CARDIAC STEM CELL THERAPY FOR INFARCTED RAT HEARTS

Suat Cheng Tan

Green Templeton College

Department of Physiology, Anatomy and Genetics

University of Oxford

Trinity Term 2011

Supervisors:

Prof. Kieran Clarke

Prof. Kay E. Davies

Dr. Carolyn A. Carr

ACKNOWLEDGEMENT

First and foremost, I would like to extend my deepest appreciation and thanks to my supervisors, Prof. Kieran Clarke, Prof. Kay Davies and Dr. Carolyn Carr.

I am grateful to Prof. Kieran for her tremendous support, patience and trust in me to carry out this project. I would like to thank her for giving me a golden opportunity to work towards a DPhil in her laboratory.

I am very much indebted to Dr. Carolyn as I would not have been able to complete this long and demanding journey towards the DPhil without her guidance. Many thanks for her countless hours of reflecting, reading, encouraging, and most of all, the patience throughout the entire process.

A special thank to Prof. Kay for allowing me access to her laboratory for genetic and molecular work, and I must thank everyone else from Kay's laboratory who had helped me a lot – Benjamin Edwards, Dr. Alice Kwok and Dr. Mattea Finelli.

There are a number of people whose contributions of time and effort I would like to acknowledge. Dr. Daniel Stuckey, Dr. Jun Jie Tan, Dr, Renata Gomes, Dr. Georgina Ellison, Prof. Christopher Schofield, Kar Kheng Yeoh, Dr. Lisa Heather, Emma Carter, Lucy Ambrose, Vanessa Fairfield and Khadijeh Pakzad for contributing their expertise and work to the realisation of partly of this research.

Thanks also to all the researchers, students and staff in the CMRG, who were extremely helpful throughout the entire period to complete my research. Special thanks to Damien, Mark, Lowri, Amira, Yvonne and Fiona in helping me to solve the problems that I faced in the research. I have learnt so many things from this wonderful laboratory.

I wish to express my most sincere appreciation to the stem cell group members, Lien-Cheng, Lucy and Vanessa, who had worked together with me over so many weekdays, weekends, Easter holidays, summer holidays and even during the Christmas period in the stem cell laboratory, for the sake of maintaining stem cell culture. We shared so much fun and joy working together.

I also would like to thank Universiti Sains Malaysia and the Malaysian Ministry of Higher Education, for sponsoring my DPhil studies at the University of Oxford.

Last but not least, I would like to thank my parents and friends for giving me never-ending support and encouragement throughout this period. I appreciate all their support and love from afar. I dedicate this thesis to my late mother.

CARDIAC STEM CELL THERAPY FOR INFARCTED RAT HEARTS

Suat Cheng Tan

Green Templeton College, University of Oxford, Trinity Term 2011

Infarction irreversibly damages the heart, with formation of an akinetic scar that may lead to heart failure. Endogenous cardiac stem cells (CSCs) are a promising candidate cell source for restoring lost tissue and thereby preventing heart failure. CSCs would be most beneficial if administered soon after infarction, thus the aim of this project was to optimize CSC culture conditions to enhance their therapeutic potential for myocardial infarction. CSCs were isolated and expanded *in vitro* via the formation of cardiospheres to give cardiosphere-derived cells (CDCs). Neonatal rat CDCs were found to be heterogenous, containing cells expressing the cardiac stem cell marker, c-Kit, pluripotent cell markers, Oct-4, Sox 2, Klf-4 and Nanog, and early cardiac specific differentiation markers, Nkx 2.5 and GATA 4. Administration of CDCs to the infarcted rat heart increased the cardiac ejection fraction by 9%, capillary density by 9% and reduced scar volume by 33%, compared to the non-treated group. The proliferation rates and the expression of c-Kit were significantly decreased in CSCs isolated from aged rats and after extended culture *in vitro*, so, CSC culture was optimized using hypoxic preconditioning. Under hypoxia, CDC proliferation rates were 1.7-fold greater, and larger cardiosphere clusters were formed. Hypoxic CDCs had an increased cardiac stem cell population, in that c-Kit was increased by 220% and CD90 and CD105 were decreased by 55% and 35%, respectively, compared to normoxic CDCs. Further, hypoxia induced the expression of CXCR-4 (~3.2-fold), EPO (~3.0-fold) and VEGF (~1.5-fold), indicating that hypoxic preconditioning may stimulate stem cell homing and neovascularization in the infarcted myocardium. Notably, hypoxic CDCs were able to switch to anaerobic glycolytic metabolism and had approximately 80% lower oxygen consumption, suggesting that they may be better adapted to survive within the hypoxic infarct scar, compared with normoxic CDCs. Culture of CDCs with hypoxia-mimicking prolyl-4-hydroxylase inhibitors (PHDIs) using DMOG, BIC and a novel compound, EDBA, induced similar effects to hypoxic culture by increasing c-Kit, EPO, VEGF, CXCR-4, decreasing CD90 and CD105 and increasing glycolytic metabolism. However, PHDI treatment for 24 hours did not alter CDC proliferation rates and cells died after 24 hours. In conclusion, CDCs are a potential cell source for therapy after myocardial infarction and their therapeutic potential can be enhanced using hypoxia or PHDI-preconditioning techniques.

CONTENTS

Abbreviations

36β4	acidic ribosomal phosphoprotein
2OG	2-oxoglutarate
5-aza	5-azacytidine
Actb	beta-actin
ATP	adenosine triphosphate
Asn	asparagine
BIC	2-(1-chloro-4-hydroxyisoquinoline-3-carboxamido)acetic acid
BMC	bone marrow cell
c-Kit	stem cell factor cytokine receptor
CAD	C-terminal transactivation domain
CBP/p300	Creb-binding protein/protein 300
CD	cluster of differentiation protein
CD90	Thy-1 cell surface antigen
CD105	endoglin
CDC	cardiosphere-derived–cell
CO_2	carbon dioxide
CSC	cardiac stem cell
CADUCEUS	CArdiosphere-Derived aUtologous Stem Cells to reverse ventricUlar dysfunction
CXCR-4	CXC chemokine receptor 4
DMOG	dimethyloxalylglycine
DNA	deoxyribonucleic acid
EDBA	ethyl 2-(2,3-dihyroxybenzamido) acetates
EDC	explant-derived cell
EPDC	epicardial-derived stem cell
DMSO	dimethylsulfoxide
ES	embryonic stem
EPC	endothelial progenitor cell
EPO	erythropoietin
Fe(II)	iron ferrous
FIH	factor inhibiting HIF
GAPDH	glyceraldehyde-3-phosphate dehydrogenase
GATA 4	GATA binding protein 4
GLUT1	glucose transporter 1
GLUT4	glucose transporter 4
HIF	hypoxia-inducible factor
HRE	hypoxia response elements.
iPS	induced pluripotent stem cells
Klf-4	Kruppel-like factor 4
Km	Michaelis–Menten kinetics
Lin	lineage
LVEF	left ventricular ejection fraction.
MSC	mesenchymal stem cells
MyHC	myosin heavy chain
Nanog	homeobox protein NANOG
Nkx 2.5	homeobox protein NKX2-5
qRT-PCR	quantitative (real-time) reverse transcriptase PCR
RT-PCR	reverse transcriptase PCR
RNA	ribonucleic acid

O_2	oxygen
OCT-4	POU class 5 homeobox 1 (Pou5f1)
ODDD	oxygen-dependent degradation domain
P	passage
PHD	prolyl-4-hydroxylase
PHDIs	prolyl-4-hydroxylase inhibitors
pVHL	von Hippel Lindau protein
Sca-1	stem cell antigen-1
SCIPIO	Cardiac Stem Cell Infusion in Patients with Ischemic Cardiomyopathy
SDF-1	stromal derived factor-1
Sox-2	SRY (sex determining region Y)-box 2
SMs	skeletal myoblasts
SP	side population
Tel	telomere
TERT	telomerase reverse transcriptase
Tnnt 2	troponin T type 2 (cardiac)
VEGF	vascular endothelial growth factor
VSELs	very small-embryonic-like cells

LIST OF UNITS

bp	base pairs
°C	degree Celsius
g	gram
in	inch
L	liter
M	molar
ml	milliliter
min	minute
mM	milimolar
nm	nanometer
ng	nanogram
ng/µl	nanogram per microliter
pH	a standard measure of the acidity of a solution
pmol	picomolar
rpm	rotation per min
sec	second
U	unit
µl	microliter
µg	microgram
µg/µl	microgram per microliter
µm	micrometer
V	volt
v/v	volume over volume

Chapter 1

Introduction

1.1 Myocardial infarction

Around 124,000 people suffer from myocardial infarction every year in the UK, with a high prevalence being diagnosed over age 54 (Figure 1.1). Despite the use of the best pharmacological and surgical therapies, myocardial infarction can progress to heart failure [1]. The death rate from heart failure remains high, with 50% of patients dying within one year of diagnosis [2, 3].

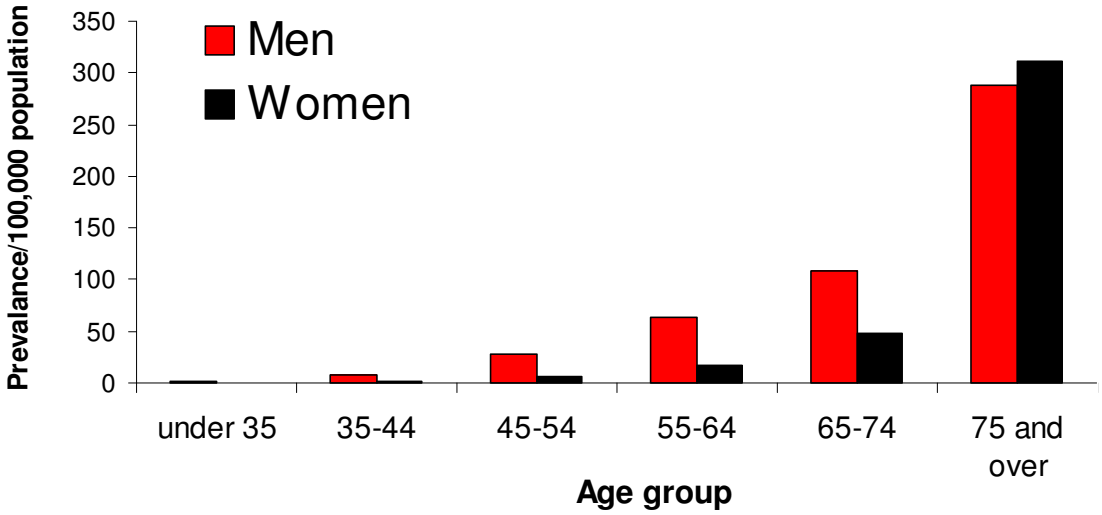

Figure 1.1 *Prevalence of coronary heart disease by age and sex in England and Wales (adapted from Coronary heart disease statistics: heart failure supplement 2010)[4].*

Myocardial infarction, commonly known as a heart attack, is caused by occlusion of one or more of the coronary arteries supplying blood to the heart. Occlusion of the blood vessels reduces the supply of nutrients and oxygen to the myocardium and results in an area of ischemia where the myocardium becomes irreversibly damaged due to cell necrosis and apoptosis [5, 6]. Acute loss of cardiomyocytes triggers the healing process through a series of molecular reactions that result in the recruitment of inflammatory cells and the formation of a non-contractile collagenous scar in the infarcted region [7]. The weakened infarcted myocardium is unable to maintain an adequate output to meet the metabolic demands of the body. Therefore, compensatory mechanisms such as cardiac dilatation and hypertrophy are initiated. This response

increases the infarcted heart's ability to circulate blood and enables it to maintain a normal stroke volume temporarily. Over time, due to the limited regenerative capability of cardiomyocytes, pathological changes occur in the heart and lead to a functional degradation and ultimately heart failure [1].

1.2 Current therapies for myocardial infarction

1.2.1 Coronary reperfusion

The cell apoptosis that occurs following myocardial infarction can be reduced if the occlusions are removed quickly and tissue reperfusion is restored [8]. Rapid restoration of blood flow to the infarcted myocardium can be achieved by administration of thrombolytic agents which digest the clot, or by physically opening the blocked vessel using a balloon catheter. In some cases, implantation of a wire mesh tube known as a stent is performed to prevent the artery from closing [9]. Where the blood vessels are permanently occluded, coronary artery bypass grafting with vessels taken from another area of the body is used to restore perfusion to the infarcted area [10].

1.2.2 Pharmacological treatment

Existing pharmacological treatment for myocardial infarction includes diuretics, angiotensin-converting enzyme (ACE) inhibitors and beta-blockers. Diuretics are important to reduce blood pressure and control fluid retention, but diuretics give possible side effects such as heart irregularities (arrhythmias) and disturbed kidney function. ACE inhibitors dilate the blood vessels, to improve the amount of oxygen-rich blood to be pumped throughout the body, whereas beta-blockers block the action of adrenalin, which reduces the heart rate and workload. Over time, ACE inhibitors and beta-blockers control the symptoms after infarction and improve the quality of the patient’s life.

1.2.3 Limitations of current therapy for myocardial infarction

Although current standard therapies allow restoration of blood supply and have significantly reduced early mortality rates [11], these treatments cannot prevent or reverse progression to the failing state because the damaged myocardium is not replaced by these therapies [2, 3]. At present, only heart transplantation can restore the failing heart [12]. However limited numbers of hearts are available for transplantation and the risk associated with surgery, such as the immunogenic response and transplant rejection, has led to the demand for an alternative therapy for heart failure and novel treatment methods for myocardial infarction.

1.3 Stem cell therapy for myocardial infarction

Cell grafting has emerged as a potential therapy for the infarcted heart. Stem cells are a population of primitive cells characterized by the ability to self-renew and differentiate into many cell types. Stem cells have a high capacity for cell division and this property is preserved throughout the life time of an organism [13]. There are three major types of stem cells, embryonic stem cells, induced pluripotent stem cells (iPS) and adult stem cells.

1.3.1 Embryonic stem cells

Embryonic stem (ES) cells originate from the inner cell mass of the blastocyst [14, 15]. Human ESCs are immortal cells, capable of perpetual self-renewal in culture while maintaining an undifferentiated phenotype and normal karyotype [16, 17]. In addition, ES cells are pluripotent, thus they are able to develop into all cells of the three germ layers (ectoderm, endoderm and mesoderm) [18]. *In vitro*, specific culturing conditions and genetic modification have been used to demonstrate that ES cells are able to differentiate into many cell types including endothelial cells [19], neuronal cells [20], pancreatic progenitor cells [21, 22] and cardiomyocytes [23]. *In vivo*, ES cells have

been shown to improve cardiac function in rodents through differentiation within the donor myocardium, contributing to a stable improvement in contractile function and ventricular remodeling in the infarcted heart [24, 25]. However, the pluripotent characteristic of ES cells results in a high chance of teratoma formation after administration [26]. Also, the allogenicity problems (ES cells provoke an immunogenic response in the recipient body) [27] and the ethical issues (ES cells can only be obtained by destroying an embryo) [28] cause ES cell transplantation to remain problematic and restrict the clinical application.

1.3.2 Induced pluripotent stem cells

Induced pluripotent stem (iPS) cells are adult cells that have been genetically reprogrammed to an embryonic stem cell–like state by being forced to express genes and factors important for maintaining the defining properties of embryonic stem cells, including Oct-4, Sox 2, Klf 4 and c-Myc [29]. Mouse iPSCs were first reported in 2006 [29], and human iPSCs were first reported in late 2007 [30]. iPS cells opened up the possibility to generate ES cell-like stem cells from recipient's somatic cells, thereby overcoming the ethical controversies and also immunogenic rejection issues of ES cells. iPS cells can be differentiated into spontaneously contracting cardiomyocytes [31, 32], providing an alternate cell source for myocardial infarction therapy. However, like ES cells, iPS cells are pluripotent, thus the risk of tumorigenesis after iPS cells transplantation remains. It was found that extended culture of iPSCs was linked to duplication of oncogenic genes [33] and that around 20% of iPS cell-derived mice developed tumours [34]. Furthermore, Lister *et al.* reported that iPSCs show significant reprogramming variability, including retaining a somatic memory of their origin. They found that iPS cell lines derived from human adipose-derived stem cells retain some somatic cell DNA methylation patterns which are resistant to resetting to an ES-cell-

like state, even at late passages (15–65 passages) [35]. Overall, iPS cells are potent cells for therapies, nevertheless, continued study of a wide variety of iPS cells and their ES cell counterparts is needed to understand the full range of epigenomic variability, and to potentially identify factors that enable complete reprogramming of iPS cells to occur [35, 36].

1.3.3 Adult stem cells

Adult stem cells are undifferentiated cells found among differentiated cells in tissue throughout the body. They are able to self-renew and also to differentiate to yield some or all of the major specialized cell types of the tissue or organ where they are found. Adult stem cells are low in number and were thought to be organ- or tissue-restricted stem cells, however recent research has demonstrated that these cells are multipotent and able to transdifferentiate into developmentally unrelated cells [37, 38]. Several different sources of adult stem cells have been used for myocardial infarction therapy, including bone marrow stem cells, endothelial progenitor cells, mesenchymal stem cells, skeletal myoblasts and endogenous cardiac stem cells.

1.3.3.1 Bone marrow-derived stem cells

Bone marrow cells (BMCs) comprise a complex assortment of cells that generate blood cells, bone, cartilage, fat, fibrous connective tissue and a diverse multipotent stem and progenitor cell population [39-41]. Evidence for the potential therapeutic value of bone marrow cells in the treatment of cardiovascular disease first appeared in *Nature* in 2001 [42]. Early studies showed that c-Kit$^+$ Lin$^-$ BMCs injected into injured myocardium transdifferentiated into cardiomyocytes, smooth muscle, endothelial cells and thus improved cardiac function [42, 43]. The promising findings of these early experiments resulted in rapid translation of stem cell therapy to the clinic. To date, over 25 clinical trials of autologous BMC therapy for the heart have been carried out

[44]. However, most clinical trials showed a small or no significant effect of autologous BMCs on left ventricular function in patients with acute myocardial infarction [45-47] (Table 1.1).

Table 1.1 *Comparison of outcomes of several clinical trials of intracoronary infusion of bone marrow-derived cells following acute myocardial infarction.*

Ref.	Trial	Year	Duration	No. of patient	Clinical outcome
[48]	Straeur *et al.*	2002	3 months	20	Infarct region decreased from 30 ± 13% to 12 ± 7% P = 0.005.
[49]	BOOST	2004	6 months	60	LVEF increased 6%
[50]	Bartunek *et al.*	2005	4 months	35	LVEF increased 7.1%
[51]	BOOST #	2006	18 months	60	N.D
[45]	ASTAMI	2006	6 months	100	N.D
[52]	REPAIR-AMI	2006	4 months	204	LVEF increased 2.5%
[53]	HEBE	2008	12 months	26	LVEF increased 2.2%
[54]	REGENT	2009	6 months	200	N.D
[55]	SCAMI	2010	6 months	42	N.D
[56]	HEBE #	2010	4 months	200	N.D
[57]	BONAMI	2010	3 months	101	Myocardial viability improved in 34% patients

= follow-up study; N.D = no significant different compared with non-treated group; LVEF = left ventricular ejection fraction.

1.3.3.2 Endothelial progenitor cells

Endothelial progenitor cells (EPCs) are VEGFR-2, CD133 and CD34 expressing cell isolated from adult bone marrow, peripheral circulation blood or umbilical cord blood [58]. EPCs have been shown to transdifferentiate into endothelial cells, smooth muscle cells and cardiomyocytes *in vivo* [59]. Functionally, transplantation of EPCs supported neoangiogenesis, increased capillary density and improved heart function in the rat [60,

61]. However conflicting results which suggested that transplanted EPC showed no contribution to the vasculature have also been reported [62, 63]. Also, there are still controversies about whether the improvement in cardiac function observed following EPC transplantation results from direct regeneration through differentiation of EPCs into cardiomyocyctes [59] or is an indirect effect due to angiogenesis induced by EPCs [64]. The controversies regarding EPC identity and function limited its application in clinical.

1.3.3.3 Mesenchymal stem cells

Mesenchymal stem cells (MSC) are fibroblast-like plastic-adherent cells isolated originally from bone marrow, and also been found in nearly every organ [65]. These cells are positive for CD105, CD90 and CD74, but negative for CD45, CD34, CD14, CD79, CD19 and HLA-DR. They are multipotent, capable of differentiating into osteoblasts, chondrocytes and adipocytes under specific culture conditions [66]. MSC are easy to expand *in vitro* and can be genetically altered by viral vectors, which make them an ideal and safe long-term vehicle for cellular gene therapy [67]. Recently, MSCs have been found to differentiate into neural cells [68], cardiomyocytes [69], and pneumyocytes [70]. MSCs have been shown to improve cardiac function in the infarcted hearts [71, 72], however conflicting results have also been reported [44].

1.3.3.4 Skeletal myoblast

Skeletal myoblasts (SMs), or satellite cells, are found in skeletal muscle where they maintain and regenerate old/damaged muscle fibers. These cells can be easily harvested from a muscle biopsy samples and proliferate abundantly *in vitro*, giving a ready source of autologous cells for transplantation [73]. SMs were the first cells injected into the ischemic myocardium as part of a cell-based therapy clinical trial [74]. Although this one year randomized controlled trial reported improvement in left

ventricular function and volume [75], little evidence showed these cells can transdifferentiate into cardiomyocytes [73, 76]. Furthermore, SMs transplantation possibly causes arrhythmias as a side effect [73, 76]. Modification of SMs by cell enhancement techniques to reduce the arrhythmias have been reported [77, 78] and further Phase II clinical studies (PERCUTANEO) are underway [79].

1.3.3.5 Very small-embryonic like cells

Very small-embryonic-like cells (VSELs) were first identified in murine bone marrow as a homogenous population of rare (~ 0.02%) CXCR-4^+ Sca-1^+ $CD45^-$ cells that express markers of pluripotent stem cells such as SSEA-1, Oct-4, Nanog and Rex-1 [80, 81]. Subsequently, these cells were identified in various other murine organs such as brain, kidneys, muscles, and pancreas [82]. As their name suggests, these cells are small (~2–4 μm) and possesses ESC-like pluripotent plasticity, thus are able to differentiate into all three germ-layer lineages. *In vitro* differentiation of VSELs demonstrated the ability of these cells to give rise to neuronal, pancreatic cells and cardiomyocytes [80]. Although VSEL transplantation improved left ventricular function in a infarcted animal model [83], the oncogenic risk and the rarity of the cells could be a drawback for translation to the clinic.

1.3.4 Endogenous cardiac stem cells

The discovery that the adult heart contains a pool of cardiac stem cells (CSCs) that can replenish the cardiomyocyte population and regenerate coronary vessels has dramatically changed the traditional view of the heart as a postmitotic organ [84-87]. Because of their natural role in the regeneration of cardiac cells, endogenous cardiac stem cells appear to be the ideal cell to expand for myocardial therapy. Different approaches have been used to isolate CSCs from heart tissue.

1.3.4.1 Cardiac side population

Hierlihy *et al.* were the first to isolate stem cells from the hearts, based on the ability to efflux Hoechst dye, yielding a putative progenitor side population (SP) cell with stem cell-like activity [88]. The unique dye efflux ability is mediated by the ATP-binding cassette transporter (Abcg2) which is then used as an identity marker for SP cells [89]. Abgc2 expression is important to endothelial cell survival migration and tubule formation after myocardial infarction. Increased numbers of cells expressing the Abcg2 marker have been observed in the border zone after myocardial infarction [89]. Moreover, these cells are capable of differentiating into the cardiomyocyte lineage in coculture experiments with primary cardiomyocytes [90], with the greatest potential for cardiomyogenic differentiation being restricted to cells co-expressing stem cell antigen-1 (Sca-1, a stem cell marker) [91]. However, SP cells were found in low amounts in the postnatal mouse heart (~1% of the total cell number) [88] and to date no study has evaluated the regenerative potential of SPs *in vivo*.

1.3.4.2 Stem cell antigen-1$^+$ cells

Stem cell antigen-1$^+$ (Sca-1$^+$) cells have been isolated from the resident population of cardiac progenitor cells [87]. These cells express telomerase reverse transcriptase (TERT), a reverse transcriptase that synthesizes telomere repeats on the telomere ends at the tips of chromosomes during each cell division [92, 93]. In various types of stem cells, telomerase functions to ensure long term self-renewal capacity via maintenance of telomere length [94, 95]. Coincident with the expression of TERT, Sca-1$^+$ cells have been found to associate with self-renewal potential [87]. Furthermore, Sca-1$^+$ cells are multipotent, and can be differentiated into cardiomyocytes when stimulated with 5-azacytidine (5-aza) in culture [87]. Functionally, intravenous injection of Sca-1$^+$ cells into mice after infarction increased the left ventricular ejection fraction, and induced

myocardial neovascularisation and modest cardiomyocyte regeneration [96]. However, as with SP cells, very low numbers of Sca-1$^+$ cells are found in the heart (~0.3%) [97].

1.3.4.3 c-Kit$^+$ cells

Beltrami *et al.* [86] first reported the discovery of a distinct resident population of CSCs expressing the receptor for stem cell factor, c-Kit (also known as CD117), but not the haematopoietic lineage markers (Lin$^-$). These c-Kit$^+$Lin$^-$ cells are self-renewing, clonogenic, multipotent, and can differentiate into cardiomyocytes, smooth muscle cells, and endothelial cells [86]. Some of these cells express transcription factors Nkx2.5, GATA4 and MEF2, indicating that they are at the early stage of cardiac myogenic differentiation and are committed to the cardiac lineage [86]. In the adult rat myocardium, c-Kit$^+$ Lin$^-$ cells are relatively rare (1 per 104 myocytes). However, the cells can be expanded *in vitro* for up to 40 passages without altering the cell phenotype [98]. Furthermore, transplantation of c-Kit$^+$ cells into infarcted rat hearts has been shown to increase viable myocardium in the infarcted region, reduce fibrosis in the non-infarcted region, improve left ventricular ejection fraction and activate the endogenous cardiac stem cells [99]. This encouraging preclinical evidence has led to a clinical trial (Cardiac Stem Cell Infusion in Patients with Ischemic Cardiomyopathy (SCIPIO) [100].

1.3.4.4 Islet-1 cells

Homeobox gene islet-1$^+$ cells were identified within the adult heart in 2005 by Laugwitz *et al.* [101]. These cardiovascular progenitor cells are multipotent and give rise to three major cell types in the heart: cardiac, smooth muscle, and endothelial cells [102]. Unlike other putative resident cardiac progenitor populations, Islet-1$^+$ cells do not express Sca-1 and c-Kit. However, they do express Nkx2.5 and GATA4 and most importantly they can be differentiated into cardiomyocytes *in vivo* [101] Nonetheless,

islet-1^+ cells have only been isolated from very young animal and human specimens, and the number of isl-1^+ cells dramatically falls over the first few weeks after birth [103], thereby limiting clinical potential.

1.3.4.5 Epicardial-derived stem cells

Another source of adult cardiac progenitor cells with potential for the regeneration of infarcted heart is the epicardium [104]. During cardiac development, the epicardium is the source of multipotent mesenchymal cells, which give rise to endothelial and smooth muscle cells in coronary vessels and also to cardiomyocytes [104]. These cells are termed epicardial-derived stem cells (EPDCs). In 2009, Smart *et al.* reported that quiescent EPDCs can be activated using a naturally occurring protein called thymosin beta 4 (Tβ4). Tβ4 brings the EPDCs out of dormancy and induces them to become mature cardiomyocytes [105]. In mice that were infused with Tβ4, the heart progenitor stem cells were activated and migrated from the epicardium to the area of damage and became mature cardiomyocytes [105]. In a recent publication in June 2011, they reported that activated adult mouse EPDCs express the key embryonic epicardial gene, Wilm's tumour 1 (*Wt1*) which ultimately contributes to *de novo* cardiomyocyte formation in the injured mouse heart [106]. EPDC-derived cardiomyocytes were structurally and functionally integrated with resident muscle and gave significant improvement in functional parameters, including increased ejection fraction, reduced end diastolic/systolic volumes and reduced scar volume. Stimulation of EPDCs to give rise to *de novo* cardiomyocytes has emerged as a new resident-cell-based therapy for heart disease.

1.3.4.6 Cardiosphere and cardiosphere-derived cells

In 2004, Messina *et al.* developed a method to isolate CSCs from human and murine heart and expand them as cardiospheres [107]. These cardiospheres were clonogenic,

expressed cardiac stem cell markers, c-Kit and Sca-1 and the endothelial progenitor cell marker, CD34. Cardiospheres have been shown to be able to spontaneously differentiate into contracting cardiomyocytes, confirming that these cells possess cardiomyogenic potential. These cardiospheres were expanded *in vitro* to obtain sufficient cardiosphere-derived cells (CDC) for transplantation [108]. It has been found that transplantation of cardiospheres and CDCs leads to myocardial regeneration and functional improvement in infarcted rodent hearts [107, 108]. Clinical application of CDCs is already under investigation by the CADUCEUS trial (Clinical Trials.gov. Identifier NCT00893360) [109]. In this thesis, the potential of CDCs as a therapeutic tool for myocardial infarction is investigated further. A summary of all cell types discussed in this chapter, with respect to their markers, sources, advantages and disadvantages for the treatment of myocardial infarction disease is listed in Supplement data 1.

1.4 Hypoxia

Hypoxia is a pathological condition in which the whole body (generalized hypoxia) or a region of the body (tissue hypoxia) is deprived of an adequate oxygen supply. Generalized hypoxia may occur due to a deficiency of oxygen in the atmosphere (high altitude) or during strenuous physical exercise. Tissue hypoxia occurs at the cellular level, as a result of reduced blood supply to a particular region of tissue or organ, for example following a myocardial infarction.

Hypoxia triggers a number of physiological and cellular mechanisms to adapt to reduced oxygen. Many processes involved in oxygen homeostasis are mediated by the hypoxia-inducible factor (HIF) transcriptional complex, which regulates the expression of a large number of genes including erythropoietin (EPO), which regulates production

of red blood cells [110], vascular endothelial growth factor (VEGF), which triggers neovascularisation [111-113], proliferation and remodelling of the vascular wall [114], glucose transporter 1 (GLUT1), a metabolic gene which is responsible for the low-level of basal glucose uptake required to sustain respiration in all cells [115, 116] and CXC chemokine receptor 4 (CXCR4), a cytokine receptor of stromal derived factor-1 (SDF-1) which plays a role in the regulation of stem cell trafficking and homing based on the CXCR-4/SDF-1 axis [117, 118].

The transcriptional complex HIF was discovered by Semenza et al. [119] in 1992. Further biochemical purification led to the identification of the HIF-α and HIF-β subunits. HIF-α protein is only detectable under hypoxic conditions while HIF-β protein is constitutively stable. Subsequently, HIF-2α and HIF-3α were discovered and showed similar regulation in response to hypoxia [120, 121].

1.4.1 Regulation of HIF in hypoxia

In the presence of oxygen, the HIF-α subunit is downregulated via two pathways: hydroxylation by prolyl-4-hydroxylase (PHD) enzymes [122] or by factor-inhibiting HIF (FIH) enzyme [122, 123] (Figure 1.2).

1.4.1.1 Pathway I - HIF-α degradation via hydroxylation by prolyl-4-hydroxylase (PHD)

PHDs are dioxygenase enzymes that split molecular oxygen. One oxygen atom is inserted into the HIF-α peptide at the prolyl residue in the oxygen-dependent degradation domain (ODDD) (hydroxylation of HIF-α) while the other converts 2-oxoglutarate (2OG) to succinate, yielding CO_2 as a by-product. Thus, this pathway can only occur in the presence of oxygen with 2-OG as co-substrate. Upon

hydroxylation of the prolyl residue in ODDD, HIF-α is recognized by von Hippel Lindau protein (pVHL) which is a part of an ubiquitin ligase and characterizes the protein to the ubiquitinylation machinery, leading to proteasomal degradation [122] (Figure 1.2).

1.4.1.2 Pathway II -HIF-α inactivation via hydroxylation by factor-inhibiting HIF (FIH)

FIH is an asparaginyl hydroxylase which catalyses the splitting of molecular oxygen, using one oxygen atom for hydroxylation of the target asparagine (Asn) within the C-terminal transactivation domain (CAD) of HIF-α, and the other for oxidising the co-substrate 2OG as above. The CAD recruits CBP/p300 (Creb-binding protein/protein 300), which is essential to link HIF-α to the hypoxia response element (HRE) transcriptional factor and initiate the transcriptional machinery of the HIF system. Hydroxylation of this single asparagine residue was found to be sufficient to prevent the interaction of the CAD with the essential transcriptional coactivator CBP/p300, thus silencing the HIF-α transcriptional ability [122, 123] (Figure 1.2a).

Under hypoxia, HIF-α escapes the prolyl and asparaginyl hydroxylation, translocates to the nucleus and dimerises with HIF-1β at the Per ARNT SIM (PAS) domain to form functional heterodimeric HIF. Activated HIF then binds to the hypoxia response elements (HREs), leading to a transcriptionally active complex which activates the expression of hundreds of genes including EPO, VEGF and GLUT-1 (Figure 1.2b).

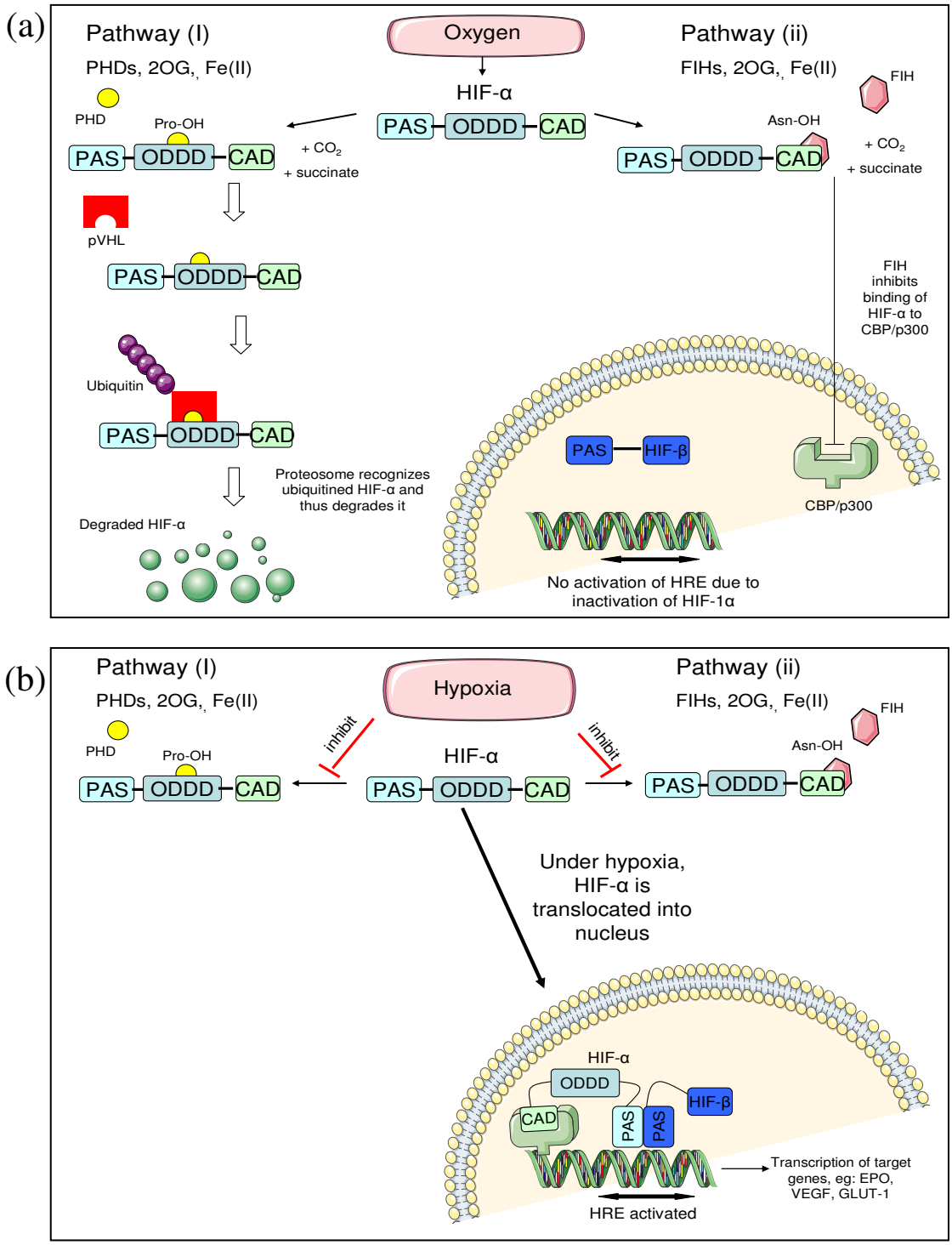

Figure 1.2 *(a) Regulation of HIF-α via two pathways under normal oxygen levels. Left panel: Pathway (I) - PHDs hydroxylate prolyl residue of HIF-α in ODDD domain, in the presence of 2OG and Fe(II). Hydroxylated HIF-α is recognized by pVHL which labels the protein to proteasomal degradation by ubiquitin protein. Right panel: Pathway (II) – FIHs hydroxylate asparagine residue of HIF-α in the CAD domain, in the presence of 2OG and Fe(II). Hydroxylated HIF-α is blocked to interact with the essential transcriptional coactivator CBP/p300, thus silencing the HIF transcriptional ability. (b) Under hypoxia, pathway (I) and pathway (II) are inhibited, HIF-α translocates to nucleus, dimerises with HIF-β and activates the HIF system.*

HIF = hypoxia-inducible factor; FIH = factor inhibiting HIF; 2OG = 2-oxoglutarate; Fe(II) = iron ferrous; ODDD = oxygen-dependent degradation domain; pVHL = von Hippel Lindau protein; CAD = C-terminal transactivation domain; CBP/p300 Creb-binding protein/protein 300; PAS = Per ARNT SIM;HRE = hypoxia response elements.

1.4.2 Prolyl-4-hydroxylase inhibitors

As described, HIF activation is negatively regulated by the PHD enzymes, a conserved subfamily of dioxygenases that catalyze the post-translational hydroxylation of HIF-α subunits. While oxygen concentration plays a major role in determining the efficiency of PHD catalyzed reactions, the sensitivity of these enzymes also depends on the co-substrate, 2OG and co-factor, iron. Thus, inhibition of the 2OG, or of iron, or of the specific active site of PHD enzyme using a small molecular weight compound, could inhibit the enzymes activity and thus potently activate the HIF response [124-127].

1.4.2.1 Oxygen

Oxygen (O_2) is the key substrate for hydroxylation. The *Km*[*] value for O_2 of all three PHD isoforms (PHD 1-3) is within the range of 230-250 μM, slightly above the O_2 concentration in aqueous solutions saturated by ambient room air [128]. The high *Km* values for O_2 indicate that PHDs are sensitive to O_2 concentration in the cytoplasm, therefore, activity of PHDs are inhibited in slightly reduced O_2 concentrations despite all other substrate and cofactors being present at adequate levels [128].

While in most cells, HIF-α protein is degraded under normoxia, however, it has been shown that HIF-1α protein was constitutively expressed *in vitro* under normoxic conditions in some cancer cell types such as lymphoma and leukemia cells derived from the hematopoietic system [129], pancreatic cancer cell line [130] and prostate cancer (PCA) PC-3 cells [131]. The HIF-1α expression in these cancer cells is further increased in response to hypoxia [131]. Although the detailed mechanism of HIF expression under normoxia is unknown, it has been postulated that the phosphatidylinositol 3′-kinase (PI3K)/protein kinase B (Akt) pathway might play a role [132]. Zhang *et al.* reported that stem cell factor/c-Kit signaling activated multiple signal transduction pathways including the PI3K/Akt pathway [133]. Thus, it is

[*] *Km* = Michaelis–Menten kinetics
Km value = the substrate concentration at which the reaction rate is half of maximation rate, V_{max}.

possible that the expression of c-Kit expressing cardiac stem cells could activate HIF-1α under normoxia via a PI3K/Akt-dependent mechanism [133].

1.4.2.2 Competitive inhibition by 2-oxoglutare analogues

2-oxoglutarate (2OG), an intermediate of the tricarboxylic acid (TCA) cycle, is an essential co-substrate for PHDs [134]. Administration of a 2OG analogue such as dimethyloxalylglycine (DMOG) or 3,4-dihydroxybenzoate (DHB) can inhibit PHD enzymes. These 2OG analogues compete against 2OG to bind to the catalytic site of PHD and cause a molecular inhibition of the enzyme function. Although mitochondria generate inhibitory TAC cycle intermediates, including succinate and fumarate, which are also able to compete with 2OG for binding to the PHD active site [135], under normal circumstances these molecules do not significantly interfere with PHD function because of their low cytosolic concentrations [136]. DMOG is the most commonly used 2OG analogue both *in vitro* and *in vivo* to stabilize and activate HIF [137-139]. DMOG activates the HIF system with enhanced transcription of target genes which might have a role in the therapy for ischemic disease [140, 141]. Animals pre-conditioned with DMOG showed reduced inflammatory infiltration after ischemia-reperfusion, associated with a significant reduction in myocardial infarct size [142]. In this thesis, the function of DMOG in stabilizing HIF is evaluated in CSCs.

1.4.2.3 Intracellular Fe(II) concentration

PHD enzymes require iron to catalyze the HIF prolyl hydroxylation reaction, therefore iron chelators are routinely used to inhibit PHD enzyme activity and thus stabilize HIF. *In vivo* studies in both neonatal and adult rats have shown that preconditioning with desferrioxamine (DFO) (iron chelator) or cobalt chloride ($CoCl_2$) (competitive inhibitor of iron) protects against hypoxic-ischemic injury in neonatal rat brain, possibly due to the activation of HIF [143-145]. However, not all reports are consistent with beneficial

effects of DFO and $CoCl_2$. A recent publication showed that DFO and $CoCl_2$ inhibit the cell proliferation in lung tissue explants culture [146]. In this thesis, a novel potential iron chelator, ethyl 2-(2,3-dihyroxybenzamido) acetate (EDBA) synthesized by our collaborators, Kar Kheng Yeoh and Prof. Chris Schofield from the Chemistry Research Laboratory, University of Oxford, is tested in cardiac stem cells.

1.4.2.4 Specific prolyl-4-hydroxylase inhibitor

Hydroxylation occurs within the oxygen-dependent degradation domains (ODDD) of the HIF-α subunit [147]. 2-(1-chloro-4-hydroxyisoquinoline-3-carboxamido)acetic acid), FibroGen 2216, hereafter called BIC, is a specific PHD antagonist that fuses into the ODDD region of HIF-α subunit, blocking the hydroxylation of PHD and binding of pVHL to the HIF-α subunit. The HIF-α subunit that escapes from the pVHL binding is not recognized by the proteosomal degradation machinery, and therefore is stabilized. This specific PHD inhibitor is patented by FibroGen Inc. and has already been administered to healthy control subjects [148] and to patients with chronic kidney disease (CKD) [149] in clinical trials. Specifically, BIC was found to enhance the mobilization and expression of the cytokine erythropoietin (EPO). However, during one of the Phase II clinical trials, a female patient developed fatal hepatic necrosis that was temporally related to the introduction of this compound [150]. The possible reason for this incident is that inhibition of the PHDs activates a wide range of pathophysiological processes, not only the activation of EPO, but at least 100 other genes including VEGF [111-113] and GLUT1 [115, 116]. Since the reported effects of BIC are variable, therefore it is in our interest to re-evaluate the specific effects of this inhibitor using cardiac stem cells. A simplified schematic showing the use of low O_2 cell culture (hypoxia) and three different PHD inhibitors to stabilize HIF system is shown in Figure 1.3.

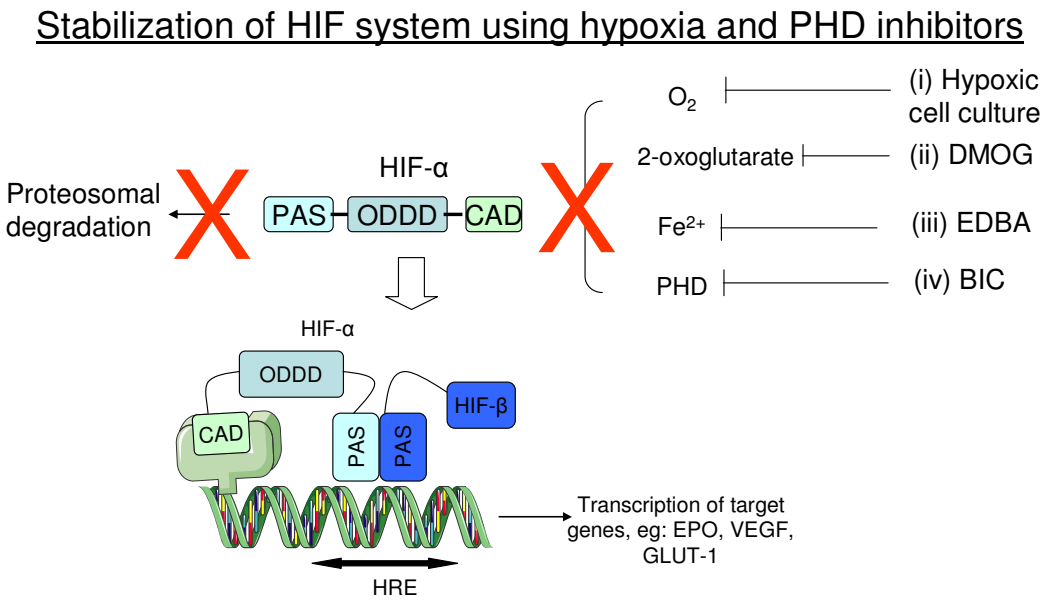

Figure 1.3 *Stabilization of HIF system using hypoxia and PHD inhibitors. There are four methods discussed in this thesis, (i) inhibit the oxygen supply using hypoxic cell culture, (ii) inhibit the co-substrate of PHD, 2-oxoglutare using 2-oxoglutarate analogue – DMOG, (iii) inhibit the co-factor of PHD, Fe(II) using iron chelator – EDBA and (iv) inhibit the PHD enzyme using specific PHD inhibitor – BIC.*

HIF = hypoxia-inducible factor; FIH = factor inhibiting HIF; 2OG = 2-oxoglutarate; Fe(II) = iron ferrous; ODDD = oxygen-dependent degradation domain; pVHL = von Hippel Lindau protein; CAD = C-terminal transactivation domain; CBP/p300 Creb-binding protein/protein 300; PAS = Per ARNT SIM;HRE = hypoxia response elements.

1.5 Objectives

The objective of the work in this report was to develop a reliable therapeutic technique to repair the infarcted heart. Specifically, the aims were to:

- Establish an *in vitro* protocol to isolate, expand and charcterize cardiosphere-derived cells (CDCs) for *in vivo* study in the infarcted rat hearts.
- Evaluate the effects of hypoxic and PHD inhibitor preconditioning on cardiac stem cell (CSC) proliferation, differentiation, metabolism, translational and transciptional changes.
- Determine the effects of ageing on CSC proliferation, differentiation, metabolism, translational and transcriptional changes.
- Optimize the CSC isolated from older rat hearts using hypoxic and PHD inhibitor preconditioning.

Chapter 2

General methods

2.1 Animals

This study used wild type Sprague Dawley (SD) and transgenic Sprague Dawley (SD-Tg(GFP)2BalRrrc) rats, which express the green fluorescent protein (GFP) gene. The SD rats were obtained from a commercial breeder (Harlan, Oxon, UK), whilst the SD-GFP rats originated from the Rat Resource and Research Centre (Missouri) and were bred in Oxford BSU from animals generously donated by Dr. Cesare Terracciano (Imperial College, UK). Animals were kept under controlled conditions for temperature, humidity and light, with water and rat chow available ad libitum, except where indicated. SD-Tg(GFP)2BalRrrc rats were used to obtain GFP expressing cardiac stem cells, an important cell marker. At the end of each experiment, rats were anaesthetised with sodium pentobarbital (270 mg/kg body weight, IP; Euthatal, Merial, UK) to allow tissue removal. Body and heart weights were routinely recorded. All procedures performed had the necessary UK Home Office and local ethical approval.

2.2 Isolation and expansion of cardiac stem cells (CSCs)

Unless otherwise stated, all cells culture was performed at 37°C in 5% CO_2:21% O_2:74% N_2.

2.2.1 Explant culture

Neonatal (1-3 days) and adult (4 months) rat hearts were excised and washed with phosphate buffered saline (PBS) (Invitrogen) twice to remove blood. The heart was then minced into 1 mm explant tissue fragments in trypsin (Invitrogen) and plated on 60 X 30 mm petri dishes, which had been pre-coated with 2 ml PBS containing 2 µl fibronectin (Sigma) and incubated at 37˚C for at least 30 mins before use. After plating the explants, 1.5 ml Complete Explants Medium (CEM) (Appendix 1) was added to each dish.

2.2.2 Harversting Explant Derived Cells (EDC)

Explants derived cells (EDC) grew out from the explants as round, phase bright cells overlying a layer of thin fibroblast-like cells, which emerged from the edges of explants. EDC, once confluent, were isolated with 1 ml trypsin for 5 mins at 37˚C.

2.2.3 Cardiosphere (Csp) culture

EDC were resuspended in Cardiosphere Growth Medium (CGM) (Appendix 1) and seeded onto 24-well plates, which had been pre-coated with 0.5 ml PBS (each well) containing 10 µg poly-D-lysine (Gibco, Invitrogen) and incubated at 37˚C for at least 30 mins before use. EDCs were plated at a density of 3 X 10^4 cells per 300 µl of CGM (each well). Spherical cell clusters, known as cardiospheres, formed from the EDC and were harvested after 4 days by mechanical trituration using a pipette.

2.2.4 Cardiosphere-derived cell (CDC) expansion

Isolated cardiospheres were resuspended in CEM, plated onto fibronectin-coated T75 flasks for expansion into cardiosphere-derived cells (CDCs). At 80-90% confluency, CDCs were passaged and split into 2 new fibronectin-coated flasks at a concentration of 5 x 10^5 cells/flask for further expansion. Media was replaced every 4 days. Cell viability was assessed at every passage.

2.3 Cell viability test

Cell viability was assessed using a dye-exclusion assay and a lactate dehydrogenase (LDH) assay. In the dye-exclusion assay, cells were trypsinized and stained with trypan blue (Sigma), a compound that traverses only the membrane of dead cells and stains them blue. Healthy cells with intact membrane integrity remained unstained. The numbers of dead cells (blue) were counted manually under a light microscope. LDH is a stable cytoplasmic enzyme present in most cells, but is released into the culture

medium upon cell death due to the damage of the plasma membrane. The increase in LDH activity in the culture supernatant is proportional to the number of lysed cells. In the LDH assay, the cell culture medium was collected after the experiment and run through the ABX Pentra 400 Chemistry Analyzer (Horiba Ltd., USA), using LDH CP enzyme reagent (A11A01824, Horiba Ltd.) (performed by Emma E. Carter).

2.4 Cell Differentiation Assay

2.4.1 Adipogenesis

Approximately 2 X 10^5 CDCs were plated in each well of a six-well plate. The cells were allowed to form a confluent monolayer and then subjected to 3 cycles of induction with adipogenic induction medium (AIM) and maintenance in maintenance medium (MM) (Appendix 2) to stimulate adipogenic differentiation. Each cycle consisted of 3 days of incubation with AIM, followed by a change of medium to MM for 2 days. Negative controls were fed on the same schedule, but only MM was used. After 7 days of incubation in MM, the medium was gently aspirated, and cells were fixed in 10% buffered formalin and stained with Oil red O. Only cells with neutral lipid vacuoles appeared red. Stained cells were observed under the microscope and images were acquired for analysis. Cells were washed with distilled water and allowed to dry at room temperature. One ml of 100% isopropanol was added into each well for 10 mins with gently shaking, and pipetting up and down several times, to elute the Oil red O. The solution was transferred into a 96-well plate reader and the optical density (OD) was measured at 500 nm, with 100% isopropanol as the blank sample.

2.4.2 Cardiomyocyte differentiation

Approximately 2 X 10^5 CDCs were plated in each well of a six-well plate pre-coated with 0.1% gelatine (Sigma, UK). When confluent, cardiomyocyte differentiation was induced using cardiomyocyte differentiation medium (CDM) (Appendix 3) containing

5-azacytidine (5-aza) or dimethylsulfoxide (DMSO) (Sigma, UK). For 5-aza treatment, 2 ml of CDM with 40 µl of 5 µM 5-aza were added to each well. For the next 2 days, 40 µl of fresh 5 µM 5-aza were added into each well every 24 hours. Then, 5-aza medium was removed and cells were incubated with 2 ml of fresh CDM for 2 days. For DMSO treatment, 2 ml of CDM and 1 µM of DMSO were added to each well. The medium was changed every two days for 6 days.

After 5-aza and DMSO treatment, all cells were aspirated with PBS to remove the dead cells and 2 ml CDM plus 50 µl of 1 µM ascorbic acid were added. The medium was changed every 2 days for the following 6 days before the cells were harvested for analysis of protein or RNA.

2.5 Polymerase chain reaction (PCR)

In this study, two PCR techniques were used: conventional reverse transcriptase PCR (RT-PCR) and real-time (quantitative) reverse transcriptase PCR (qRT-PCR). A general description is outlined from 2.4.1 to 2.4.3, with specific details for each PCR technique outlined in 2.4.4 and 2.4.5.

2.5.1 Primer design and optimization

Primer pairs were using Primer3 software based on interpretation of GenBank or Ensembl Genome Browser designed (Appendix 4). Primer specificity was enhanced by designing a primer pair that flanked the exon-exon border of the gene of interest. This can avoid the primers amplifying genomic DNA that may be contained in samples. Primer specificity was confirmed by BLASTing the primer sequence against genomic databases available at NCBI. No significant homology sequence should been found, to ensure gene specific amplification rather than amplification of several transcripts with one primer pair.

2.5.2 Primer efficiency test

For the primer efficiency test, a series of 2-fold dilutions of cDNA were prepared and amplified with consistent concentration of primer using the qRT-PCR machine. The threshold cycle (Ct) value was obtained after the PCR procedure and plotted against log cDNA dilution. Primer amplification efficiency was calculated as $E = (\exp^{-1/m} - 1)$ X 100% where E is the amplification efficiency and m is the slope of the dilution curve.

2.5.3 DNA extraction

DNA was extracted using the QIAGEN® Blood and Cell Culture DNA kits (QIAGEN GmbH, Hilden, Germany) according to the manufacturer's instructions. This kit extracted and purified the DNA. The concentration and purity of DNA was determined by measuring the absorbance at 260 nm (A260) and 280 nm (A280) using a Nanodrop ND-1000 spectrophotometer (Nanodrop Technologies Inc., USA). A ratio of A260/A280 ≈ 1.8 is generally accepted as pure DNA.

2.5.4 RNA extraction and DNase treatment

Total RNA was extracted from cultured CDCs and rat whole heart tissue using Trizol reagent (Sigma) according to the manufacturer's instructions. DNase treatment was performed using Turbo DNA-free (Ambion) to degrade any DNA present. The concentration and purity of RNA was determined by measuring the absorbance at A260 and A280 using a Nanodrop ND-1000 spectrophotometer. A ratio of A260/A280 ≈ 2.0 is generally accepted as pure RNA.

2.5.5 Reverse transcription (complementary DNA synthesis)

Complementary DNA (cDNA) was synthesized from the RNA template using the AB high capacity transcriptase kit (Applied Biosystem). Every 1 ug RNA sample was

reverse transcribed using 1 µl reverse transcriptase, 2 µl random primer, 0.8 µl dNTPs (10 mM each), 2 µl buffer and topped up by RNase free water to a total volume of 20 µl. The reaction mixture was subjected to incubation for 10 mins at 25°C, 120 mins at 37°C and 5 secs at 85°C.

2.5.6 Conventional PCR

2.5.6.1 PCR amplification

PCR was used to amplify the specific genes of interest. The total volume of each PCR starting material was 50 µl. The PCR starting material was prepared by adding 5 µl REDTaq PCR reaction buffer (Sigma, UK), 2.5 µl REDTaq DNA Polymerase (Sigma, UK), 1 µl deoxynucleotide mix (Roche, UK), 1 µl forward primer, l µl reverse primer, 1 µl cDNA template and topped up with 38.5 µl of distilled water (ddH2O). The PCR program was set up with an initial heat activation step at 94°C for 30 secs. Then, 25 cycles of thermocycling were performed with a denaturation step at 94°C for 15 secs; an annealing step at 60°C for 30 secs and an extension step at 72°C for 30 secs. The final extension temperature was 72ºC for 7 mins and finally the PCR products were held at 4ºC until next further analysis.

2.5.6.2 Evaluation of PCR products using 4% Agarose Gel Electrophoresis

After the PCR procedure, amplified PCR products were verified by running 4% agarose gel electrophoresis. The gel was prepared by dissolving 4 g agarose powder (Promega, USA) into 100 ml 1X TBE buffer (Appendix 5) with microwave heating for 3 mins. The boiling mixture was poured into a gel plate. A comb was quickly inserted in the gel plate and the gel was left for 30 mins at room temperature to solidify. The comb was then removed from the plate before use. 1X TBE buffer was loaded into the tank of a mini gel electrophoresis system (Labnet International Inc.) and the 4%

agarose gel was immersed in 1X TBE buffer. Each well of agarose gel was loaded with 25 µl of PCR product or 10 µl of 100 bp DNA ladder (Promega, Gene Ruler^{Tm}) and the gel was run at 100 volts for 45 mins. The gel was visualized by using Chemimager version 5.5 (Alpha Innotech Corporation) and the image of the gel was captured. PCR product bands were quantified using Un-Scan-It, Version 6.1 (Silk Scientific, USA).

2.5.7 Real time PCR

Real time PCR amplification was performed using the Applied Biosystems StepOnePlus Real-Time PCR System (AB International, CA). The real-time PCR mastermix was prepared by adding 10 µl AB Sybrgreen PCR mastermix (AB International, CA), 1 µl reverse primer, 1 µl forward primer, 1 µl cDNA and 7 µl distilled water. The total volume for each real-time PCR reaction was 20 µl. The PCR program was set up with an initial heat activation step at 95°C for 10 mins. Forty cycles of thermocycling were performed with a denaturation step at 95°C for 15 secs, an annealing step at 60°C for 30 secs and an extension step at 72°C for 30 secs. Fluorescence was measured at the end of each extension step.

After amplification, a melting curve was acquired by heating the product at 4°C/sec to 95°C, cooling it at 4°C/sec to 70°C, keeping it at 70°C for 20 secs, and then slowly heating it at 4°C/sec to 95°C. Fluorescence was measured through the slow heating phase. Melting curves were used to determine the specificity of PCR products.

2.5.7.1 qRT-PCR data analysis

Housekeeping genes were validated and qRT-PCR data normalization analysis method were developed (Appendix 8, manuscript submitted). All the real time PCR data in this study were analyzed as previously described (Appendix 8).

2.6 Western Blot

Whole tissue lysates and cell lysates were used in this study. A general description of the technique is outlined below, with variations for the specific proteins in Table 2.2.

2.6.1 Tissue lysate preparation

Rat hearts were excised and freeze-clamped in liquid nitrogen. Frozen tissue was crushed using a pestle and mortar. A 50 mg sample was added to 500 µl of lysis buffer containing protease inhibitor (Appendix 5). The sample was homogenized using a Polytron homogenizer for 30 secs. The lysates were boiled for 5 mins and centrifuged at 13,000 rpm, 4 °C for 5 mins. An aliquot of 20 µl was taken for determination of protein concentration using a BCA protein assay kit (Thermo Scientific, USA) while the remaining supernatant was stored at -80 °C.

2.6.2 Cell lysate preparation

Culture medium was removed from the tissue culture flask and 1 ml lysis buffer per T75 flask was added. The flask was incubated on ice for 10 min. Lysate was removed, boiled for 5 mins and centrifuged at 13,000 rpm, 4 °C for 5 mins. An aliquot of 20 µl was taken for determination of protein concentration using a BCA protein assay kit (Thermo Scientific, USA) while the remaining supernatant was stored at -80 °C.

2.6.3 Polyacrylamide gel electrophoresis and protein transfer

Lysate solutions were diluted to (50 µg/µl) following the protein assay. For every sample, 35 µl of diluted lysates with 5% beta-mercaptoethanol (v/v) (Bio-rad Laboratories, UK) were loaded onto 10% polyacrylamide gel and run at 120 V for approximately 2 hours. The proteins were then transferred to nitrocellulose membranes (Pall Corporation) using a semi-dry transfer cell (Bio-rad Laboratories, UK) at 0.07 mA per gel for 1 hour.

2.6.4 Immunoblotting, detection and band quantification

After protein transfer, the nitrocellulose membrane was washed with TBS-Tween (Appendix 5) and blocked in 12.5 ml of 5% (w/v) dried milk in TBS-Tween for 1 hour. The membrane was washed with TBS-Tween for 1 hour, with the solution changed every 10 min. The specific primary antibody (Table 2.1) was diluted in 5% milk in TBS-Tween and incubated on the membrane at 4°C overnight. The membrane was washed with TBS-Tween for an hour, with the solution changed every 10 min. The appropriate horseradish peroxidase-conjugated secondary antibody (Table 2.1) (Santa Cruz, USA) was diluted in 5% milk in TBS-Tween and incubated on the membrane for an hour. The membrane was again washed for an hour, with the solution changed every 10 min. After washing, the membrane was covered with ECL Western blotting detection solution (GE Healthcare, Amersham) and sandwiched between two sheets of acetate. Photographic film was then placed on top of the blots in a dark room, and left for varying time periods before being developed (Compact X4 automatic X-ray film developer, X-ograph Imaging Systems). Protein bands were quantified using Un-Scan-It, Version 6.1 (Silk Scientific, USA).

Table 2.1 Primary antibodies and incubation time for immunoblotting

Primary antibody	**Primary antibody supplier**	**Dilution**	**Secondary antibody**	**Dilution**
Rabbit anti-HIF-1α	Novus, NB100-479	1:2000	Goat anti-rabbit	1:2000
Rabbit anti-glucose transporter-1 (GLUT-1)	Abcam, AB652	1:2000	Goat anti-rabbit	1:1000
Rabbit anti-glucose transporter-1 (GLUT-4)	Gift: G. Holman, University of Bath, UK	1:4000	Goat anti-rabbit	1:2000
Rabbit anti-citrate synthase	Apha Diagnostic, CISY11-A	1:2000	Goat anti-rabbit	1:2000

2.7 Enzyme-linked immunosorbent assay (ELISA) for VEGF

Cell culture medium was collected after the experiment and the protein concentration of the medium was determined using a BCA protein assay kit (Thermo Scientific, USA). A 96-well plate was coated with 100 µl/well VEGF capture antibody (R&D System, UK) overnight. An ELISA assay was performed according to the manufacturer's instruction.

2.8 Clarke-type oxygen electrode

Cell oxygen consumption rates of were measured using a Clark-type oxygen electrode (Strathekelvin Instrument, Scotland) (assisted by Lucy Ambrose). Two million cells were suspended in 500 µl respiratory medium (Appendix 6) and incubated in a stirred chamber at 30°C. Respiration was measured under basal unstimulated conditions for 5 mins, following by the addition of substrates, pyruvate and malate, the ATP synthase inhibitor, oligomycin, and the metabolic uncoupler, carbonyl cyanide p-(trifluoromethoxy) phenylhydrazone (FCCP). Table 2.2 lists the concentration, volume and incubation time required for each solution. Cell oxygen consumption rates in each solution were traced and recorded. Traces were then analyzed using Strathekelvin 782 Oxygen System v3.0 software.

Table 2.2 Concentration, volume and incubation time for each solution used in Clarke-type oxygen electrode measurement of cellular oxygen consumption rates

Solution	Concentration	Volume	Incubation time
Pyruvate	10 mM	5 µl	3 min
Malate	5 mM	5 µl	3 min
Oligomycin	2 mM	1 µl	1 min
FCCP	10 mM	10 µl	3 min

Abbreviations: FCCP = carbonyl cyanide p-(trifluoromethoxy) phenylhydrazone

2.9 Glucose uptake and lactate metabolism

The glucose and lactate levels were determined using the ABX Pentra 400 Chemistry Analyzer (Horiba Ltd., USA), an automated analyzer for *in vitro* diagnostic of a wide range of chemical compounds. To run this assay, cell culture medium was collected after the experiment and ran through ABX Pentra with glucose reagent (A11A01668, Horiba Ltd.) and lactate reagent (A11A01721, Horiba Ltd.). These reagents bound to the glucose and lactate molecules present in the medium, respectively, and fluoresced. The analyzer detected the signal and analyzed the concentration of glucose and lactate (performed by Emma E. Carter).

2.10 Statistical analysis

Data obtained were expressed as mean ± standard error of the mean (SEM). All statistical analysis was performed using Excel and SPSS software. The statistical differences of measurement made in the same animals were analysed using a paired T-test, whereas multiple comparisons between groups were analysed using a one-way analysis of variance (ANOVA). Repeated Measures ANOVE was performed to compare curves. Tukey post hoc test was used to analyse statistical difference between groups or curves. A value of $p < 0.05$ was considered statistically significant.

Chapter 3

Cardiosphere-derived cells for infarcted rat hearts

3.1 Abstract

Resident cardiac stem cells (CSCs) are found in the heart, and can be isolated and expanded *in vitro* via the formation of cardiospheres (Csp) to give cardiosphere-derived cells (CDCs). Administration of CDCs to the infarcted heart improves cardiac function in rodents [108], however, a full understanding of the mechanism by which CDCs act in the infarcted myocardium is not known. One of the objectives of this work was to isolate, and characterize CDCs from neonatal rat heart. The second aim was to assess the changes in function and morphology in infarcted rat hearts after CDC therapy. CDCs contained pluripotent cells expressing markers such as Oct-4, Sox 2, Klf-4 and Nanog and some cells expressing early cardiac specific differentiation genes such as Nkx 2.5 and GATA 4. CD90 mRNA expression in CDCs was 14-fold higher than in neonatal rat heart, while CD105 and c-Kit mRNA expression were 42% and 4.1% of that in neonatal heart, respectively, suggesting that CDCs were a heterogenous population resembling a more $CD90^+$ $CD105^+$ mesenchymal cell phenotype. Adipogenesis and cardiomyocyte differentiation were induced in passage 2 CDCs to test their differentiation potential. Approximately 30% of the cells transdifferentiated into adipocytes, while Nkx 2.5, troponin T and myosin heavy chain were upregulated in cells differentiated towards cardiomyocytes compared with control. For the *in vivo* animal study, a total of 6 x 10^6 CDCs were administrated to infarcted rats (n = 7). CDC-treated and non-treated (control) infarcted rat hearts were assessed using *in vivo* magnetic resonance imaging (MRI) for up to 16-weeks. In CDC-treated hearts, the ejection fraction was 9% higher than a control infarcted rat heart after 6 weeks, an improvement in function that was maintained for 16 weeks. After 16 weeks, the hearts were isolated, cryosectioned and stained with alkaline phosphatase, Picro-sirius red and H&E (n = 5). A significant increase in capillary density (9.2%) and decrease in scar volume (33%) were found in CDC-treated hearts, compared with control infarct. However, there was no significant difference in the number of inflammatory cells between CDC-treated and non-treated hearts. A significant positive correlation (R^2 = 0.86) was achieved between the scar volume measured using *in vivo* MRI and *ex vivo* histology, suggesting that MRI can be used to monitor scar size non-invasively at multiple time points. In conclusion, transplantation of CDC, expressing stem cells markers improved cardiac function by reducing scar size and increasing capillary density.

3.2 Introduction

Cardiac stem cells (CSCs) were first identified within the heart in 2003 [86]. The presence of CSCs challenged the generally accepted paradigm that the heart is a postmitotic organ [5, 13]. Different approaches have been used to isolate CSCs from heart tissue. Hierlihy *et al.* were the first to isolate CSCs from the adult hearts, based on their ability to efflux Hoechst dye, yielding a putative progenitor side population (SP) cell with stem cell-like activity [88]. Others isolated CSCs based on a specific single cell marker, such as c-Kit [86] or Sca-1 [87, 151]. Both of these methods generated a homogenous cell population, which was capable of differentiating into cardiac myocytes [86-88]. Nonetheless, they generated relatively low number of CSCs, as only 1% of SP cells of all cells were found. Similarly, the c-Kit based isolation method was only able to provide one c-Kit^{+ve} cell for every 104 myocytes [97].

In 2004, Messina *et al.* developed a method to isolate CSCs from human and murine heart and expand them as cardiospheres [107]. These cardiosphere were clonogenic, expressed stem and endothelial progenitor cell antigens/markers, and appeared to have the properties of adult cardiac stem cells. The cardiospheres were expanded to obtain sufficient cardiosphere-derived cells (CDC) for transplantation [108]. Cardiospheres and CDCs derived from heart explant culture *in vitro* lead to myocardial regeneration and functional improvement when injected into the infarcted mouse heart [107, 108]. In this thesis, the potential of CDCs as a therapeutic tool for myocardial infarction was further investigated.

In spite of the information gleaned to date on isolating CDCs, a full understanding of the mechanism whereby CDCs regenerate infarcted myocardium is unknown. The observed improvement in function after transplantation of CDCs into the infarcted

mouse heart [107, 108], may result from stem cells differentiating into cardiomyocytes, secreting paracrine factors, or recruiting peripheral stem cells to the ischemic territory [152]. Therefore, one of the objectives in this study was to assess the changes in morphology and function of infarcted myocardium after delivery of CDCs. MRI was used as a non-invasive method to assess heart function *in vivo*, whereas histological staining was used to assess myocardial morphology and cellular changes *ex vivo*. A combination of these two techniques provided a detailed insight into the mechanism of CDC repair of the infarcted myocardium at a cellular level [153].

The aims of this study were to:

- Isolate and expand CDCs from neonatal rat hearts.
- Characterize the mRNA expression profile of CDCs.
- Induce adipogenesis and cardiomyocyte differentiation of CDCs.
- Assess the functional and morphological changes after myocardial infarction and CDC therapy using histology. Compare histological data with MRI measurements of morphology to confirm the MRI results.

3.3 Methods

3.3.1 Isolation, expansion and characterization of cardiosphere-derived cells

Neonatal Sprague Dawley (SD) rat hearts were excised, minced and plated to give explant-derived cells (EDCs). Cardiosphere-derived cells (CDCs) were generated from EDCs according to Smith's protocol [108] (Chapter 2). All experiments in this chapter used CDCs at passage 2 (P2), unless otherwise stated. Genotypic characterization of CDCs was assessed using reverse transcriptase PCR (RT-PCR) and quantitative (real time) reverse transcriptase PCR (qRT-PCR). Specific cardiac stem cell markers (c-Kit), pluripotent stem cell markers (Oct-4, Sox 2, Klf-4, and Nanog), cardiac differentiation transcription factors (Nkx 2.5 and GATA 4), matured cardiomyocyte markers (Troponin T and myosin heavy chain) and mesenchymal stem cell markers (CD90 and CD105) (see Appendix 4 for primer sequences) were investigated. All RT-PCR data were normalized to GAPDH as the reference gene while, all qRT-PCR data were normalized to GAPDH as the reference gene and neonatal rat whole heart total RNA as the control samples. The differentiation potential of CDCs was determined using adipogenesis induction medium with 1-methyl-3-isobutylxanthine, dexamathasone and indomethacin (Appendix 2) or cardiomyocyte differentiation medium with 5-azacytidine (5-Aza) or dimethyl sulfoxide (DMSO) (Appendix 3).

3.3.2 Animal study design

The *in vivo* animal study in this chapter was performed in collaboration with other researchers in the group. Specific experimental methodologies are described below.

3.3.3 Myocardial infarction and CDC administration

Female Sprague-Dawley (SD) rats were used in this study. The left anterior descending coronary artery was occluded to induce myocardial infarction, with reperfusion of the artery after 50 mins. For the CDC-treated group (n = 7), 2 X 10^6 CDCs were injected

10 mins after infarction and another 4 X 10^6 CDCs were infused via the tail vein 2 days later. For the control group (n = 7), the culture medium (CEM) was injected. In sham operated animals (n = 4), the thoracotamy was performed, but no stitch was placed in the heart, and the chest was closed. Cardiac function and morphology were assessed using magnetic resonance imaging (MRI) (Appendix 7) for up to 16 weeks (work done by Dr Carolyn Carr, Dr. Daniel Stuckey and Dr. Jun Jie Tan).

3.3.4 Tissue preparation

At the end of the study, the animals were sacrificed and the hearts were excised. Rat hearts were cut in half transversely and embedded in Tissue-tek optimal temperature cutting (OCT) compound and frozen over dry ice. The tissue blocks were stored at -80˚C.

3.3.5 Frozen section

Tissue blocks were sliced into sections of 10 µm in thickness using a cryostat at -20˚C. Tissue slices were selected to correlate with the MRI slices (Figure 3.1). Using the apex of the heart as reference point, the heart block was moved forward 1400 µm to the start position. Twenty slices of 10 µm were taken, the block was moved forward 550 µm and twenty slices of 10 µm were taken. This step was repeated until the end of the tissue block was reached. For the basal slices, the top of the heart tissue was used as the reference point. The block was sliced until the left ventricle became apparent. Then, twenty slices of 10 µm were taken, the block was moved forward 550 µm and twenty slices of 10 µm were taken. This step was repeated until the end of the tissue block was reached. This sectioning resulted in sections from approximately 8 positions from the apex and 8 from the base. All the slides were air dried at room temperature for 1 hour, and then were kept at -20˚C until used.

Figure 3.1 *MRI image of rat heart. Red lines indicate the position for tissue slicing, each slice is approximately 200 μm width. 14 to 16 slices acquired from each heart.*

3.3.6 Immunohistochemistry and immunocytochemsitry

3.3.6.1 Tissue and cell fixation

Tissue sections or CDCs (grown on a Nunc Lab-Tek® 4-well chamber slide precoated with 10 μg/ml fibronectin) were fixed with 4% paraformaldehyde (Sigma, UK) on ice for 15 mins and then washed with washing buffer (PBS with 0.1% Tween) 5 times, with washing buffer changed every 2 mins. After washing, tissue sections or CDC slides were blocked with 10% donkey serum (Biosera, UK) in 0.1% PBS-tween for an hour at room temperature.

3.3.6.2 Primary antibody staining

Blocking solution was aspirated and the fixed tissue or cells were incubated with the primary antibody (Table 3.1) diluted in PBS, overnight at 4^{o}C in a humidified chamber. Tissue sections or cell slides were washed 5 times for 2 mins each with washing buffer. The appropriate secondary antibodies (Table 3.1) were added to tissue sections or cell slides and were incubated at 37^{o}C for an hour. Tissue sections or cell slides were washed as before. Slides were mounted by putting 1 drop of VectaShield

hardest mounting medium with DAPI (Vector laboratories, UK) on each tissue section or cell slide and covering the sample with a coverslip. Slides were kept at 4°C, protected from sunlight, until further analysis using confocal microscopy (Zeiss LSM510) (cardiac troponin and GFP immunostaining, confocal microscopy and confocal image analysis were by Dr. Georgina Ellison, Dr. Jun Jie Tan and Dr. Renata S. M. Gomes).

Table 3.1 *Primary antibodies and incubation time for immonohistochemistry*

Primary antibody	Manufacture	Dilution	Secondary antibody	Dilution
Cardiac troponin T (Tnnt)	Ab10214, Abcam, UK	1:100	donkey anti mouse lgG-FITC (AF488)	1:1000
Cardiac troponin I (cTnI)	SC-15368, Santa Cruz, USA	1:100	donkey anti rabbit lgG-FITC (AF488)	1:1000
GFP	Ab290, Abcam, UK	1:50	donkey anti rabbit lgG-FITC (AF488)	1:1000
Integrin αX (CD11c)	SC-26692, Santa Cruz, USA	1:200	donkey anti goat lgG-FITC (AF488)	1:1000

3.3.7 Histology

3.3.7.1 Haematoxylin and eosin (H&E) staining

Sections were fixed in acetic alcohol (3% acetic acid in 95% methanol) for 1 min. Fixed sections were washed in running tap water and then stained in haematoxylin for 10 mins. Sections were washed in running tap water until it ran clear, then dipped in differentiation solution (1% HCl in 70% ethanol) and washed again in running tap water. Sections were ‘blued’ in Scotts tap water substitute for 30 secs, washed in running tap water and stained in filtered Eosin for 2 mins. Sections were then rinsed in

water and dehydrated through serial alcohols (70%, 95%, 100%). After complete dehydration, sections were taken through xylene baths and a coverslip was applied with DPX mounting medium. Haematoxylin stained cell nuclei purple/black, whereas eosin stained most components of the cell cytoplasm pink/red. The amount of positive staining was quantified using ImagePro analysis software on three specific regions, the infarct, peri-infarct and remote area. In each region, 2 to 3 digital images of H&E stained sections were taken from 14 to 16 fields (14 to 16 tissue sections from base to apex, Section 2.8) at 10X magnification. All acquired images were of 744 X 560 pixels in an area measuring 690 X 520 μm.

3.3.7.2 Picro-sirius red staining

Sirius red stain was prepared by dissolving 0.5 g of powdered direct red 80 (Sigma, UK) in 45 ml distilled water. Ethanol (50 ml; 99%) was added, followed by 1 ml of 1% sodium hydroxide. Drops of 20% sodium chloride were slowly added until a slight precipitate persisted. The mixture was left overnight and filtered before use. Sections were fixed in acid alcohol (1% HCl in 70% ethanol) for 5 mins. Fixed sections were washed in acid water (0.5% acetic acid) for 1 min before staining in picro-sirius red (10% sirius red stain in a saturated picric acid solution) for 30 mins. Sections were then washed in acid water for 1 min twice and dehydrated through serial alcohols (70%, 95%, 100%). After complete dehydration, sections were taken through xylene baths and a coverslip was applied with DPX mounting medium. Cytoplasm stained yellow whereas collagen fibers stained red by Picro-Sirius red stain. Digitized images of picro-sirius red-stained tissue sections were taken and arranged from base to apex. All the acquired images were of 520 X 520 pixels in an area measuring 1.35 X 1.35 cm. The amount of positive staining was quantified using ImagePro image analysis software.

3.3.7.3 Alkaline phosphatase staining

Sections were fixed in acetone for 5 mins. Slides were allowed to air dry at room temperature. 5-Bromo-4-chloro-3-indolyl phosphate and nitroblue-tetrazolium (BCIP/NBT kit, Vector Labs) was used to stain capillaries black. BCIP/NBT substrate working solution was prepared by adding 2 drops of Reagent 1 into 5 ml of 100 mM Tris-HCl buffer (pH 9.5). The mixture was mixed well before 2 drops of each of Reagent 2 and Reagent 3 were added. BCIP/NBT solution was prepared freshly. Tissue sections were incubated with BCIP/NBT solution at room temperature for 25 mins in a tray to avoid light affecting the quality of the stain. Sections were rinsed with distilled water for 2 mins. This step was repeated 3 times. Then the slides were mounted directly with aqueous mounting medium (Vecta Mount AQ) immediately before use. Alkaline phosphatase stained blood vessels black. The amount of positive staining was quantified using ImagePro image analysis software on three specific regions, the infarct, peri-infarct and remote area. In each region, 2 to 3 digital images of stained sections were taken from 14 to 16 fields (14 to 16 tissue sections from base to apex, Section 2.8) at 10X magnification. All acquired images were of 744 X 560 pixels in an area measuring 690 X 520 μm.

3.4 Results

3.4.1 Cardiac stem cell isolation and expansion

3.4.1.1 Explant-derived cells (EDC)

SD-GFP neonatal rat heart (0.07 to 0.10 g) was explanted into 6 fibronectin-coated dishes. Explants adhered well to the fibronectin and generated a layer of thin, flat fibroblast-like cells after 1-2 days (Figure 3.2a). Round phase bright cells were observed growing out from the explants and migrated over this fibroblast-like cell layer after 4 days (Figure 3.2b). One neonatal rat heart generated approximately 1 x 10^6 explant-derived cells (EDCs) after 7 days. The explants could be harvested up to 3 times with an interval of 1 week between each harvest.

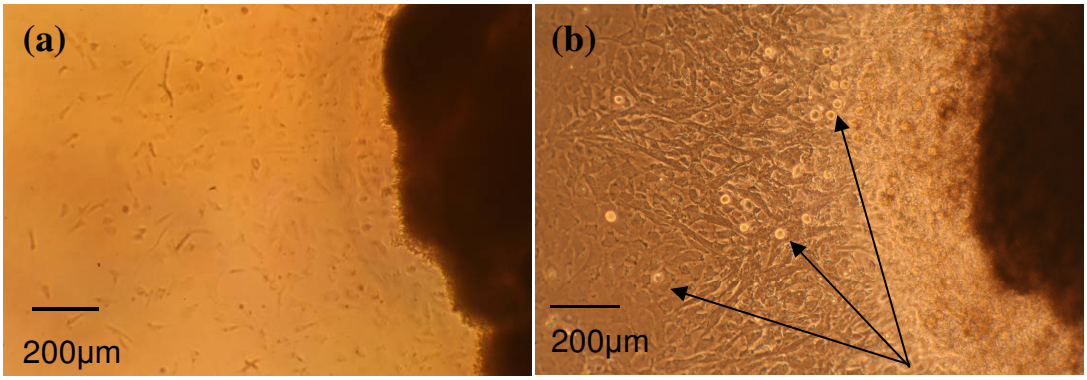

Figure 3.2 *Explant derived cells. (a) fibroblast-like cells generated after 2 days (b) round phase bright cells grew on top of the fibroblast layer after 4 days.*

3.4.1.2 Cardiosphere and cardiosphere-derived cells (CDC)

EDCs were allowed to grow on poly-D-lysine–coated 24-well plates with CGM (Appendix 1). Cardiospheres, spherical clusters of cells, with an average size of 80-100 μm, formed after 2 days of incubation (Figure 3.3). Approximately 400 cardiospheres were obtained from each well of a 24-well plate after 4 days of incubation.

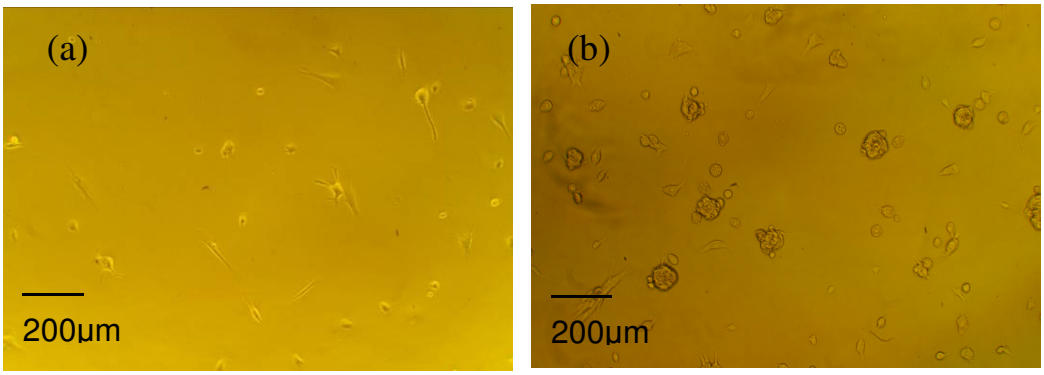

Figure 3.3 *Cardisopheres: (a) after 24 hours, (b) after 4 days*

Cardiospheres loosely adhered to the culture surface or remained in suspension and thus could easily be isolated by pipetting and replating into a T75 flask for expansion. Isolated cardiospheres were cultured in CEM (Appendix 1) and formed cardiosphere-derived cells (CDCs) after 3-4 days of incubation. CDCs reached 80-90% confluency within 5 to 7 days and were subsequently passaged in the ratio 1:2 for further expansion up to passage 2 (Figure 3.4). A total of approximately 2 x 10^7 CDCs were obtained from each neonatal heart at the end of passage 2.

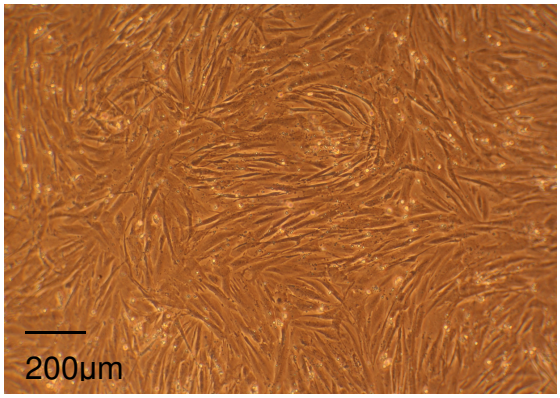

Figure 3.4 *Passage 2 cardiosphere-derived cells*

3.4.2 Characterization of CDCs

3.4.2.1 RNA isolation and cDNA synthesis

Total RNA was isolated from passage 2 CDC and neonatal heart tissue lysates. The purity of total RNA was verified using a Nanodrop ND-100 spectrophometer (Nanodrop Technologies Inc, USA) and showed a ratio of A260/A280 ≈ 2.0, indicating pure RNA.

cDNA was synthesized using reverse transcriptase enzyme with pure RNA as the template. The purity of cDNA was enhanced by running DNase treatment before the cDNA synthesis procedure. All synthesized DNA showed a ratio of A260/A280 ≈ 1.8 which indicated pure cDNA.

3.4.2.2 Efficiency and specificity of target specific primers

A total of 11 pairs of primer sequences were designed for RT-PCR and qRT-PCR analysis of selected target genes. Glyceraldehyde 3-phosphate dehydrogenase (GAPDH) was used as the housekeeping gene because this gene has been shown to be the most consistently expressed gene in P2 CDCs among all 6 genes under investigation (Appendix 8, manuscript submitted). To test the primer efficiency, a series of 2-fold dilutions of cDNA were amplified with consistent concentration and primer amplification efficiency, E, was calculated as $E = (\exp^{-1/m} - 1) \times 100\%$ where m is the slope of the linear dilution plot dilution curve. For example, the linear regression plot for GAPDH primer is shown in Figure 3.5.

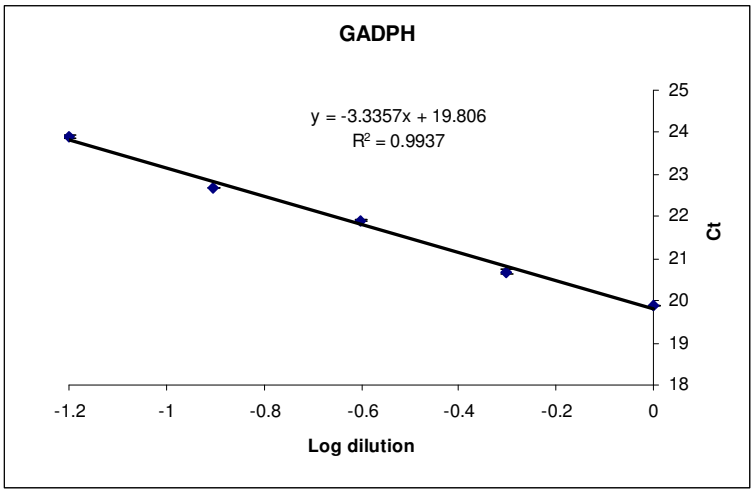

Figure 3.5 *Linear regression plot (Ct value against log cDNA dilution) for GAPDH primer efficiency (n = 4). Y=mX + C, m = slope of the linear regression plot; R^2= correlation coefficient.*

Correlation coefficients (R^2) for all primers ranged from 0.90 to 0.99 and efficiencies for all primers ranged from 91% to 110%. This indicates that all the designed primers worked successfully and gave consistent results throughout efficiency testing (Table 3.2).

Table 3.2 *Primer efficiency*

Primer / Gene	**Slope of the linear regression plot (m)**	**Primer efficiency**, $E = (\exp^{-1/m} - 1) \times 100\%$	**Correlation coefficient (R^2)**
GAPDH	-3.34	99%	0.99
c-Kit	-3.28	102%	0.95
Oct 3/4	-3.32	100%	1.00
Sox 2	-3.70	86%	0.99
Klf-4	-3.37	98%	0.99
Nanog	-3.10	110%	0.99
Nkx 2.5	-3.38	98%	0.98
GATA 4	-3.49	93%	0.90
Tnnt	-3.57	91%	1.00
MyHC	-3.50	93%	0.99
CD105	-3.42	96%	0.98
CD90	-3.11	110%	0.95

Amplified products were dissociated after the qRT-PCR. All primers showed only one peak in the dissociation curve (melt curve). This indicates the specificity of the primer amplification function. The melt curve for GAPDH is shown in Figure 3.6.

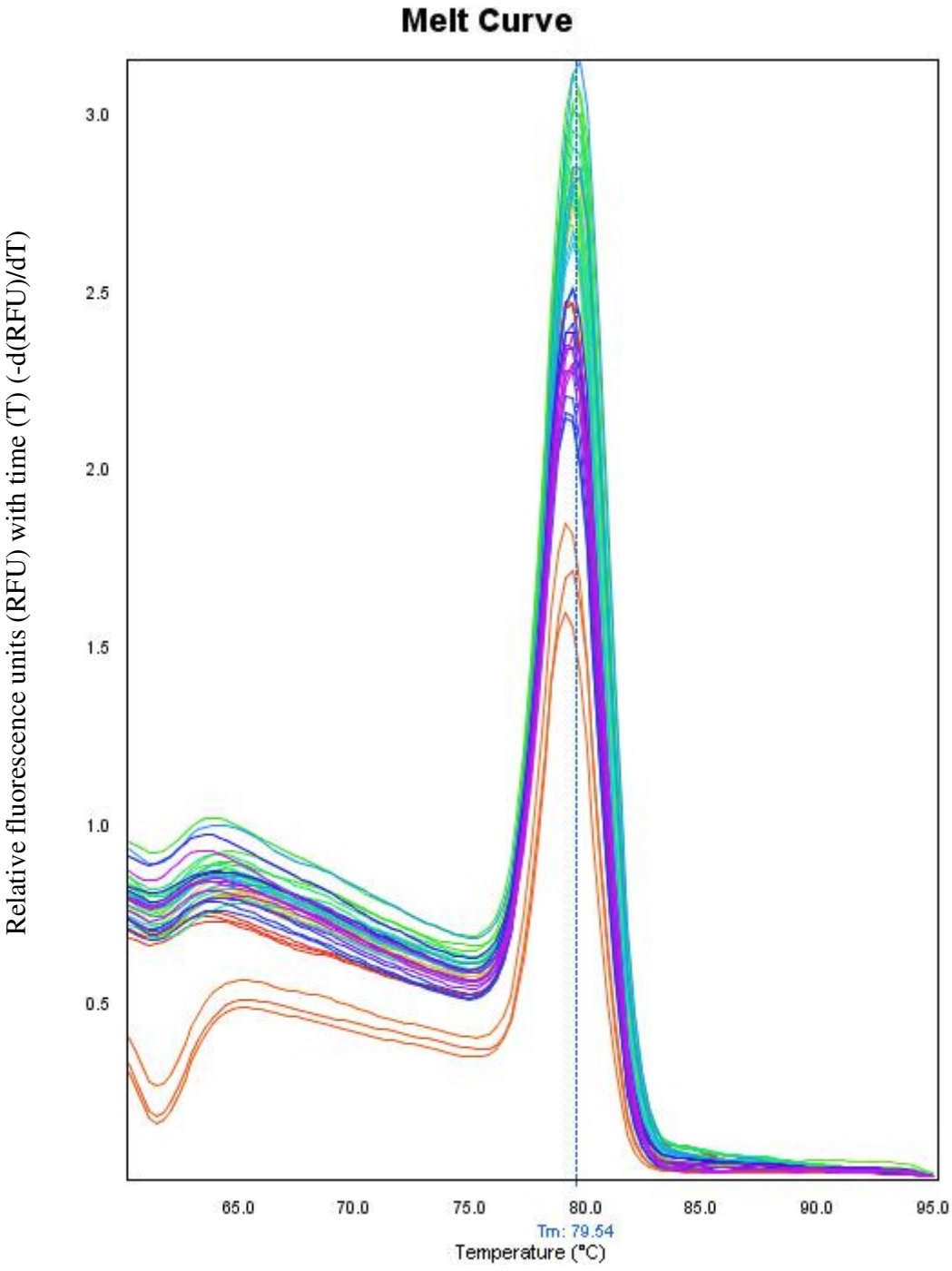

Figure 3.6 *Melt (or dissociation) curve for primer GAPDH.*

3.4.2.3 CDCs expressed pluripotent stem cell and cardiac differentiation markers

Conventional RT-PCR revealed that P2 CDCs isolated from 1 or 2 day old neonatal wild type SD rat hearts represented a mixed cell population consisting of cardiac stem cells and progenitor cells expressing c-kit, Oct-4, Klf4 Sox2 and Nanog; cardiac differentiating cells (Nkx 2.5 and GATA 4) with weak expression of mature cardiomyocyte markers (Tnnt and MyHC); and mesenchymal cells (CD90 and CD105) (Figure 3.7).

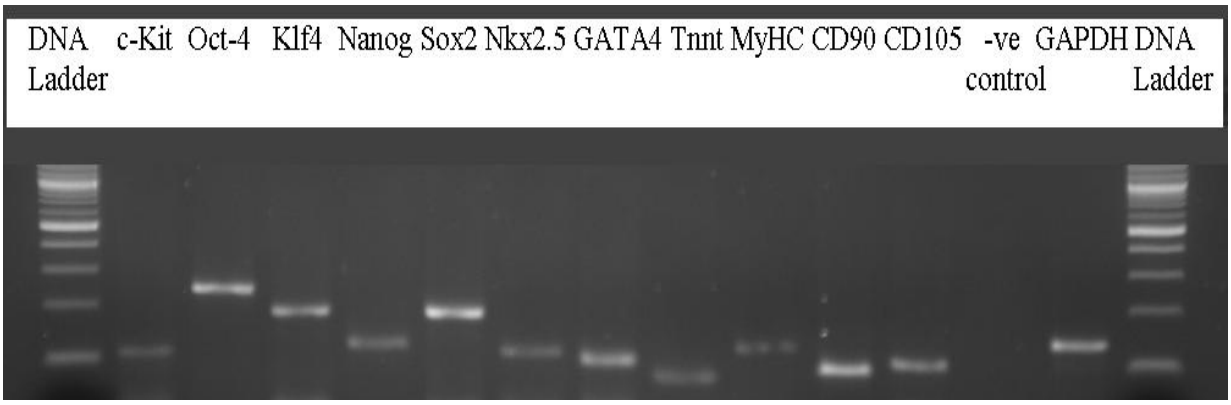

Fig. 3.7 *Representative gel electrophoresis image (of three independent experiments) of RT-PCR characterization of neonatal P2 CDCs. GAPDH was used as housekeeping gene to validate the RNA extraction and cDNA synthesis procedure. -ve control = PCR amplification without cDNA template; DNA ladder = 100 bp DNA ladder (N3231S, BioLabs).*

3.4.2.4 CDCs comprised cardiac progenitor and mesenchymal cells

Using quantitative (real time) RT-PCR (qRT-PCR), relative mRNA levels of neonatal CDCs were compared to the rat heart total mRNA levels to determine the ratio of cardiac stem/progenitor cells isolated *in vitro* to the endogenous cardiac stem/progenitor cell population. qRT-PCR results showed that rat P2 CDCs expressed significantly lower c-Kit (4.1 ± 0.3%) and CD105 (42 ± 17%), compared with whole neonatal rat hearts (indicated as 100%), with very high expression of CD90 (14.1 ± 1.3-fold increase *vs.* neonatal rat heart) (Figure 3.8). These data indicated that P2 CDCs comprised c-Kit$^+$/CD105+ cardiac progenitor cells and CD90$^+$/CD105$^+$ cardiac mesenchymal cells, but the majority of CDCs had a CD90$^+$/CD105$^+$mesenchymal stem cell phenotype.

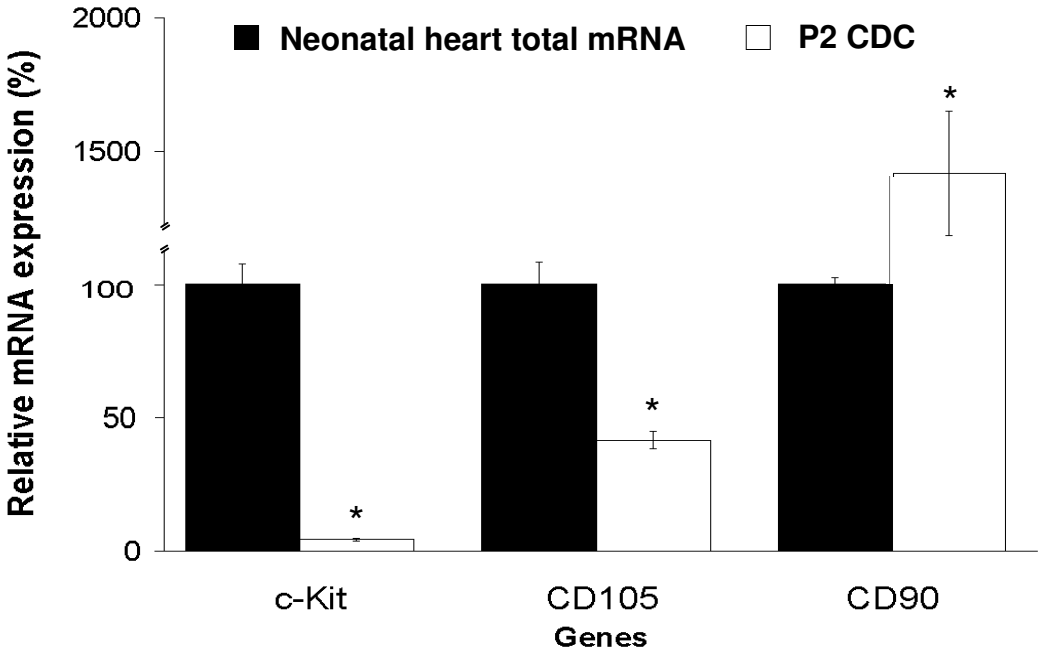

Figure 3.8 *The relative mRNA expression of c-Kit, CD105 and CD90 for neonatal P2 CDC (n = 4) using qRT-PCR. All values were normalized to GAPDH (housekeeping gene) and neonatal whole heart total mRNA (indicated as 100%). P2 CDC mRNA abundance was expressed relative to the neonatal rat heart.* $p < 0.01$ vs. neonatal whole heart total mRNA. Y axis scale is segmented for clarity.*

3.4.3 CDC functional studies (*in vitro*)

3.4.3.1 CDCs could be transdifferentiated into adipocytes

Approximately 30% of passage 2 CDCs stained red by Oil red O after 3 cycles of adipogenic induction medium (AIM) (Appendix 3). This showed that a portion of the CDCs were able to be transdifferentiated into adipocytes (Figure 3.9).

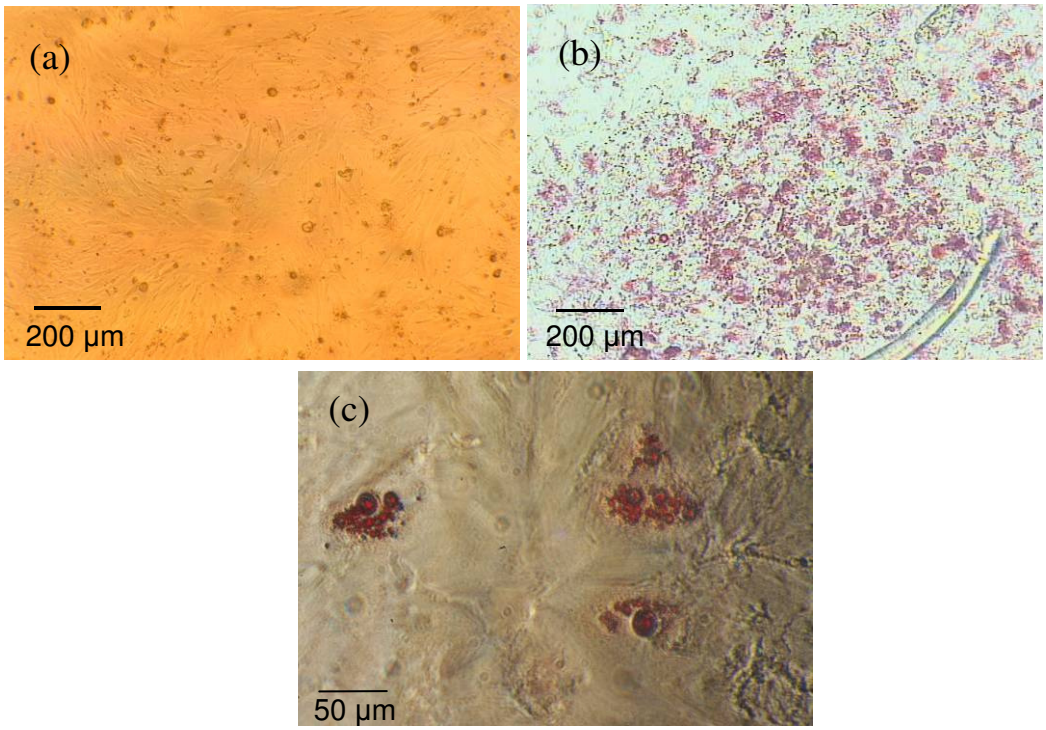

Figure 3.9 *Representative images (of four independent experiments) of (a) non-treated CDCs, (b) neonatal CDCs treated with 3 cycles of adipogenic induction medium resulted in differentiation into adipocytes, identified by staining with Oil red O, (10X magnification) and (c) Oil red O stained adipocytes (40X magnification).*

3.4.3.2 CDCs were capable of transdifferentiating into cardiomyocytes

The cardiomyogenic potential of neonatal P2 CDCs was tested *in vitro* over 2 weeks with cardiomyocyte differentiation medium (CDM) containing the cardiomyogenic inducers, 5-azacytidine (5-aza) or dimethyl sulfoxide (DMSO). Negative control cells were treated with complete explant medium (CEM), the basal culture medium for CDCs, for either 5 days or 2 weeks.

CDCs treated with CEM (Figure 3.11a), 5-aza (Figure 3.10b), or DMSO (Figure 3.10c), had a confluent morphology after 2 weeks, compared with normal CEM-treated CDCs at day 5 post plating (Figure 3.10d).

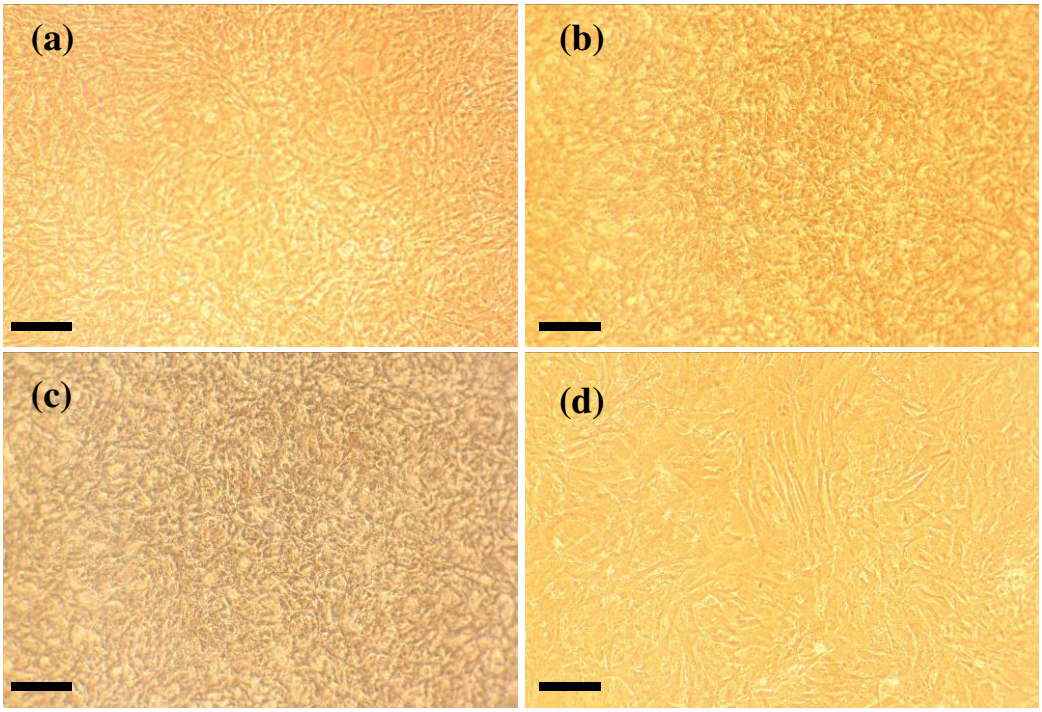

Figure 3.10 *Representative images (of three independent experiments) of cell morphology of P2 CDCs two weeks after treatment with (a) CEM, (b) 5-aza, (c) DMSO, compared with (d) P2 CDCs 5 days after treatment with CEM. Scale bars = 200 μm.*

Nkx 2.5 and Tnnt mRNA levels were significantly increased in neonatal CDCs treated with CEM for 2 weeks, compared with those treated with CEM for 5 days (Figure 3.11), indicating that CDCs have the potential to spontaneously differentiate into cardiomyocytes after 2 weeks in culture without passaging. For 5-Aza and DMSO treated CDCs, Nkx 2.5, Tnnt and MyHC mRNA levels were significantly increased, compared with CDCs treated with CEM for 5 days (Figure 3.11). In addition, Tnnt mRNA was significantly higher in CDCs treated with 5-aza and DMSO, compared to those treated with CEM for 2 weeks (Figure 3.11), indicating that although CDCs could spontaneously differentiate into cardiomyocytes, adding the cardiomyogenic inducers enhanced the differentiation potential.

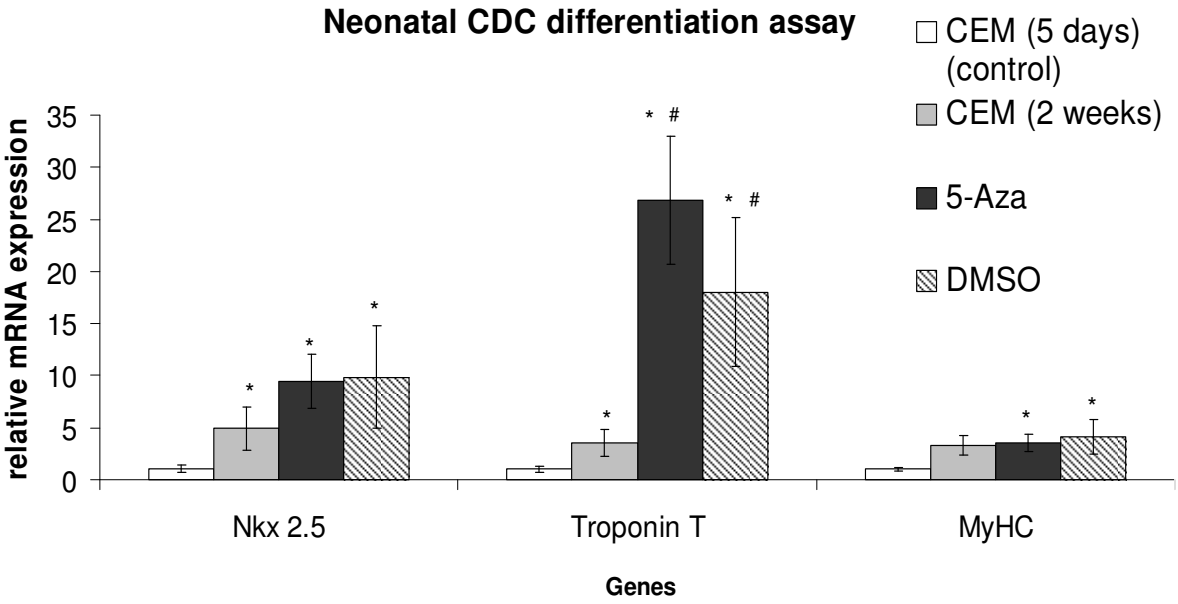

Figure 3.11 *The relative mRNA expression of Nkx 2.5, Tnnt and MyHC for neonatal P2 CDC (n=3) using qRT-PCR. All values were normalized to GAPDH (housekeeping gene) and CEM (5 days) (control). CEM (2 weeks), 5-Aza- and DMSO-treated CDC mRNA abundance was expressed relative to the control. * $p < 0.05$ vs. control; # $p < 0.05$ vs. CDCs treated with CEM (2 weeks).*

Immunocytochemistry for Tnnt also revealed that CDCs, at about 30-40% confluecy (3 days after plating), did not express Tnnt, while CDCs at over 90% confluency (2 weeks after plating) showed positive staining for Tnnt. This could be due to the cell-to-cell contact which induced the CDCs to initiate differentiation along the cardiomyocyte lineage. The Tnnt staining became more obvious and the structure of cardiomyocyte-like cells became organized after DMSO treatment, compared to non-treated cells after 2 weeks, validating the importance of DMSO in inducing cardiomyocyte differentiation (Figure 3.12). However, no beating cells were observed in any of these cultures. Negative control also was included in this experiment to validate the immunostaining data. No signal was detected on the negative control (data not shown).

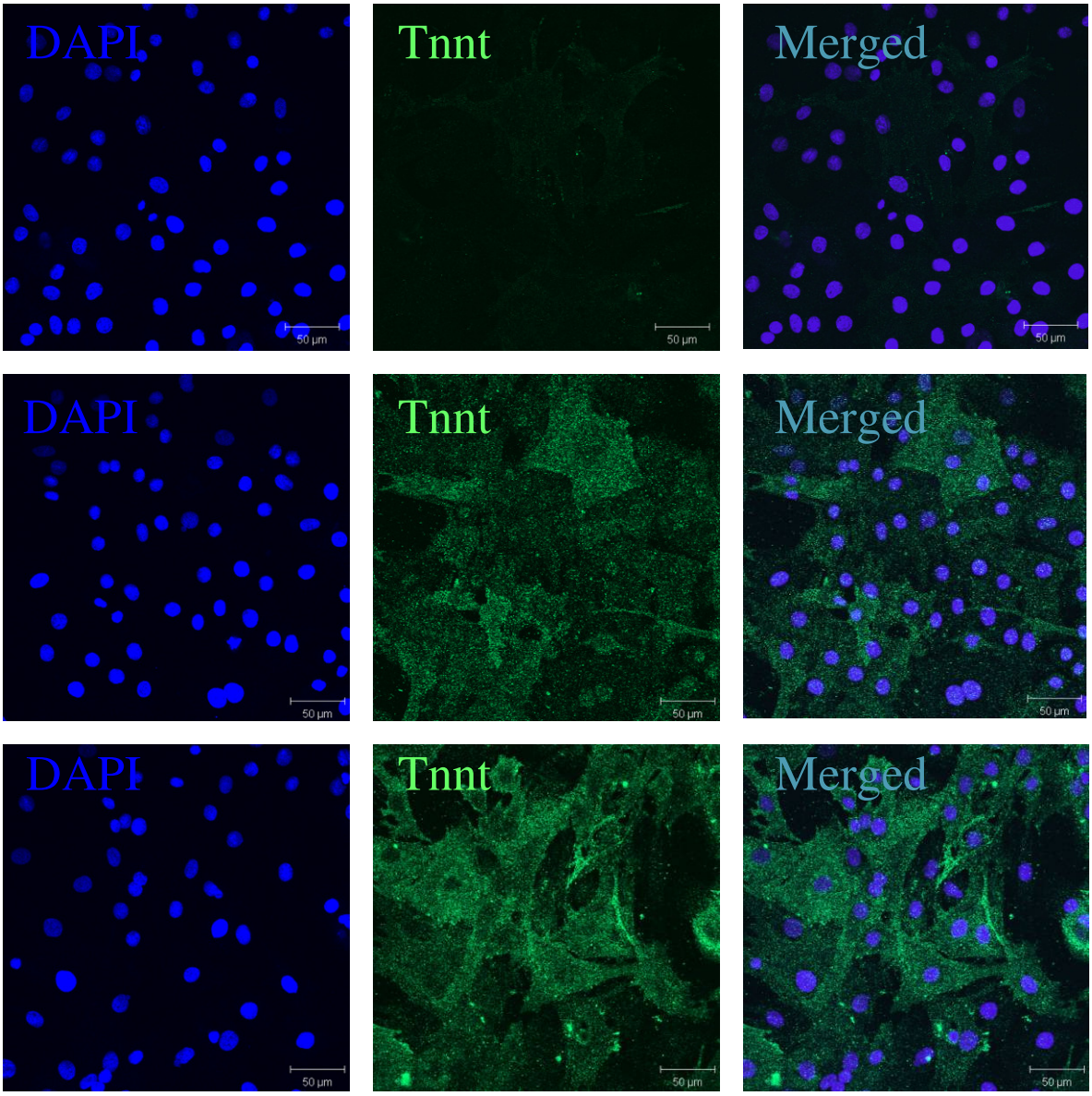

Figure 3.12 Cardiomyocyte differentiation of P2 CDCs. *Representative confocal images (of three independent experiments) of the DMSO differentiation protocol. Top panel: 30-40% confluent CDCs, middle panel: over 90% confluent CDCs, bottom panel: CDCs treated with DMSO over two weeks. At the end of the differentiation protocol, an equal number of cells (8 x 105 per chamber) of each condition were trypsinized and seeded on 4-well chamber slides coated with fibronectin (10 μg/ml) and stained with DAPI and Tnnt. Scale bars = 50 μm.*

3.4.4 CDC functional studies (*in vivo*)

To investigate the regenerative potential of CDCs *in vivo*, P2 CDCs generated from neonatal transgenic Sprague Dawley (SD-Tg(GFP)2BalRrrc) rats, which express the green fluorescent protein (GFP) gene, were administered to surgically infarcted female Sprague Dawley (SD) rats. Injected CDCs were labeled with fluorescent dye to assist the detection of the cells after injection. *In vivo* CDC cardiomyogenic differentiation was confirmed using immunohistochemical staining and heart function was measured using MRI over 16 weeks.

3.4.4.1 Detection of injected CDCs in infarcted myocardium after 16 weeks

P2 GFP-CDCs were labeled with bright green fluorescent micron-sized particles of iron oxide (MPIO) and red DiI cell tracker dye prior to administration into the infarcted rat heart. Sixteen weeks after injection, rat hearts were excised, sliced and counterstained with DAPI. MPIO and DiI fluorescent cells were detected in the infarcted myocardium under fluorescent microscope (Figure 3.13 a and b). This shows that the injected CDCs remained in the infarcted myocardium for 16 weeks after injection. Although green fluorescent GFP-CDCs were used in this study, the detection of GFP-CDCs directly under fluorescent microscope was not practical due to the natural autofluorescent of cardiac tissue. Therefore, GFP-CDCs were identified using specific GFP immunostaining (Figure 3.13c).

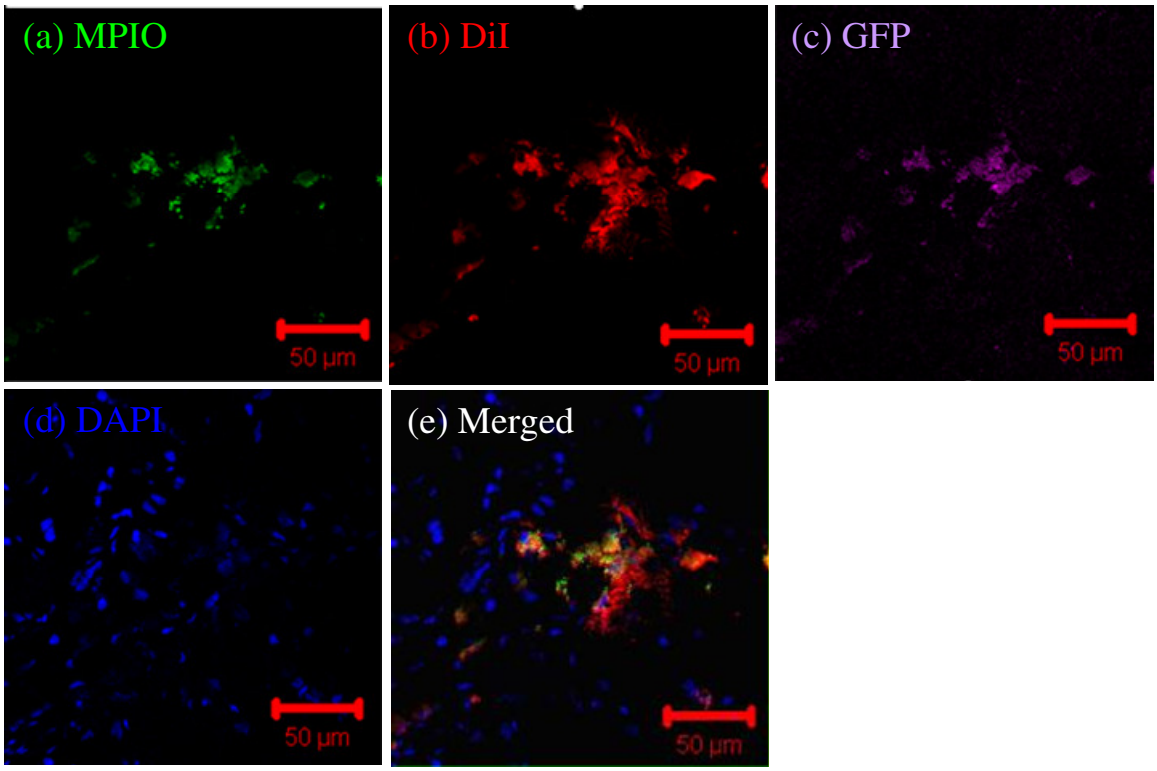

Figure 3.13 *Representative confocal images (of five independent experiments) of the CDCs labeled with (a) MPIO particles, (b) red DiI cell tracker dye and (c) GFP-immunostained CDCs were detected in infarcted rat heart tissue 16 weeks after injection. (d) Tissue was counterstained with DAPI which stains nuclei blue.*

3.4.4.2 In vivo CDC cardiomyocyte differentiation

Sixteen weeks after CDC injection, the rat hearts were excised, cryosectioned and stained with cardiac troponin I (cTnI) to detect *in vivo* CDC cardiomyocyte differentiation. Quantification of positive cTnI was from at least 10 representative fields from 3 CDC-treated hearts. About 49 ± 3% cells with MPIO and red DiI cell tracker dye were co-localized with cTnI staining (Figure 3.14), indicating that some portion of injected CDCs were retained in the infarcted myocardium and differentiated into cardiomyocytes 16 weeks after injection. Although green fluosrescent GFP-CDCs were used in this study, the detection of GFP-CDC was not practical due to the natural autoflurescent of cardiac tissue.

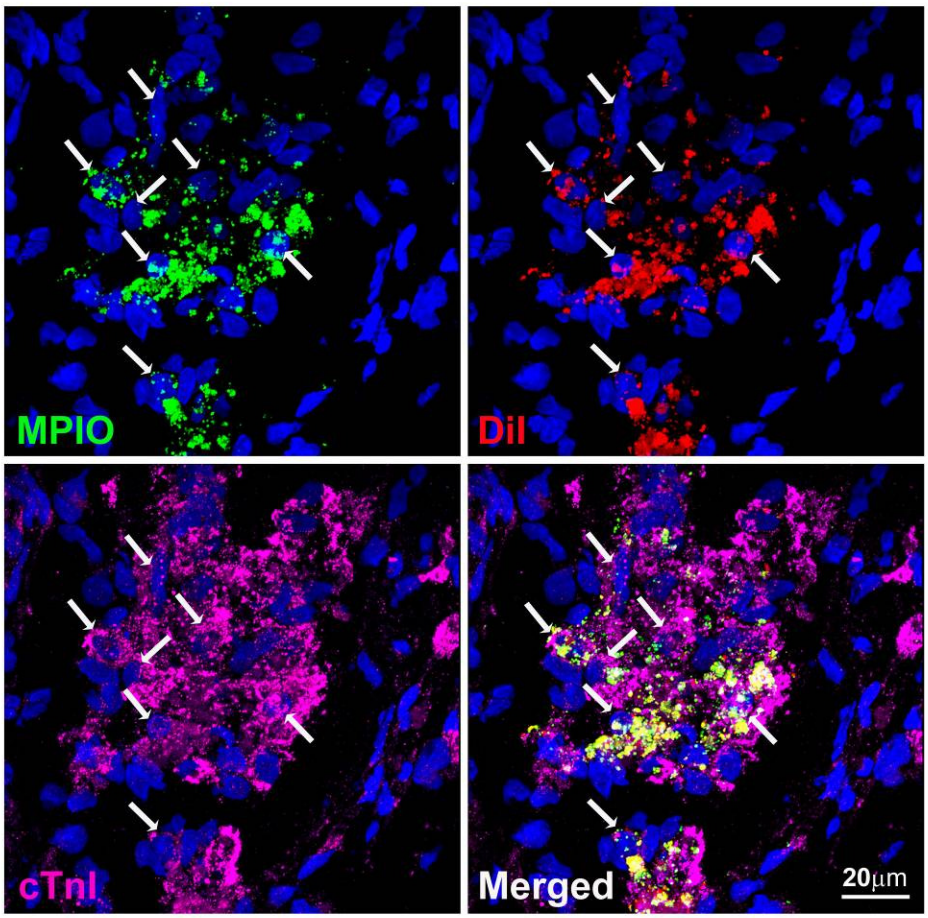

Figure 3.14 *In vivo CDC differentiation. Representative confocal images (of five independent experiments) of the infarct region of the CDC-treated rat heart showed that MPIO and DiI-labelled cells co-localised with cardiac troponin I staining, suggesting cardiomyogenic differentiation of transplanted CDCs in vivo.*

3.4.4.3 CDC transplantation increased infarcted heart function

Cine-MRI was used to measure cardiac function at baseline (2 days post MI) and at 2, 6, 10, 16 weeks after MI and the administration of CDCs. At baseline, there were no significant differences between control and CDC-treated hearts in ejection fraction (EF). However, after 2 weeks, a sharp fall in EF was observed in non-treated infarcted hearts (52 ± 2%) and CDC-treated infarcted hearts (55 ± 2%), but not in sham operated hearts (68 ± 1%). By 6 weeks, the EF in CDC-treated infarcted hearts was 9 ± 2% ($p < 0.05$) higher than that of the non-treated infarcted hearts, and the difference persisted for up to 16 weeks (Figure 3.15).

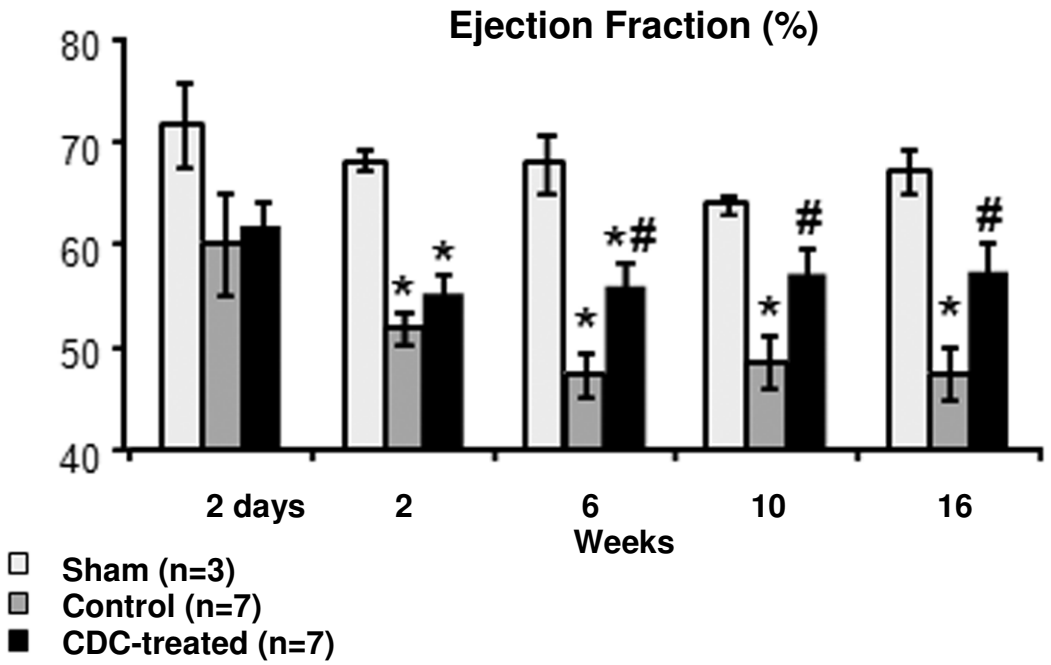

Figure 3.15 *Ejection fraction (EF) measured using cine-MRI. In sham operated animals (n=3), no significant changes in EF was observed over 16 weeks. By 6 weeks, a significant improvement in EF was found in CDC-treated hearts (n = 7) and maintained for 16 weeks, compared with the non-treated hearts (control) (n = 7). * P< 0.05 vs sham; # P< 0.05 vs control.*

3.4.5 CDC functional studies (ex vivo) - assessment of cardiac morphology using histology

Following MRI, hearts from a sub-set of non-treated and CDC-treated animals (n = 5 each group) were excised and cardiac morphology was assessed using histology.

3.4.5.1 Wavy fibers formed and inflammatory cells invaded after infarction

Haematoxylin and eosin (H&E) staining revealed the structure of cardiac tissue in all groups (Figure 3.16). Wavy fibers were found in the infarcted tissue due to the pull on the dead myocardium by live myocardium (Figure 3.16a). Contractile muscle cells were replaced by pale white collagen, forming the scar of the infarction. Moreover, the infarcted area was invaded by a high density of cells, indicated by the haematoxylin

stain which stained nucleic blue (Figure 3.16b), compared to non-infarcted area (Figure 3.16c). Soon after infarction, the interstitium at the margin of the infarcted area was initially infiltrated with neutrophils, then with lymphocytes and macrophages, which phagocytose myocyte debris [154]. Although it was not possible to specifically identify the cell types in the infarct region using this staining technique, the observed morphology suggested that most of the nuclei were inflammatory cells, further, immunohistochemistry using specific antibody for inflammatory cells was used to verify this hypothesis.

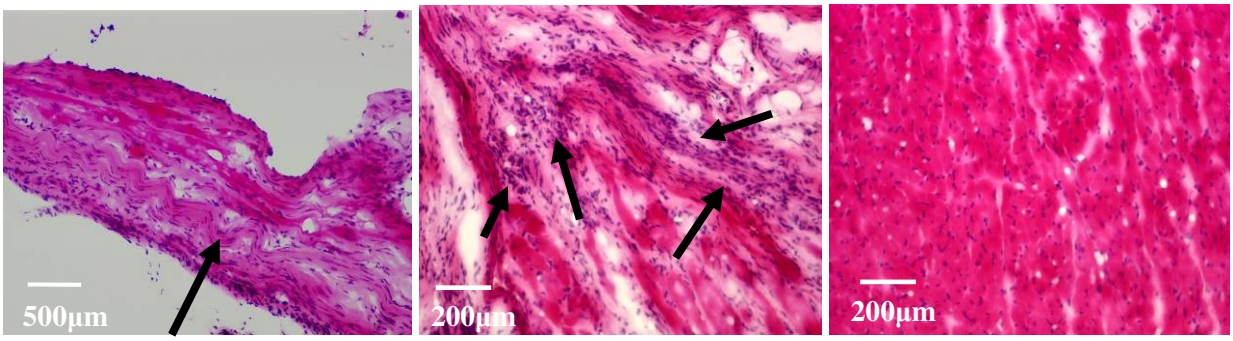

Figure 3.16 *Representative images (of five independent experiments) of rat heart tissue stained with haematoxylin and eosin. (a) Wavy fibers, 4X (marked with arrow) (b) pale white collegen scar and invading leukocytes, 10X (marked with arrow) and (c) normal healthy myocardium, 10X, for comparison.*

3.4.5.2 Identification of inflammatory cells using immunohistochemistry

In order to verify the cell types that invaded the infarcted area, tissue sections were stained with Integrin αX (CD11c). CD11c is a type I transmembrane protein found at high levels on several important inflammatory cell types such as monocytes, macrophages, neutrophils and some B cells. The confocal images showed positive staining in infarcted myocardium but not in healthy non-infarcted myocardium, confirming that the cells that invaded the infarcted myocardium were predominantly inflammatory cells expressing CD11c (Figure 3.17).

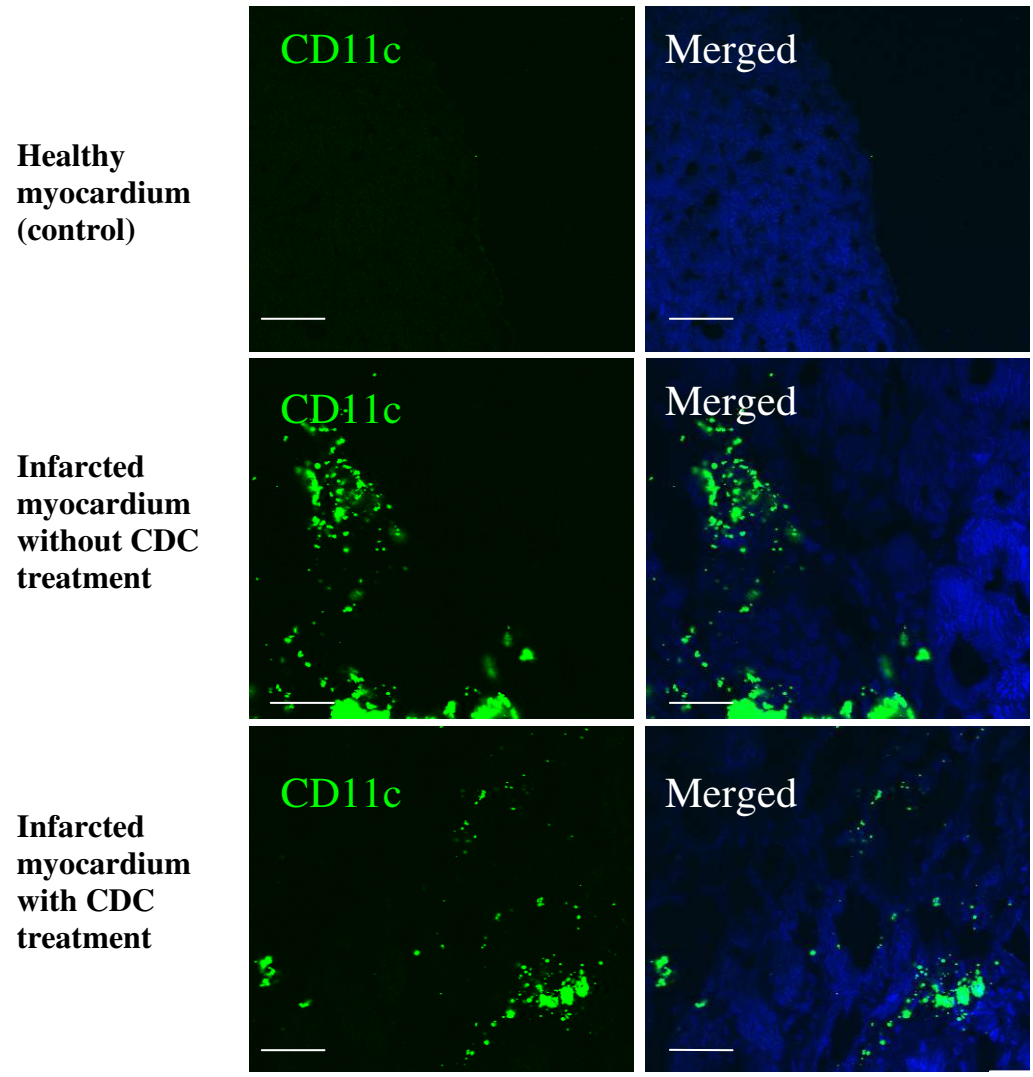

Figure 3.17 *Immunostaining of inflammatory cells. Representative confocal images (of three independent experiments) of the normal healthy myocardium, infarcted myocardium without CDC treatment and infarcted myocardium with CDC treatment (from top to bottom) immunostained with CD11c antibody. Green = CD11c; blue = DAPI. Scale bars = 50μM*

3.4.5.3 *Quantification of invading inflammatory cells*

Quantification of invading inflammatory cells (based on H&E staining) was performed on three specific regions, the infarct, peri-infarct and remote areas of CDC-treated and non-treated infarcted rat heart tissue (Figure 3.18).

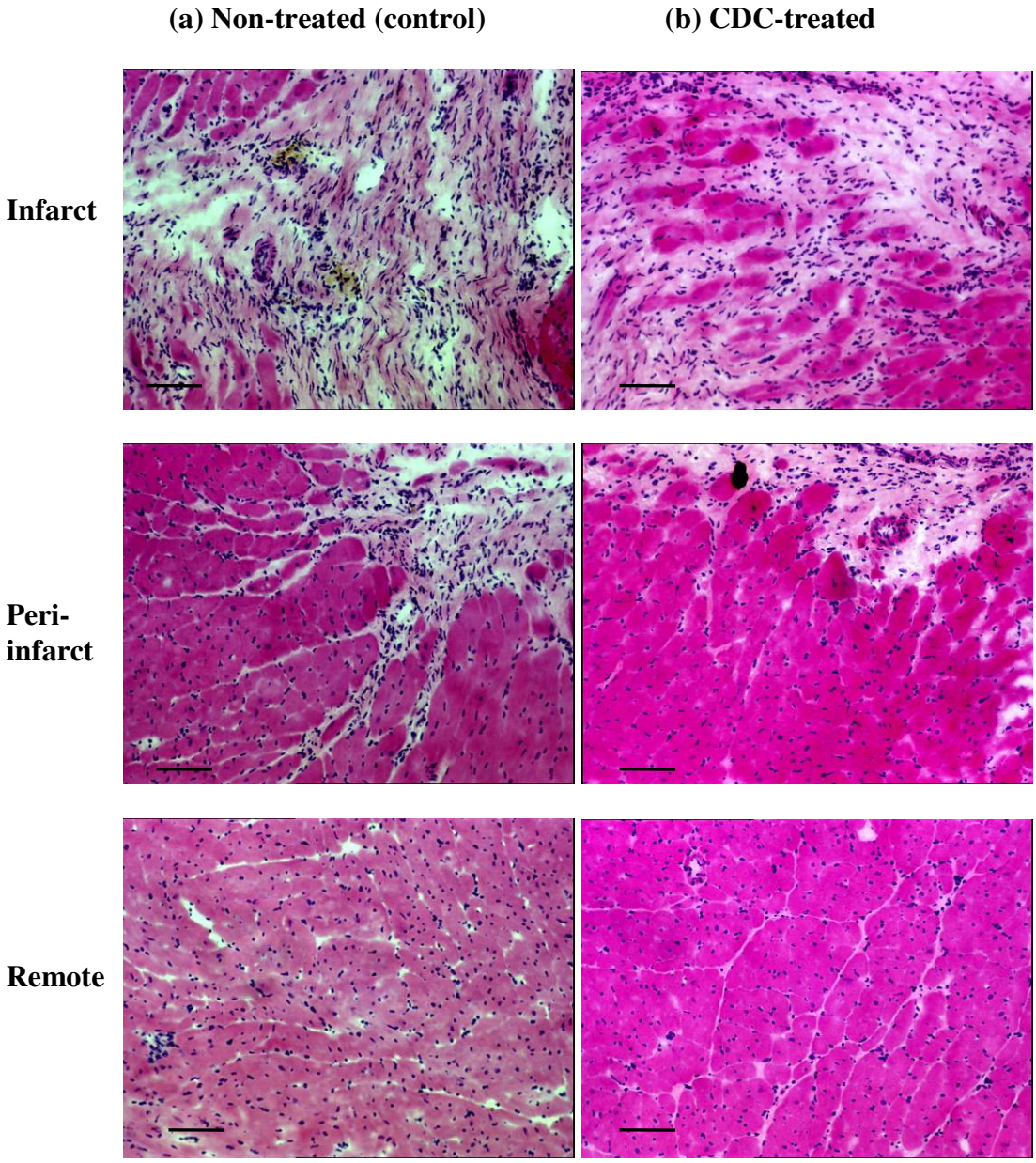

Figure 3.18 *H&E staining, 10X, revealed leukocyte invasion in different regions in cardiac tissue sections. (a) non-treated group (n = 5) (b) CDC-treated group (n = 5). (From top to bottom: infarcted area, peri-infarct area, remote area). Scale bars = 200μm*

The infarct zone had increased infiltrating inflammatory cells (hematoxylin stain) compared with the non-infarcted remote area in both groups ($p < 0.01$). However, there was no significant difference in the number of infiltrating inflammatory cells between the two groups (Figure 3.19). (Non-treated group vs. CDC-treated group, infarct zone = 27 ± 3% vs. 24 ± 2%, peri-infarct zone = 20 ± 3% vs. 17 ± 1%, remote zone = 10 ± 2% vs. 10 ± 1%).

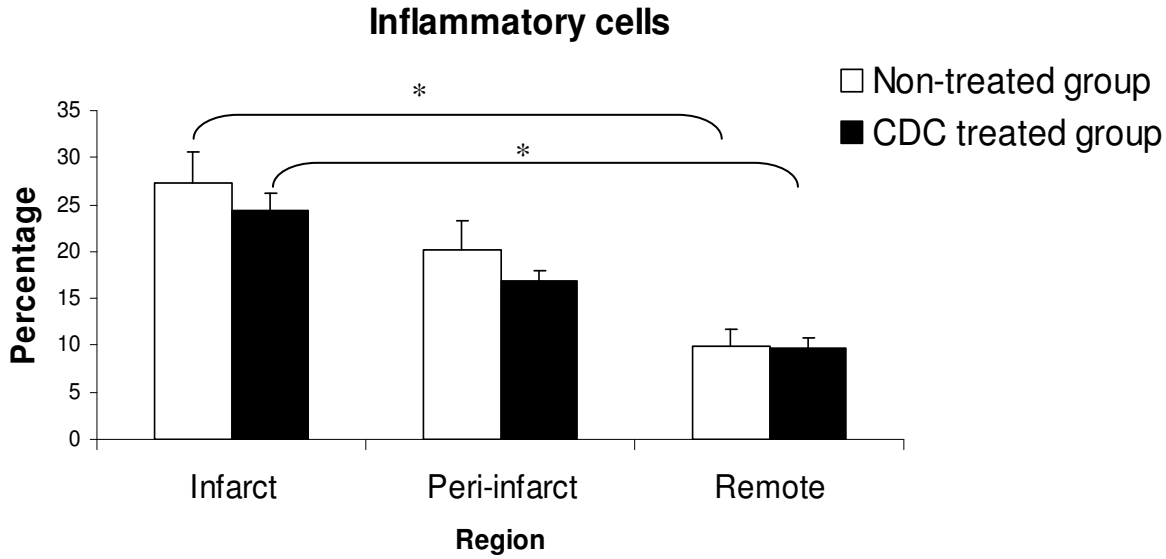

Figure 3.19 *Hematoxylin staining indicated increased infiltration by inflammatory cells in the infarcted, compared with the remote myocardium in the non-treated group (n=5) and CDC-treated group (n = 5). * = significantly different between the infarct and remote region at p < 0.01.*

3.4.5.4 Capillary density reduced after myocardial infarction

The myocytes in the infarcted myocardium were replaced by a collagenous scar with permanent loss of cardiac contractility and a reduced number of blood vessels. The area was unstained by alkaline phosphatase due to the absence of blood vessels. In the normal myocardium, alkaline phosphatase stains capillaries black. Quantification of capillary density (number of capillary per mm^2 of myocardium area) was performed on three specific regions, the infarct, peri-infarct and remote area of CDC-treated and non-treated groups (Figure 3.20).

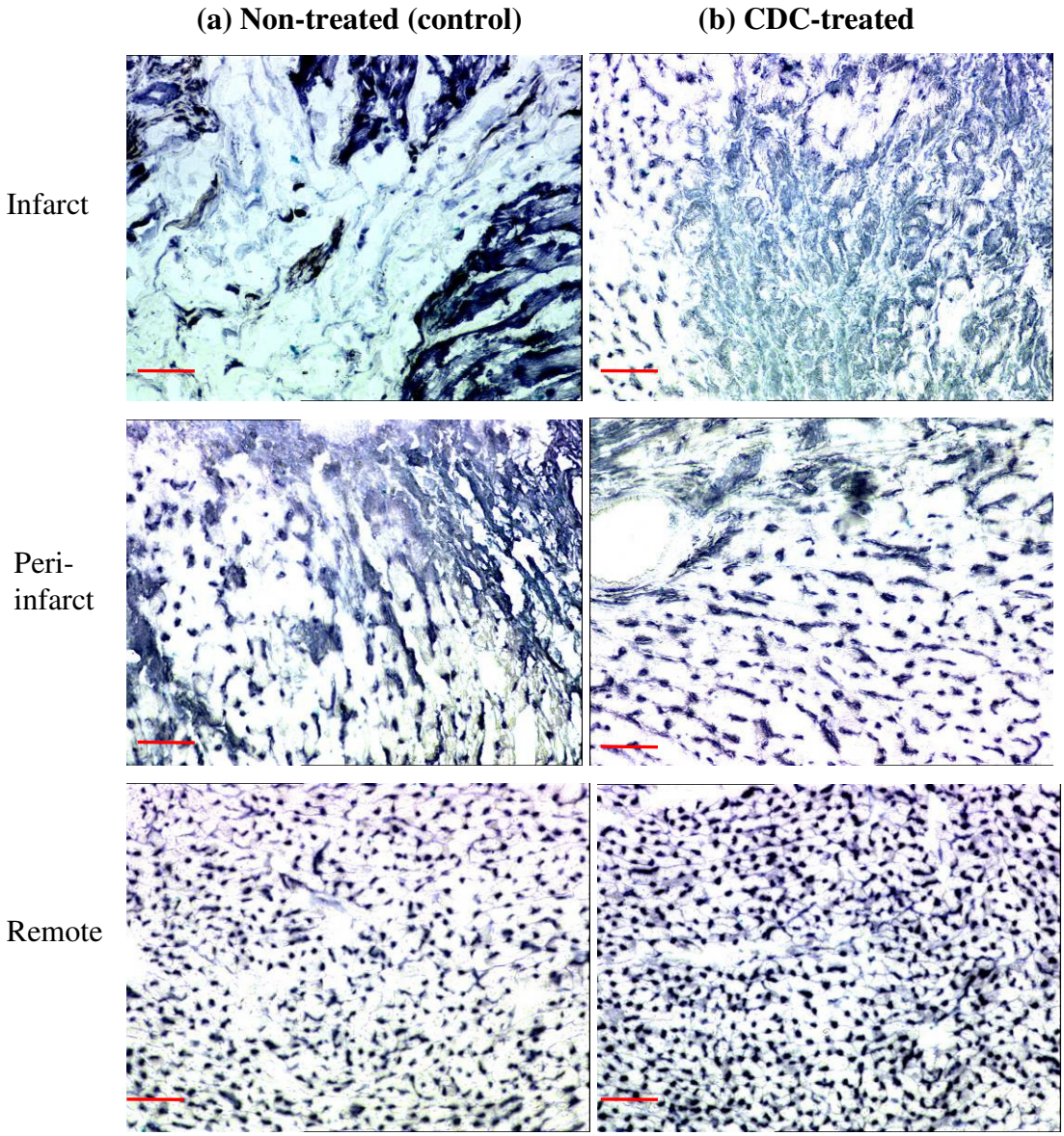

Figure 3.20 *Alkaline phophatase staining, 10X, revealed capillary density in different region in cardiac tissue sections. (a) non-treated group (n = 5) (b) CDC-treated group (n = 5). (From top to bottom: infarcted area, peri-infarct area, remote area). Scale bars = 200μm.*

Infarct zones showed a significant decrease in capillary density compared to the peri-infarct and remote areas in both the treated and non-treated groups. In the non-treated group, the number of capillaries per mm^2 of myocardium in the infarcted zone was 376 ± 34 compared to 745 ± 12 in the peri-infarct zone and 1337 ± 89 in the remote zone. Whereas, for the CDC-treated group, the number of capillaries per mm^2 of myocardium area in the infarcted area was 430 ± 48 compared with 813 ± 31 in the peri-infarct area and 1413 ± 112 in the remote area (Figure 3.21). A significant 9.2%

increase in capillary density was found in the CDC-treated group, compared to non-treated group, in the peri-infarct region (Figure 3.21).

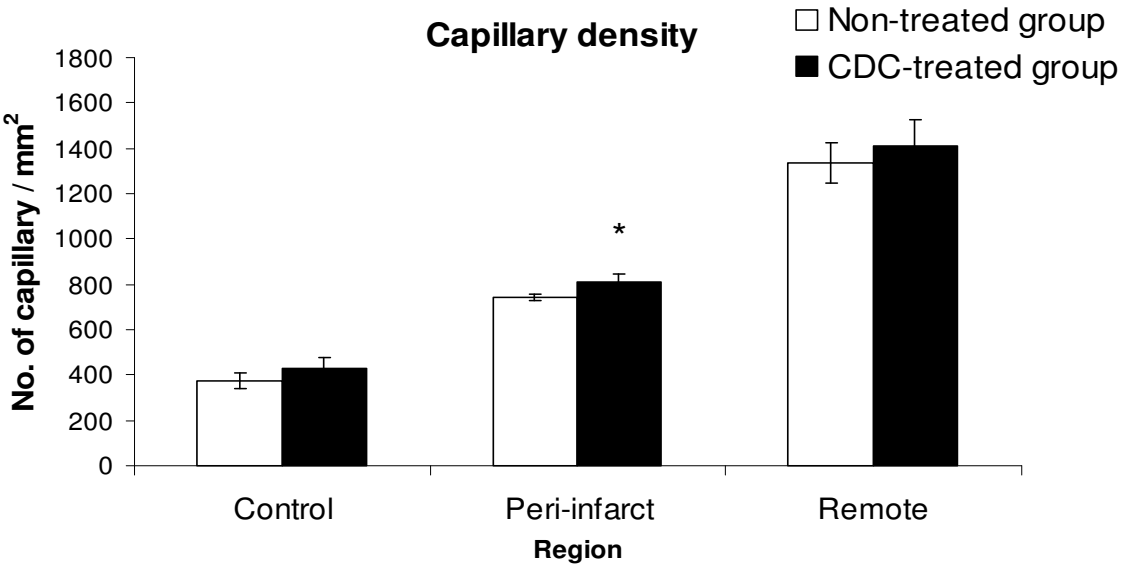

Figure 3.21 *Alkaline phosphatase staining showed increased capillary density in peri-infarct myocardium in the CDC-treated group (n = 5) compared with the non-treated group (n = 5). * $p < 0.05$ vs. non-treated group.*

3.4.5.5 Collagen tissue formed as scar tissue in the infarcted area

Picro-sirius red staining revealed a clear difference between healthy and infarcted tissue (Figure 3.22). Healthy myocardium stained yellow due to the cytoplasm, whereas myocardium was replaced with collagen and stained red in the infarcted region.

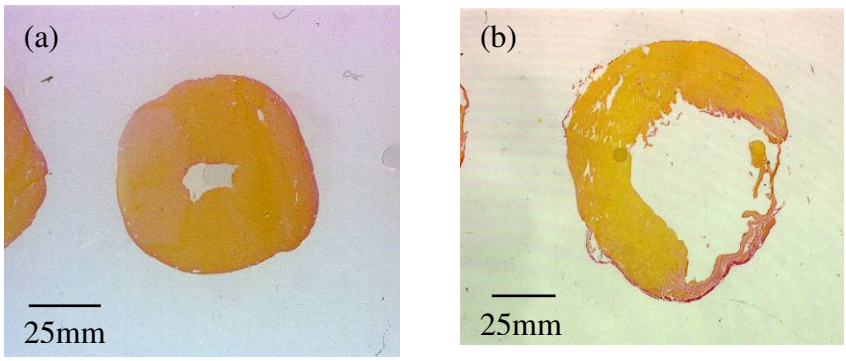

Figure 3.22 *Representative images (n = 5) of rat whole heart transverse tissue slices stained with picro-sirius red. (a) normal heart (b) infarcted heart.*

Figure 3.23 shows a comparison of the alkaline phosphatase stain and the picro-sirius red stain on a comparable region of the same infarcted rat heart. The infarcted region, which was unstained by alkaline phosphatase due to the absence of capillaries was stained red by the picro-Sirius red stain due to the formation of the collagen scar.

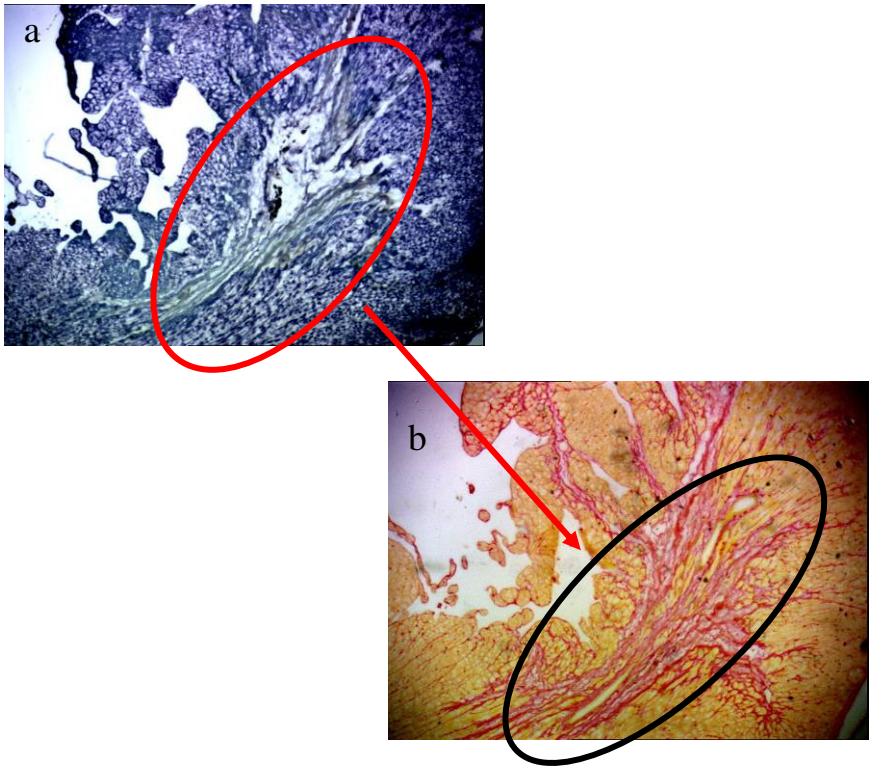

Figure 3.23 *Comparison of (a) alkaline phosphatase staining, 4X and (b) picro-sirius red staining, 4X on a comparable region of the same infarcted rat heart (shown in circle). Infarcted (circle) tissue was replaced with collagen which stained red by the picro-sirius red. The collagenous scar did not contain blood vessels, thus no alkaline phophatase stain was observed in this area.*

3.4.5.6 Quantification of scar volume

A significant decrease in total scar volume on whole heart tissue sections was found in the CDC-treated group compared to the non-treated group (Figure 3.24). The total scar volume for the CDC-treated group was 65.4 ± 8.2 mm^3, 33.3% decreased compared with the non-treated group.

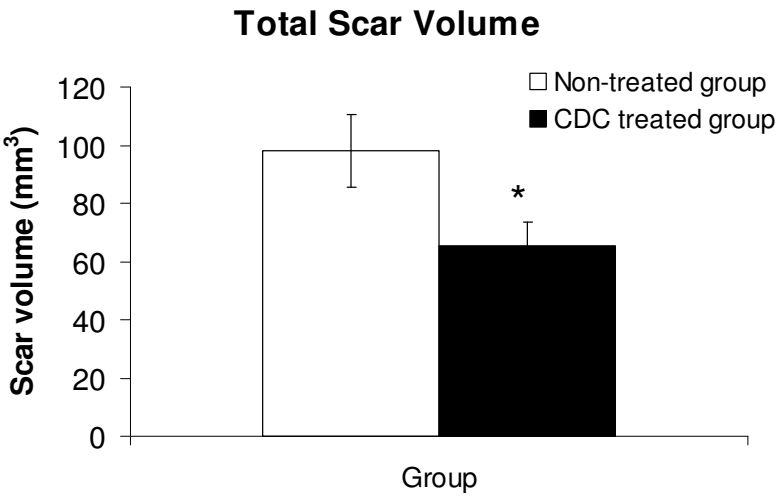

Figure 3.24 *Total scar volumes in whole heart tissue sections of non-treated and CDC-treated groups (n = 5). * p < 0.05 vs non-treated group.*

3.4.6 Comparison between *in vivo* MRI and *ex vivo* histology

The morphology of the infarcted rat heart was assessed using MRI. Seven contiguous short axis cine MRI slices of 1.5 mm thickness were acquired and the images at end systole and end diastole were analyzed using Image J (Figure 3.25).

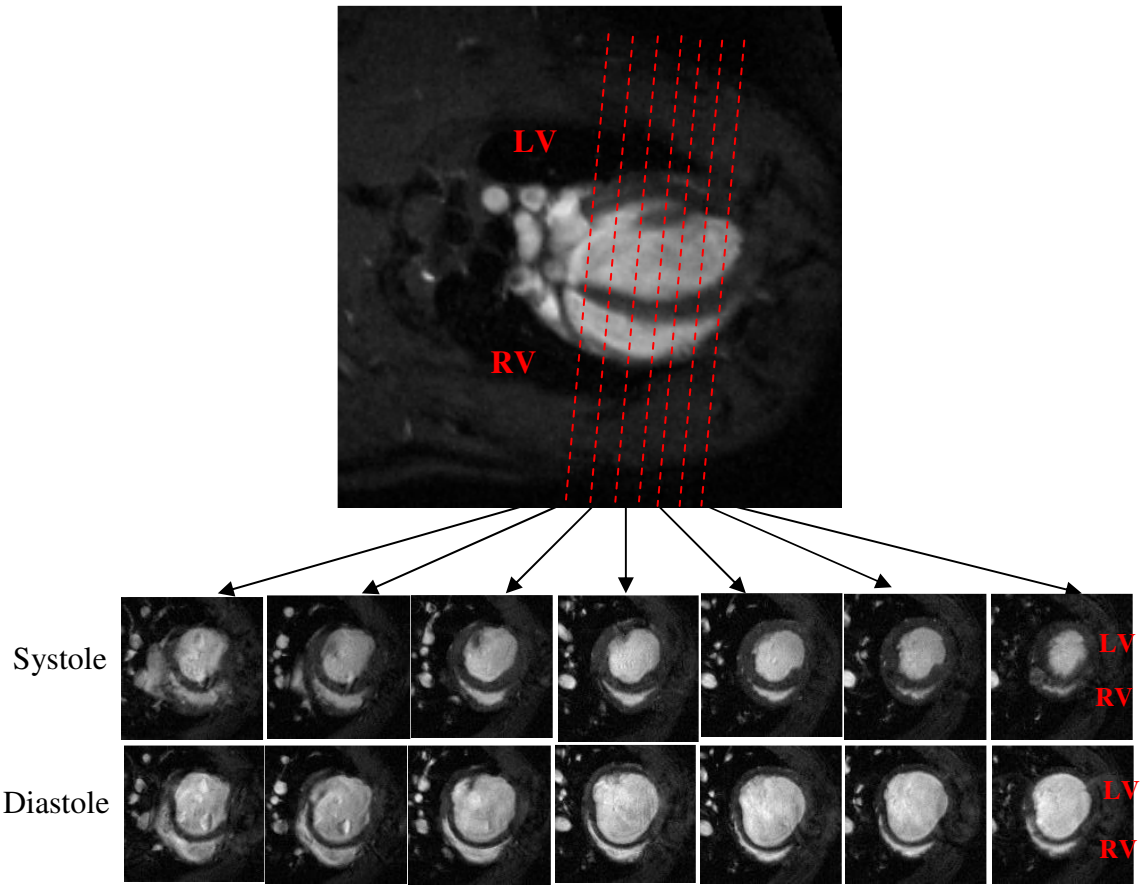

Figure 3.25 *MR image of an infarcted rat heart. Top panel: Long axis. Bottom panel: Short axis shown at end systole and end diastole. Lines perpendicular to the long axis of the heart indicate the location of short axis slices, planned from the long axis image.*

The akinetic region was identified in MR images as an area of myocardium lacking contractility, wall motion and wall thickening (Figure 3.26). Absolute scar size was calculated as the sum of the akinetic segment of the seven parallel, sequential short axis cine MRI slices, with 1.5mm thickness each, covering the entire LV. A significant positive correlation was found between scar volume measured using MRI and picro-sirius red stained tissue section in all groups ($R^2 = 0.86$) (Figure 3.27).

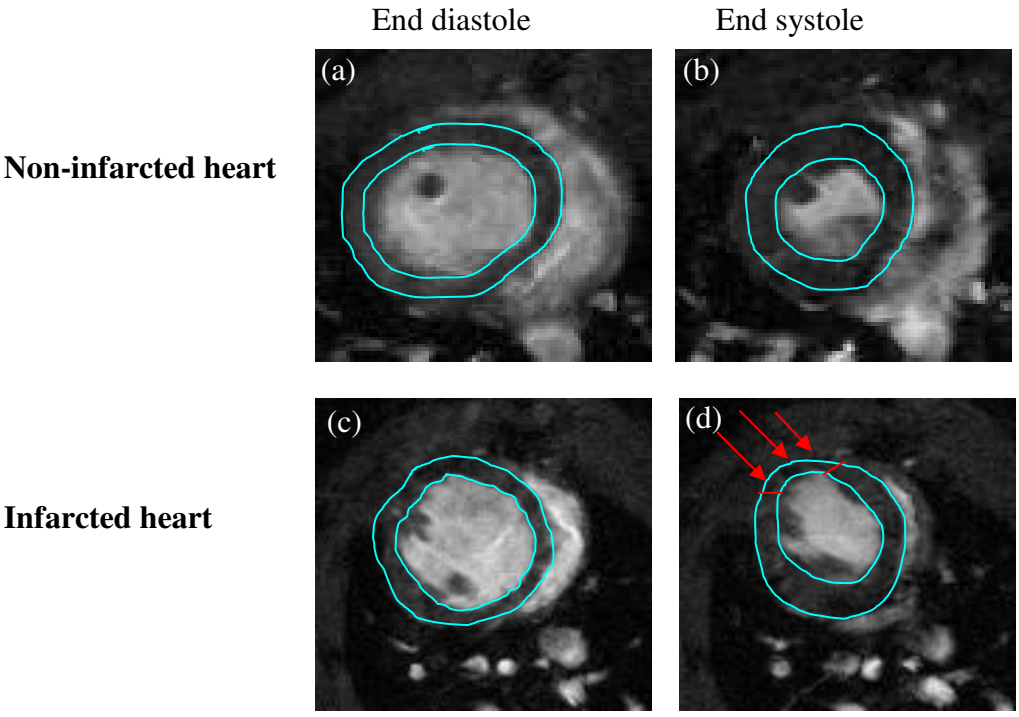

Figure 3.26 *Short axis MRI slices obtained for non-infarcted heart (a & b) and infarcted heart (c & d) during end diastole (a & c) and systole (b & d). LV epicardial and endocardial areas were outlined using free hand drawing function. Note the lack of wall motion and thickening in the akinetic area of infarcted heart during systole (d), while the non-infarcted heart (a & b) exhibits wall motion and thickening. The akinetic area was selected (red arrow and red line in d) and the area bounded by the red line was measured.*

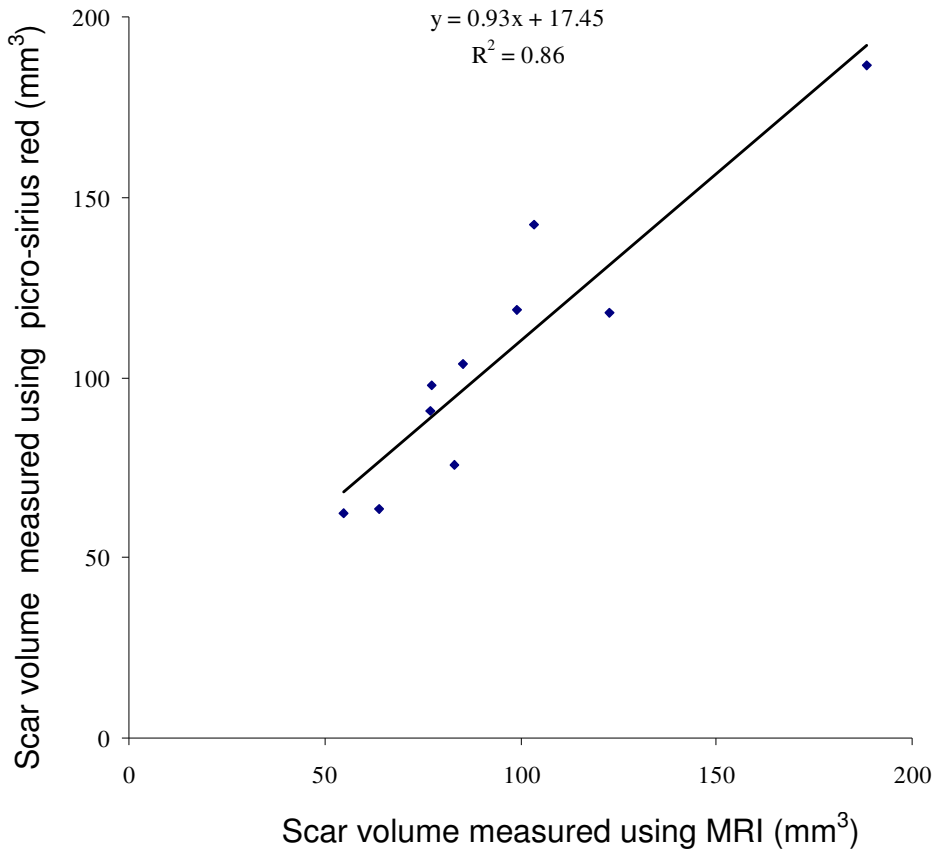

Figure 3.27 *A positive correlation was found between scar volume measured using MRI and picro-sirius red staining for non-treated groups (n = 5) and CDC-treated groups (n = 5). Each point represents the correlation of MRI and picro–sirius red staining for each animal.*

Moreover, there was agreement between *in vivo* short axis MRI images and *ex vivo* histological staining at the equivalent position in almost every slice (Figure 3.28). The dark akinetic infarct area could be seen in diastolic and systolic MR images, corresponding to the red stained collagen scar in the tissue section.

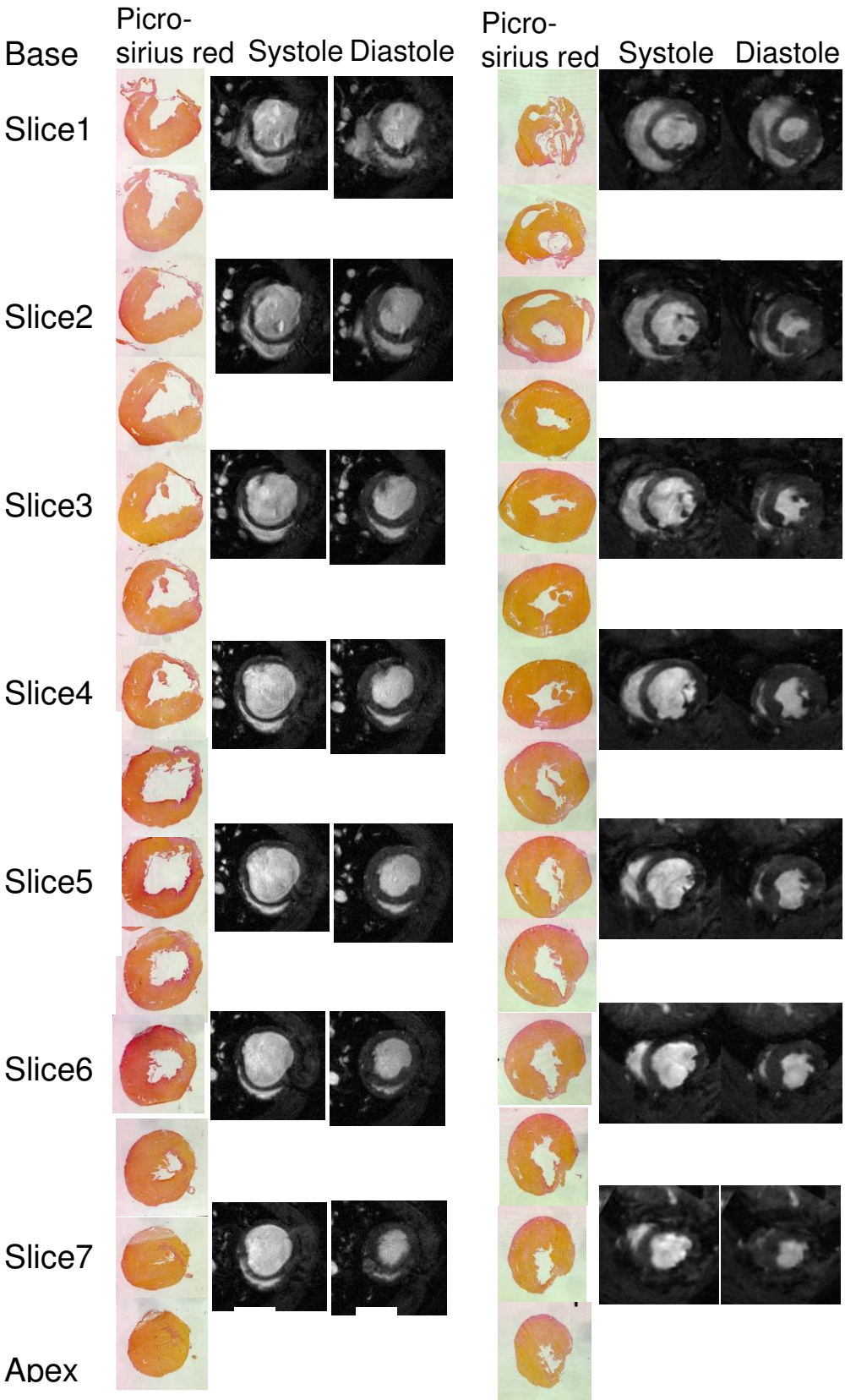

Figure 3.28 *Contiguous heart slices from base (top) to apex (bottom), with Picro-sirius red stained tissue section and short axis cine MR image at systole and diastole, 16 weeks after surgery. Left panel: non-treated group. Right panel: CDC-treated group. MRI slices (Slice 1 to Slice 7) were 1.5mm apart and histological sections were collected so that they accurately matched the region of the heart shown in the MR images.*

3.5 Discussion

The aims of the work described in this chapter were to isolate, characterize and differentiate P2 CDCs *in vitro*, and assess the potential of these cells as a therapeutic agent for myocardial infarction using *in vivo* MRI techniques and *ex vivo* histology.

CDC culture, expansion and characterization

In this study, we used the cardiosphere culture method to expand CDCs generating a heterogenous mixture of cells, which contains cardiac stem cells [107, 108]. This approach was used for two reasons: firstly, CDCs have been shown to give functional improvement in infarcted animal models [107, 108] and secondly, the number of cells generated in a few weeks from this approach is many fold greater than obtained by selection for c-Kit or Sca-1 [97]. Approximately 6 x 10^6 CDCs were obtained from neonatal rat heart within 28 days, comparable to Smith *et al.,* who obtained 1.7 ± 0.4 x 10^6 CDCs from human biopies within 45 ± 7 days using the same technique [108].

CDCs isolated in the present study were characterized using both RT-PCR and qRT-PCR. The selection of target genes for PCR in this study was based on important molecular signals involved in cardiac stem cell identification and differentiation.

Based on the RT-PCR findings, it was clear that the CDCs obtained from the heart explant culture *in vitro* were a heterogenous cell population, which included cardiac stem cells and progenitor cells expressing c-kit, Oct-4, Klf-4 Sox2, Nanog and mesenchymal cells (CD90 and CD105). There were also cardiac differentiating cells (GATA-4 and Nkx 2.5) and a low level of more mature cardiomyocytes (Tnnt and MyHC). This is in agreement with Smith *et al.,* which have shown that CDCs were a mixed population comprising of c-Kit$^+$ progenitor cells and CD90$^+$ CD105$^+$ mesenchymal cells that could be transdifferentiated into cardiomyocytes [108].

In line with the RT-PCR data, qRT-PCR showed that rat P2 CDCs expressed a low level of c-Kit (4.1%) and much higher levels of CD105 (42%) and CD90 (14.1-fold increase), compared to neonatal rat hearts. Thus most CDCs had a $CD90^+/CD105^+$mesenchymal stem cell phenotype, as was also shown by Tateishi *et al.* [155]. c-Kit, also known as CD117, is the stem cell factor receptor expressed on the surface of many stem cell types [156-160], and is used as surface marker to identify endogenous cardiac stem cells [86]. A substantially lower level of c-Kit expression was found in this study, compared with that of Smith *et al.* who showed (using flow cytometry) that 20% of that CDCs expressed c-Kit and approximately 40% were $CD90^+$ [108]. It is not possible to make a direct comparison between our results and those of Smith's, as our data were obtained using cardiospheres and CDCs isolated from whole neonatal rat hearts, while the latter isolated CDCs from adult human heart septal wall biopsies. Different sources of tissue explants may account for the different proportions of cell populations. This hypothesis is supported by Davis *et al.* [109] who showed, using flow cytometry, approximately 4.9% c-Kit positive cells in a rat CDC population. Nevertheless, the precise mechanism underlying the discrepancy between rat and human CDC populations is unknown and requires further investigation.

CDCs were cardiomyogenic and adipogenic pluripotent stem cells

Recently, Andersen *et al.* suggested that cardiospheres from neonatal rat hearts were largely composed of cardiac fibroblasts and $CD45^+$ hematopoietic cells, with no cardiomyogenic potential [161]. Although the $CD90^+$ cells may include cardiac fibroblasts, the detection of Oct-4, Sox 2, Klf-4 and some Nanog using RT-PCR and qRT-PCR confirmed the presence of pluripotent stem cells within the CDC population. Oct-4 was discovered by Scholer *et al.* [162] as an early developmental control gene expressed in pre-implanted mouse embryos. Together with Sox 2, Klf4 and Nanog,

Oct-4 regulates genes controlling stem cell function and maintaining stem cell pluripotency [163, 164]. In the adult, these pluripotent markers are generally believed to be expressed exclusively in germ cells, however, recent evidence suggested that these genes are also present in adult stem cell populations. Oct-4 expression was reported for multipotent adult progenitor cells [165] and haemapoietic stem cells [166], Sox 2 in human Műller stem cells [167] and dermal stem cells [168, 169], Klf4 in gastrointestinal epithelia [170] and Nanog in spermatogonial stem cells [171, 172].

Furthermore, treatment with cardiomyocyte differentiation medium containing 5-aza or DMSO for 2 weeks induced CDC differentiation along the cardiomyocyte lineage, with up-regulation of the cardiomyocyte differentiating marker, Nkx 2.5 and mature cardiomyocyte markers, Tnnt and MyHC. 5-aza and DMSO are DNA demethylating agents which modulate the cell epigenetic transcriptional profile via DNA demethylation [173, 174]. Under the influence of 5-aza, cells obtained a wide range of changes in gene regulation with distinct functional categories[173]. In some cells, such as Sca-1^+ cells [87] and mesenchymal stem cells [175], the cardiomyocyte transcriptional profile was activated after treatment with 5-aza and the cells obtained a spontaneously beating myocyte-like cell phenotypes [87]. Interestingly, it was found that neonatal CDCs had the potential to spontaneously differentiate into cardiomyocytes without cardiomyogenic inducers when they were over confluent. Yoon *et al.* reported that direct cell-to-cell interaction is one of the microenvironmental factors that induce transdifferentiation of adult stem cells into cardiomyocytes [176]. However, no changes of MyHC mRNA expression level and no beating cells were observed after 2 weeks of induction with CEM, indicating that the cardiomyocytes were not fully mature. A longer treatment period or higher seeding cell number is thus suggested to increase the cell-to-cell contact and ultimately stimulate the cells to beat.

In this study, CDCs have been first proven to be capable of undergoing adipogenesis upon proper induction by a supplementation of growth medium with dexamethasone, indomethacin, 1-methyl-3-isobutylxanthine and insulin. This was evidenced by Oil red O staining. Since CDCs have the ability and potential to be transdifferentiated into several specific cell types, they are thought to represent *ex vivo* expansion of resident progenitor cells. The discrepancy observed in Andersen's report [161] maybe due to the modification and technical variations which they introduced to the protocol, such as prolonged enzymatic treatment and filtration of the cell suspension after enzymatic digestion [109].

CDC improved cardiac function

Transplanted CDCs were retained in the infarcted myocardium after injection and 49% were found to express troponin I (cTnI) 16 weeks after injection. MRI measurements of cardiac function showed that CDC-treated hearts had a significantly greater ejection fraction (EF) than control hearts, 6 weeks after infarction and CDC administration. This difference in EF was maintained for up to 16 weeks after infarction. The results were confirmed by quantitative histological analysis, which showed a significantly decreased scar size and an increase in capillary density 16 weeks after the CDC treatment. Despite the relatively lower c-Kit level expressed by CDCs in this study, it has been shown that these CDCs have the capacity to regenerate the infarcted myocardium (reduce scar size) through cell differentiation and to induce neoangiogeneis (increase capillary density) and recruit endogenous cardiac stem cells (retention of CDCs in infarcted myocardium) through paracrine effects. These data are in agreement with Davis *et al.* [177] who reported direct outgrowth from cardiac tissue explants, which contain sub-populations resembling endothelial and mesenchymal cells, capable of cardiomyocyte differentiation and post MI functional benefits. Also, it

has been shown that a mixed cell population of cardiac mesenchymal stem cells and c-Kit$^+$ cells provide greater functional improvement than c-Kit$^+$ cells alone [178].

Comparison of in vivo MRI and ex vivo histological studies

Notably, this was the first study to compare cardiac function and morphology in CDC treated and non-treated hearts using *in vivo* MR images with corresponding *ex vivo* histological sections taken from the same heart. Short axis *ex vivo* heart sections were found to correlate well with the *in vivo* MRI slices in the gross morphology of the myocardium and actual scar size area. The infarcted area, which was observed in MRI images as a dark akinetic area was also observed in corresponding *ex vivo* heart sections, with positive picro-sirius red staining. There was also a significant correlation of scar size measured using MRI with that using histological staining,16 weeks after infarction. This confirmed that measurement of the akinetic region using MRI revealed the true amount of scarred collagenous tissue. Thus, non-invasive MRI can be used to monitor scar size non-invasively at multiple time points.

3.7 Conclusion

This project investigated the therapeutic potential of CSCs for infarcted rat hearts. Heart tissue explant culture yielded sufficient CDCs for therapy within 4 weeks. These cells expressed c-Kit and had the ability to transdifferentiate into adipocytes and cardiomyocytes, and thus were thought to represent CSCs *in vitro*. Although, undoubtedly, CDCs cultured *in vitro* were a different cell type to the pure c-Kit$^+$ CSCs in heart tissue *in vivo*, it was found that the CDC-treated infarcted rat hearts showed a significant improvement in cardiac function using *in vivo* MRI assessment, while e*x vivo* histological assessment further confirmed that CDCs improved the heart condition by reducing the scar size and increasing the capillary density.

Chapter 4

Hypoxic Preconditioning to Enhance the Therapeutic Potential of Cardiosphere-Derived Cells

4.1 Abstract

Infarction irreversibly damages the myocardium, with formation of an hypoxic scar and impaired cardiac function. In *Chapter 3,* it was shown that transplantation of CDCs into infarcted rat hearts improved cardiac function when administered at the time of infarction. However, the protocol used required at least one month to obtain sufficient CDCs for therapy. Hence, this chapter describes work to optimize CDC culture to shorten the culture period and enhance the therapeutic potential for myocardial infarction by preconditioning the CDCs under hypoxia. Neonatal rat heart explants were cultured under normoxia (21% O_2) or hypoxia (2% O_2) to generate explant-derived cells (EDC). EDCs were isolated, cultured to form Csp and expanded into monolayer CDCs. EDC and CDC proliferation was 1.7-fold greater and larger cardiosphere clusters were formed under hypoxia. Approximately 6 x 10^6 CDCs were obtained from hypoxic explant within 21 days, a week faster than the normoxic explant. qRT-PCR confirmed that hypoxia increased the proportion of c-Kit$^+$ cardiac progenitor cells and decreased CD90$^+$ CD105$^+$ mesenchymal cells in the CDC population. Proliferating hypoxic cells maintained pluripotency and fewer cells spontaneously transdifferentiated into cardiomyocyte, compared with cells cultured under normoxia. Nonetheless, these cells retained their ability to differentiate into adipocytes or cardiomyocytes when induced with adipogenic or cardiomyogenic stimuli. Further, hypoxia induced the expression of the erythropoietic cytokine, EPO (2.1-fold) and the angiogenic cytokine, VEGF (2.4-fold), compared with normoxia, indicating that hypoxic CDCs may provide a potent stimulus for neovascularization in infarcted myocardium. Hypoxia also induced the expression of CXCR-4 (4.3-fold), which plays a role in the regulation of stem cell trafficking and homing to SDF-1 in the infarcted myocardium. Notably, hypoxic CDCs were able to switch to anaerobic glycolytic metabolism and had approximately 80% lower oxygen consumption, suggesting that the hypoxic-preconditioned CDCs may be better adapted to survive within the hypoxic infarct scar, compared with normoxic CDCs. In conclusion, hypoxic preconditioning may enhance the potential of CDC therapy for myocardial infarction by shortening the culture period by one week and stimulating various stem cell functions, including increasing the proliferation rate and the expression of the cardiac stem cell marker, c-Kit, with induction of several important cytokines involved in stem cell homing and neovascularization.

4.2 Introduction

Adult heart contains stem cells that are able to partially repair the heart following a heart attack or throughout the course of progressive heart failure [86]. However, endogenous cardiac stem cells (CSCs) are limited in quantity [97] and the number and functional capacity of these reparative stem cells may decrease with increased age [179]. Therefore, it is necessary to isolate and expand the CSCs *in vitro t*o generate sufficient cells for transplantation.

Work described in *Chapter 3* was the development of an efficient method to isolate CSCs using a tissue explanation technique. Using this method, cardiosphere-derived cells (CDCs) were isolated from rat heart tissue explants via the formation of explant-derived cells (EDC) and cardiospheres (Csp). CDCs obtained using this method showed stem cell properties and increased cardiac function *in vivo*. Clinical application of CDCs is under investigation by the CADUCEUS trial (Clinical Trials.gov. Identifier NCT00893360) [180]. However, it has been shown by us and others, that CDCs need to be expanded *in vitro* over weeks in order to obtain sufficient cells for transplantation [107, 108]. During this period, the infarcted heart will undergo the initial stages of scar formation and remodeling. Therefore, CDCs may be of more benefit to treat the infarcted heart if they are administered as soon as possible after infarction. Hence, optimization of the current CDC culture protocol to increase the cell proliferation rate without compromising stem cell properties was the main objective of the work in this chapter.

Stem cells reside in complex microenvironments, termed niches [181]. Niches play an important role in signaling stem cell division, function and differentiation [182, 183]. The oxygen (O_2) level is one of the most important factors in the stem cell niche [181]. To date, most *in vitro* tissue cultures are routinely maintained at atmospheric levels of

21% oxygen. However, natural cell microenvironments contain much lower oxygen tensions [184]. The average oxygen concentration at tissue level *in vivo* is about 2-9%, with considerable variation based on location, whereas the mean oxygen tension is even less in the embryo [184-186]. Similarly, adult stem cell niches are hypoxic, with some oxygen levels as low as 1-2% [184] . Thus, *in vitro* cultivation of stem cells in a traditional incubator supplied by room air (74% nitrogen and 21% oxygen), buffered with 5% CO_2, does not represent the *in vivo* physiological condition and could result in a gradual loss of stem cell primitive characteristics and self-renewal properties [187]. Therefore, in order to fully evaluate the therapeutic potential of cardiac stem cells, it is important to isolate and culture the cells under physiologic oxygen levels.

Recently, enhanced cell proliferation rates have been reported for human and rat mesenchymal stem cells (MSCs) [188, 189], neural stem cells [190-192], embryonic stem cells [193] and adipose-derived stem cells [194] when cultured under low oxygen concentrations (2% – 6% O_2). In the same stem cell populations, reduced apoptosis was observed under low oxygen conditions [190, 195-197]. These findings lead to the hypothesis that hypoxic preconditioning might promote cell proliferation and thus could shorten the period required to obtain sufficient cells for therapy. Therefore, in this study, CDC culture was optimized using hypoxia. Rat CDCs were isolated and cultured under physiological oxygen levels (2% oxygen; termed hypoxia) and the resulting changes in CDCs self-renewal, differentiation, gene expression and ultimate function *in vitro* were investigated and compared with those cultured under atmospheric oxygen (21% oxygen; termed normoxia).

The aims of this study were to:

- Optimize cardiac stem cell culture using hypoxia.
- Investigate the stem cell self-renewal/proliferation and differentiation after hypoxic preconditioning.
- Characterize and compare gene expression profiles of hypoxic cells to those of cells cultured under normoxia.
- Evaluate the potential benefits of hypoxic preconditioning on cardiosphere-derived cells (CDCs) in promoting therapeutic cytokine production.
- Investigate the effects of hypoxic preconditioning on CDC respiration and metabolism.

4.3 Methods

4.3.1 Isolation and expansion of cardiosphere-derived cells under hypoxia

Two incubators (Wolf Laboratories, UK) adjustable to different O_2 concentrations by infusion of nitrogen (N_2), were used for cell culture. Normoxic cell culture was set at 21% O_2 (atmospheric oxygen levels), whereas hypoxic cell culture was set at 2% O_2 (physiologic oxygen levels). The O_2 concentration was monitored continuously using an oxygen sensor (Wolf Laboratories, UK). Neonatal Sprague Dawley (SD) rat hearts were excised and heart weight was measured (0.07-0.10 g, n = 4). Each heart was separated into two portions of equal weight and allocated to two groups (hypoxia and normoxia). Heart tissues were minced and plated on petri dishes to give explant-derived cells (EDCs). Cardiosphere-derived cells (CDCs) were generated from EDC via the formation of cardiosphere, in either hypoxic or normoxic incubators (see *Chapter 2*).

4.3.2 Characterization of hypoxic cells

Genotypic characterization of hypoxic EDC, cardiospheres and CDCs used qRT-PCR. Specific target genes such as hypoxia-induced factor-1 alpha (HIF-1α), vascular endothelial growth factor (VEGF), erythropoietin (EPO), telomerase reverse transcriptase (TERT) and C-X-C chemokine receptor type 4 (CXCR-4), were investigated to show the effects of hypoxia on CDC culture (see Appendix 4 for primer sequence). In addition, 11 primer pairs that were designed for P2 CDC characterization in *Chapter 3* were also used to evaluate the effects of hypoxia on CDC gene expression profile. All qRT-PCR data were normalized to a combination of GADPH and Actb as housekeeping genes, as validated in a previous study (Appendix 8, manuscript submitted).

4.3.3 Differentiation of normoxic and hypoxic CDCs

Hypoxic and normoxic P2 CDCs were subjected to adipogenesis using adipogenic induction medium (AIM) (Appendix 3) under normoxic culture conditions (21% O_2; 5% CO_2; 74% N_2). After 3 cycles of adipogenic induction by AIM, cells were stained with Oil Red O and images were captured under a light microscope. To quantify the positive Oil Red O staining, cells were eluted using isopropanol and the solution was transferred into a 96-well plate reader and optical density (OD) was measured at 500 nm, with 100% isopropanol as a blank sample.

P2 normoxic and hypoxic CDCs were induced to form cardiomyocytes by incubation with cardiomyocyte differentiation medium (Appendix 3) containing either 5-azacytidine (5-aza) or dimethyl sulfoxide (DMSO) for 2 weeks. Negative control cells were treated with normal CDC culture medium (CEM, Appendix 1) for 5 days or 2 weeks, with CEM changed every 2 days. After 5 days or 2 weeks, RNA was isolated from cells and mRNA levels for the cardiomyocyte markers, Nkx 2.5, Troponin T (Tnnt) and myosin heavy chain (MyHC) were evaluated using qRT-PCR.

4.3.4 Western blotting

Metabolic characteristics of normoxic and hypoxic CDCs were determined by western blotting for HIF-1α, GLUT-1, GLUT-4 and citrate synthase. Bands were quantified using UN-SCAN-IT gel software (Silk Scientific, USA).

4.3.5 ELISA for VEGF

Cell culture medium was collected from normoxic and hypoxic CDCs and the VEGF protein concentration in the medium was determined using a DuoSet VEGF ELISA Development kit (R&D System, USA) according to the manufacturer's instructions.

4.3.6 Hypoxic cell metabolism

Effects of hypoxia on CDC oxidative respiration were determined using Clarke-type oxygen electrode while glucose metabolism in CDCs was investigated using ABX 400 Chemistry Analyzer (see *Chapter 2*).

4.4 Results

4.4.1 Effects of hypoxia on cardiac stem cell proliferation

4.4.1.1 Explant-derived cells (EDCs)

Neonatal rat heart explants were cultured under normoxia (21% O_2) or hypoxia (2% O_2) (Figure 4.1a). After 3 days in both normoxic and hypoxic culture, explants became adherent to the dishes and fibroblast–like cells started to migrate away from the edge of the explants (Figure 4.1b). At day 6, small, round, phase bright cells were observed to grow more vigorously on top of the fibroblast-like cell layer from the edge of explants in hypoxic culture, compared with normoxia (Figure 4.1c). This observation became more obvious at day 9 (Figure 4.1d).

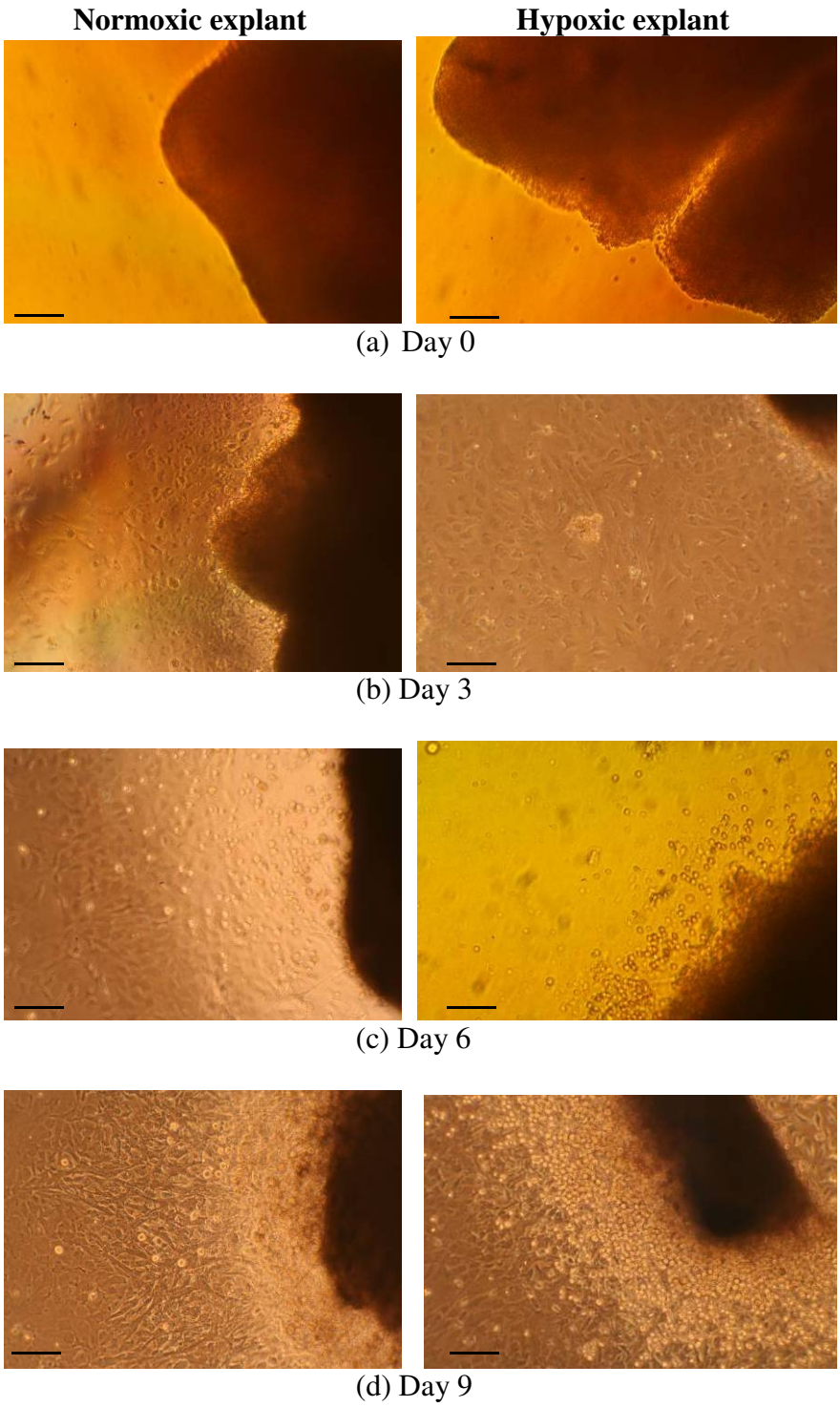

Figure 4.1 *Rat cardiac explants cultured under normoxia (left panel) and hypoxia (right panel) for (a) 0, (b) 3, (c) 6 and (d) 9 days. The layer of fibroblast-like cells grew from the edge of explants after 3 days in culture. Phase bright cells were observed to grow more vigorously under hypoxia after 6 days in culture. Scale bars = 200 μm.*

Typically, under hypoxia, EDCs became confluent and ready for harvesting within 5 days of plating. On the other hand, under normoxia, EDCs normally became confluent 7 days after plating. In order to evaluate the cell proliferation rates under normoxia and hypoxia, EDCs were harvested using trypsin and cell numbers were counted using a hematocytometer at days 3, 6 and 9. After 6 days in culture, 0.1 g hypoxic explants generated approximately 15 ± 0.3 x 10^5 EDCs, 1.7 fold more than those generated from normoxic explants (9 ± 1 x 10^5 EDC). These rates were maintained up to day 9, with hypoxic explants generating 1.8-fold more cells compared to normoxic explants (34 ± 3 x 10^5 vs. 19 ± 4 x 10^5 EDCs) (Figure 4.2).

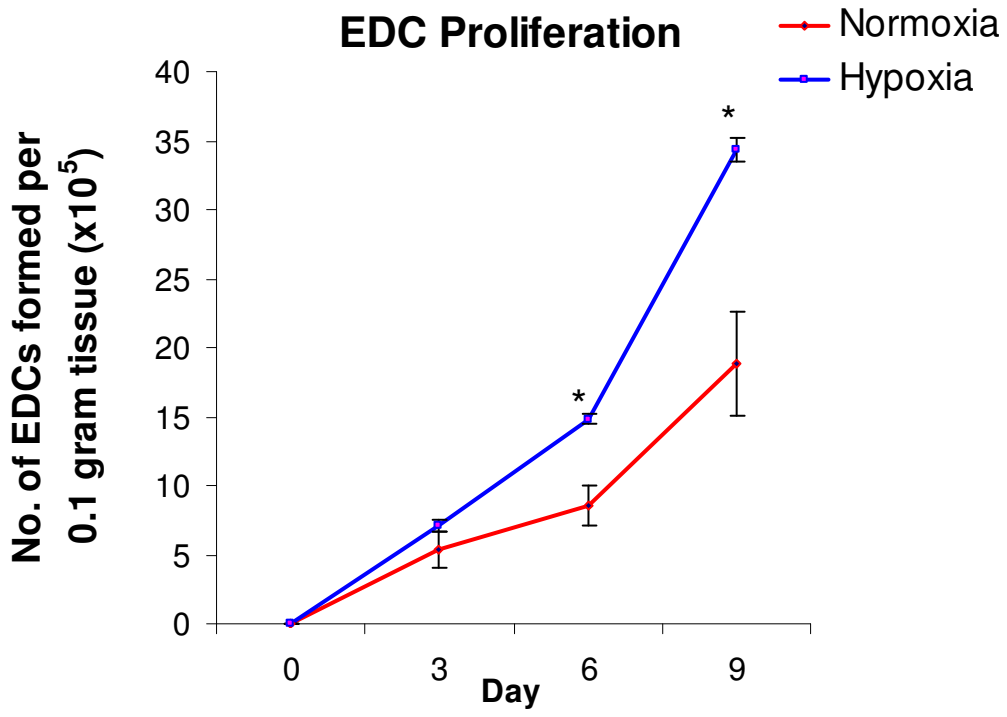

Figure 4.2 *Normoxic and hypoxic EDC proliferation assay (n =4). Cells were harvested and counted at days 3, 6 and 9. * $p < 0.01$ vs. normoxia.*

4.4.1.2 *Cardiospheres*

EDCs were plated at a density of 3 x 10^4 cells per well. Cells aggregated to form cardiospheres after 2 days in culture. Approximately 400 cardiospheres were obtained from each well after 4 days of incubation under normoxia or hypoxia (Figure 4.3), with hypoxic cardiospheres forming larger cell clusters (0.018 ± 0.003 mm^2) compared with those under normoxia (0.033 ± 0.004 mm^2) (Figure 4.4).

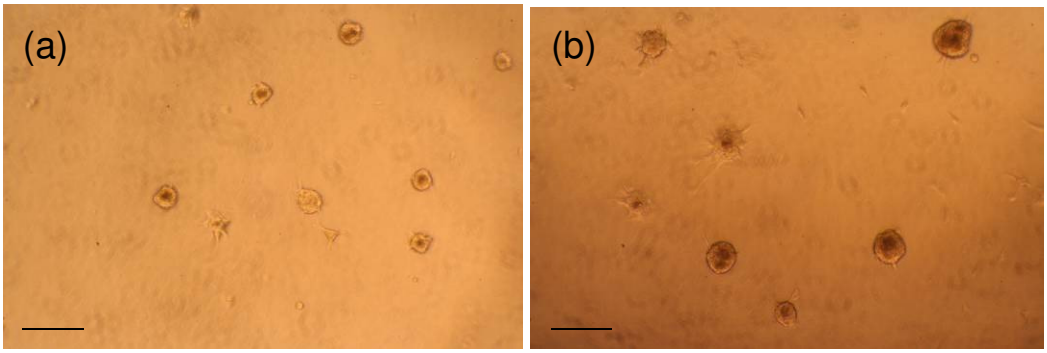

Figure 4.3 *Representative images of cardiosphere cultured under (a) normoxia (b) hypoxia for 4 days (n = 4). Scale bars = 200 μm.*

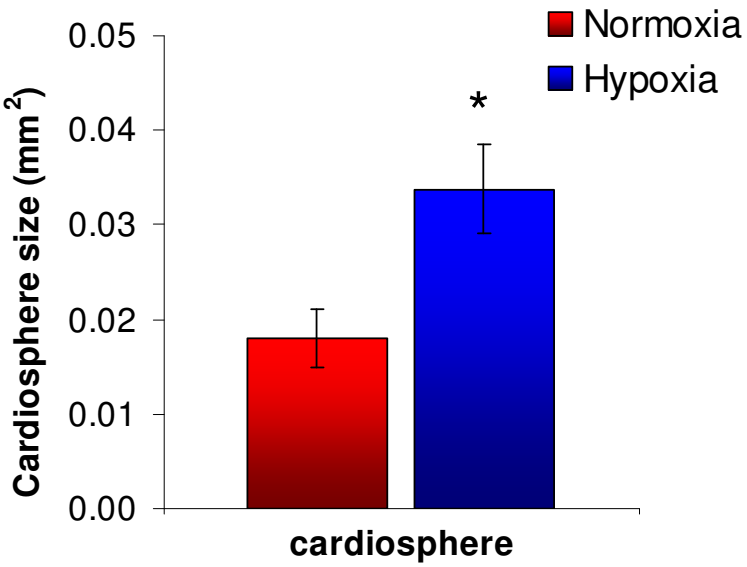

Figure 4.4 *Sizes of cardiospheres cultured under normoxia and hypoxia (n = 4). Images of 20 random unfixed cardiospheres from each group were captured under the microscope and the sphere sizes were measured using ImageJ. * $p < 0.05$ vs. normoxia.*

4.4.1.3 Gene expression of hypoxic EDCs and hypoxic cardiospheres

qRT-PCR showed that hypoxic preconditioning significantly increased the expression of HIF-1α in EDCs (1.6 ± 0.3-fold) and cardiospheres (2.1 ± 0.3-fold), cultured under hypoxia for 7 days and 4 days, respectively. In addition, VEGF levels were upregulated in hypoxic cardiospheres by 2.4 ± 0.6-fold, compared with normoxic cardiospheres (Figure 4.5). Both EDCs and cardiospheres expressed the stem cell marker, c-Kit and mesenchymal cell markers, CD90 and CD105 however, the expression levels of these genes were not upregulated under hypoxia (Figure 4.5).

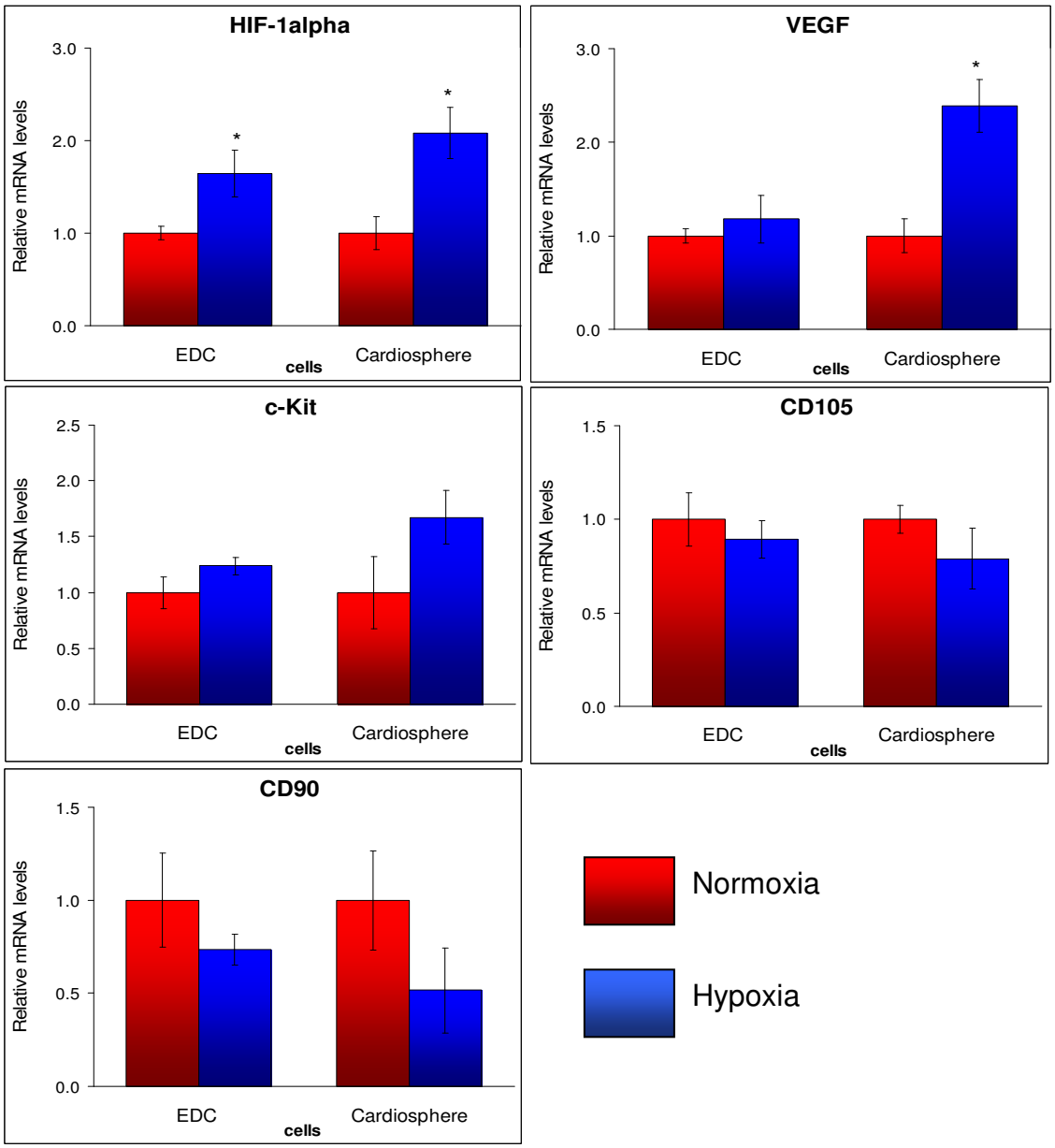

Figure 4.5 *The relative mRNA expressions of HIF-1α, VEGF, c-Kit, CD105 and CD90 in EDCs and cardiospheres cultured under normoxia and hypoxia (n = 4), respectively. The mRNA expression of hypoxic cells was normalized to the geometric mean of GAPDH and Actb (housekeeping genes) and normoxic cells (calibrator). * p < 0.05 vs. normoxia.*

4.4.1.4 Cardiosphere-derived cells (CDCs)

(i) Comparison of growth potential between normoxic and hypoxic CDCs from passage 1 to passage 5

After culture under both normoxic and hypoxic conditions, cardiospheres were harvested and transferred into cell culture flasks to form cardiosphere-derived cells (CDCs). Normoxic and hypoxic CDCs were passaged every 5 days and cell numbers were counted at the end of every passage. Hypoxia yielded higher cell numbers than normoxia at day 5 of each passage from passage 1 until passage 5 (Figure 4.6). On average, 5.3 ± 0.3-fold expansion was observed at each passage for hypoxic cells, whereas normoxic CDCs maintained a 3.1 ± 0.1-fold increase during each passage.

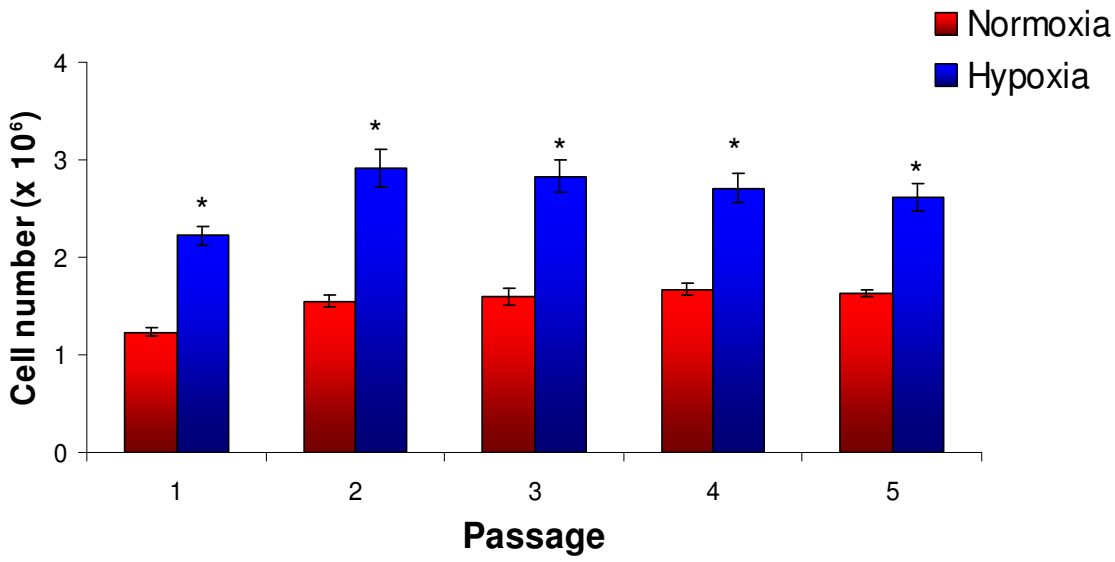

Figure 4.6 *Normoxic and hypoxic CDC growth potential from passage 1 to passage 5 (n = 4). * p < 0.01 vs. normoxia.*

(ii) Comparison of growth kinetics for chronic hypoxia, acute hypoxia, reoxygenation and normoxia

The effects of hypoxia on CDC growth kinetics were determined using P2 CDCs exposed to different oxygen. Four different oxygen conditions were used: 1) long term normoxia (control group) – cells were maintained under normoxia from explant culture up to P2 CDCs, 2) chronic hypoxia (long term hypoxia) – cells were maintained under hypoxia from explant culture up to P2 CDCs, 3) acute hypoxia (short term hypoxia) – long term normoxic cells were exposed to hypoxia for the period of the assay (8 days), and 4) reoxygenation – long term hypoxic cells were returned to normoxia for the period of the assay (8 days). In each group, cells were plated at 1 x 10^5 cells/flask and were harvested at days 2, 4, 6 and 8 in triplicate. The number of cells harvested was calculated by an experimentally-blinded investigator (performed by Vanessa Fairchild).

In the first 4 days, there was no significant difference in the number of cells cultured under the four conditions, indicating that hypoxic preconditioning (chronic or acute) did not stimulate the cells to grow faster than those cultured under normoxia. By day 6, all the cells cultured under normoxia (reoxygenated group and long term normoxic group) had slowed growth as cell confluency was achieved. On the other hand, all the cells cultured under hypoxia (chronic hypoxic group and acute hypoxic group) kept proliferating beyond the point of confluency and therefore generated significantly higher viable cell numbers compared with the normoxic groups at day 6. This observation was maintained up to day 8 (Figure 4.7).

Chronic hypoxia increased cell numbers more than acute hypoxia at day 6 (chronic vs. acute = 5.1 ± 0.3 x 10^5 vs. 4.4 ± 0.1 x 10^5) ($p < 0.05$) and at day 8 (6.1 ± 0.5 x 10^5 vs. 4.9 ± 0.2 x 10^5). Furthermore, the response to hypoxia was reversible, as the

reoxgenated group showed a similar growth pattern to that of the long term normoxic group (Figure 4.5). These data indicated that hypoxic CDCs had increased proliferative potential, but this effect was not permanent and could be reversed by altering the oxygen levels.

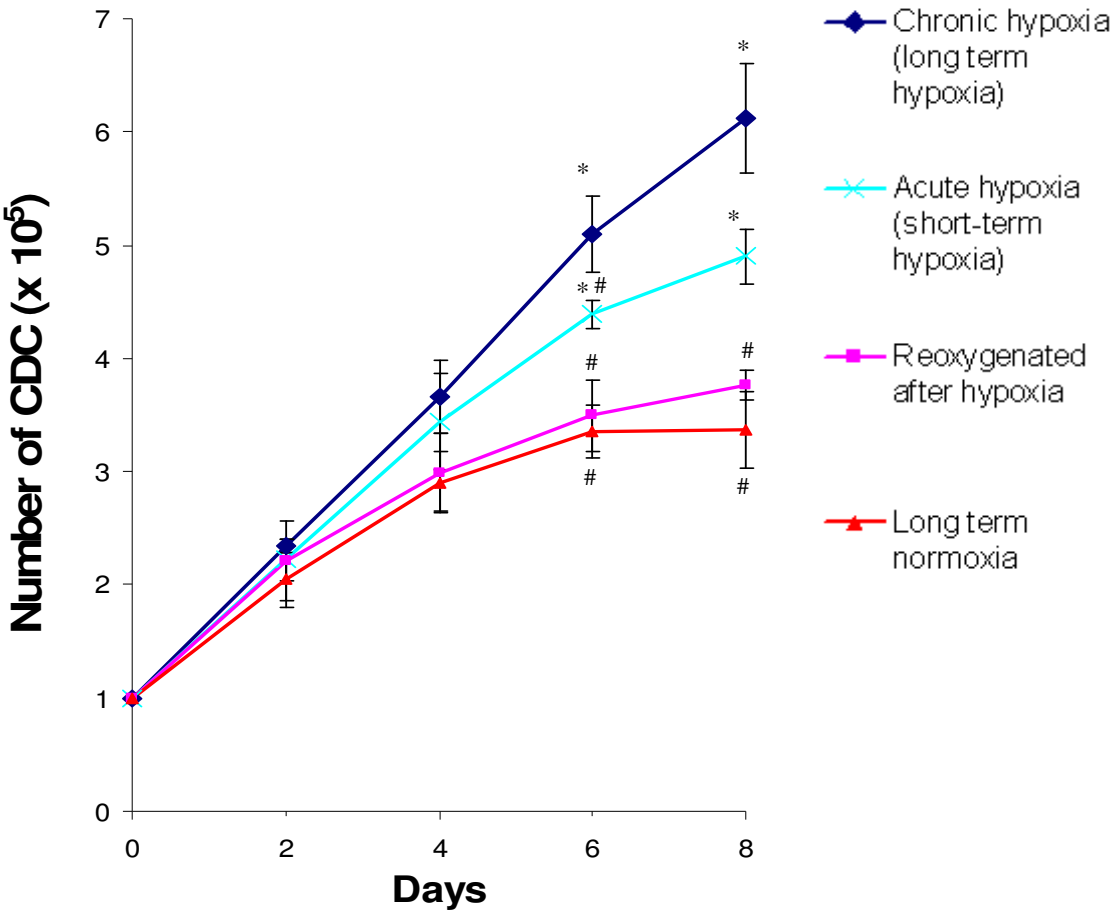

Figure 4.7 *Growth kinetics of P2 CDCs (n = 4) cultured under four different oxygen conditions: chronic hypoxia, acute hypoxia, reoxgenated after hypoxia and long term normoxia. For reoxygenated and long term normoxic groups, the growth rate was slowed after 4 days as confluency was achieved, while for the chronic and acute hypoxic groups, the low oxygen level stimulated cells to grow beyond the point of cell confluency, resulting in significantly higher cell numbers. * $p < 0.05$ vs long term normoxic group; # $p < 0.05$ vs. long term hypoxic group.*

4.4.2 Characterization of hypoxic CDCs

4.4.2.1 Hypoxic CDCs expressed HIF-1α and HIF-1α regulated genes

qRT-PCR results showed that CDCs cultured under hypoxia expressed significantly higher HIF-1α mRNA (2.1 ± 0.5-fold), compared with normoxic CDCs (Figure 4.8a). In line with this, HIF-1α protein levels were also found to significantly increase by 3.9 ± 0.7-fold in hypoxic CDCs, compared with normoxic CDCs (Figure 4.8b). The increased of HIF-1α mRNA was consistent with the HIF-1α protein levels, confirming that hypoxic treatment activate the CDC HIF system.

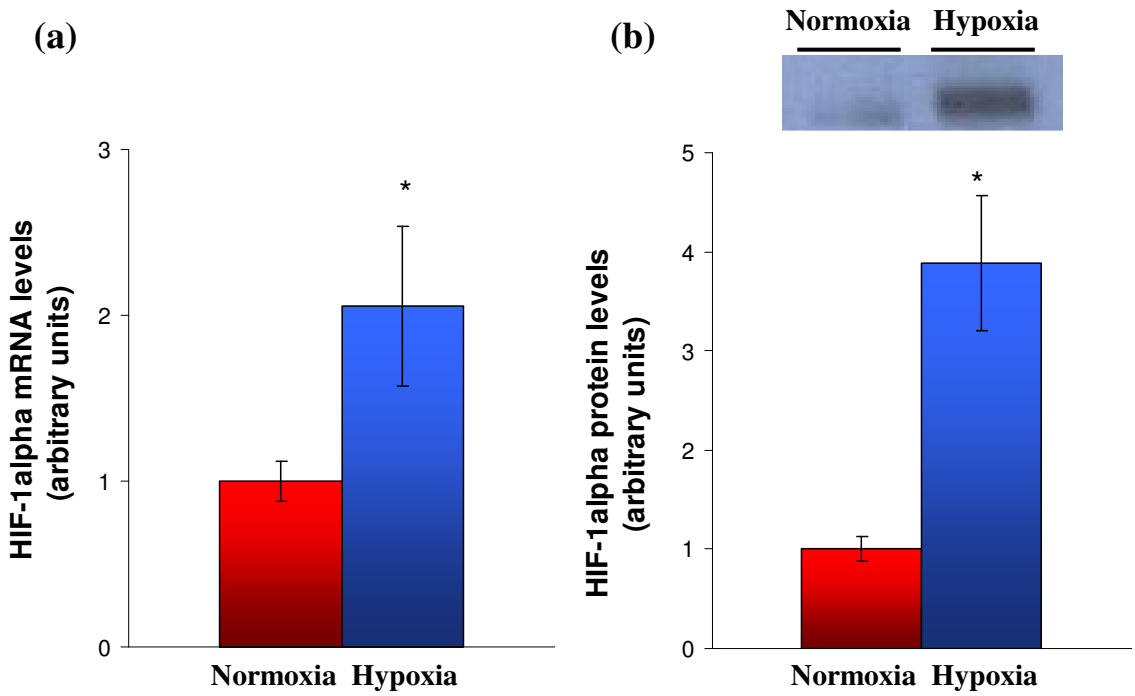

Figure 4.8 *The relative (a) mRNA and (b) protein expression of HIF-1α for normoxic and hypoxic neonatal P2 CDC (n = 4). mRNA and protein expression of hypoxic cells were expressed in arbitrary units, with hypoxic CDCs relative to normalized normoxic CDCs. * $p < 0.05$ vs. normoxia.*

Activation of HIF-1α under hypoxia subsequently upregulated several important HIF-regulated genes including EPO (2.1 ± 0.5-fold), VEGF (2.4 ± 0.7-fold), TERT (3.7 ± 0.7-fold) and CXCR-4 (4.3 ± 1.6) (Figure 4.9).

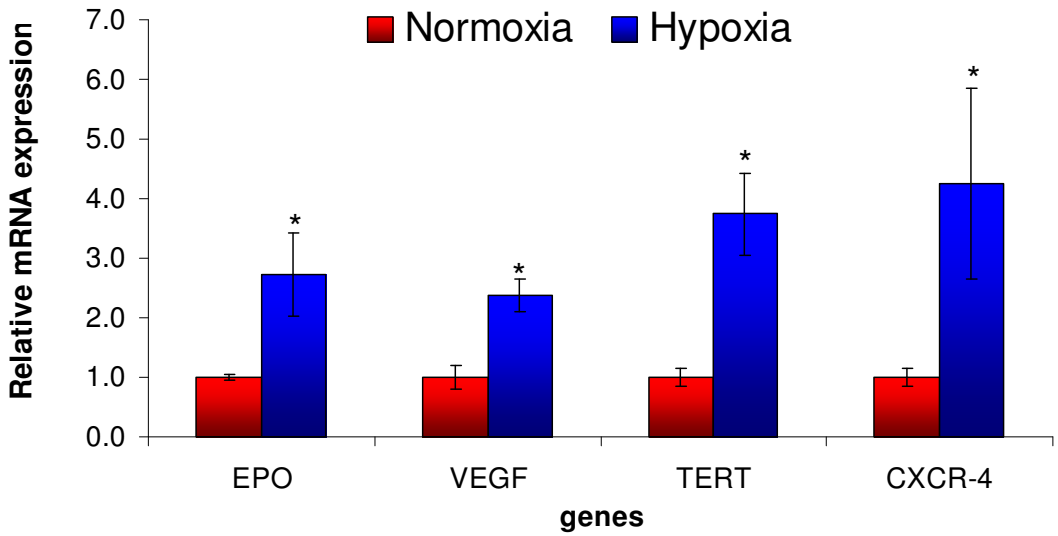

Figure 4.9 *The relative mRNA expression of EPO, VEGF, TERT and CXCR-4 for normoxic and hypoxic P2 CDC (n = 4) using qRT-PCR. mRNA expression in hypoxic cells was normalized to the geometric mean of GAPDH and Actb (housekeeping genes) and normoxic cells (calibrator). * $p < 0.01$ vs. normoxia.*

4.4.2.2 VEGF protein expression

Biologically active VEGF proteins secreted by CDCs from day 0 to day 5 after plating were measured using the VEGF ELISA kit to verify the transcriptional activation of the VEGF gene, as found in qRT-PCR (as shown in Figure 4.9), and also to determine the expression pattern of the VEGF protein over the culture period.

The VEGF ELISA assay revealed that VEGF protein accumulated in the CDC culture medium from day 2 after plating, and was elevated at day 3. Repeated Measures Anova validated the significant different of both normoxic and hypoxic curves. In agreement with the activation of transcription levels, the post translation level of VEGF was found to be significantly higher under hypoxia from day 2 up to day 5 (Figure 4.10).

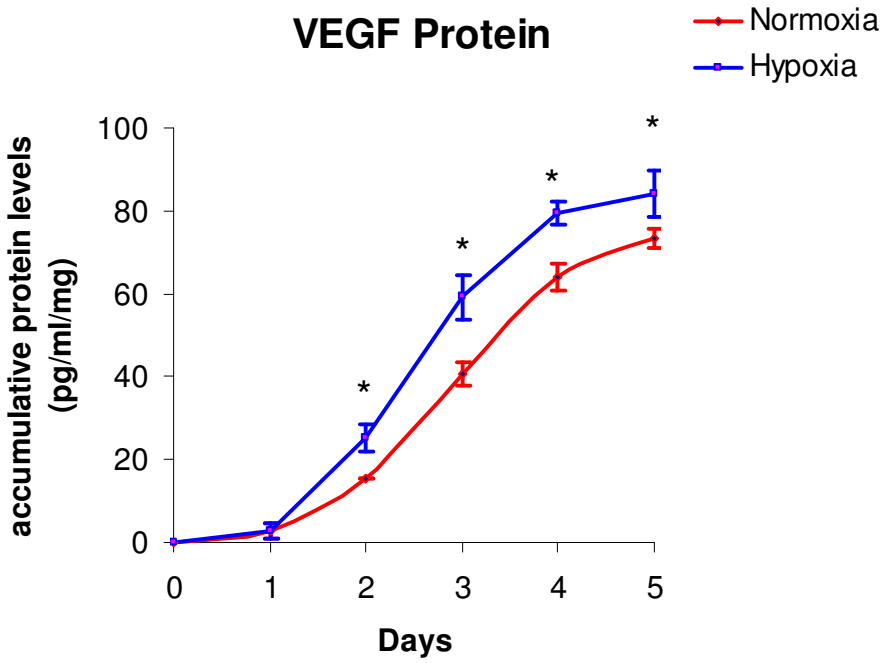

Figure 4.10 *The accumulative VEGF protein in normoxic and hypoxic CDCs (n = 3). Repeated Measures Anova validated the significant different between normoxic and hypoxic curves ($p < 0.05$). * $p < 0.01$ vs. normoxia at specific time point.*

4.4.2.3 Hypoxia increased cardiac stem cell markers in the CDC population

Under hypoxia, CDCs showed significant increases in c-Kit (2.0 ± 0.3-fold) and pluripotent markers, including Oct-4 (1.9 ± 0.3-fold), Klf4 (2.3 ± 0.4-fold), Nanog (3.1 ± 0.1-fold) and Sox 2 (3.8 ± 0.6-fold). On the other hand, under hypoxia, the expression of CD90 and CD105 was reduced by 36% and 66%, respectively. These data indicated that hypoxia increased the proportion of c-Kit$^+$ cardiac progenitor cells and of Oct-4, KLf4, Nanog and Sox 2 expressing progenitor cells and decreased the proportion of CD90$^+$CD105$^+$ mesenchymal cells (Figure 4.11 a-g).

The mRNA expression of cardiac differentiation markers (Nkx 2.5 and GATA 4) and the matured cardiomyocyte marker (Tnnt) was not significantly different after hypoxic treatment. However, hypoxic CDCs had significantly lower MyHC mRNA expression (0.4 ± 0.2-fold), compared with normoxic CDCs (Figure 4.11 h-k).

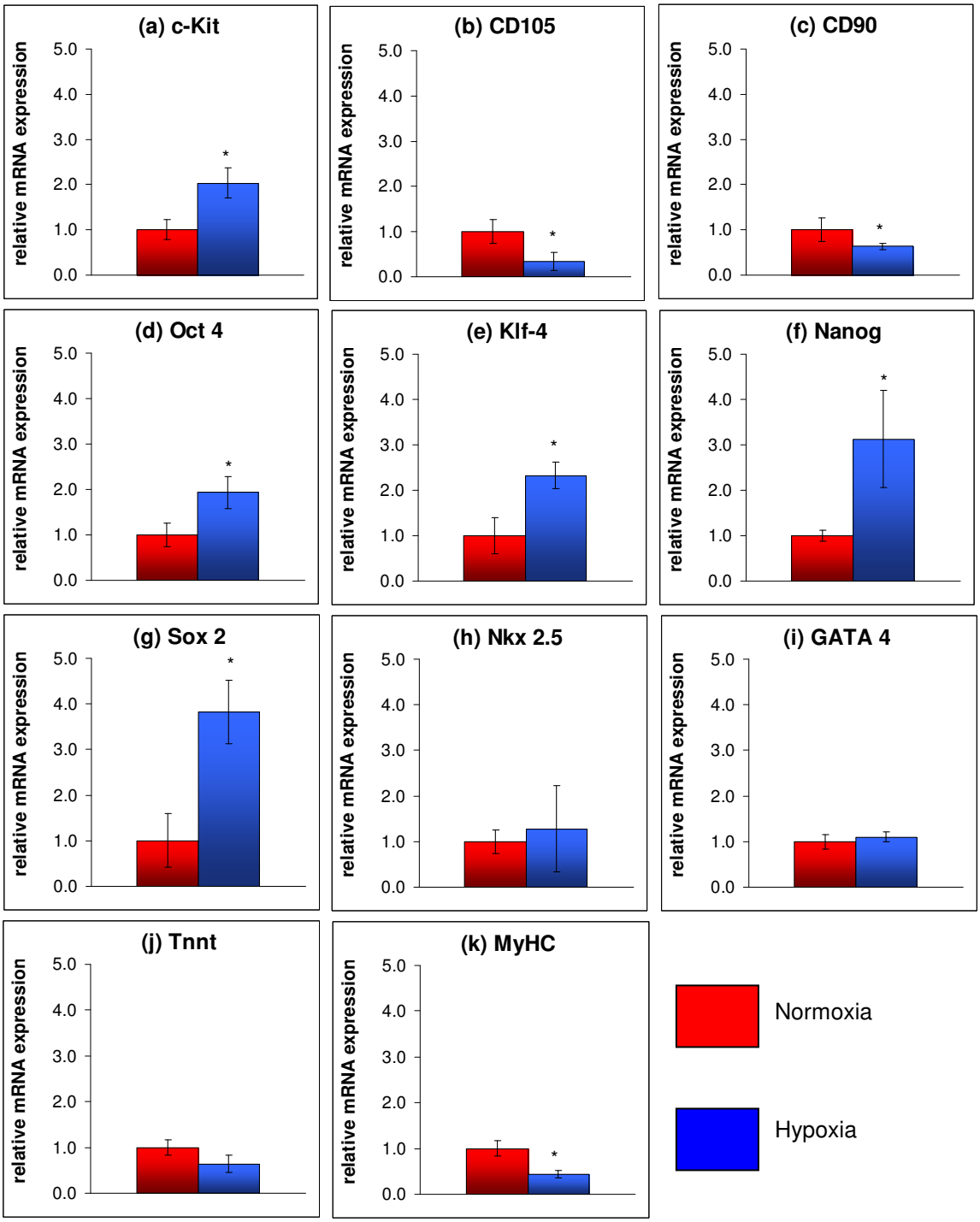

Figure 4.11 *The relative mRNA expression of (a) c-Kit, (b) CD105, (c) CD90, (d) Oct-4, (e) Klf-4, (f) Nanog, (g) Sox 2, (h) Nkx 2.5, (i) GATA 4, (j) Tnnt and (k) MyHC for normoxic and hypoxic P2 CDC (n=3) using qRT-PCR. Abundance of mRNA expression of hypoxic P2 CDCs was normalized to GAPDH and Actb (housekeeping genes) and normoxic P2 CDCs (calibrator). * $p < 0.01$ vs. normoxic P2 CDCs.*

4.4.3 Cardiosphere-derived cell differentiation

4.4.3.1 Adipogenesis

Hypoxic and normoxic P2 CDCs were subjected to adipogenesis using adipogenic induction medium (AIM) (Appendix 3) under normoxic culture conditions. After 3 cycles of adipogenic induction by AIM, some of the normoxic and hypoxic CDCs exhibited typical adipocyte morphology and stained positive with Oil Red O, confirming the differentiation of CDCs into adipocytes (Figure 4.12). To quantify the amount of adipocytes in AIM-treated normoxic and hypoxic CDCs, positive Oil Red O staining were eluted using isopropanol and the optical density (OD) was measured at 500 nm. The density of Red O Oil stain eluted from hypoxic CDCs was only 0.1-fold of that eluted from normoxic CDCs, indicating hypoxic preconditioning significantly diminished the ability of CDCs to be transdifferentiated into adipocytes (Figure 4.13)

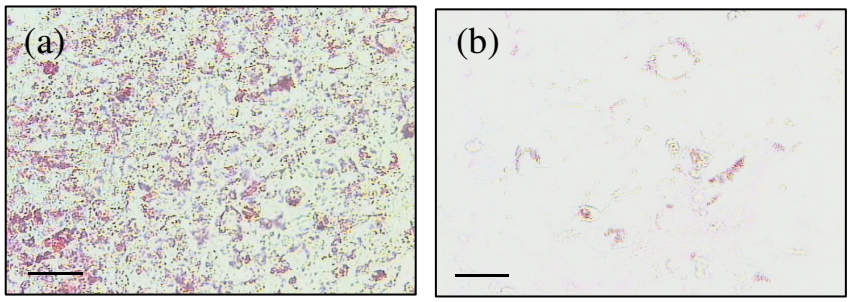

Figure 4.12 *Treatment with 3 cycles of adipogenic induction medium of (a) normoxic CDCs and (b) hypoxic CDCs caused differentiation into adipocytes, identified by staining with Oil Red O (10X). Scale bars = 200 μm.*

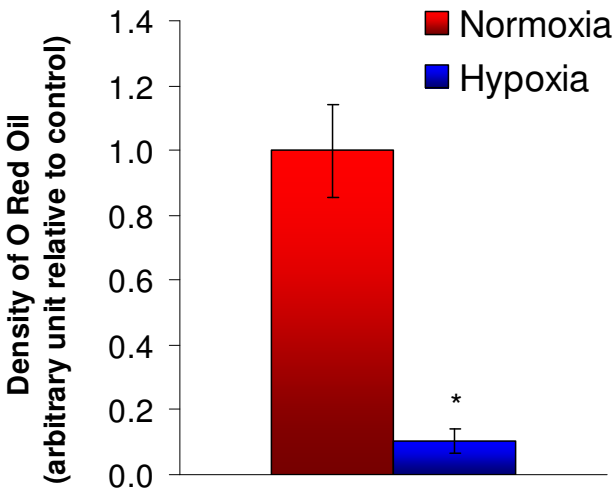

Figure 4.13 *Density of Red O Oil stain eluted from normoxic and hypoxic P2 CDCs subjected to adipogenesis (n = 4). Density of Red O Oil eluted from hypoxic CDCs was expressed relative to the normoxic CDCs (control group). * $p < 0.01$ vs. normoxia.*

4.4.3.2 Cardiomyocyte differentiation

Hypoxic CDCs were treated with either normal cell culture medium (negative control) or differentiation medium for 2 weeks. qRT-PCR showed that differentiation medium containing 5-aza significantly increased Nkx 2.5 and Tnnt mRNA expression by 2.2 ± 0.5-fold and 3.1 ± 0.2-fold, respectively, compared with non-treated hypoxic CDCs. Similarly, DMSO-treatment significant induced Nkx 2.5 (1.4 ± 0.1-fold) and Tnnt (2.0 ± 0.3-fold) mRNA levels, compared with non-treated hypoxic CDCs. These results indicated that hypoxic CDCs were able to differentiate into cardiomyocytes when treated with cardiomyogenic stimuli (Table 4.1 and Figure 4.14).

Table 4.1 *The relative mRNA expression of Nkx 2.5, Tnnt and MyHC in (a) non-treated hypoxic CDC, (b) 5-aza-treated hypoxic CDCs and (c) DMSO-treated hypoxic CDCs (n = 3). mRNA expression of 5-aza- and DMSO-treated hypoxic cells was normalized to the geometric mean of GAPDH and Actb (housekeeping genes) and non-treated hypoxic cells (calibrator) * p < 0.05 vs. non-treated hypoxic CDCs.*

Genes	(a) Non-treated hypoxic CDCs	(b) 5-aza-treated hypoxic CDCs	(c) DMSO-treated hypoxic CDCs
Nkx 2.5	1.0 ± 0.1	2.2 ± 0.5*	1.4 ± 0.1*
Tnnt	1.0 ± 0.3	3.1 ± 0.2*	2.0 ± 0.3 *
MyHC	1.0 ± 0.5	2.0 ± 0.4	1.8 ± 0.3

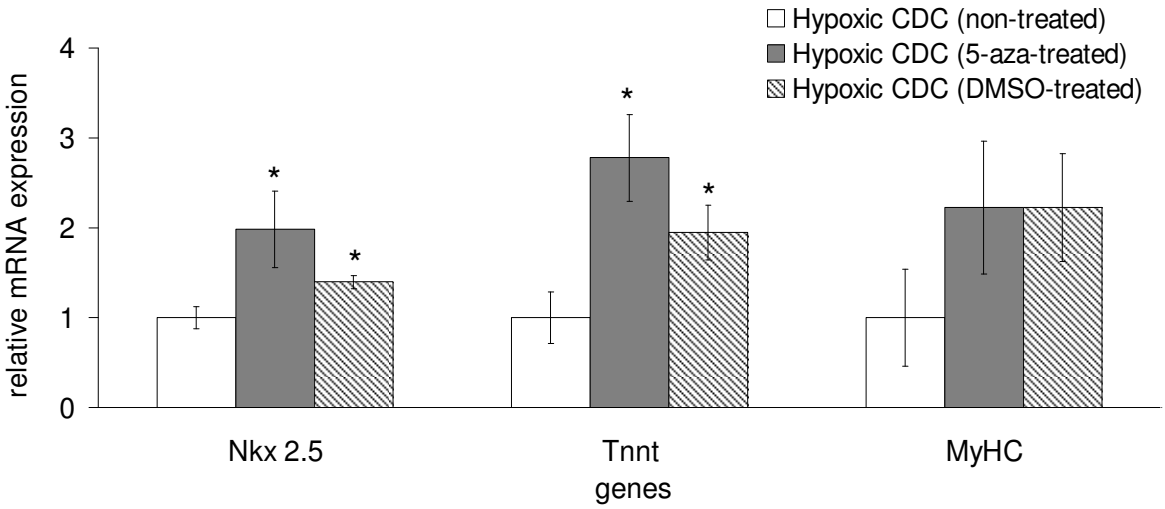

Figure 4.14 *The relative mRNA expression of Nkx 2.5, Tnnt and MyHC for non-treated, 5-aza-treated and DMSO-treated hypoxic P2 CDCs (n = 3). mRNA expression of 5-aza- and DMSO-treated hypoxic cells was normalized to the geometric mean of GAPDH and Actb (housekeeping genes) and non-treated hypoxic cells (calibrator). * p < 0.05 vs. non-treated hypoxic CDCs.*

However, it was found that the levels of Nkx 2.5, Tnnt and MyHC in 5-aza–treated hypoxic CDCs were significantly lower by 68%, 58% and 61%, respectively, compared to 5-aza–treated normoxic CDCs (Table 4.2 and Figure 4.15). Similarly, the DMSO-treated hypoxic CDCs also showed significantly lower Nkx 2.5 (60%), Tnnt (45%) and MyHC (40%), compared to DMSO-treated normoxic CDCs (Figure 4.15).

Taken together, these findings indicated that cells cultured under hypoxia retained the ability to differentiate into cardiomyocytes, however, this ability was attenuated after hypoxia culture.

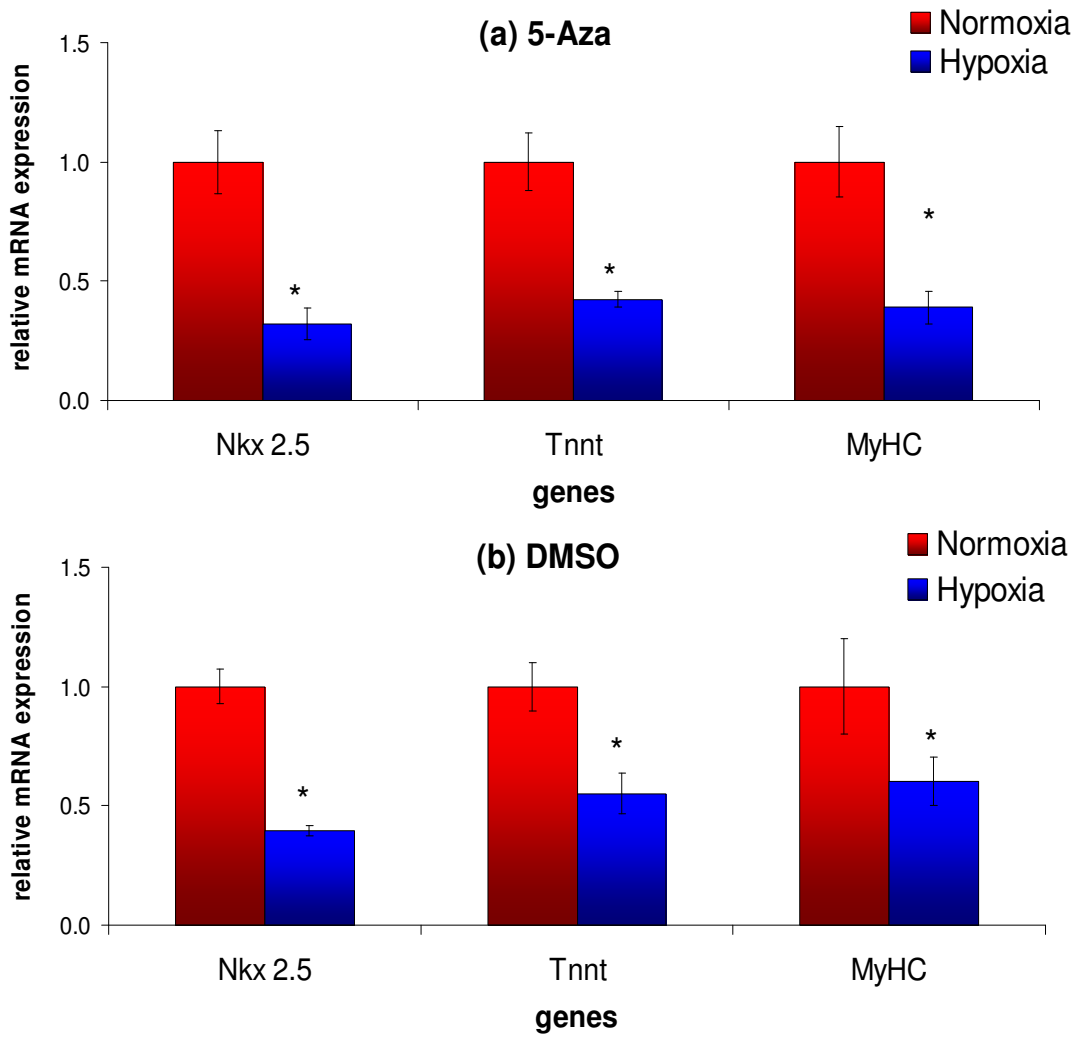

Figure 4.15 *The relative mRNA expression of Nkx 2.5, Tnnt and MyHC for normoxic and hypoxic neonatal P2 CDC (n = 3) after treatment with cardiomyogenic induction medium containing (a) 5-Aza and (b) DMSO for 2 weeks. mRNA expression of hypoxic cells was normalized to the geometric mean of GAPDH and Actb (housekeeping genes) and normoxic cells (calibrator). * $p < 0.05$ vs. normoxia.*

4.4.4 Metabolism of hypoxic CDCs

4.4.4.1 Reduced oxygen uptake by hypoxic CDCs

Cellular oxygen consumption was measured after acute (24 hours) and chronic (4 days or long term) exposure to hypoxia. A schematic diagram of an oxygen consumption trace in long term normoxic CDCs and long term hypoxic CDCs is shown in Figure 4.16.

The basal respiration rates were significantly reduced by 49% after 24 hours under hypoxia, 75% after 4 days under hypoxia and 82% under long term hypoxia. The respiration rates were also significantly reduced after the addition of substrate, indicating that hypoxic cells had adapted to the lower oxygen condition by reducing oxidative metabolism, independent of substrate supply (Table 4.3 and Figure 4.17).

Subsequently, cells were treated with oligomycin, an inhibitor of ATP-synthase which halted electron transport in mitochondria and reduced oxidative phosphorylation of ADP to ATP. In the presence of oligomycin, mitochondrial respiration was inhibited and all normoxic and hypoxic cells showed the same oxygen respiration rate (Table 4.3).

Respiration was then maximally stimulated by adding carbonyl cyanide p-trifluoromethoxyphenylhydrazone (FCCP) to the cells. FCCP is an uncoupling agent which dissipates the proton gradient across the mitochondrial inner membrane and restores more rapid oxidative respiration to synthesize more ATP. Although the respiration rates increased in all cells after the addition of FCCP, the respiration rates remained low in hypoxic cells, compared with normoxic cells. Respiration rates were significantly reduced by 51% in 24 hour hypoxic cells, 62% in 4 days hypoxic cells

and by 80% in long term hypoxic cells, compared with normoxic cells (Table 4.3 and Figure 4.17).

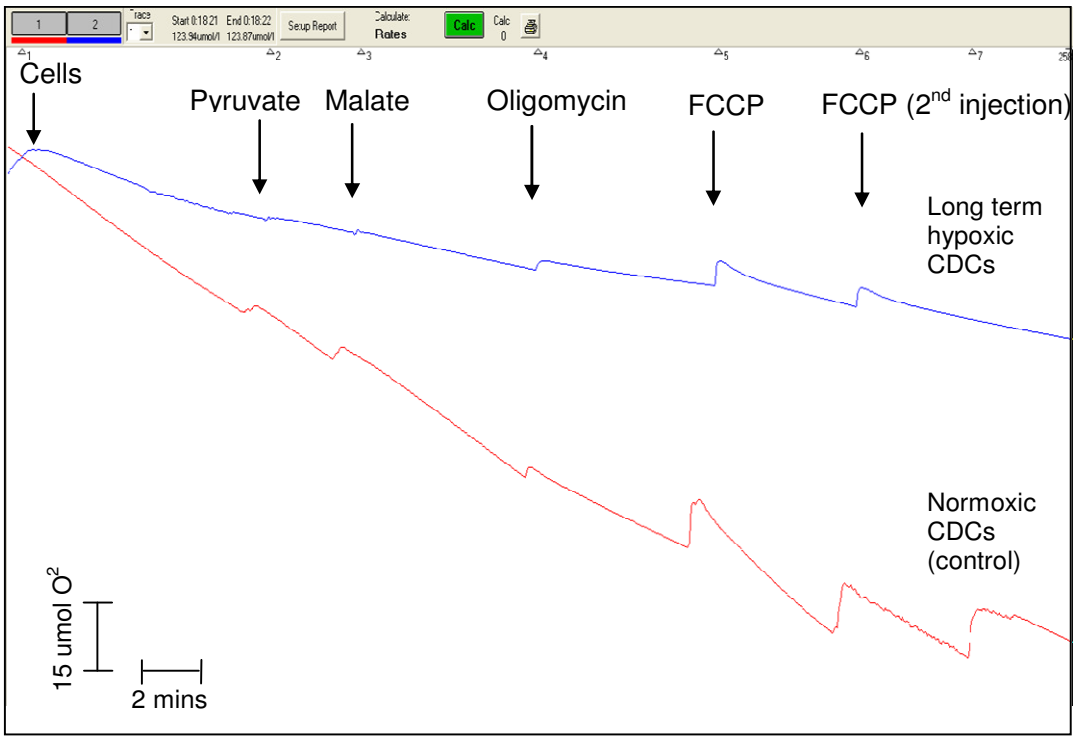

Figure 4.16 *Representative oxygen consumption recording of long term normoxic CDCs (red line) and long term hypoxic CDCs (blue line). The Y axis represents the amount of remaining oxygen detected by the Clarke-type electrode, the X axis represents the time period. The amount of oxygen decreased over time as cells took up oxygen for metabolism. Cell respiration rates were measured based on the slope of the trace. Arrows indicate time points when cells (normoxic or hypoxic CDCs), pyruvate, malate, oligomycin or FCCP were injected into the oxygen chambers.*

Table 4.3 *Oxygen consumption measurements in long term normoxic, 24 hour hypoxic, 4 day hypoxic and long term hypoxic P2 CDCs (n = 3). All measurements were standardised to nmol of oxygen uptake per min per milligram of protein present (nmol O_2/min/mg protein). * $p < 0.05$ vs. normoxia (control).*

	Normoxia (control)	**24 hour hypoxia**	**4 day hypoxia**	**Long term hypoxia**
Basal	13.4 ± 1.7	6.8 ± 0.7 *	3.3 ± 0.3 *	2.4 ± 0.8 *
Substrate-stimulated respiration	13.7 ± 2.4	6.3 ± 1.7 *	3.2 ± 0.7 *	3.2 ± 0.9 *
Oligomycin	6.2 ± 3.0	3.7 ± 1.0	2.2 ± 0.5	1.8 ± 0.5
FCCP-uncoupled respiration	22.8 ± 2.9	11.1 ± 0.3 *	8.6 ± 2.5 *	4.4 ± 0.6 *

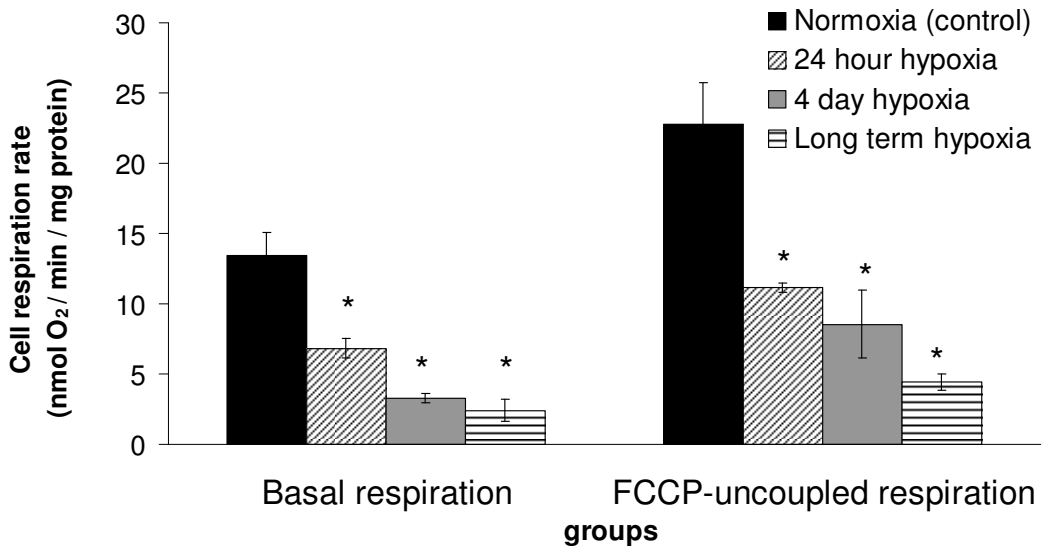

Figure 4.17 *Basal and FCCP-uncoupled respiration rates of normoxic (control), 24 hour hypoxic, 4 day hypoxic and long term hypoxic P2 neonatal CDCs (n = 3). * $p < 0.05$ vs. normoxia (control).*

4.4.4.2 Hypoxia did not change citrate synthase protein levels

Citrate synthase is a quantitative enzyme marker for the presence of intact mitochondria. Under long term hypoxia, the protein levels of citrate synthase were not significantly different to those of the normoxic controls, suggesting that hypoxia did not alter the number of intact mitochondria in CDCs (Figure 4.18).

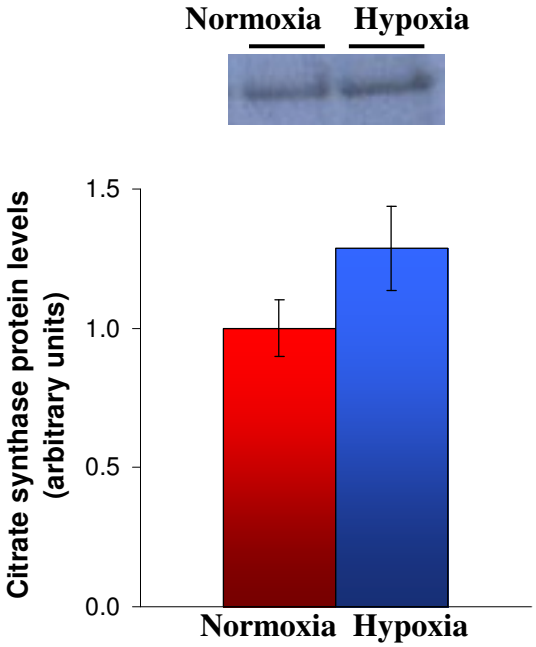

Figure 4.18 *Citrate synthase protein expression in normoxic and hypoxic neonatal P2 CDCs (n = 4). Protein levels were expressed in arbitrary units, with hypoxic CDC expressed relative to normalized normoxic CDC averages. No significant difference in citrate synthase protein levels were detected between normoxic and hypoxic CDCs.*

4.4.4.3 Effects of hypoxia on glucose metabolism in CDCs

Western blot analysis revealed that neonatal CDCs expressed negligible levels of the insulin sensitive GLUT-4 protein, whereas GLUT-1 protein was clearly detected (Figure 4.19). The expression level of GLUT-1 protein was increased by 7 ± 2-fold under hypoxia, compared to normoxia (Figure 4.20).

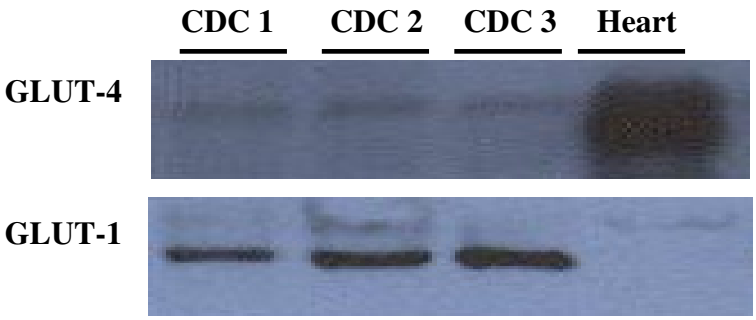

Figure 4.19 *Western blot showing that CDCs expressed GLUT-1 but not GLUT-4 (n = 4). Neonatal SD rat heart lysates were used as positive controls. CDC1 = cardiosphere-derived cell lysate replicate 1; Heart = rat heart lysate.*

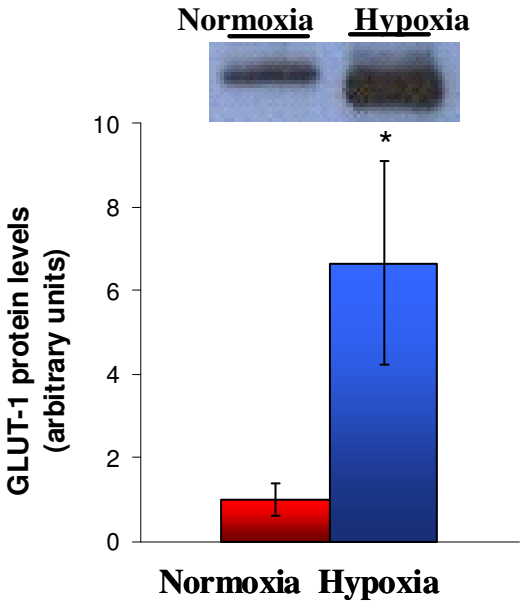

Figure 4.20 *GLUT-1 protein expression in normoxic and hypoxic neonatal P2 CDCs (n = 4). Protein levels were expressed in arbitrary units, with hypoxic CDC expressed relative to normoxic CDCs. * $p < 0.05$ vs. normoxia.*

Culture medium was collected from normoxic and hypoxic CDCs at 24 hours and 4 days. Glucose consumption and lactate production rates in neonatal CDCs expanded under different oxygen tensions were determined. Over 24 hours, hypoxic CDCs utilized 4 ± 1 mM glucose per million cells, 48% more than normoxic CDCs. At day 4,

glucose utilization remained higher by 60% in hypoxic CDCs, compared with normoxic CDCs (Figure 4.21a). In line with this, hypoxic CDCs produced 10 ± 1 mM lactate per million cells after 24 hours under hypoxia, 51% more than those produced under normoxia. At day 4, the lactate production rate of hypoxic CDCs was 59% higher than normoxic CDCs (Figure 4.21b).

Taken together, these data suggest that under hypoxia, CDCs adapted to low oxygen conditions by reducing oxygen consumption, increasing the expression of GLUT-1 and switching into glycolytic metabolism, indicated by the increased glucose consumption and lactate production.

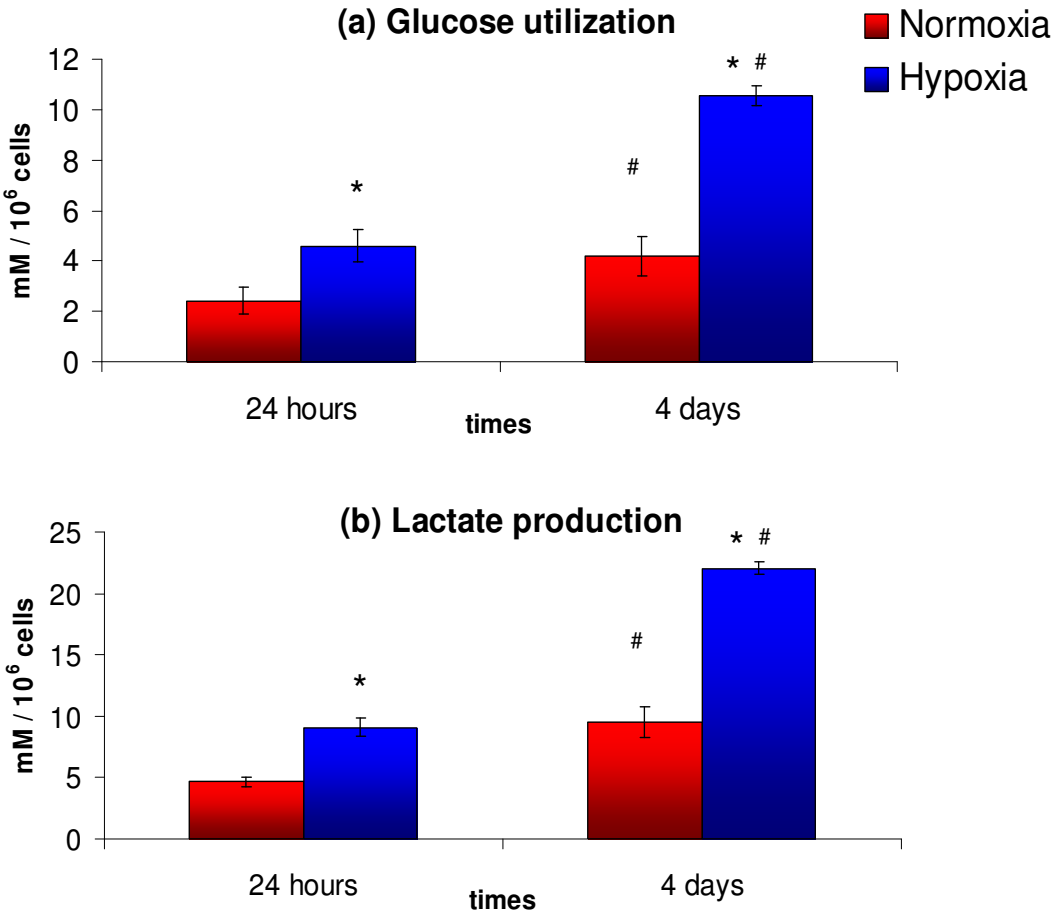

Figure 4.21 *Levels of (a) glucose utilization and (b) lactate production in normoxic and hypoxic CDCs at 24 hours and 4 days after passaging (n = 3). Glucose utilization and lactate production are expressed as mM of glucose/lactate per million cells. * $p < 0.05$ vs. normoxia. # $p < 0.05$ vs. 24 hours.*

4.5 Discussion

The work in this chapter determined the effects of oxygen as an important factor in cardiac stem cell proliferation, differentiation, gene expression and metabolism.

Hypoxia increased cardiac progenitor cell proliferation rates

As hypothesized, the proliferation rates of EDCs and CDCs were significantly increased under hypoxia. There was an almost 2-fold increase in EDC and CDC cell numbers in hypoxia compared to those cultured under normoxia. Moreover, larger cardiosphere cell clusters were formed under hypoxia, in agreement with studies that showed that low oxygen environments enhanced stem cell division or proliferation [188, 198, 199].

It was found that EDCs expressed c-Kit, as reported by others [107, 200, 201]. Although hypoxic pre-treatment did not induce a significant increase in c-Kit gene expression after EDC culture, rapid cell proliferation of hypoxic EDCs could be beneficial for clinical application as rapid culture of stem cells is crucial. Longer cell expansion time *in vitro* could lead to loss of c-Kit expression [202, 203]. Therefore, we postulated that hypoxia is important to rapidly expand better quality EDCs.

EDCs formed three-dimensional (3D) spheroids in culture, with hypoxic EDCs generating bigger spheres, compare with normoxic EDCs. The larger sizes of hypoxic cardiospheres most likely resulted from rapid proliferation of cardiac stem cells in the core of the sphere. Our hypothesis was supported by Li *et al.,* who suggested that cardiospheres are cellular aggregates that structurally provide 3D, niche-like microenvironments that favour c-Kit cell proliferation in the interior core of the spheres [204]. Under hypoxia, cardiospheres showed a significant increase in the expression of vascular endothelial growth factor (VEGF), raising the possibility that

hypoxic pre-treatment improves the cardiosphere's ability to generate vascular networks [205]. This is in agreement with Bartosh *et al.* [206] who also demonstrated a size-dependent increase of VEGF transcription in cardiospheres and that differentiation of these cells in microvascular endothelial cell medium induced the formation of vascular endothelial and smooth muscle cell types with the potential to form vascular networks.

It has been estimated that 10^8-10^9 CDCs need to be effectively delivered to the human heart to repair a medium-sized infarct [207]. *In vitro* expansion of CDCs under hypoxia successfully yielded adequate cell numbers for transplantation within 21 days, a week faster than those cultured under normoxia. Investigation of the CDC growth kinetics revealed that the hypoxic environment improved CDC expansion by inducing a proliferative state beyond the confluency point, when normoxic CDC growth was halted due to inhibitory signals [188, 208]. The cancer cell-like limitless replicative potential of the hypoxic CDCs maybe due to the hypoxia-induced upregulation of c-Myc transcriptional activity, which promotes cell cycle progression and contributes to tumor growth in many cancer cell types [209]. c-Myc overexpression stimulates cell proliferation, presumably through DNA over-replication without entering the cell senescent phase [210]. This is supported by our finding that the enzyme activity of telomerase reverse transcriptase (TERT) was upregulated under hypoxia. TERT is a reverse transcriptase that synthesizes telomere repeats on the telomere ends at the tips of chromosomes, protecting the chromosomes from deterioration and also maintaining the overall genomic stability [92, 93]. In various types of stem cells, telomerase functions to ensure long term self-renewal capacity via maintenance of telomere length [94, 95]. In this study, it is possible that hypoxic CDCs bypassed the cell senescence arrest by activating telomerase. As a consequence, hypoxic CDCs generated more cells

compared to normoxic CDC culture. However, unlike cancer cells, the proliferative effect was not permanent in CDCs *in vitro*. CDCs response to hypoxia was reversible, as reoxygenated CDCs changed to the normal cell growth pattern under normoxic culture. This is important in eliminating the possibility of uncontrollable cell proliferation, or teratoma formation, after transplantation.

Hypoxia increased c-Kit$^+$ cardiac progenitor cells and reduced CD90$^+$CD105$^+$ cardiac mesenchymal cells in the CDC population

In *Chapter 3*, normoxic CDCs at passage 2 were found to be functionally competent. However, their therapeutic effects may be limited by the relatively low c-Kit level [108]. Here, hypoxic preconditioning successfully increased the proportion of c-Kit$^+$ cardiac progenitor cells and reduced the CD90$^+$CD105$^+$ cardiac mesenchymal cells, enhancing the therapeutic potential of CDCs with a shorter culture period. In other studies, implantation of cells cultured under 5% oxygen into infarcted hearts of mice resulted in greater cell engraftment and better functional recovery than with conventionally cultured cells [211]. However, the 2% oxygen culture used in this study is more relevant to stem cell niche [212, 213], thus, an *in vivo* study is planned to inject hypoxic cells cultured at 2% oxygen into infarcted rat hearts.

Hypoxia maintained CDC pluripotency and diminished differentiation in vitro

Stem cells are characterized by the ability to self-renew and differentiate into specific cell types. In a balanced niche, adult stem cells maintain self-renewal and provide a long-lived ability to generate pluripotent cells [214]. Genes such as Oct-4, Klf-4, Sox 2 and Nanog are among the essential factors for maintaining stem cell pluripotency. The expression of these genes in CDCs was elevated under hypoxia, in agreement with previous findings [164, 188, 215, 216]. In line with this, the adipogenic and cardiomyogenic ability of CDCs was attenuated under hypoxia, suggesting that

undifferentiated cell proliferation was favoured [184, 188]. Conversely, some investigators have argued that hypoxia is a potent stimulus for differentiation in other stem cell types [217, 218]. But, as suggested by Abdollahi *et al.*, [219], the stem cell differentiation potential under hypoxia is likely to be cell-type dependent. For example, Fink *et al.* demonstrate that culture in 1% oxygen induced an adipose phenotype in bone marrow-derived mesenchymal stem cells [220], while Csete *et al.* reported that skeletal muscle stem cells were more likely to undergo myogenesis than adipogenesis in lower oxygen, compare with 20% oxygen [221]. Yun *et al.,* reported that 2% oxygen inhibited adipocyte differentiation of mouse embryonic fibroblasts (MEF) [222], in agreement with the data here. In brief, the effect of the oxygen concentration on cell differentiation involves a more complex mechanism and a further investigation on the detailed pathway of cardiac stem cell differentiation under hypoxia is required.

Hypoxia stimulated cytokine production in CDCs

(i) VEGF and EPO

Preconditioning under hypoxia significantly increased HIF-1α mRNA expression in EDCs, Csp and CDCs, as shown in previous studies [198, 199, 223-225]. HIF-1α is a potent inducer of several important cytokines *in vitro*. Ramirez-Bergeron *et al.* [226] showed that HIF-1α was stabilized prior to the induction of VEGF expression during acute ischemia in the human heart and Beguin *et al.* [227] demonstrated that intense EPO stimulation was produced by prolonged hypoxia. Here, hypoxic preconditioning elevated VEGF and EPO mRNA levels and induced secretion of biologically active VEGF protein in CDC culture. As shown in the previous chapter, following infarction, the myocardium surrounding the infarcted area comprised a hostile environment with few blood vessels and a large number of invading inflammatory cells [228]. The hypoxic nature of the tissue may cause apoptosis of the administered cells and limit the

effectiveness of cardiac cell therapy. Thus, transplantation of hypoxic CDCs expressing the paracrine factors, VEGF and EPO, could optimize the cell therapy by stimulating angiogenesis in the infarcted area [226, 229-231].

(ii) CXCR4

After infarction, the ischemic heart produces numerous cytokines, chemokines, and growth factors that may influence stem cell–mediated repair [232, 233]. As shown by Dr. Daniel Stuckey in previous work [234], levels of stromal cell–derived factor (SDF)-1 in rat heart tissue peaked at day 1 and remained elevated at day 3 post infarction. SDF-1 is critically involved in the recruitment and tissue retention of hematopoietic cells, based on the interaction with its receptor, CXC chemokine receptor 4 (CXCR4) [117, 118]. Here, the expression of CXCR4 was upregulated in hypoxic CDC culture, demonstrating hypoxic preconditioning could increase the recruitment of intravenously administered CXCR4 expressing CDCs to the SDF-1 expressing ischemic myocardium, therefore resulting in higher cell retention rate in the infarcted heart and enhancing the benefit of CDC therapy for treatment of myocardial infarction.

Hypoxic CDCs switched to glycolytic metabolism with reduced oxygen uptake and increased glucose utilization and lactate production

The glucose transporter (GLUT) family comprises integral membrane transport proteins that catalyze the entry of monosaccharide sugars such as glucose into mammalian cells [235]. In this study, CDCs isolated from rat hearts showed very low expression of insulin-sensitive GLUT-4, which is commonly expressed in heart tissue [236]. On the other hand, GLUT-1 was expressed in CDCs and the expression of this isomer was elevated under hypoxia, coinciding with an increase in glucose uptake and

lactate production. In addition, hypoxic CDCs had reduced oxygen uptake, despite the presence of intact mitochondria at similar levels to those found in the normoxic CDCs. Taken together, hypoxic CDCs had a metabolic switch from mitochondrial oxidative phosphorylation to glycolysis for adenosine triphosphate (ATP) generation, as an adaptation to the low oxygen condition [237]. Under glycolytic metabolism, more than 90% of the glucose carbons are converted to lactate to generate only 2 ATP [238, 239]. Although the yield of ATP per glucose was low, in proliferating cells cultured in abundant glucose but low oxygen, high glycolytic flux could produce ATP at levels that exceed that produced from oxidative phosphorylation in the mitochrondia to support the proliferative state of the cells [240-243]. Here, high glycolytic flux was shown by the increase in glucose uptake and lactate production.

4.6 Conclusion

These results provide important insights into how hypoxic culture favors the expansion of rat cardiac stem cells *in vitro,* which would be advantageous for the maximization of cell yield in a clinical-scale cardiac stem cell expansion process. Hypoxia mimics the stem cell niche and generated stem cell with enhanced stemness properties, indicating by upregulation of cardiac stem cell marker, c-Kit and pluripotent cell markers, Oct-4, Klf-4, Nanog and Sox 2 and a downregulation of differentiation potential. Hypoxia also activated the expression of HIF-1α and its regulated genes, increased the expression of therapeutic cytokines, EPO and VEGF and of CXCR-4 which is involved in stem cell homing. Hypoxic cells had reduced oxygen respiration and adapted anaerobic metabolism, and thus could survive better in the hypoxic infarcted myocardium after transplantation. In conclusion, hypoxic preconditioning of CDCs optimizes their potential for therapy and could have a direct clinical impact on the treatment of myocardial infarction.

Chapter 5

HIF-1α Stabilization using

Prolyl-4-hydroxylase Inhibitors

5.1 Abstract

In *Chapter 4*, it was shown that hypoxic preconditioning generated CDCs with greater therapeutic potential *in vitro*. Here, low molecular weight inhibitors of hypoxia-inducible factor (HIF) prolyl-4-hydroxylases (PHD) were used to mimic the effects of hypoxic preconditioning. The potential utility of three PHD inhibitors (PHDIs): dimethyloxaloylglycine (DMOG), ethyl 2-(2,3-dihydroxybenzamido)acetate (EDBA) and 2-(1-chloro-4-hydroxyisoquinoline-3-carboxamido) acetic acid (BIC), to activate the CDC HIF system were investigated. This was the first study using PHDIs for HIF activation in CDC culture, thus a careful time-dose cytoxicity test was performed to determine a sublethal PHDI concentration and culture period. The optimal PHDI treatment for CDCs, with respect to their negative cytotoxicity effects and optimal potential to activate HIF-1α and GLUT-1 expression, was found to be 1 mM DMOG, 0.5 mM EDBA and 30 μM BIC for 24 hours. Cell proliferation was not affected by PHDI treatment over this time period. Coincident with GLUT-1 upregulation, PHDI-preconditioned CDCs showed decreased oxygen consumption and increased glucose uptake and lactate production, indicating that CDCs had adapted to the PHDI-induced 'hypoxic' condition by reducing oxygen consumption and switching to glycolytic metabolism. Further, EDBA significantly increased c-Kit mRNA levels by 1.5-fold and all three PHDIs significantly reduced cardiac mesenchymal cell markers, CD90 and CD105, giving an increased cardiac stem cell population in CDC culture. In addition, all three PHDIs significantly induced the expression of CXCR-4. EPO mRNA was increased in CDCs treated with EDBA (2.1-fold) and BIC (2.5-fold) while VEGF mRNA was increased in those treated with DMOG (2.9-fold) and EDBA (2.8-fold), compared with controls. DMOG and BIC treatment showed no significant effects on the potential for cardiomyogenic differentiation, but EDBA-treated CDCs showed a significantly reduced Tnnt protein level after induction of differentiation using 5-azacytidine. In conclusion, DMOG, EDBA and BIC stabilized and activated HIF, which induced metabolic changes and several important cytokines in the CDCs. This work could improve the potential of CDC therapy for myocardial infarction.

5.2 Introduction

Preconditioning of stem cells to enable survival in the hypoxic environment has been postulated to improve cell retention within the infarcted heart [244]. It has been shown by us and others, that hypoxic preconditioning activated hypoxia-inducible factor (HIF) and its regulated genes, resulting in broad changes encompassing a wide variety of cellular processes, including stem cell proliferation, differentiation, cytokine production and energy metabolism, thereby generating cardiosphere-derived cells (CDCs) with possibly greater potential for cell therapy [211]. A study using hypoxic CDCs in the infarcted mouse heart supports this hypothesis by demonstrating efficacy of hypoxic CDCs to generate greater cell engraftment and better functional recovery after transplantation [211].

HIF activation is negatively regulated by the prolyl-4-hydroxylase (PHD) enzyme, a conserved subfamily of dioxygenases that catalyzes the post-translational hydroxylation of specific prolyl residues of HIF-α subunits. Upon hydroxylation, the HIF-1α subunit is recognized by the von Hippel-Lindau protein which targets the subunit to proteasomal degradation and thus deactivates the HIF system [119, 245-249]. PHDs are identified as a crucial target to augment the transcriptional activity of HIF and subsequently activate the adaptive machinery regulating oxygen homeostasis in cells. While oxygen concentration plays a major role in determining the efficiency of PHD-catalyzed reactions, the sensitivity of PHD hydroxylase capacity also depends on its co-substrate, 2-oxoglutarate and co-factor, iron. Thus, inhibition of the 2-oxoglutarate or iron could inhibit the PHD activity and thus potently activate the HIF response [124-127].

Here, three different prolyl-4-hydroxylase inhibitors (PHDIs) were used for HIF stabilization in CDC culture, dimethyloxaloylglycine (DMOG) – a cell permeable,

competitive inhibitor of 2-oxoglutarate [125], ethyl 2-(2,3-dihyroxybenzamido) acetate (EDBA) – an aspirin metabolite that acts as an iron chelator to activate the HIF system via generic 2-oxoglutarate oxygenase inhibition [250] and 2-(1-chloro-4-hydroxyisoquinoline-3-carboxamido)acetic acid) (BIC, also known as FibroGen 2216, FG2216) – a specific PHD inhibitor patented by FibroGen Inc. which has been used in clinical trials as a pro-angiogenic compound acting via the HIF-1α system [126]. This study was a novel study investigating the effects of PHDI-treatment on CSCs. EDBA was an in-house PHDI synthesized by our collaborators, Kar Kheng Yeoh and Prof. Chris Schofield from the Chemistry Research Laboratory, University of Oxford and this was the first application of this PHDI for cardiac stem cell research. One of the advantages of stimulating an hypoxic response by using PHDIs was that manipulation using a pharmaceutical maybe more practical and specific to scale up rather than physiological manipulation of oxygen levels. Our hypothesis was that chemical inhibition of PHDs results in stabilisation of HIF and the associated genetic modifications, mimicking the effects of hypoxic preconditioning.

Inhibition of PHDs has been shown to be a promising drug target in the treatment of diseases such as myocardial infarction, stroke, peripheral vascular disease, inflammation, diabetes and severe anemias, as inhibition of PHDs activates the HIF response and thereby generates beneficial angiogenesis [251, 252]. Here we investigated the effects of PHDI treatment on CDC to enhance the therapeutic potential for myocardial infarction.

The aims of this study were to:

- Mimic hypoxic preconditioning using three different prolyl-4-hydroxylase inhibitors (PHDIs): DMOG, EDBA and BIC.
- Determine the optimal concentration and culture period of DMOG, EDBA and BIC for CDC culture.
- Investigate the stem cell self-renewal/proliferation and differentiation after PHDI preconditioning.
- Investigate the effects of hypoxic preconditioning on cell respiration and metabolism.
- Characterize the gene expression profile of PHDI-treated CDCs
- Evaluate the potential benefits of PHDI-preconditioning of CDCs in promoting therapeutic cytokine production.

5.3 Methods

Neonatal passage 2 cardiosphere-derived cells (CDCs) (see *Chapter 2*) were used in this study, unless otherwise stated.

5.3.1 Evaluation of cytotoxicity of PHDIs in CDCs

This was the first study using PHDI treatment in CDC culture, thus a careful cytotoxity test across a gradient of PHDI drug concentrations and treatment periods was carried out to determine an optimal, sublethal PHDI treatment for CDCs. DMOG, EDBA and BIC (generous gift from Kar Kheng Yeoh and Prof. Chris Schofield, Chemistry Research Laboratory, University of Oxford, UK) were dissolved in CEM (Appendix 1) to give final concentrations ranging from 0.01 mM to 2 mM (Table 5.1). Concentrations of PHDIs were selected based on doses used in the literature [127, 146, 253]. Neonatal P2 CDCs at 70 to 80% confluency were treated with the inhibitors at defined concentrations for up to 4 days. Cell culture medium was collected at 0 hour, 24 hour and 4 day to measure the concentration of lactate dehydrogenase (LDH) using an ABX Pentra 400 Chemistry Analyzer (See Chapter 2). LDH is a cyoplasmic enzyme that is released into the cell culture medium upon cell lysis. The LDH assay, therefore, was a measure of cell viability.

5.3.2 Western blotting

Protein expressions of CDCs treated with DMOG, EDBA and BIC at ranging concentrations (Table 5.1) were determined by western blotting for HIF-1α and GLUT-1 antibodies. Bands were quantified using UN-SCAN-IT gel software (Silk Scientific, USA). A housekeeping gene, GADPH was used as the internal control to normalize the band density.

Table 5.1 List of drug abbreviation, chemical name, chemical structure, molecular weight and amount of drug (mg) dissolved per ml of CEM to give a desired final concentration.

Drug Abbreviation	Chemical name	Chemical structure and molecular weight (MW)	Amount of drug dissolved in 1ml of CEM (mg)	Final concentration (mM)
DMOG	Dimethyloxaloylglycine	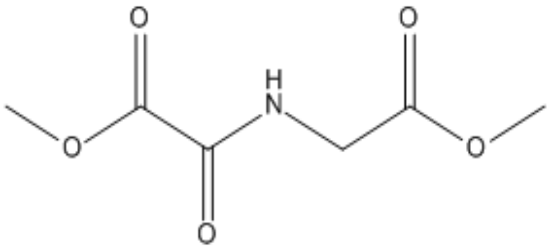 MW: 175.14	0	0
			0.018	0.1
			0.090	0.5
			0.180	1
			0.360	2
EDBA	ethyl 2-(2,3-dihyroxybenzamido) acetate	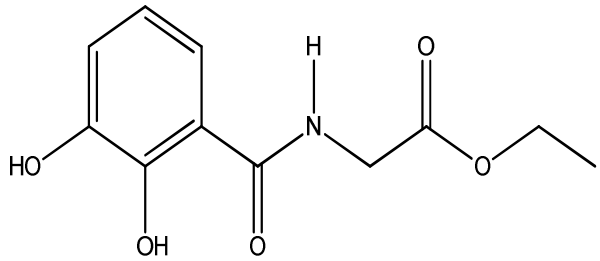 MW: 239.22	0	0
			0.024	0.1
			0.120	0.25
			0.240	0.5
			0.480	1

Table 5.1 (continued) List of drug abbreviation, chemical name, chemical structure, molecular weight and amount of drug (mg) dissolved per ml of CEM to give a desired final concentration.

Drug Abbreviation	Chemical name	Chemical structure and MW	Amount of drug dissolved in 1ml of CEM (mg)	Final concentration (µM)
BIC	2-(1-chloro-4-hydroxyisoquinoline-3-carboxamido)acetic acid	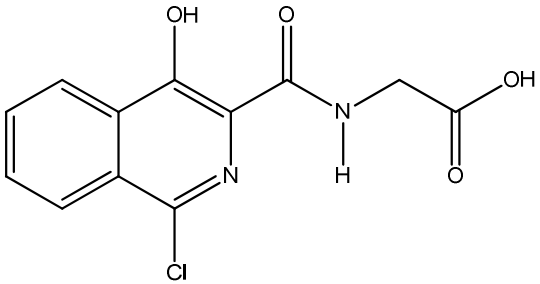 MW: 280.22	0	0
			0.003	10
			0.009	30
			0.014	50
			0.028	100

In the following experiments, 1 mM DMOG, 0.5 mM EDBA and 30 μM BIC were used to treat neonatal passage 2 CDCs for 24 hours, unless otherwise stated.

5.3.3 Cell proliferation of PHDI-preconditioned CDCs

Cell proliferation was measured by counting the viable cells manually under the microscope at 6, 12, 24, 72 and 120 hours after treatment with PHDIs. Live/dead cells were distinguished based on tryphan blue dye which only traverses the membrane of a dead/damaged cell and stains it blue.

5.3.4 Oxygen consumption and glucose metabolism

Effects of PHDI-preconditioning on CDC oxidative respiration were determined using Clark-type oxygen electrode which measures the rate of cellular oxygen uptake. Cell culture supernatants after PHDI-treatment were collected, and concentrations of nutrient (glucose) and metabolite (lactate) were determined using the metabolite analyzer (see *Chapter 2*).

5.3.5 Cardiomyocyte differentiation assay

The cardiomyogenic potential of PHDI-treated CDCs was tested using cardiomyocyte differentiation medium with 5-Aza or DMSO (Appendix 3) for 2 weeks. RNA was isolated from cells and mRNA levels for the cardiomyocyte markers, Nkx 2.5, Tnnt and MyHC were evaluated using qRT-PCR.

5.3.6 Gene expression in PHDI-preconditioned CDCs

The effects of PHDI-induced hypoxia on CDC gene expression were investigated using culture qRT-PCR. All qRT-PCR data were normalized to a combination of GADPH and Actb as housekeeping genes, as validated in a previous study (Appendix 8, manuscript submitted).

5.4 Results

5.4.1 Evaluation of cytotoxicity of PHDIs in cardiosphere-derived cells (CDCs)

The toxic effects of PHDIs were investigated using the LDH assay. In order to verify the maximum toxicity levels, 5 x 10^5 CDCs were plated per flask and exposed to detrimental level of 5 mM EDBA. All cell died under 5 mM EDBA for 24 hours, confirmed by the tryphan blue staining. The LDH levels of maximum cytoxicity levels were found to be 149 ± 3 U/L. This value represented LDH levels of 100% cell death and was used as normalization factor to determine the cytotoxicity of other PHDI treatments.

For DMOG cytotoxicity test, gradient concentrations of 0.1 mM, 0.5 mM, 1 mM and 2 mM were used to treat 5 x 10^5 CDCs for either 24 hours or 4 days. Prolonged DMOG treatment (4 days) and high concentration (> 0.5 mM) caused significantly 70-90% cell death (Figure 5.1a). For EDBA, gradient concentrations of 0.1 mM, 0.25 mM, 0.5 mM and 1 mM were used to treat equal amount of CDC number. EDBA at concentrations above 1 mM for 24 hours or above 0.5 mM for 4 days caused at least 75% of cell death (Figure 5.1b). For BIC, lower concentrations of 10 μM, 30 μM, 50 μM or 100 μM were used to treat CDCs for either 24 hours or 4 days as suggested [253]. BIC was not toxic to the cells under any of these conditions, indicated by the significantly lower percentage of cell death, compared to the positive control group (maximum LDH levels) (Figure 5.1c).

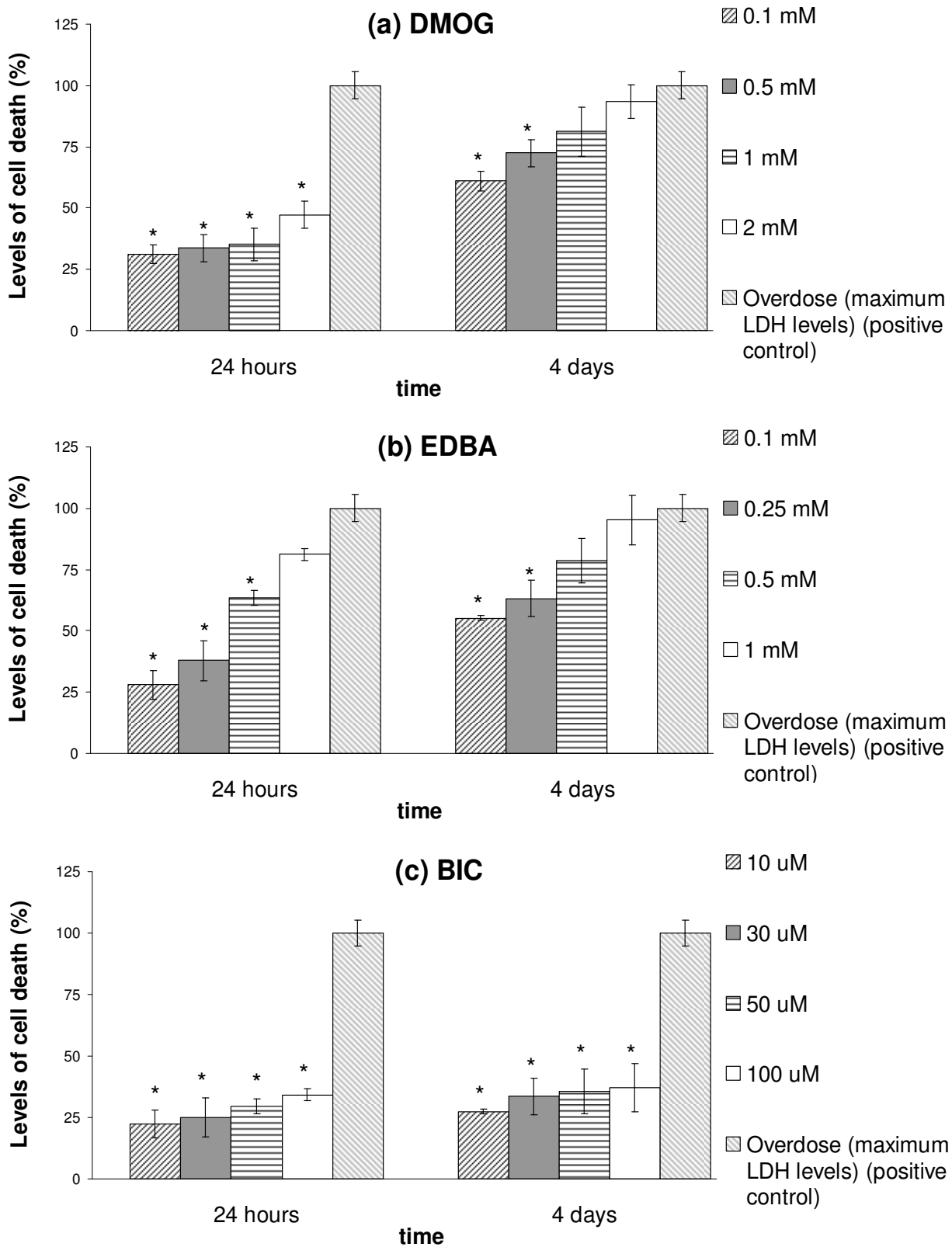

Figure 5.1 *Levels of cells death under (a) DMOG, (b) EDBA and (c) BIC at varying concentrations for 24 hours and 4 days (n = 4). * $p < 0.05$ vs. overdose (maximum LDH levels) (positive control).*

5.4.2 Effects of PHDI-preconditioning on HIF-1α and GLUT-1 expression in CDCs

Protein levels of HIF-1α and its regulated gene, GLUT-1 in P2 CDCs treated with DMOG, EDBA and BIC in gradient concentrations for 24 hours and 4 days were determined. We found that HIF-1α activation by DMOG was time and concentration dependent, being maximal after 24 hours of 0.5 mM or 1 mM DMOG treatment. On the other hand, high DMOG concentration (2 mM) or prolonged DMOG treatment (4 days) inhibited the expression of HIF-1α. Coincident with HIF-1α expression, GLUT-1 expression peaked after treatment with 1mM DMOG for 24 hours but decreased after prolonged or high concentrations of DMOG treatment (Figure 5.2 (i)).

For EDBA, HIF-1α protein levels peaked after treatment with 0.5 mM for 24 hours (2.4 ± 0.3-fold), compared with non-treated control cells. GLUT-1 protein expression was significantly upregulated in 0.1 mM EDBA (3.3 ± 0.3-fold), 0.25 mM EDBA (3.4 ± 0.3-fold), and 0.5 mM EDBA (4.0 ± 0.3-fold) treated cells, compared with the non-treated control cells. As anticipated, no HIF-1α and GLUT-1 protein expression was observed with EDBA treatment at high concentrations and after a prolonged culture period as this had been shown to be toxic to the cells (Figure 5.2 (ii)).

BIC is a specific PHD inhibitor and thus was able to significantly upregulate both HIF-1α and GLUT-1 at the low concentration of 30 μM. Also, due to the non-toxic nature of this drug, CDCs treated with BIC at higher concentrations for 4 days did not show decreased HIF-1α and GLUT-1, compared to non-treated cells, as seen in DMOG- and EDBA-treated CDCs (Figure 5.2 (iii)). Taken together, 1 mM DMOG, 0.5 mM EDBA and 30 μM BIC treatment for 24 hours was predicted to be the optimal culture condition to activate HIF in CDCs. Thus, this concentration and culture period were applied in all the following experiments.

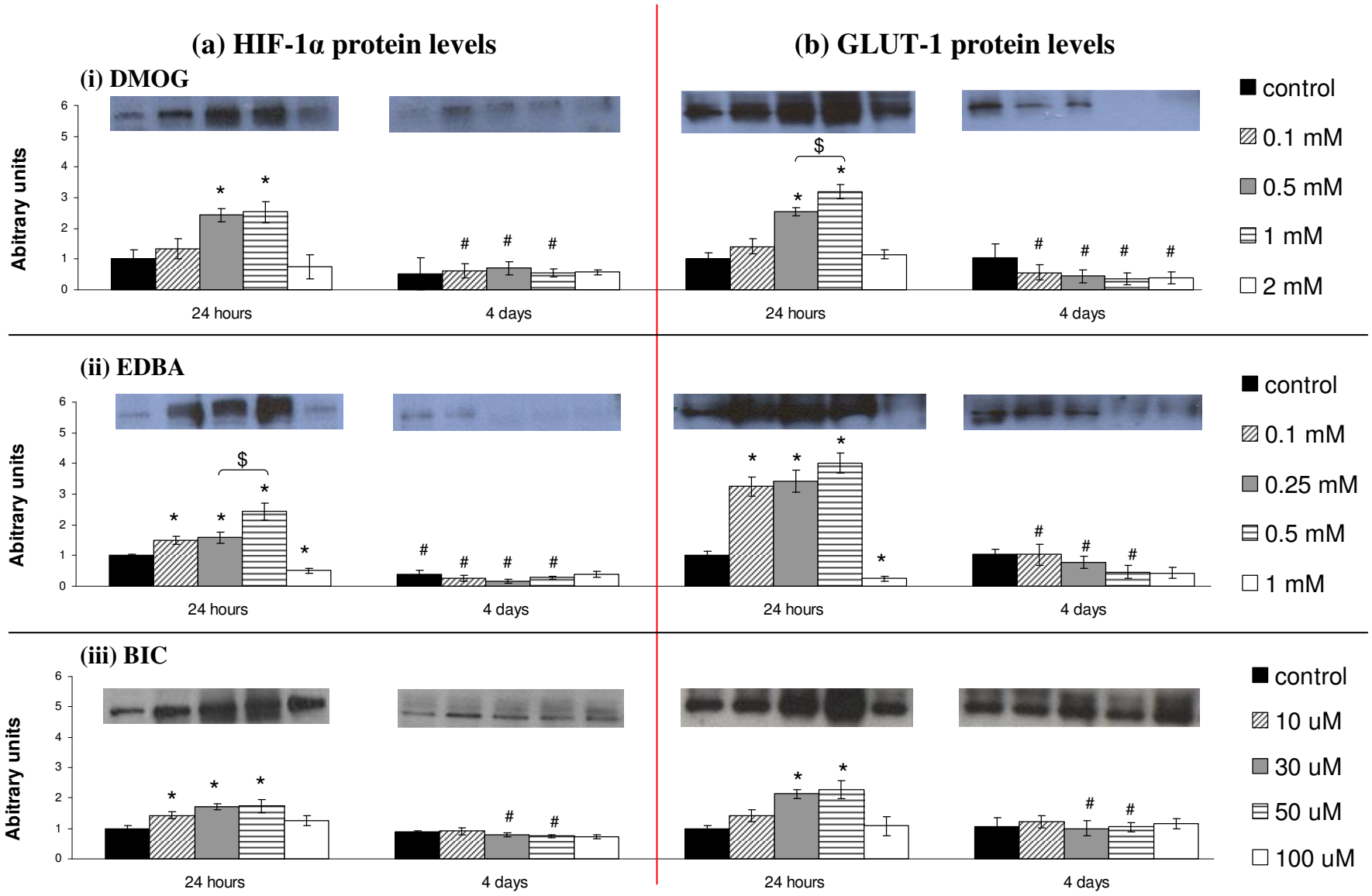

Figure 5.2 *Western blot analysis of (a) HIF-1α (left panel) and (b) GLUT-1 (right panel) protein levels in neonatal P2 CDCs treated with (i) DMOG, (ii) EDBA and (iii) BIC with a range of concentrations for 24 hours or 4 days (n = 3). Protein levels were expressed in arbitrary units relative to cells treated with control at 24 hours. * $p < 0.05$ vs. control at 24 hours; # $p < 0.05$ vs. correspond concentration at 24 hours; $ $p < 0.05$ between the two groups linked with arrow.*

5.4.3 Effects of PHDI-preconditioning on CDC proliferation

After identification of the optimal drug concentrations, CDCs were exposed to the three PHDIs at the defined sublethal concentration for 6 hours, 12 hours, 24 hours, 72 hours and 120 hours and viable cell numbers were counted. As shown in Figure 5.3, PHDI-treatment did not result in a significant increase in CDC proliferation. In fact, cell growth decreased upon exposure to these PHDIs for 72 hours, compared with non-treated control cells.

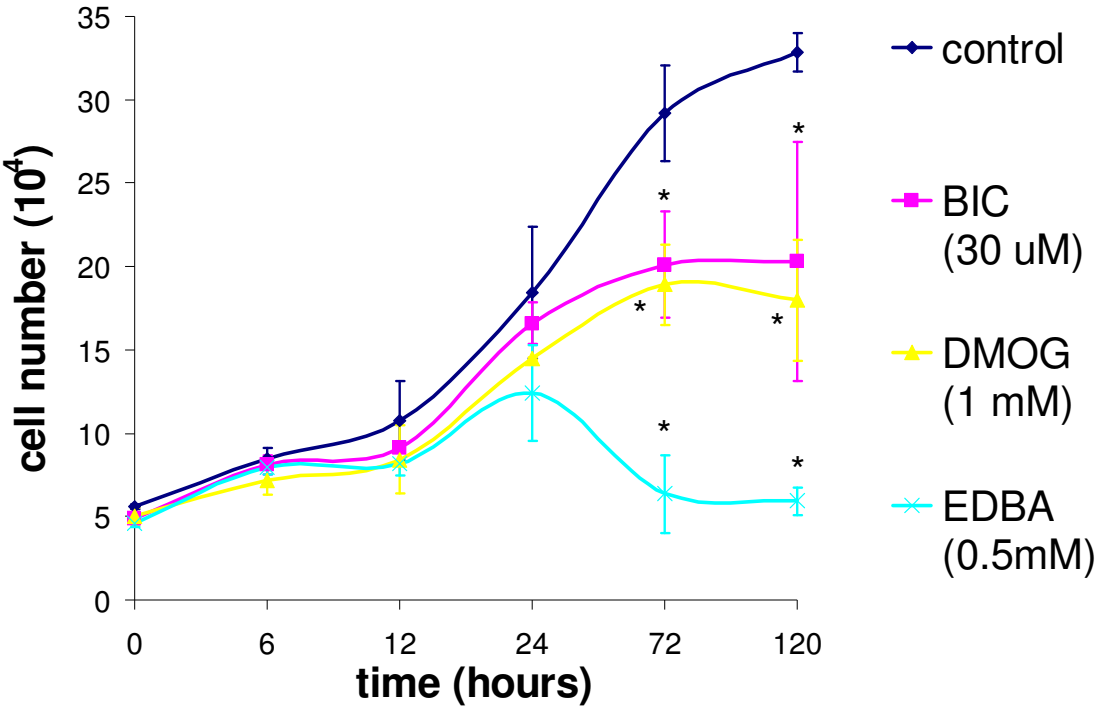

Figure 5.3 *PHDI-treated CDC proliferation assay (n = 4). Cells were harvested and counted 6 hours, 12 hours, 24 hours, 24 hours, 72 hours and 120 hours after treatment with 30 μM BIC, 1 mM DMOG and 0.5 mM EDBA. * p < 0.01 vs. control.*

5.4.4 Metabolism of PHDI-preconditioned CDCs

Following upregulation of GLUT-1 in CDCs treated with 1 mM DMOG (3.2-fold), 0.5 mM EDBA (4.0-fold) and 30 μM BIC (2.1-fold) (values obtained from Figure 5.2), a significant upregulation of glucose uptake and lactate production were also observed (Figure 5.4).

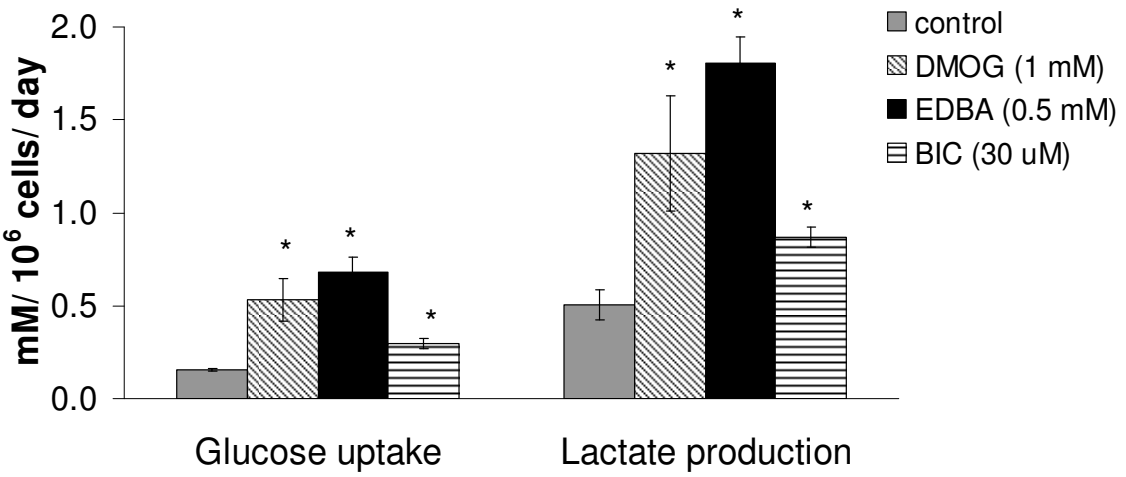

Figure 5.4 *Levels of (a) glucose uptake and (b) lactate production in non-treated control CDCs and CDCs treated with 1 mM DMOG, 0.5 mM EDBA and 30 μM BIC (n = 3). Glucose utilization and lactate production are expressed as mM of glucose/lactate per million cells per day. * $p < 0.05$ vs. control.*

There was a positive correlation between expression of GLUT-1 and upregulation of glucose uptake and lactate production (Figure 5.5).

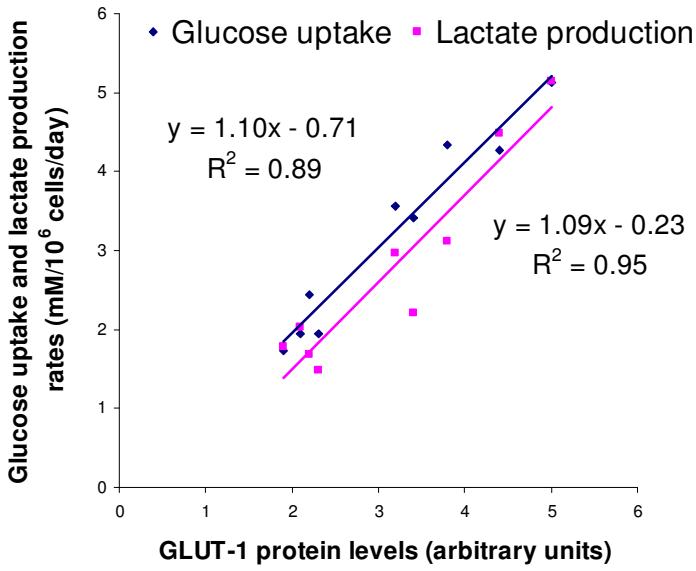

Figure 5.5 *The rate of glucose uptake and lactate production increased with increasing GLUT-1 protein levels (n =3).*

In addition, a significant reduction of basal oxygen respiration rates by 30%, 55% and 50%, were observed in 1 mM DMOG, 0.5 mM EDBA and 30 μM BIC-treated cells, respectively (Table 5.2 and Figure 5.6). The respiration rates remained significantly reduced after the respiration was stimulated by addition of substrate (malate and pyruvate) (DMOG = 31%, EDBA = 58% and BIC = 35%) or uncoupling agent, carbonyl cyanide p-trifluoromethoxyphenylhydrazone (FCCP) (32%, 47% and 35%), indicating that PHDI-preconditioned CDCs had adapted to the 'hypoxic' condition induced by PHDIs, by reducing oxygen consumption and switching to glycolytic metabolism, confirmed by the increased glucose consumption and lactate production levels.

Table 5.2 *Oxygen consumption measurements in non-treated control CDCs and CDCs treated with 1 mM DMOG, 0.5 mM EDBA and 30 μM BIC (n = 3). All measurements were standardised to nmol of oxygen uptake per min per milligram of protein present (nmol O_2/min/mg protein). * $p < 0.05$ vs. non-treated (control).*

	Non-treated (control)	**DMOG 1mM**	**EDBA 0.5 mM**	**BIC 30 μM**
Basal	10.0 ± 1.2	6.9 ± 0.4 *	3.2 ± 0.9 *	5.0 ± 0.6 *
Substrate-stimulated respiration	10.3 ± 1.4	7.0 ± 0.7 *	3.0 ± 0.5 *	6.6 ± 1.2 *
Oligomycin (to halt respiration)	6.6 ± 0.5	6.3 ± 0.9	3.1 ± 0.7	5.0 ± 1.2
FCCP-uncoupled respiration	20.0 ± 0.6	13.5 ± 1.2 *	10.7 ± 0.3 *	12.9 ± 1.5 *

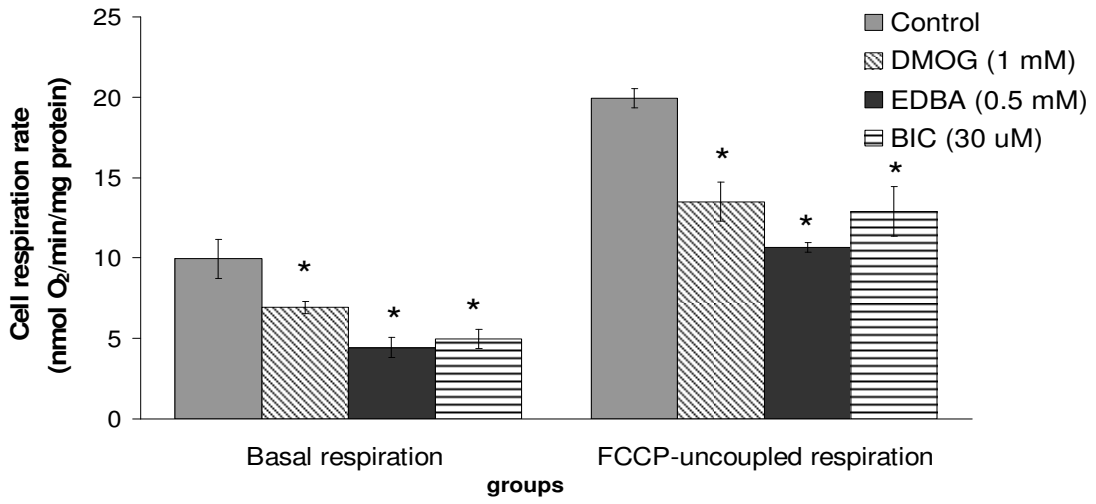

Figure 5.6 *Basal and FCCP-uncoupled respiration rates of non-treated CDCs (control) and CDCs treated with 1 mM DMOG, 0.5 mM EDBA and 30 μM BIC for 24 hours (n = 3). * $p < 0.05$ vs. control.*

5.4.5 Effects of PHDI-preconditioning on cardiac stem cell population

c-Kit levels were significantly increased after treatment with EDBA (1.5 ± 0.1-fold) but not after treatment with DMOG or BIC, compared with non-treated CDCs (Figure 5.7). All three PHDIs significantly reduced the expression levels of CD90 and CD105. DMOG reduced CD90 by 19% and CD105 by 21%, EDBA reduced CD90 by 28% and CD105 by 29% whereas BIC reduced CD90 by 28% and CD105 by 22% (Figure 5.9). There was no significant difference in the c-Kit, CD90 and CD105 expression levels between DMOG, EDBA and BIC-treated CDCs.

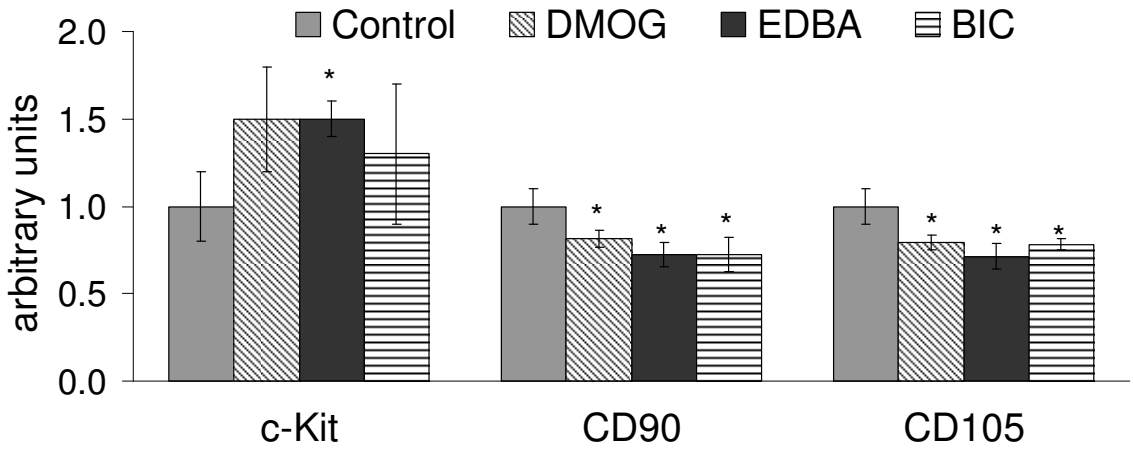

Figure 5.7 *The relative mRNA expression of c-Kit, CD90 and CD105 in non-treated P2 CDCs (control) and CDCs treated with 1 mM DMOG, 0.5 mM EDBA and 30 μM BIC for 24 hours (n = 4). mRNA expression in DMOG-, EDBA- and BIC-treated cells was normalized to the geometric mean of GAPDH and Actb (housekeeping genes) and non-treated control cells (calibrator). * p < 0.05 vs. control.*

5.4.6 Effects of PHDI-preconditioning on CDC pluripotent cell markers expression and differentiation potential

CDCs treated with DMOG, EDBA and BIC for 24 hours did not show any significant difference in the mRNA levels of Oct-4, Klf 4, Sox 2 and Nanog (data not shown). However, there was a significant reduction of GATA 4 mRNA levels by 21% in DMOG-treated CDCs and by 18% in EDBA-treated cells (Figure 5.8).

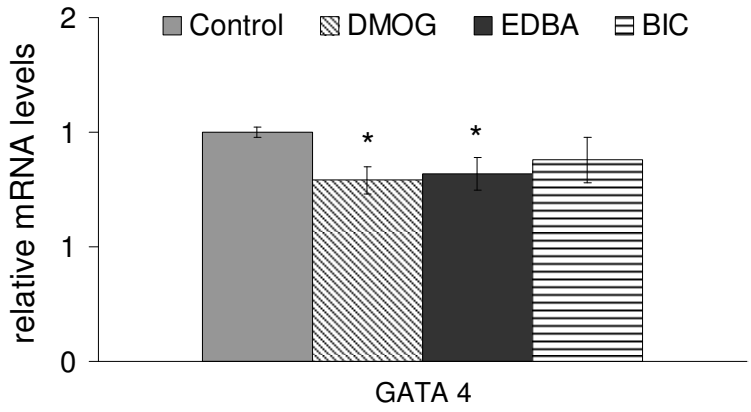

Figure 5.8 *The relative mRNA expression of GATA 4 in non-treated P2 CDCs (control) and CDCs treated with 1 mM DMOG, 0.5 mM EDBA and 30 μM BIC for 24 hours (n = 4). mRNA expression in DMOG-, EDBA- and BIC-treated cells was normalized to the geometric mean of GAPDH and Actb (housekeeping genes) and non-treated control cells (calibrator). * $p < 0.05$ vs. control.*

The cardiomyogenic potential of PHDI-treated cells was tested by inducing cardiomyogenic differentiation using 5-Aza and DMSO. However, there was no significant difference in expression of cardiomyocyte markers, Nkx 2.5, Tnnt and MyHC, compared with non-treated CDCs, indicating that PHDI treatment has no effect on the cardiomyocyte differentiation potential of CDCs (data not shown). In order to verify the qRT-PCR data, western blotting for Tnnt protein was performed by an experimentally blinded investigator, Vanessa Fairfield. Western blot data indicated that DMOG and BIC-treated CDCs did not show significantly different in Tnnt levels after 5-aza or DMSO treatment. However, EDBA-treated CDCs showed decreased Tnnt

expression by 38% after 5-aza treatment, compared with non-treated cells, indicating some inhibition of CDC differentiation by PHDI treatment (Figure 5.9).

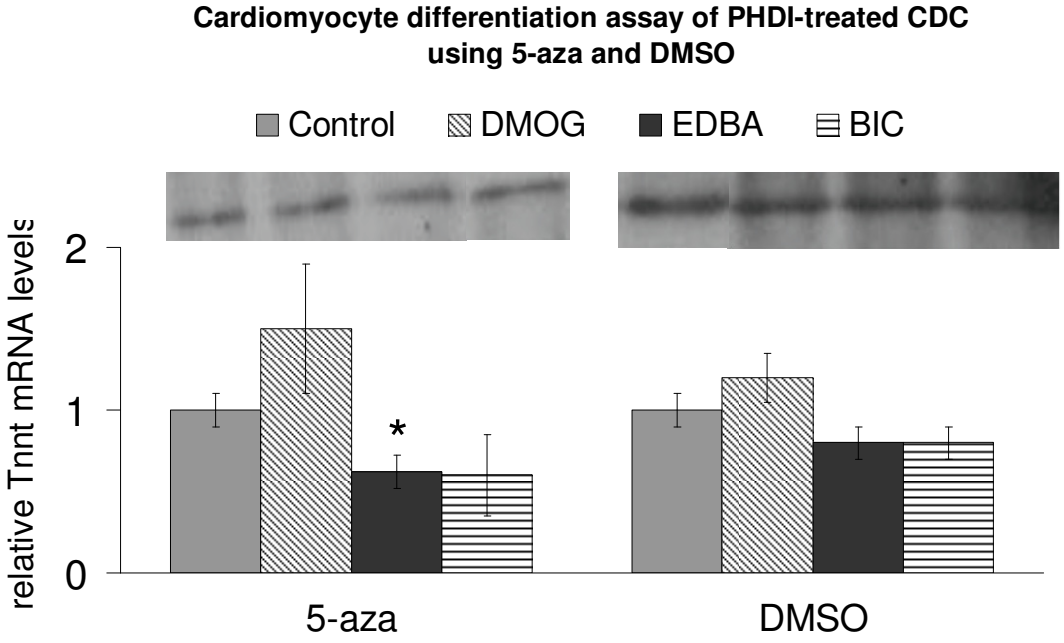

Figure 5.9 *Tnnt protein expression in non-treated P2 CDCs (control) and CDCs treated with 1 mM DMOG, 0.5 mM EDBA and 30 μM BIC for 24 hours (n = 3). Protein levels were expressed in arbitrary units relative to non-treated control. * $p < 0.05$ vs. control.*

5.4.7 Effects of PHDI-preconditioning on CDC cytokine production

DMOG and EDBA treatment significantly induced the mRNA levels of CXCR-4 in CDCs, compared with non-treated CDCs (Figure 5.10). Also, EPO mRNA levels were significantly increased in EDBA (2.1 ± 0.1-fold) and BIC (2.5 ± 0.1-fold) treated CDC, while VEGF levels were significantly upregulated in DMOG (2.9 ± 0.7-fold) and EDBA (2.8 ± 0.4-fold) treated CDCs, compared with non-treated CDCs (Figure 5.10). DMOG-treated CDCs showed significant higher CXCR-4 expression by 29%, compared with BIC-treated CDCs while BIC-treated CDCs showed significant higher EPO expression by 16%, compared with EDBA-treated CDC (Figure 5.10).

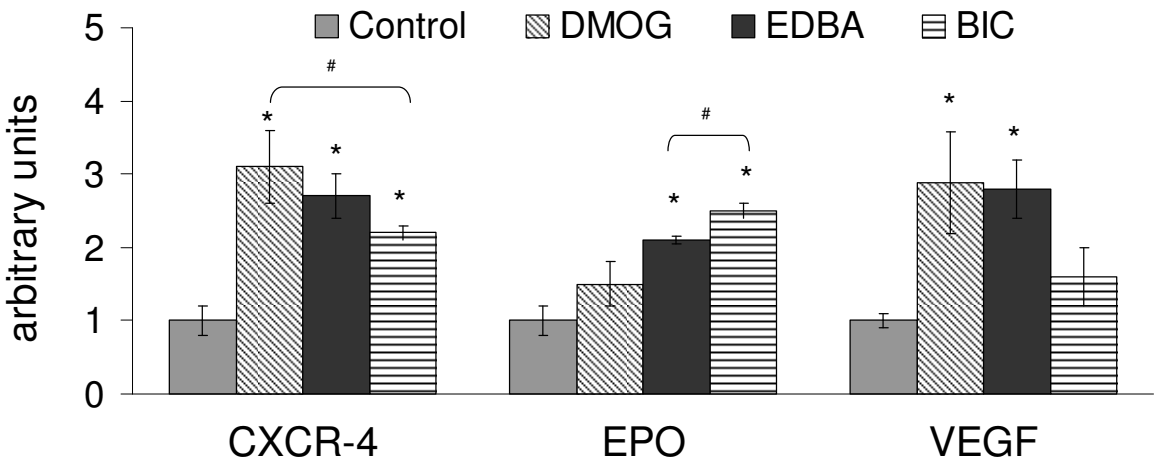

Figure 5.10 *The relative mRNA expression of CXCR-4, EPO and VEGF in non-treated P2 CDCs (control) and CDCs treated with 1 mM DMOG, 0.5 mM EDBA and 30 μM BIC for 24 hours (n = 4). mRNA expression in DMOG-, EDBA- and BIC-treated cells was normalized to the geometric mean of GAPDH and Actb (housekeeping genes) and non-treated control cells (calibrator). * $p < 0.05$ vs. control. # $p < 0.05$ between two groups linked with arrow.*

5.4.8 Comparison of the effects of DMOG, EDBA and BIC preconditioning in CDCs

Although all three PHDIs investigated here activated HIF in CDCs, different PHDIs contributed differentially to specific HIF-regulated gene expression. Table 5.3 presents the effects of DMOG, EDBA and BIC on HIF-1α level, glucose metabolism, cellular oxygen consumption, cell growth, differentiation and survival, expression of cardiac stem/mesenchymal cell markers and synthesis of cytokines involved in stem cell trafficking, erythropoiesis and angiogenesis.

Table 5.3 *Lists of fold-changes in CDC genotypic and phenotypic levels after (a) DMOG, (b) EDBA and (c) BIC treatments. All non-treated CDC values were normalized to '1', and all DMOG, EDBA and BIC-treated CDC values were expressed relative to the normalized non-treated CDCs.*

** $p < 0.05$ vs. non-treated control; $^{\#}$ $p < 0.05$ vs. DMOG and $^{\$}$ $p < 0.05$ vs. EDBA.*

No.	Evaluation	(a) DMOG	(b) EDBA	(c) BIC
1.	Sublethal concentration and culture period (cytotoxicity assay)	< 2 mM < 24 hours	< 0.5 mM < 24 hours	Showed no toxicity at the highest concentration (100 μM) up to 4 days
2.	Optimal drug concentration and culture period used in this study	1 mM for 24 hours	0.5 mM for 24 hours	30 μM for 24 hours
3.	HIF-1α protein levels	2.5 ± 0.3 *	2.4 ± 0.3 *	1.6 ± 0.9 * $^{\$}$
4.	GLUT-1 protein levels	3.2 ± 0.2 *	4.0 ± 0.3 * $^{\#}$	2.1 ± 0.1 * $^{\# \$}$
5.	Cell proliferation rate	No change	No change	No change
6.	Glucose uptake	3.6 ± 0.6 *	4.3 ± 0.6*	1.9 ± 0.1* $^{\# \$}$
7.	Lactate production	2.6 ± 1.1 *	3.6 ± 0.9*	1.7 ± 0.2 * $^{\# \$}$
8.	Basal respiration rate	0.70 ± 0.04 *	0.45 ± 0.06 * $^{\#}$	0.50 ± 0.06 * $^{\# \$}$
9.	FCCP-uncoupled respiration rate	0.68 ± 0.06 *	0.53 ± 0.01* $^{\#}$	0.65 ± 0.08 * $^{\$}$
10.	<u>mRNA levels</u> c-Kit	1.5 ± 0.3	1.5 ± 0.1 *	1.3 ± 0.4
11.	CD90	0.80 ± 0.1 *	0.73 ± 0.1 *	0.72 ± 0.1 *
12.	CD105	0.81 ± 0.1 *	0.7 1± 0.1 *	0.78 ± 0.1 *
13.	GATA 4	0.79 ± 0.1 *	0.82 ± 0.1 *	0.88 ± 0.1
14	CXCR-4	3.1 ± 0.5 *	2.7 ± 0.3 *	2.2 ± 0.1 *
15.	EPO	1.5 ± 0.5	2.1 ± 0.1 *	2.5 ± 0.1 * $^{\# \$}$
16.	VEGF	2.9 ± 0.7 *	2.8 ± 0.4 *	1.6 ± 0.4
17.	Cardiomyocyte differentiation potential	No changes	Tnnt protein levels reduced by 38% after 5-aza treatment.	No changes

5.5 Discussion

The work in this chapter determined the effects of pharmacologically-induced hypoxia, resulting from the three different prolyl-4-hydroxylase inhibitors (PHDIs): DMOG, EDBA and BIC, on CDC proliferation, differentiation, gene expression and metabolism. To our knowledge, this was the first study to demonstrate the effects of PHDIs on CDCs.

Pilot study of PHDI-activated HIF pathway in CDC culture

CDCs were pretreated with PHDIs in a range of gradient concentrations for a defined treatment period from a few hours up to 4 days. This preliminary testing of PHDIs was crucial because studies have shown cytotoxicity from a range of PHDI concentrations. For example, DMOG at more than 0.5 mM for 24 hours was found to be toxic to embryonic lung explant culture [146], but not in villious placental explant treated for the same time period [254]. The discrepancies in PHDI cytotoxicity in different tissues or cell types are mainly due to the different degree of diffusion or penetration of inhibitors into the specific cell types [255]. Therefore a careful evaluation of the cytotoxicity of DMOG, EDBA and BIC was performed with CDCs.

In CDC culture, maximal HIF stabilization was achieved using 1 mM DMOG, 0.5 mM EDBA or 30 μM BIC for 24 hours. Under these sublethal culture conditions, optimum HIF-1α and GLUT-1 protein expression were achieved without affecting the CDC proliferation. As anticipated, high concentrations and prolonged PHDI treatments triggered cell death in the CDCs, due to the detrimental anoxic condition after over exposure to PHDIs [146, 256].

Here, all PHDIs successfully inhibited the PHD enzyme activity and subsequently activated HIF-1α protein in CDC culture, as observed in other cell types [125-127].

However, due to the diverse roles of PHDs in many different processes and the presence of three different PHD isoforms (PHD1–3), inhibition of PHDs by different PHDIs could trigger multi-faceted physiological changes in cells [257, 258]. Groenman *et al.* [146] showed that fetal lung development can be impaired or stimulated in different ways by different PHD inhibition. For example, they demonstrated that both DMOG and desferrioxamine (DFO) increased HIF-1 α protein levels and VEGF mRNA expression, but DMOG alone stimulated vascularization in embryonic lung explant culture. In this study, DMOG, EDBA and BIC induced different effects on CDCs. Each of these PHDIs has its unique advantages as a candidate agent for myocardial infarction therapy. An *in vivo* animal study using the PHDI-treated CDCs to treat infarcted rat hearts is planned for further evaluation of the effects of these PHDIs *in vivo.*

Effects of DMOG preconditioning on CDCs

Here, we found that 1 mM DMOG significantly inhibited PHD enzyme activity and upregulated HIF-1α CDCs, as shown in previous studies [124, 146, 259]. DMOG inhibited the PHD enzyme activity by mimicking 2-oxoglutarate, the essential co-factor of the PHD enzymes in activating their reaction [140, 260]. Coincident with HIF-1α expression, a significantly increased GLUT-1 level was observed, which subsequently induced the glucose uptake and lactate production, switching the CDCs into glycolytic metabolism, confirmed by the reduced cellular oxygen consumption rates [259, 261]. In addition, DMOG preconditioning also induced the production of CXCR-4, which plays a role in trafficking stem cells to the infarcted myocardium based on the SDF-1/CXCR-4 axis [262, 263], and VEGF which induces angiogenesis [112]. Although DMOG did not significantly change the c-Kit levels, CD90 and

CD105 levels were significantly reduced by DMOG preconditioning, giving a reduced mesenchymal cell population within the heterogenous CDC population.

Limitation and advantages of non-specific PHD inhibitors

DMOG is a nonspecific PHD inhibitor which could inhibit any other mechanism involving 2-oxoglutarate, for example, collagen synthesis [264]. Therefore, DMOG might be associated with undesired side effects in tissue or cells. Groenman *et al.* reported that inhibition of collagen synthesis by DMOG could impair lung growth, because of the essential role of matrix proteins in the developing lung [146]. On the other hand, this 'side effect' may be beneficial in certain situations. For example, Song *et al.* reported that DMOG treatment significantly decreased macrophage infiltration and reduced fibrosis in rats with subtotal nephrectomy, by decreasing type IV collage expression [259]. Following myocardial infarction, excessive non-contractile fibrosis in the infarct zone may lead to myocardium remodelling which ultimately may lead to heart failure [1]. In this case, *in vivo* DMOG treatment could be beneficial to reduce fibrosis after infarction and thereby may improve heart function [142, 251, 252]. This is in agreement with Kobayashi *et al.* who reported that identification of a therapeutic target for limiting fibrosis could provide a method to improve function after myocardial infarction [265].

In addition, the induction of CXCR-4 by DMOG treatment could also increase the recruitment of CDCs to the infarcted myocardium, where they could induce angiogenesis due to increased secreted cytokine, VEGF. Further, DMOG-treated CDCs had adapted to hypoxia and thus could better survive in the infarcted myocardium. All taken together, pharmacological inhibition of PHD using DMOG functionally activated

HIF and could possibly enhance the therapeutic potential of CDCs for myocardial infarction.

Effects of EDBA preconditioning on CDCs

In this study, EDBA at a concentration of less than 0.5 mM was found to significantly induce HIF-1α, in agreement with Lienard *et al.* who reported an induced HIF-1α stabilisation by EDBA in human Hep3β cell lines in a concentration-dependent manner [127]. Structurally, EDBA is another 2-oxoglutarate analogue compound, thus it was predicted to inhibit the PHD enzyme activity by mimicking the 2-oxoglutarate. However, addition of 2-oxoglutarate to EDBA-treated Hep3β cell did not reduce the activity of EDBA to activate HIF-1α as observed in DMOG-treated Hep3β cells [127]. Thus it was postulated that the *in vivo* mechanism of EDBA action may be more complex than as a simple 2-oxoglutarate analogue. Currently, the mechanism of EDBA inhibition is still under investigation. The hypothesis is that EDBA plays a role as a iron chelator to inhibit the PHD which require the ferrous iron-dependent oxygenases for their activity [266]. Further, as reported by Lienard *et al.,* EDBA was found to be more potent in inducing HIF-1α stabilisation in cells than DMOG. Although HIF-1α protein levels were not significantly different between EDBA-treated and DMOG-treated CDCs, we found that EDBA induced significant expression of c-Kit levels, not seen with DMOG- or the BIC-treated CDCs. This data is further supported by the observation of a significant increase of both EPO and VEGF in EDBA-treated CDCs, whereas, in contrast, DMOG preconditioning only significantly induced VEGF while BIC was only able to induce EPO. Activation of both the erythropoietic EPO cytokine and the angiogenic VEGF cytokine in EDBA-treated CDCs could provide more potent candidate cells for neovascularization in the infarcted myocardium, compared with DMOG- or BIC-treated CDCs. Also, we found that EDBA-treatment showed

significantly reduced cardiomyocyte differentiation potential after 5-aza treatment, as seen with the hypoxic preconditioning which was found to maintain CDC pluripotency and diminish differentiation *in vitro,* in *Chapter 4.* All taken together, EDBA-treated CDCs mimicked the hypoxic-preconditioning of CDCs more comprehensively, compared with DMOG and BIC-treated CDCs [127].

Effects of BIC preconditioning on CDCs

Unlike DMOG and EDBA, BIC is a specific inhibitor for PHD. Due to its specificity, this drug was found to give significant upregulation of HIF-1α and its regulated genes GLUT-1 and CXCR-4 at low concentrations. The cytotoxicity test revealed that this drug was not toxic to the cells at high concentrations, even at levels 10 times higher than the previous study (100 μM vs. 10 μM) [253]. The non-toxicity of BIC found in this study was in agreement with the previous patent literature review which showed that BIC (patent name: FG2216) was orally bioavailable and chronic oral dosing in male rhesus macaques was well tolerated *in vivo* [253, 267]. Further, we found that the levels of EPO expression in BIC-treated CDCs were significantly higher than those treated with DMOG and EDBA, in agreement with the previous reports which shown that BIC induced significant and reversible EPO expression both *in vitro* (Hep3B cells) and *in vivo* (oral administration of BIC in nonhuman primates) [253]. Also, it was found BIC treatment induced glycolytic metabolism and reduced $CD90^{+}CD105^{+}$ cardiac mesenchymal cell marker expression, similar to cells treated with DMOG and EDBA.

5.6 Conclusion

In conclusion, PHDI preconditioning of CDCS, using a short, sublethal PHDI treatment, mediated the activation of HIF and its regulated genes. Due to the diverse roles of PHDs in many different processes, each PHD inhibitor used in this study showed different effects on CDCs. Each of these PHDI has its unique advantages as a candidate for therapeutic treatment of myocardial infarction. As a non-specific PHD inhibitor, DMOG could have double effects in myocardial infarction therapy, in which DMOG could inhibit excessive fibrosis formation if given *in vivo* and at the same time induce the *in vitro* hypoxic phenotype on CDCs by activating the HIF and HIF-regulated genes. On the other hand, EDBA was found to be the most potent PHD inhibitor in inducing HIF-1α stabilisation, as it significantly upregulated both EPO and VEGF, and most importantly EDBA is the only PHDI which upregulated the cardiac stem cell marker, c-Kit in CDCs. Last but not least, BIC is a specific PHD inhibitor which can be safely administered orally. This drug has been proved to induce EPO expression in nonhuman primates and also has been recruited for a clinical trial. Despite the fact that each PHDI showed different effects on CDCs, all these PHDI-treated cells showed reduced oxygen consumption and increased glycolytic metabolism, enhancing their survival within the hypoxic infarcted myocardium. Future investigations are needed to explore *in vivo* specificity of PHDI-treated CDCs and their differential roles in activating different biological processes after transplantation into infarcted hearts.

Chapter 6

Effects of Ageing on Isolation of CSCs

and

Optimization of Adult Rat CDC Culture

6.1 Abstract

Clinically, cardiovascular risk increases with age, however, a full understanding of the mechanism which underlies the age-associated effects on CDC isolation and expansion was unknown. Thus, one of the objectives of this work was to isolate and characterize CDCs from neonatal and adult rat hearts, from the atrium and apex, to investigate the effects of ageing and stem cell niche location on CDC functional studies *in vitro.* Neonatal rat explants successfully yielded 6 x 10^6 CDCs approximately 10 days faster than adult atrial explants and 16 days faster than adult apical explants. EDCs isolated from atrial tissue showed significant higher expression of c-Kit (31%) and CD105 (27%), compared with apical EDCs, indicating that resident stem cells were found more densely in the atrial region. qRT-PCR confirmed that adult CDCs had lower cardiac stem/progenitor and mesenchymal stem cell markers (c-Kit, Oct-4, Klf4, Sox 2, CD105) but higher cardiac differentiation markers (Nkx 2.5, GATA4, Tnnt and MyHC), compared with neonatal CDCs. In line with this, it was found that the adult CDCs were more committed to differentiate into the cardiomyocyte lineage rather than into the adipocyte lineage. Increasing age of the donor was also associated with telomere shortening and reduced TERT enzyme expression. Further, *in vitro* propagation of cardiac stem cells, from EDCs up to P10 CDCs, downregulated the c-Kit expression and upregulated the expression of CD105 and CD90 genes. In the second part of this chapter, adult CDC culture was optimized by preconditioning the CDCs under hypoxia or with prolyl-4-hydroxylase inhibitors (PHDIs). Preconditioned cells showed increased expression of c-Kit, HIF-1α and several important cytokines such as CXCR-4, EPO and VEGF. These hypoxic and PHDI-preconditioned cells also had reduced oxygen consumption rate and increased glucose metabolism. In conclusion, CDCs grown from adult atrial and apical tissue had adult stem cell characteristics, however increasing age of donors and *in vitro* cellular ageing was associated with reduced stem cell numbers and proliferation potential. Hypoxic- and PHDI-preconditioned stem cells may be better adapted to survive in infarcted tissue and may provide better tissue regeneration after transplantation. In future work, optimized adult CDCs will be transplanted into infarcted rat hearts to investigate the *in vivo* therapeutic potential of adult CDCs for myocardial infarction.

6.2 Introduction

Myocardial infarction is one of the major causes of morbidity and mortality worldwide [268-272]. Transplantation of endogenous adult stem cells represents a promising therapy for the disease because these cells are autologous and would not induce an immunogenic response after transplantation. However, clinically, myocardial infarction predominantly affects the elderly population [268-272]. It has been argued that cardiovascular risk increases with age and the age-associated decline in cardiac and vascular regenerative capacity may contribute to dysfunction of endogenous cardiac stem and progenitor cells [273, 274]. Reports have shown that some of the intrinsic stem cell characteristics change with ageing, such as reduced self-renewal capacity [275] and decreased stem cell function [276, 277]. Also, ageing of the stem cell supportive niche or systemic environment can have negative effects on stem cell isolation as seen in aged skeletal muscle satellite cells [278].

Thus, in order to fully investigate the therapeutic potential of CSCs, the effects of ageing on CSC isolation must be determined. In this study, CSCs were isolated from neonatal and 4 month old adult rat hearts to evaluate the transcriptional, translational and functional changes of CSCs isolated from postnatal heart and fully developed matured adult heart *in vitro*. Our hypothesis was that aged donors have depleted progenitors and precursor cells and might have impaired functional characteristics which may influence the ability to promote the cardiovascular repair in the disease heart.

Further, it was reported that although CSC clusters were scattered throughout the myocardium, their distribution appears to be conditioned by the distinct levels of wall stress [279]. In adult heart, physical forces and high wall stress can introduce an intracellular response that regulates cell behaviour and fate [280, 281]. Studies have

shown that mechanical factors influenced the differentiation of a number of stem cell types [281, 282]. Here, CSCs were isolated from three regions with different levels of wall stress: atrium, midregion (ventricle) and apex, to identify the effects of the wall stress on stem cell niches in the isolation of CSC. A detailed investigation of the distribution of CSC throughout the adult myocardium will hopefully provide new insights of the region where surgical biopsies for CSC isolation should be taken from in clinical applications for maximal potential of stem-cell based myocardial infarction therapy.

Therefore, in this study, CSCs were isolated from adult rat atrial, ventricular and apical heart tissues and were optimized using hypoxic culture and PHDI treatment, which have been proven and validated in previous chapters, to improve the therapeutic potential of adult CSCs for myocardial infarction therapy.

The aims of this study were to:

- Isolate and expand CSCs from adult rat atrial, ventricular and apical heart tissues and compare the cell proliferation rate, gene and protein expression profile of adult CSCs to the neonatal CSCs.
- To invesitigate the effects of multiple *in vitro* passaging on CSC proliferation and gene expression.
- Induce adipogenesis and cardiomyocytes differentiation of adult CDCs.
- Optimize adult CDC culture using hypoxic and PHDI-preconditioning.

6.3 Methods

There were two studies involved in this chapter: (i) Effects of ageing on CSC isolation, characterization and differentiation *in vitro*, and (ii) Optimization of adult CDC culture using hypoxic and PHDI-preconditioning.

Study one - Effects of ageing on CSC isolation, characterization and differentiation *in vitro*

6.3.1 Isolation and expansion of CSCs from neonatal and adult rat hearts

Neonatal (1-3 days) and adult (4 months) Sprague Dawley (SD) rats were used in this study (n = 4). For neonatal rats, whole heart tissue was minced and plated on fibronectin-coated dishes to give explant-derived cells (EDCs), while for adult rats, heart tissue was separated into three parts: atrium, midregion and apex, before being minced and cultured in separate dishes to generate explant-derived cells (EDCs) (Figure 6.1). Cardiosphere-derived cells (CDCs) were generated from EDCs via the formation of cardiospheres as described in *Chapter 2*.

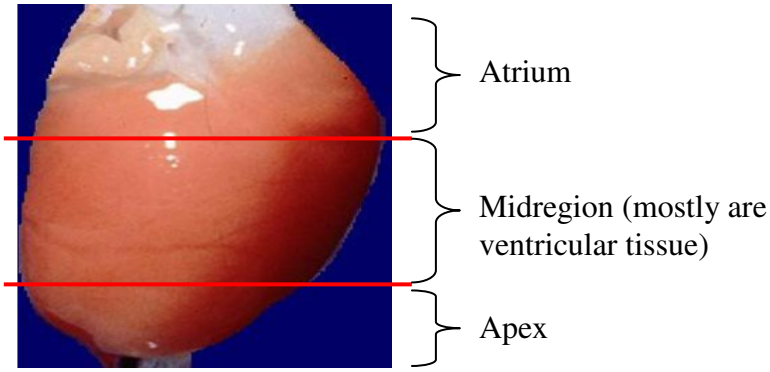

Figure 6.1 *Adult rat hearts were separated into three parts, from base to apex, before being minced and cultured in separate dishes to generate explant-derived cells (EDCs).*

6.3.2 Comparison of cell proliferation, gene expression profile and differentiation potential of neonatal and adult CSCs

Cell viability for EDCs, cardiospheres and CDCs of neonatal and adult explants were assessed using a dye-exclusion assay with tryphan blue and viable cell numbers were

counted. Genotypic characterization of hypoxic EDC, cardiospheres and CDCs used RT-PCR or qRT-PCR. Expression of the specific cardiac stem cell marker (c-Kit) and the mesenchymal stem cell markers (CD90 and CD105), pluripotent stem cell markers (Oct-4, Sox 2, Klf-4, and Nanog), cardiac differentiation transcription factors (Nkx 2.5 and GATA 4) and mature cardiomyocyte markers (Troponin T and myosin heavy chain) were investigated. Adipogenesis and cardiomyogenesis potential of adult CDCs were compared with neonatal CDCs, using adipogenesis induction medium with 1-methyl-3-isobutylxanthine, dexamathasone and indomethacin (Appendix 2) or cardiomyocyte differentiation medium with 5-azacytidine (5-Aza) or dimethyl sulfoxide (DMSO) (Appendix 3).

6.3.3 Effects of ageing on CDC telomere length and telomerase expression

Telomere length of neonatal and adult P2 CDCs was measured using an qRT-PCR assay adapted from the published method [283]. Telomere sequence in DNA was amplified using a specific primer pairs for telomeres amplification (shown in Table 2.1). The amplification of telomere was normalized to a single copy gene (SCG), 36B4 (sequence listed in Table 2.1). Telomerase expression of CDCs was measured based on the mRNA expression of telomere reverse transcriptase (TERT) enzyme normalized to housekeeping genes GADPH and Actb.

6.3.4 Effects of *in vitro* cellular ageing (multiple cell passaging) on cardiac progenitor and mesenchymal cell population

RNA was isolated from EDCs, cardiospheres, P0 CDCs, P2 CDCs, P5 CDCs and P10 CDCs. Expression pattern of selected genes, c-Kit, CD105 and CD90 were investigated using qRT-PCR.

Study two - Optimization of adult CDC culture using hypoxic and PHDI-preconditioning

6.3.5 Optimization of adult CSC culture using hypoxic or PHDI-preconditioning

For hypoxic preconditioning, adult rat atrium, midregion and apex tissue were separated into two portions of equal weight and allocated to two groups (hypoxia and normoxia) (n = 4). Heart tissues were minced and plated on petri dish to give explant-derived cells (EDCs). Cardiosphere-derived cells (CDCs) were generated from EDC via the formation of cardiospheres as outlined in *Chapter 2*, in either hypoxic (2% oxygen) or normoxic (21% oxygen) incubators. For PHDI preconditioning, atrial and apical P2 CDCs at 70% - 80% confluency were treated with 1mM DMOG, 0.5mM EDBA or 30μM BIC, for 24 hours.

6.3.6 Evaluation of the effects of hypoxic and PHDI treatment hypoxic

All the following experiments in this section used adult atrial and apical P2 CDC preconditioned with hypoxia, DMOG, EDBA or BIC, unless otherwise stated. Normoxic adult atrial and apical P2 CDCs also were included in every experiment as a negative control.

6.3.6.1 Gene expression

The effects of PHDI-induced hypoxia on CDC gene expression were investigated using culture qRT-PCR. All qRT-PCR data were normalized to a combination of GADPH and Actb as housekeeping genes, as validated in a previous study (Appendix 8, manuscript submitted).

6.3.6.2 Protein expression

HIF-1α protein expression of hypoxic and PHDI-treated adult CDCs were investigated using western blot. Bands were quantified using UN-SCAN-IT gel software (Silk Scientific, USA) (see *Chapter 2).*

6.3.6.3 Oxygen consumption and glucose metabolism

Effects of hypoxic and PHDI-preconditioning on CDC oxidative respiration were determined using Clark-type oxygen electrode. Cell culture supernatants after hypoxic and PHDI-treatment were collected, and concentrations of nutrient (glucose) and metabolite (lactate) were determined using the metabolite analyzer (see *Chapter 2*)

6.4 Results

Study one – Effects of ageing on CSC isolation, characterization and *in vitro* differentiation

6.4.1 Effects of ageing on cell proliferation

6.4.1.1 Explant-derived cell (EDC)

SD adult (4 months) rat hearts were separated into three parts: atrium, midregion (mainly ventricular tissue) and apex. Atrium and apex tissue adhered to the dishes, generated stromal-like cells after 5 days and round phase bright cells, 7 to 9 days after plating (Figure 6.2 a and b). However, tissue from the midregion of the heart showed no growth several weeks post-plating, confirming that few proliferative cardiac progenitor cells exist in the midregion of the heart. Since the cell numbers generated from midregion tissue were so slow, in the following experiments midregion tissue culture was excluded from the study (Figure 6.2c).

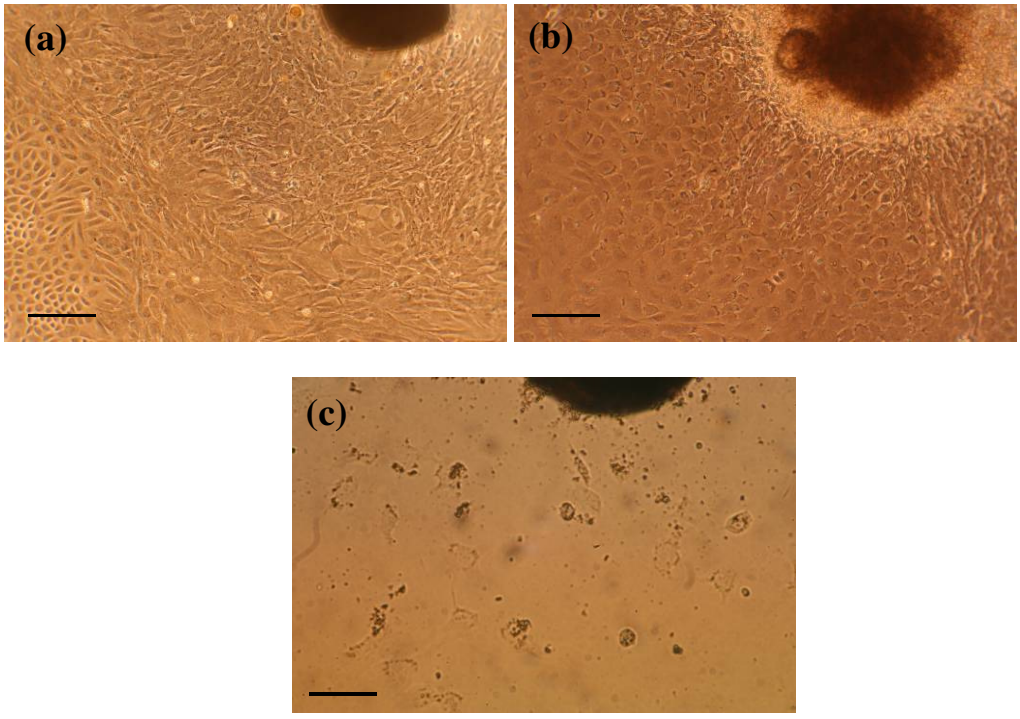

Figure 6.2 *Cells derived from different regions of adult heart, (a) atrium, (b) apex and (c) midregion (mainly ventricular tissue). Pictures were taken at day 12 post plating. Scale bars = 200 µm.*

There was a progressive increase in explant-derived cell (EDC) number from neonatal rat hearts after 3 days in culture, achieving confluency within 7 ± 2 days of plating, whereas adult tissue typically became confluent after 15 ± 2 days. To evaluate and compare the cell proliferation rate between neonatal and adult explants, EDCs were harvested using trypsin and cell numbers were counted using a hematocytometer, every 3 days up to 15 days. At day 6, explants from neonatal heart generated 1.3 ± 0.1 x 10^7 EDCs per gram tissue, approximately 4.3-fold more than those generated from adult atrium (0.3 ± 0.1 x 10^7 EDC/g) and 6-fold more from adult apex (0.2 ± 0.1 x 10^7 EDC/g). Higher proliferation rates in neonatal EDC culture were maintained up to day 9, with neonatal explants generating 1.9 ± 0.3 x 10^6 EDCs, 2-fold more than adult atrium (0.9 ± 0.1 x 10^6) and 4-fold more than adult apex (0.5 ± 0.1 x 10^6). At day 9, neonatal explants achieved confluency, but this was not observed in adult atrium and apex explants until day 12 to day 15 post plating. From day 6 to day 12, adult atrial EDC proliferated, on average, 0.6-fold faster than the apical EDC. Over 18 days in culture, explants from the midregion of the adult heart showed no cell growth at all (Figure 6.3).

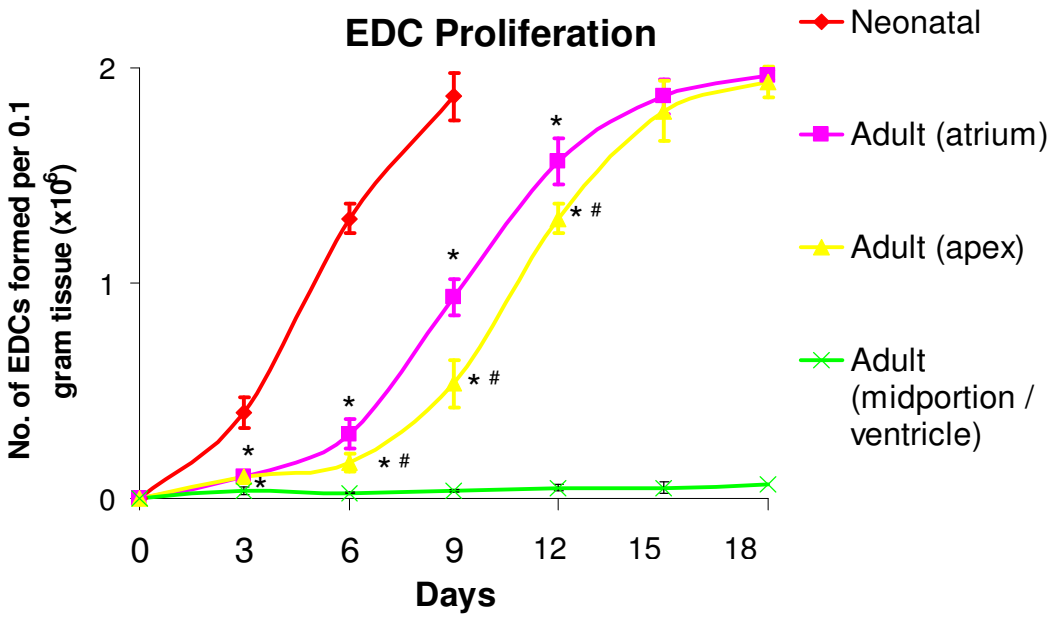

Figure 6.3 *Neonatal and adult (atrium, apex and midportion) EDC proliferation assay (n = 4). Neonatal cells were harvested and counted at days 3, 6 and 9, while adult cells were cultured until day 18 to achieve confluency. * $p < 0.01$ vs. neonatal; # $p < 0.01$ vs. adult atrium.*

6.4.1.2 Cardisphere (Csp)

EDCs were grown on poly-D-lysine–coated 24-well plates with CGM (Appendix 1). In neonatal and adult atrial culture, cells spontaneously aggregated into small colonies 24 hours after plating, and within 4 to 5 days the cells formed a suspension of cardiospheres with an average size of 50-80 μm in diameter (Figure 6.4). Cells grown from ventricular apex EDCs proliferated more slowly, forming spheres at least 8 days after plating. Approximately 400 cardiospheres were obtained from each well of a 24-well plate at the end of the experiment. Sizes of neonatal, atrial and apical cardiospheres, measured using ImageJ, were not significantly different (Figure 6.5).

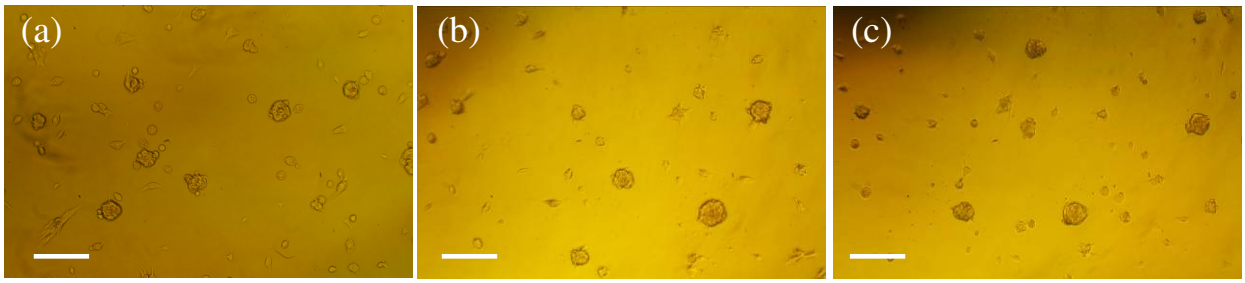

Figure 6.4 *Morphology of cardiosphere isolated from (a) neonatal whole heart, (b) adult atrial tissue and (c) adult apical tissue, under light microscope. Scale bars = 200μm*

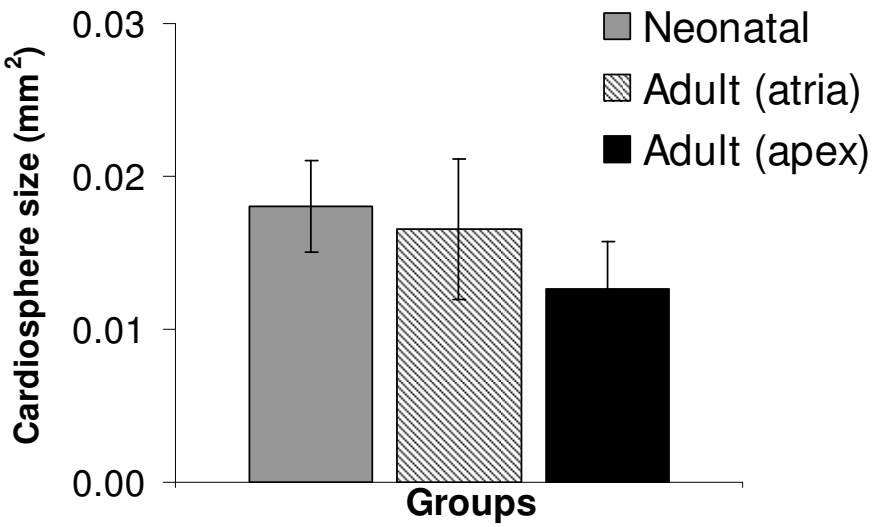

Figure 6.5 *Sizes of cardiospheres cultured from neonatal rat whole heart tissue and adult atrial and apical tissue (n = 4). Images of 20 random unfixed cardiospheres were captured under the micropscope and the sphere sizes were measured using ImageJ. * $p < 0.05$ vs. normoxia.*

6.4.1.3 Cardiosphere-derived cell (CDC)

Isolated cardiospheres formed cardiosphere-derived cells (CDCs) after 3-4 days of incubation. CDCs reached 80-90% confluency within 5 to 7 days and were subsequently passaged in the ratio 1:2 for further expansion up to passage 2 (P2) to generate sufficient cell numbers for further study. Generally, independent of donor age and tissue location in the heart, all CDCs showed similar cell morphology and proliferated at a constant rate (Figure 6.6). A total of approximately 6 x 10^6 CDCs were obtained from each heart biopsy at the end of passage 2.

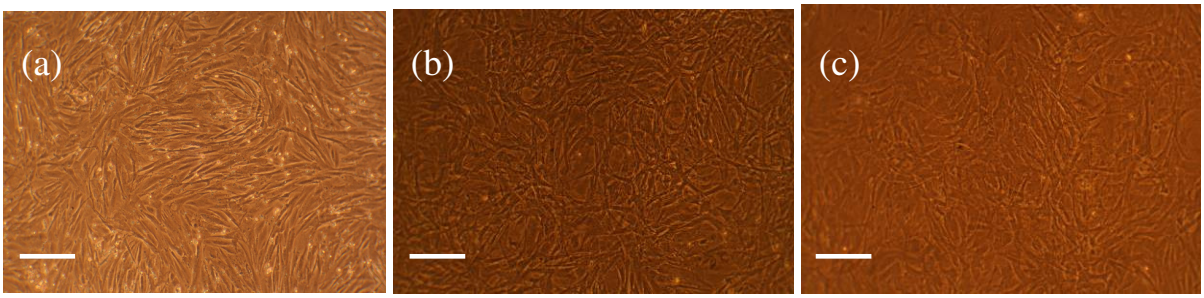

Figure 6.6 *Morphology of P2 CDCs isolated from (a) neonatal whole heart, (b) adult atrial tissue and (c) adult apical tissue, under light microscope. Scale bars = 200μm.*

A simplified schematic flow illustrating the primary cardiac stem cell culture process and a table listing the total period (days) required for each step of primary cardiac stem cell culture process are shown in Figure 6.7 and Table 6.1. Since there was variation in the time required to grow EDC (5 – 14 days) and cardiospheres (4 to 8 days), cells were harvested based on confluency for EDC and CDC and size for cardiospheres (50 to 80 μM) rather than a set time period.

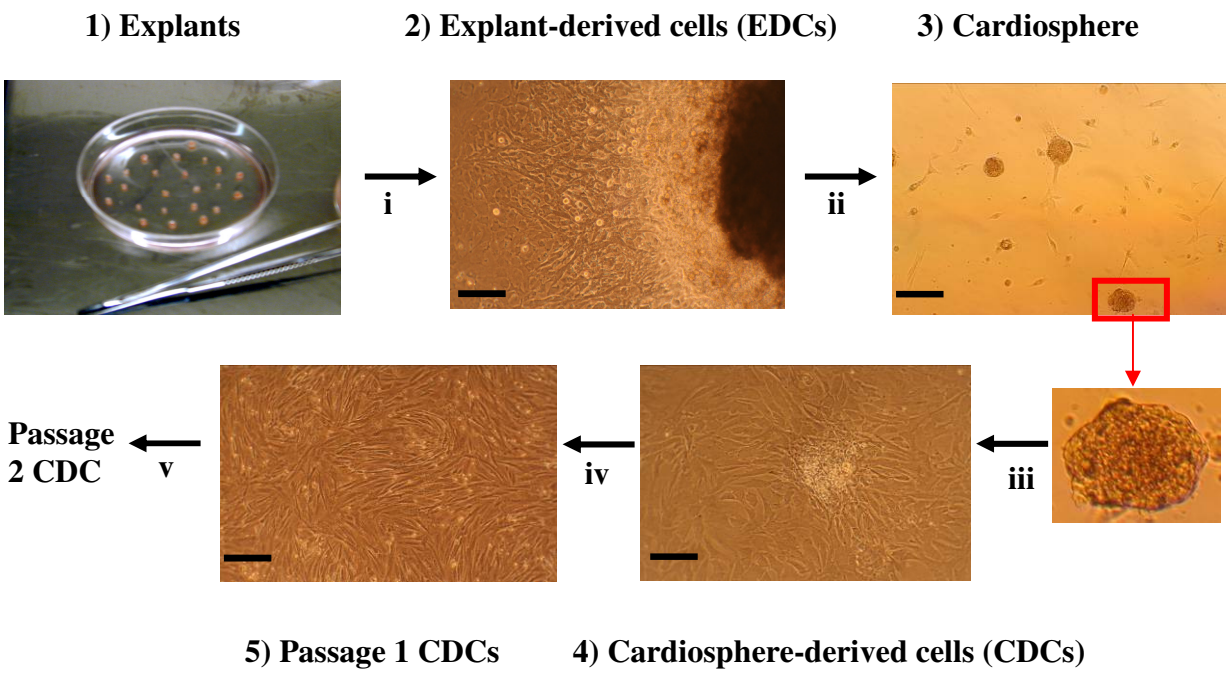

Figure 6.7 *Simplified schematic flow of the primary cardiac stem cell culture process. Scale bar = 200μm.*

Table 6.1 *Days required for each step of primary cardiac stem cell culture process for neonatal rat whole heart tissue, adult atria, adult apical and adult ventricular tissue (n = 4).*

No.	Culture step	Neonatal	Adult		
			atrial	apex	midregion
i	Generating explant-derived cells (EDC) from cardiac explant	5 ± 2	12 ± 2	14 ± 2	*ng*
ii	Generating cardiosphere from EDC	4 ± 1	5 ± 2	8 ± 2	-
iii	Cardiospheres were expanded into monolayer cardiospher-derived cells (CDCs)	5 ± 1	7 ± 1	7 ± 1	-
iv	CDCs were passaged and split in the ratio 1:2 to give passage 1 (P1) CDCs	5 ± 1	5 ± 1	6 ± 1	-
v	P1 CDCs were further passaged to give P2 CDCs	5 ± 1	5 ± 1	6 ± 1	-
	Total days required:	**24 ± 6**	**34 ± 7**	**42 ± 7**	**-**

ng = no growth observed; - = no data obtained as no cells were generated from cardiac explants.

6.4.2 Effects of ageing on CSC gene expression

6.4.2.1 EDC and cardiosphere gene expression

As shown in Figure 6.2, the gross appearance of the outgrowth from the plated tissue from animals of different ages and tissue location was morphologically similar (except for adult midregion explants which showed no cell growth at all). However, the gene expression was found to be different in neonatal and adult EDCs. qRT-PCR results revealed that the cardiac stem cell marker, c-Kit was significantly reduced by 27% in adult atrial EDC and 50% in adult apical EDCs, compared with neonatal EDCs. The expression level of the cardiac mesenchymal stem cell marker, CD105, was significantly decreased in adult atrial and apical EDCs, by 34% and 52% respectively, compared with neonatal EDCs. However, the mRNA levels of CD90 increased in adult atrial and apical EDC, by 1.5-fold and 1.8-fold respectively, compared with neonatal EDCs. Also, we found that atrial EDCs showed significantly higher c-Kit levels by 31% and CD105 by 27%, compared with apical EDCs (Figure 6.8).

A similar gene profile was observed after cardiosphere culture, in which cardiospheres from adult atrium and apex showed lower c-Kit levels, by 29% and 40%, and CD105 levels, by 20% and 22%, respectively, compared with neonatal cardiospheres. A significant increase in CD90 levels was observed in adult atrial (1.3-fold) and adult apical cardiospheres (1.4-fold). However, unlike EDCs, no significant difference in c-Kit and CD105 levels was observed between atrial and apical cardiospheres (Figure 6.9).

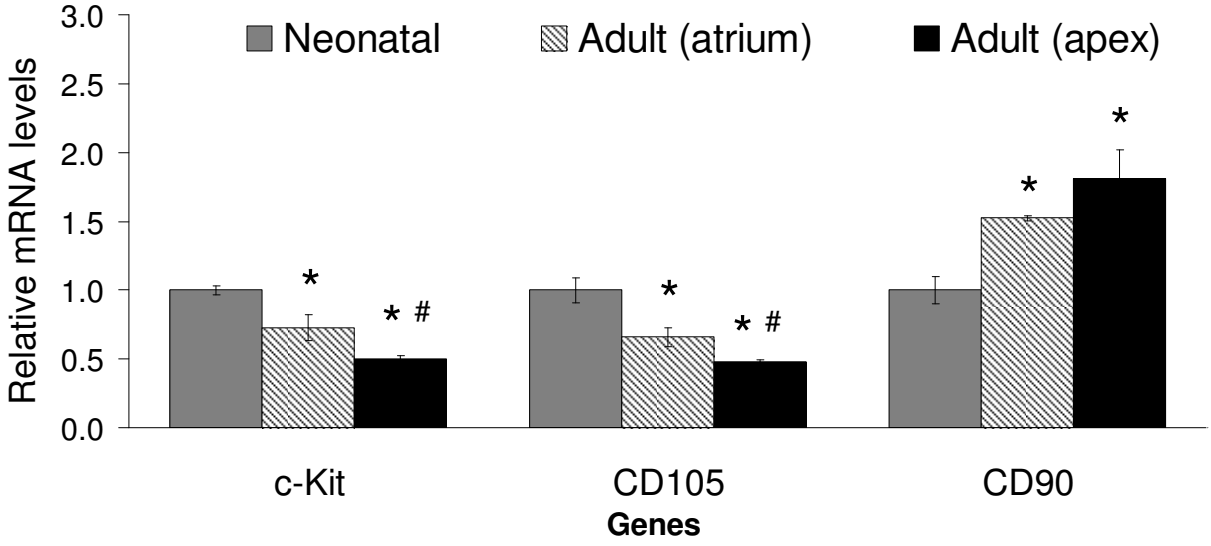

Figure 6.8 *Relative mRNA expressions of EDCs isolated from neonatal, adult atrial and adult apical tissue (n = 4). All values were normalized to the geometric mean of GAPDH and Actb as housekeeping genes and were expressed relative to neonatal EDCs. * $p < 0.05$ vs. neonatal. # $p < 0.05$ vs. adult atrium.*

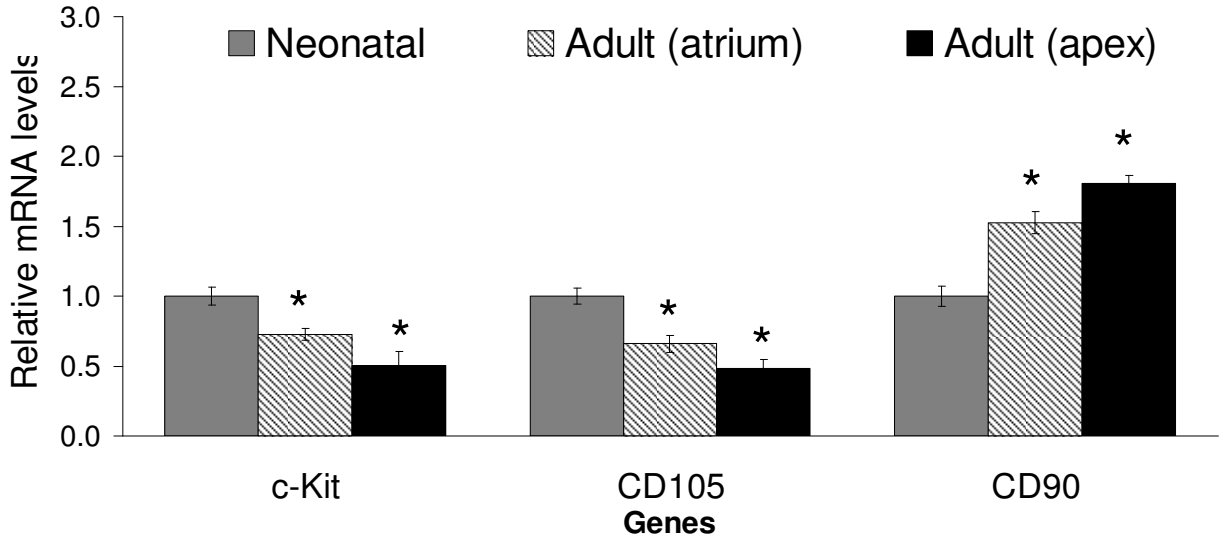

Figure 6.9 *Relative mRNA expressions of cardiospheres generated from neonatal, adult atrial and adult apical tissue (n = 4). All values were normalized to the geometric mean of GAPDH and Actb as housekeeping genes and were expressed relative to neonatal cardiospheres. * $p < 0.05$ vs. neonatal.*

6.4.2.2 Cardiosphere-derived cell (CDC) gene expression

Using conventional RT-PCR, mRNA of genes of interest was amplified using specifically designed primers and PCR products were run on gel electrophoresis. RT-PCR revealed that P2 CDCs isolated from both adult atrial and adult apical cardiac explants were an heterogeneous population containing cells which expressed the cardiac stem cell marker (c-Kit), pluripotent cell markers (Oct-4, Klf4, Sox2 and Nanog), cardiac differentiating cell markers (Nkx 2.5 and GATA 4), mature cardiomyocyte cell markers (Tnnt and MyHC) and mesenchymal cells markers (CD90 and CD105) (Figure 6.10a and b).

In order to evaluate the effects of ageing on the CDC gene expression profile, PCR product band density of adult atrial (Figure 6.10a) and apical CDCs (Figure 6.10b) were quantified using ImageJ and were expressed relative to neonatal CDCs (Figure 6.10c, also see Figure 3.8 in *Chapter 3*). Based on this analysis, it was found that adult CDCs (atrium and apex) had reduced expression levels of the cardiac stem cell marker (c-Kit) (Figure 6.11a), pluripotent markers (Oct-4, Klf-4 and Sox 2) (Figure 6.11 b, c e) and markedly increased levels of cardiac markers (Nkx 2.5, GATA 4, Tnnt and MyHC) (Figure 6.101 f-i), compared with neonatal CDCs. Further, CD105 levels were decreased by 20% in adult atrial CDCs and 38% in adult apical CDCs (Figure 6.11k), compared with neonatal CDCs. However, there was no significant difference in the expression of CD90 between neonatal and adult CDCs (Figure 6.11j).

For all the genes investigated here, there were no statistically significant differences between adult atrial CDCs and adult apical CDCs (Figure 6.11 a to j).

(a) Adult atrial CDCs

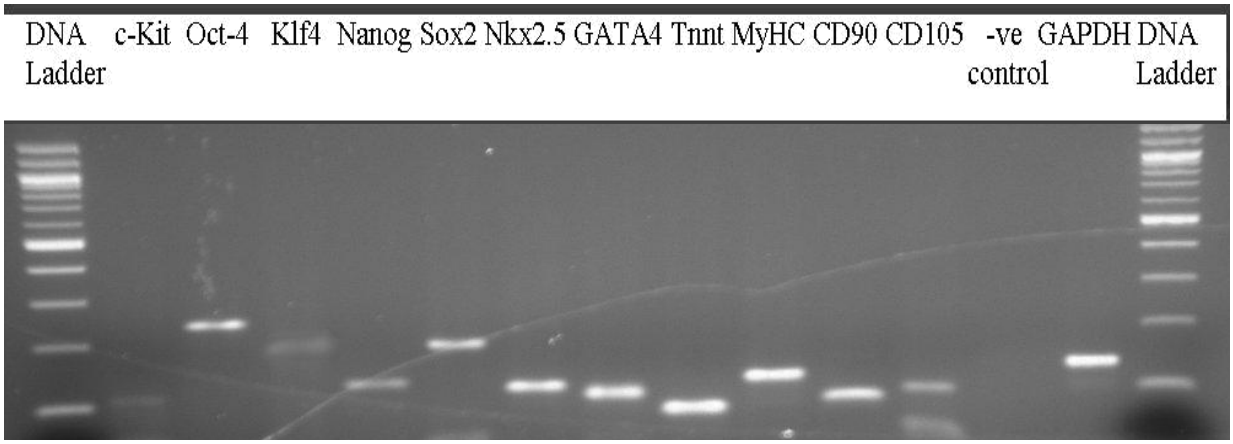

(b) Adult apical CDCs

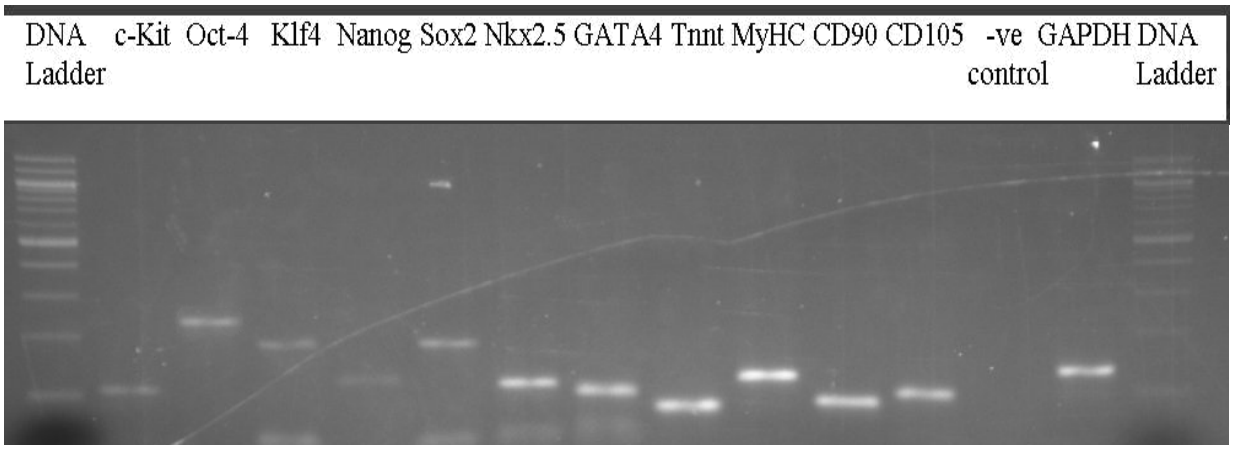

(c) Neonatal whole heart CDCs

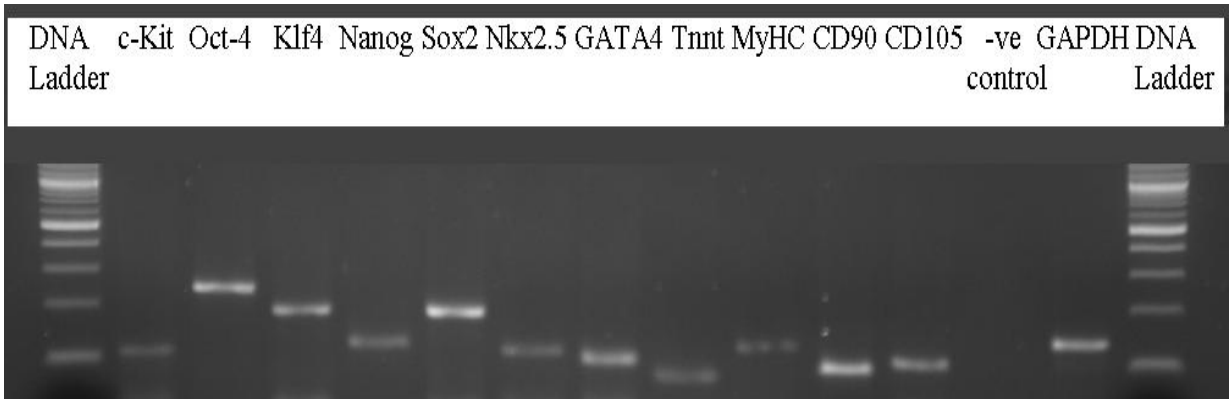

Figure 6.10 *Representative gel electrophoresis images (of three independent experiments) of RT-PCR characterization of (a) adult atrial, (b) adult apical and (c) neonatal whole heart CDCs. GADPH was used as housekeeping gene to validate the RNA extraction and cDNA synthesis procedure. -ve control = PCR amplification without cDNA template; DNA ladder = 100bp DNA ladder (N3231S, BioLabs).*

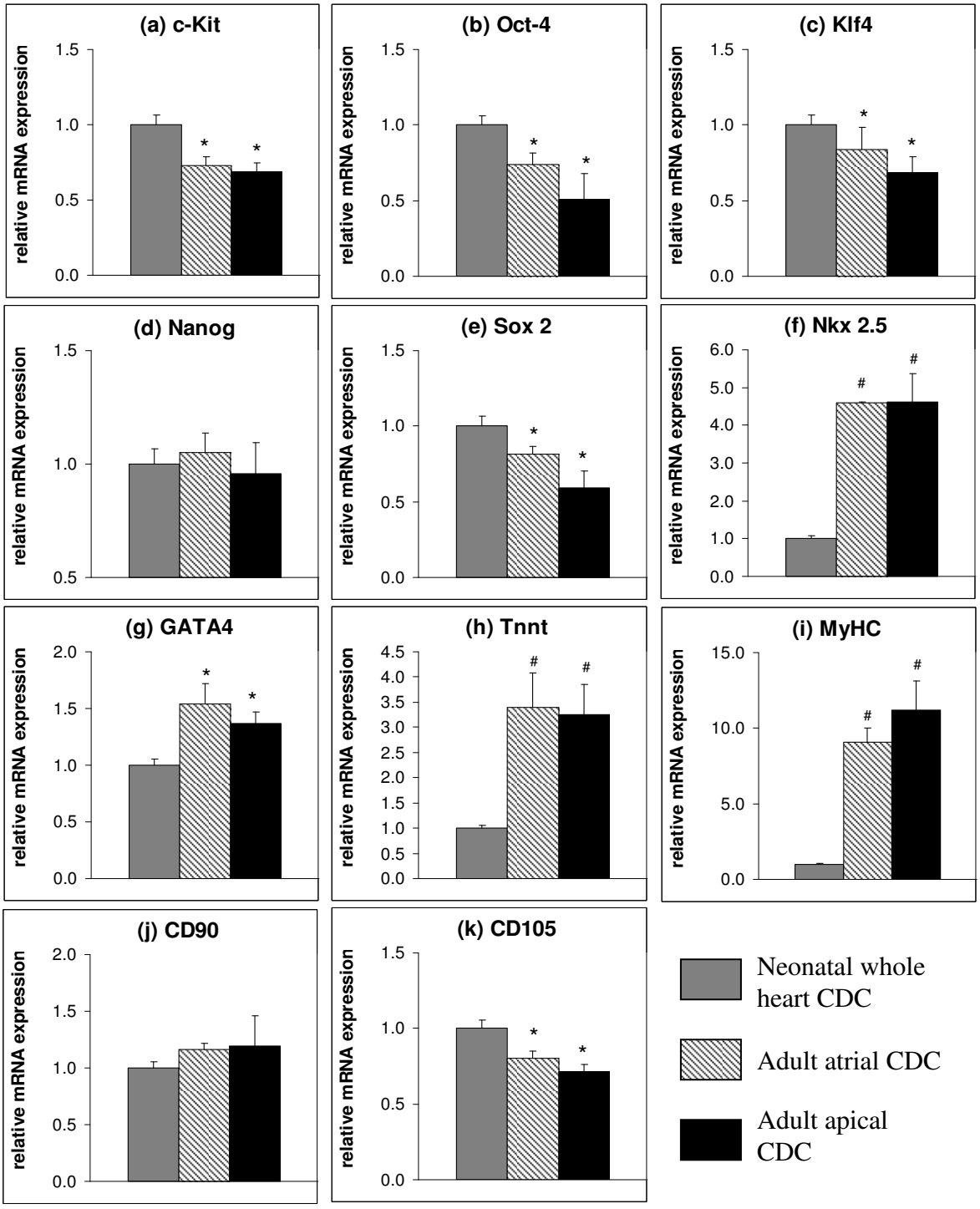

Figure 6.11 *The relative mRNA expression of (a) c-Kit, (b) CD105, (c) CD90, (d) Oct-4, (e) Klf-4, (f) Nanog, (g) Sox 2, (h) Nkx 2.5, (i) GATA 4, (j) Tnnt and (k) MyHC for neonatal, adult atrial and adult apical P2 CDCs based on the gel electrophoresis of RT-PCR amplified products (n = 3). All values were normalized to GAPDH (housekeeping gene). Abundance of mRNA expression of neonatal CDCs was set arbitrary to 1, adult atrium and adult apex CDC mRNA abundance was expressed relative to the neonatal CDCs. * $p < 0.05$ vs. neonatal. # $p < 0.01$ vs. neonatal.*

6.4.3 Effects of ageing on P2 CDC differentiation potential

6.4.3.1 Adipogenesis

Neonatal and adult P2 CDCs were induced to differentiate using adipogenic induction medium (AIM) (Appendix 3). The density of Oil Red O stain eluted from adult CDCs was only 0.4-fold of that eluted from neonatal CDCs, indicating that adult CDCs had fewer differentiated adipocytes and that ageing significantly diminished the ability of CDCs to be transdifferentiated into adipocytes (Figure 6.12). This coincided with the reduced expression of the mesenchymal stem cell marker, CD105 in adult CDCs as observed using RT-PCR.

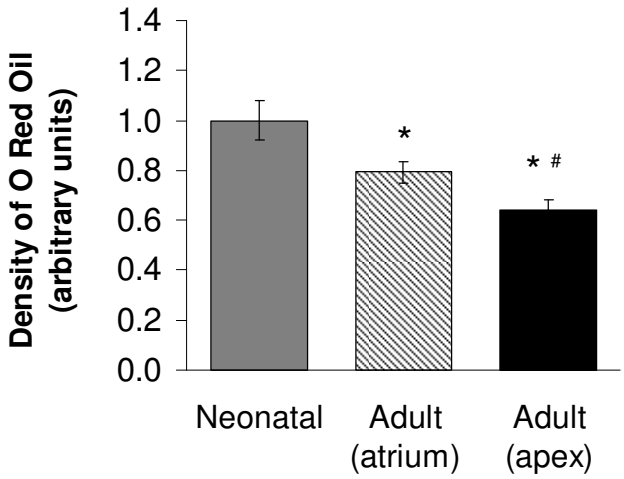

Figure 6.12 *Density of Oil Red O stain eluted from neonatal, adult atrial and adult apical CDCs subjected to adipogenesis assay under identical condition (n = 4). Density of Oil Red O eluted from hypoxic CDCs was expressed relative to the neonatal CDCs (control group). * $p < 0.05$ vs. neonatal, $^{\#}p < 0.05$ vs. adult (atrium).*

6.4.3.2 Cardiomyocytes differentiation

The cardiomyogenic potential of adult P2 CDCs was tested *in vitro* over 2 weeks with cardiomyocyte differentiation medium (CDM) containing the cardiomyogenic inducers, 5-azacytidine (5-Aza) or dimethyl sulfoxide (DMSO). Negative control cells were treated with complete explant medium (CEM), the basal culture medium for CDCs, for either 5 days or 2 weeks.

After 2 weeks culture with CEM without passaging, both atrial and apical CDCs showed upregulation of Nkx 2.5 and Tnnt, compared with CDCs treated with CEM for 5 days. CDCs treated with 5-aza or DMSO showed significant increases, not only in Nkx 2.5 and Tnnt, but also in MyHC mRNA levels, compared with CDCs treated with CEM for 5 days (Figure 6.13). However, no beating cells were observed. In order to verify the qRT-PCR data, western blotting for Tnnt protein was performed by an experimentally blinded investigator, Khadijeh Pakzad. The significant increased Tnnt protein levels in atrial CDCs confirmed the expression of Tnnt mRNA levels in cells (Figure 6.14), indicated that CEM (2 weeks), 5-aza or DMSO treatment induced differentiation along the cardiomyocyte lineage.

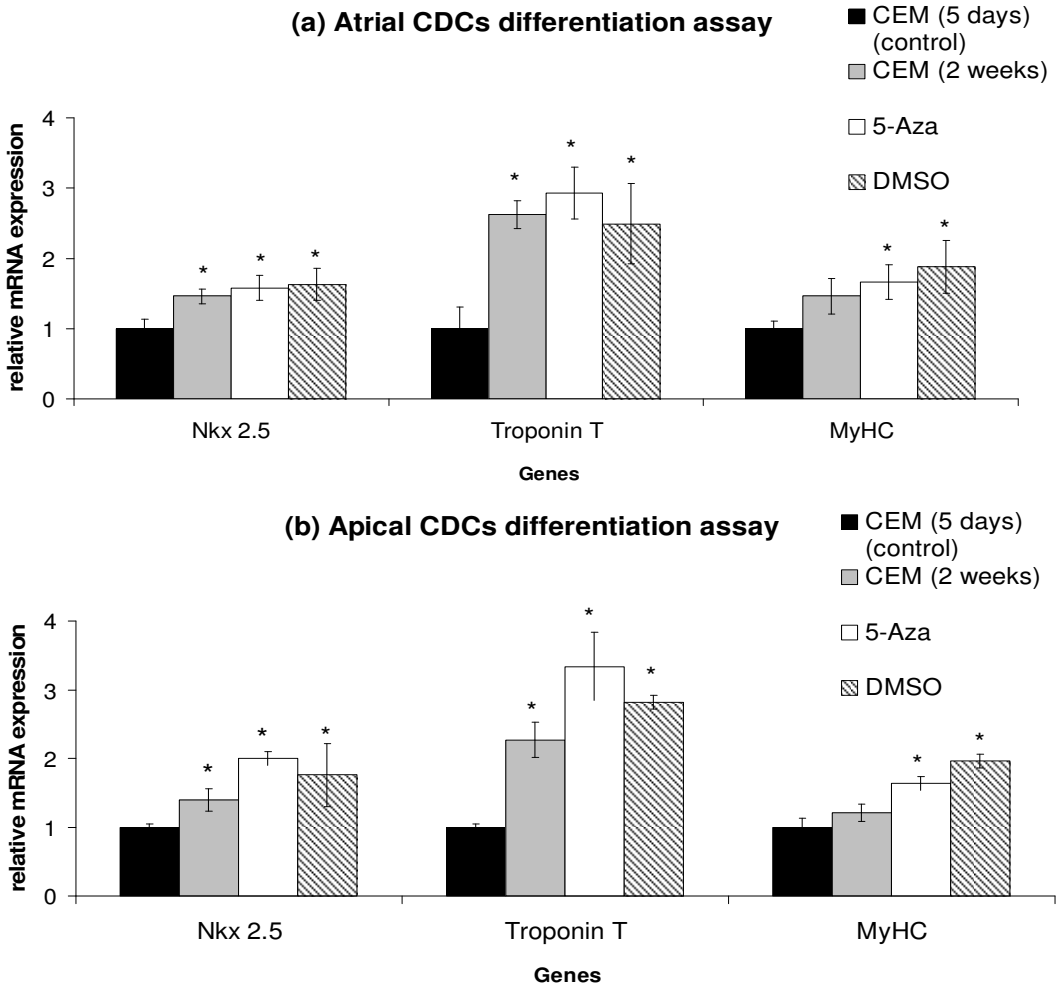

Figure 6.13 *The relative mRNA expression of Nkx 2.5, Tnnt and MyHC for (a) adult atrial and (b) adult apical P2 CDC (n = 3) using qRT-PCR. All values were normalized to GAPDH (housekeeping gene). mRNA expression in CEM (2 weeks), 5-Aza- and DMSO-treated CDC mRNA abundance was expressed relative to the CDCs treated with CEM for 5 days (control). * $p < 0.05$ vs. CEM (5 days) control; # $p < 0.05$ vs. CDCs treated with CEM (2 weeks).*

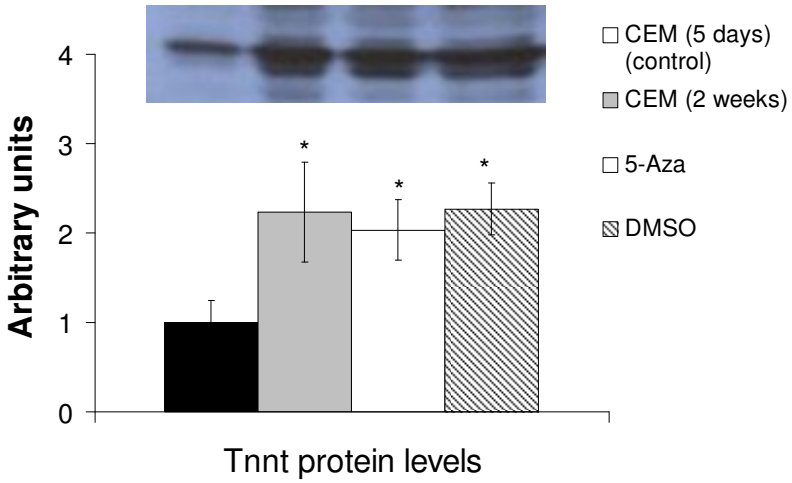

Figure 6.14 *Tnnt protein expression in CEM (5 days)-, CEM (2 weeks)-, 5-aza- and DMSO-treated adult apical P2 CDCs (n = 3). Protein levels were expressed in arbitrary units, with CEM (2 weeks)-, 5-aza- and DMSO- treated CDCs relative to normalized CEM (5 days) CDCs. * p < 0.05 vs. CEM (5 days) (control).*

6.4.4 Effects of ageing on CDC telomere length and telomere reverse transcriptase (TERT) enzyme expression

DNA of P2 CDCs isolated from 3 days, 5 weeks and 3 months old rat hearts was extracted and telomere length was measured. A gradual reduction of telomere length from young rat cells to old rat cells was observed (3 day *vs*. 5 weeks *vs* 3 months = 100% *vs.* 62% *vs.* 44%) (Figure 6.15a). In addition, TERT mRNA levels was also found to gradually decrease from 3 days old CDCs to 3 months old CDCs (100% *vs.* 69% *vs.* 47%) (Figure 6.15b).

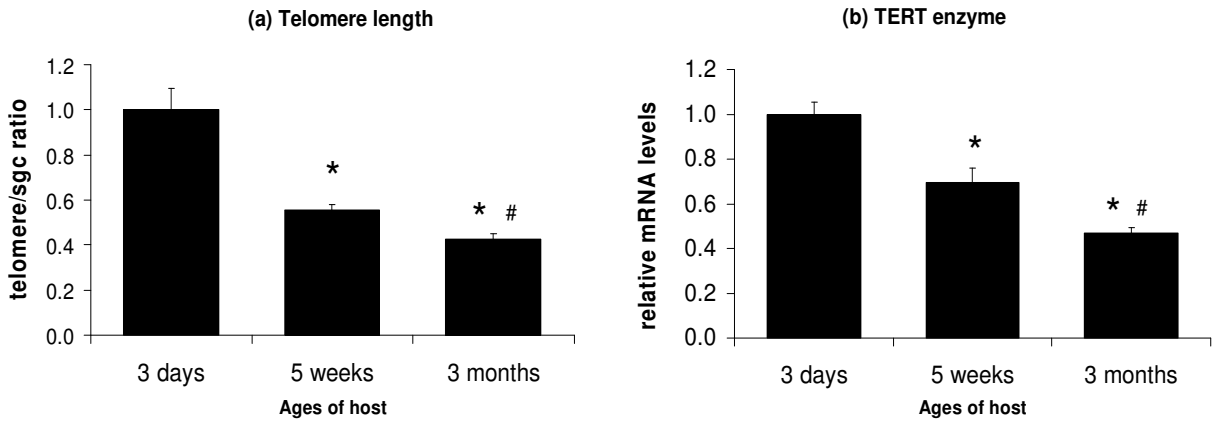

Figure 6.15 *(a) Telomere length and (b) TERT mRNA expression levels were measured in P2 CDCs isolated from 3 days, 5 weeks and 3 months old rat hearts (n = 3). * p < 0.05 vs. 3 days; # p < 0.05 vs. 5 weeks.*

6.4.5 Effects of passaging on cardiac progenitor and mesenchymal cell population

In addition to investigating the effects of the age of donor tissues on CSC isolation and characterization, the effects of cellular ageing due to multiple *in vitro* passaging of neonatal and adult rat CSC were also investigated in this study, by comparing the changes in the expression pattern of selected genes, c-Kit, CD105 and CD90, from EDCs, cardiopheres, passage 0 (P0) CDCs up to passage 10 (P10) CDCs, using qRT-PCR.

c-Kit expression gradually decreased over the *in vitro* expansion culture, with 9.0 ± 0.3% c-Kit in EDCs dropping to only 0.9 ± 0.1% in P10 CDCs, compared with neonatal whole heart total RNA (Figure 6.16). On the other hand, there was a significant up-regulation of CD105 over the *in vitro* cell expansion process, with 26.0 ± 6.8% of CD105 levels in EDCs, increasing to 59.2 ± 4.4% in P10 CDCs, both compared with neonatal whole heart total RNA (Figure 6.17 and Table 6.1).

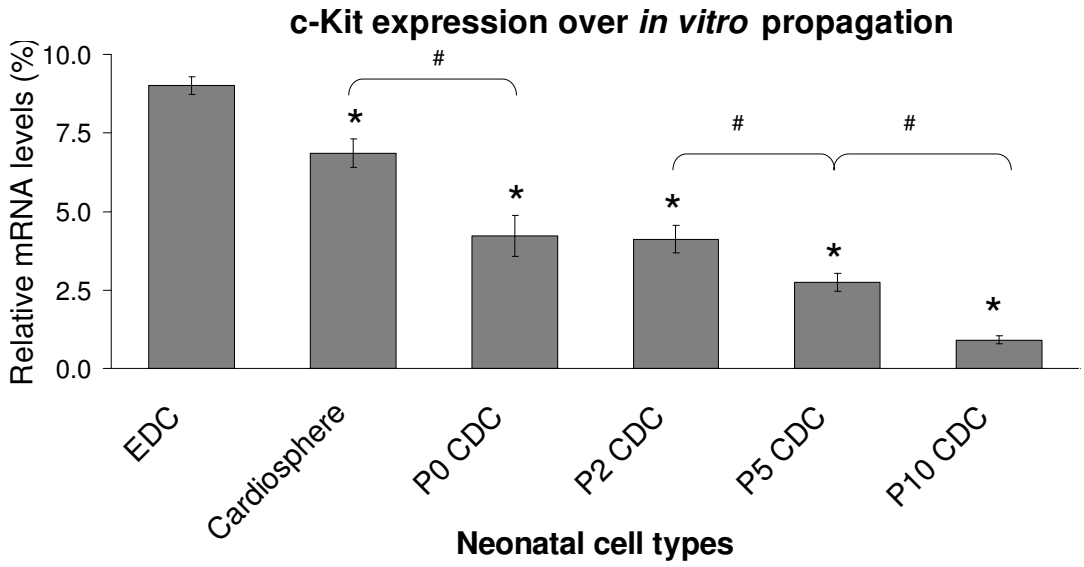

Figure 6.16 *Percentage of c-Kit mRNA expression levels of neonatal EDCs, cardiospheres, P0, P2, P5 and P10 CDCs, relative to neonatal heart total RNA (n = 3). * $p < 0.05$ vs. EDC. # $p < 0.05$ between the two groups linked with arrow.*

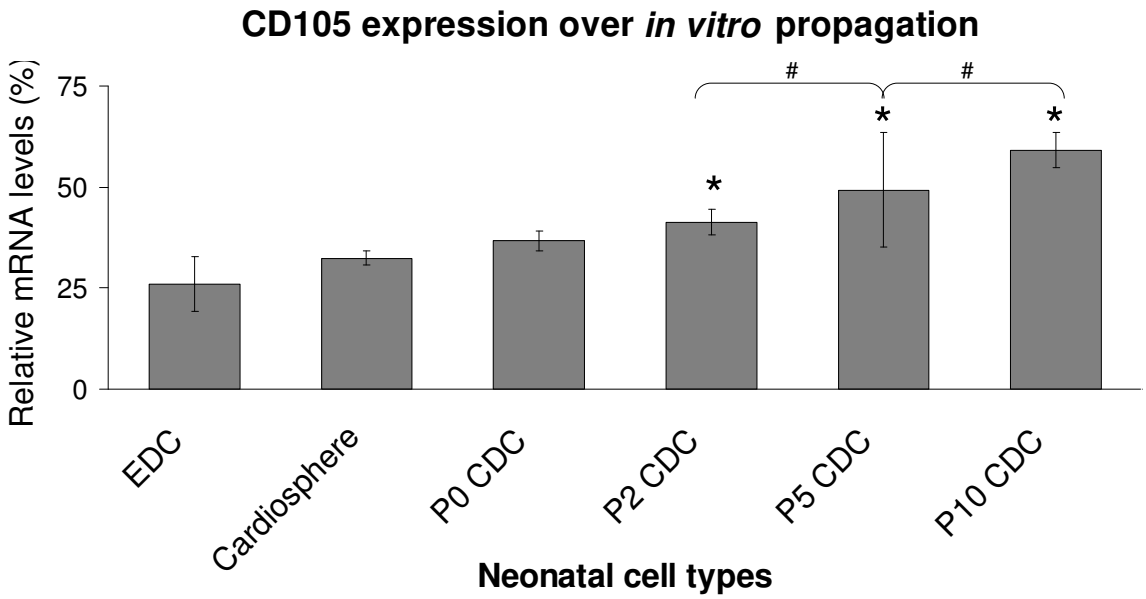

Figure 6.17 *Percentage of CD105 mRNA expression levels of neonatal EDCs, cardiospheres, P0, P2, P5 and P10 CDCs, relative to neonatal heart total RNA (n = 3). * $p < 0.05$ vs. EDC. # $p < 0.05$ between the two groups linked with arrow.*

The levels of CD90 remained high throughout the *in vitro* expansion of CSCs using the tissue explanation method. Neonatal EDCs showed a 3.6 ± 0.8-fold increase of CD90, compared with neonatal whole heart total RNA, and there was a significant gradual upregulation of CD90 expression levels from EDC up to P10 CDC culture (17.8 ±1.1-fold), with the CD90 levels increased during expansion from cardiospheres (7.6 ± 0.6-fold) into P0 CDCs (10.4 ± 2.5-fold) and also during expansion from P0 CDCs into P2 CDCs (14.2 ± 2.3-fold). CD90 levels remained high in CDC culture up to P5 (17.8 ± 2.3-fold) and P10 CDCs (17.8 ± 1.1-fold) (Figure 6.18 and Table 6.1).

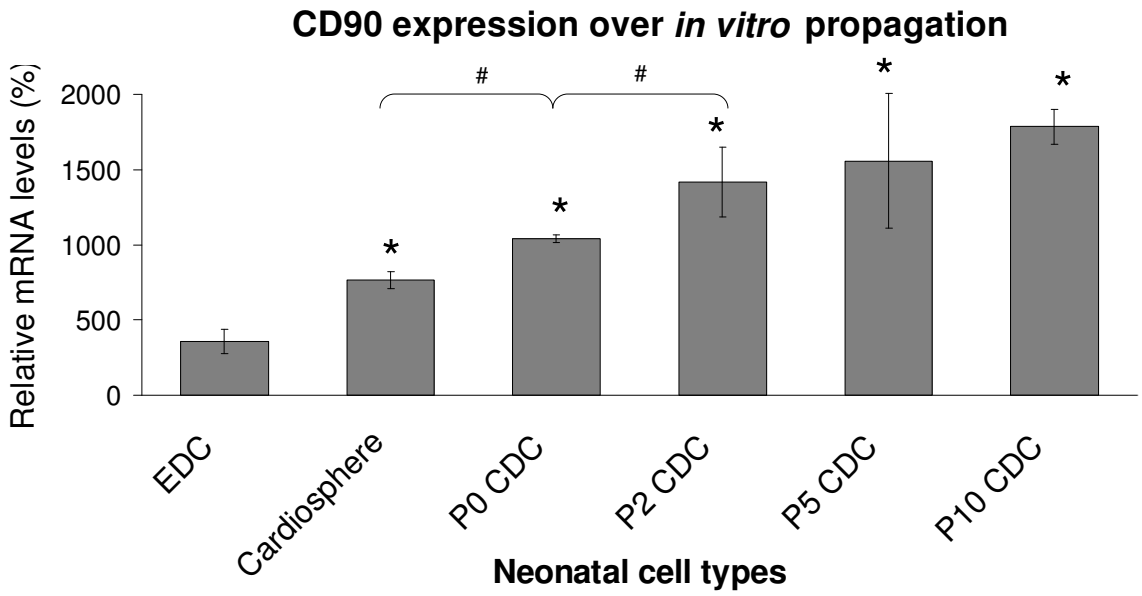

Figure 6.18 Percentage of CD90 mRNA expression levels of neonatal EDCs, cardiospheres, P0, P2, P5 and P10 CDCs, relative to neonatal heart total RNA (n = 3). ** $p < 0.05$ vs. EDC; # $p < 0.05$ between the two groups linked with arrow.*

Similar observations for c-Kit, CD105 and CD90 expression patterns from EDC to P10 CDCs culture were also found for adult atrial and apical tissue (data simplified in Table 6.1). Although adult cells showed increasing CD105 over the culture period, but overall, the expression of CD105 was still lower than the neonatal cells at similar passage (Table 6.1). All together, these data suggested that, independent of donor age, multiple passaging of isolated CSCs could induce *in vitro* cellular ageing, triggering the decease of the c-Kit$^+$ cardiac stem cell population density and increase of CD90$^+$CD105$^+$ cardiac mesenchymal cell population.

Table 6.1 *Percentage of mRNA expression levels of CD90, CD105 and c-Kit of (a) neonatal (b) adult atrial and (c) adult apical EDC, cardiosphere, P0 CDCs, P2 CDCs, P5 CDCs and P10 CDCs, relative to neonatal and adult whole heart total RNA, respectively (n = 3). All data were normalized to GADPH and Actb as housekeeping genes. * $p < 0.05$ vs. EDC.*

(a) Neonatal	**EDCs**	**Cardiospheres**	**P0 CDCs**	**P2 CDCs**	**P5 CDCs**	**P10 CDCs**
c-Kit	9.0 ± 0.3	6.8 ± 0.5 *	4.2 ± 0.6 *	4.1 ± 0.4 *	2.8 ± 0.3*	0.9 ± 0.1*
CD105	26.0 ± 6.8	32.4 ± 1.8	36.7 ± 2.4	41.3 ± 3.2 *	49.3 ± 14.2*	59.1 ± 4.4*
CD90	356 ± 79	763 ± 55.5 *	1042 ± 25*	1415 ± 233*	1557 ± 446*	1783 ± 114*

(b) Adult atrial	**EDCs**	**Cardiospheres**	**P0 CDCs**	**P2 CDCs**	**P5 CDCs**	**P10 CDCs**
c-Kit	6.5 ± 0.9	4.8 ± 0.3 *	4.8 ± 0.6 *	3.0 ± 0.2 *	1.3 ± 0.1*	0.9 ± 0.1*
CD105	20.9 ± 2.2	25.9 ± 2.0	36.0 ± 3.6 *	32.3 ± 1.8 *	48.5 ± 13.1*	53.0 ± 2.2*
CD90	664 ± 8	976 ± 59 *	1221 ± 17*	1508 ± 186*	1601 ± 441*	1747 ± 148*

(c) Adult apical	**EDCs**	**Cardiospheres**	**P0 CDCs**	**P2 CDCs**	**P5 CDCs**	**P10 CDCs**
c-Kit	4.5 ± 0.2	4.1 ± 0.7	3.2 ± 0.4 *	2.9 ± 0.2 *	1.3 ± 0.1*	1.0 ± 0.1*
CD105	15.3 ± 0.4	25.3 ± 2.2 *	24.8 ± 0.7 *	31.5 ± 2.7 *	47.5 ± 12.1*	57.8 ± 10.1*
CD90	787 ± 94	853 ± 144	1032 ± 42*	1314 ± 463*	1523 ± 91*	1912 ± 485*

Study two - Optimization of adult CDC culture using hypoxic and PHDI-preconditioning

In the first part of the study, it was shown that the proliferation and cardiac stem cells marker, c-Kit, were attenuated in CDCs isolated from aged tissue. Also, multiple passaging of CDCs *in vitro* caused reduction in c-Kit expression. Thus, in the second part of this study, adult CDCs were optimized using hypoxia and PHDI-preconditioning methods to enhance the therapeutic potential of CDCs for myocardial infarction.

6.4.6 Increased HIF-1α mRNA and protein expression

qRT-PCR results revealed that adult atrial and apical P2 CDCs cultured under hypoxia or with 1mM DMOG, 0.5mM EDBA or 30 μM BIC showed significantly higher HIF-1α mRNA and protein levels, compared with normoxic non-treated CDCs (Figure 6.19 and Figure 6.20), confirming that hypoxic and PHDI treatment activated the adult P2 CDC HIF system. There were no significant differences in HIF-1α levels, neither transcriptionally nor translationally, between adult atrial and adult apical CDCs. In both atrial and apical CDCs, hypoxic and DMOG treatment resulted in significant higher HIF-1α protein levels, by 36% and 26%, respectively, compared with BIC-treated CDCs (Figure 6.20).

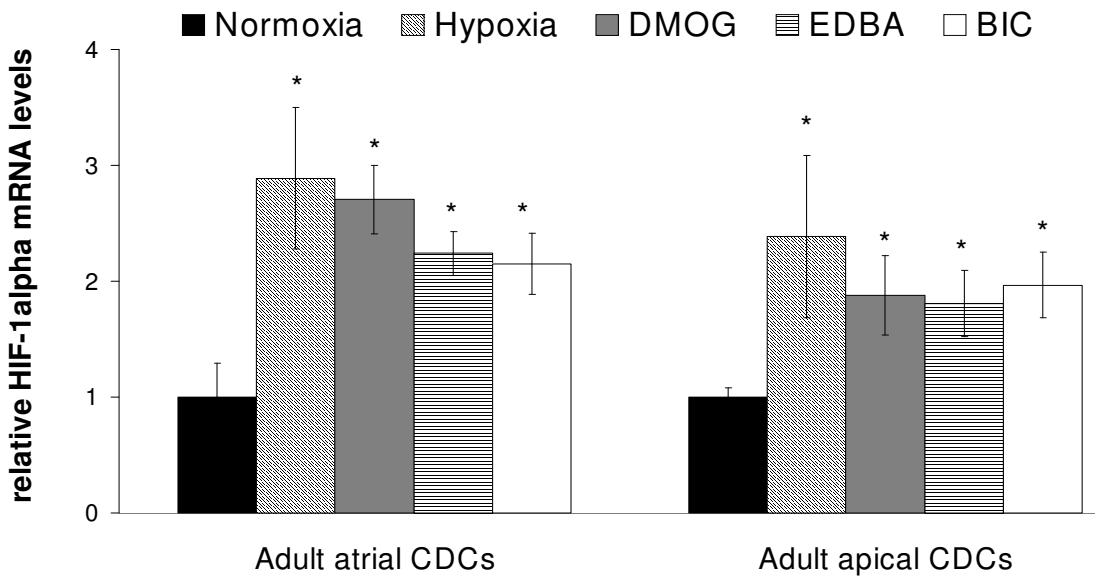

Figure 6.19 *The relative mRNA expression of HIF-1α in adult atrial and apical CDCs (n = 4) using qRT-PCR. mRNA expression in hypoxic, DMOG-, EDBA- and BIC-treated CDCs was normalized to the geometric mean of GAPDH and Actb (housekeeping genes) and normoxic cells (calibrator). * p < 0.05 vs. normoxia.*

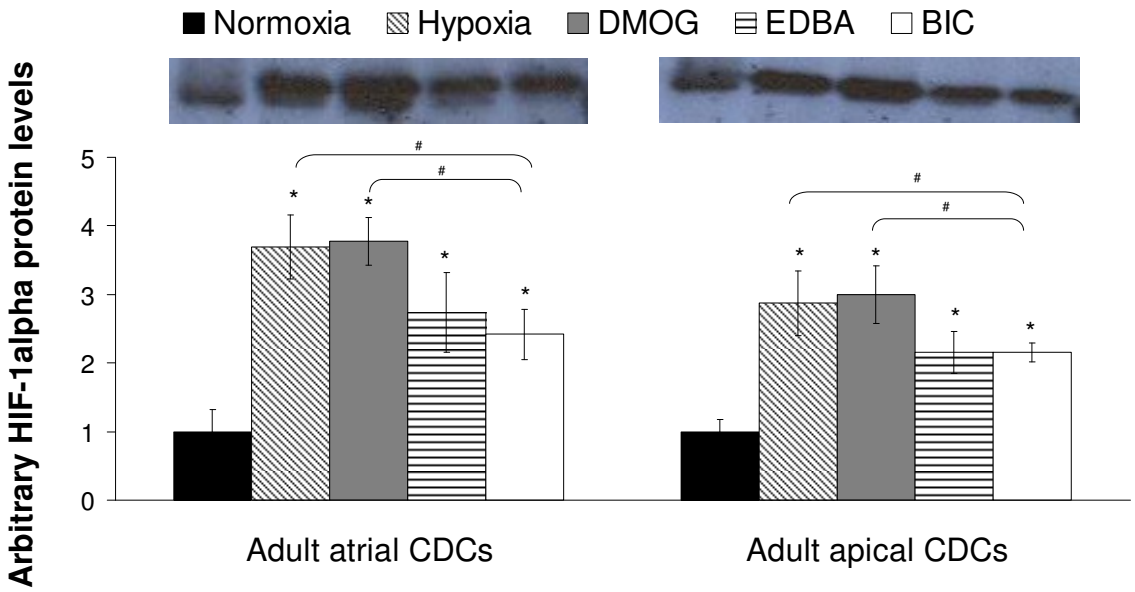

Figure 6.20 *HIF-1α protein expression in normoxic, hypoxic, DMOG-, EDBA- and BIC-treated adult atrial and apical CDCs (n = 4). Protein levels were expressed in arbitrary units, relative to normoxic CDCs. * p < 0.05 vs. normoxia; # p < 0.05 between the two groups linked with arrow.*

6.4.7 Increased CXCR-4 expression

Activation of the HIF system after hypoxic- and PHDI-preconditioning induced the expression of the HIF-regulated cytokine CXCR-4 in adult atrial and apical CDCs, compared with normoxic CDCs (Figure 6.21). Coincident with the HIF-1α mRNA and protein levels, there were no significant differences in CXCR-4 expression levels between adult atrial and adult apical CDCs.

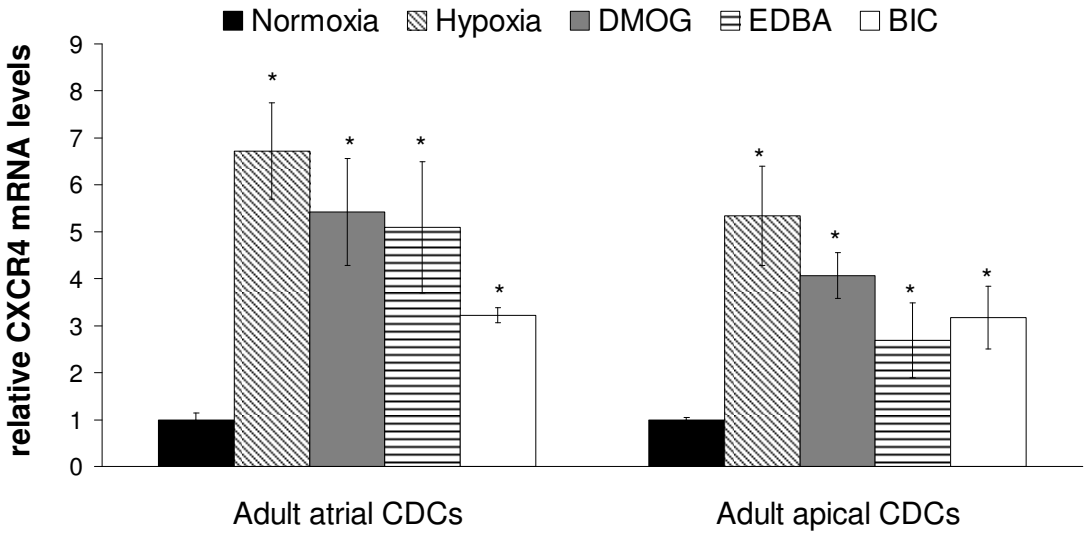

Figure 6.21 *The relative mRNA expression of CXCR-4 in adult atrial and apical CDCs (n = 4) using qRT-PCR. mRNA expression in hypoxic, DMOG-, EDBA- and BIC-treated CDCs was normalized to the geometric mean of GAPDH and Actb (housekeeping genes) and normoxic cells (calibrator). * $p < 0.05$ vs. normoxia.*

6.4.8 Increased cytokine expression – EPO and VEGF

Hypoxic, DMOG and EDBA treatment significantly increased the levels of EPO and VEGF mRNA in both atrial and apical CDCs, compared with normoxic CDCs (Figure 6.22 and Figure 6.23).

Notably, BIC-treated CDCs reacted to the HIF activation in a different way to that seen in hypoxic, DMOG and EDBA-treated CDCs. Firstly, BIC-treated atrial CDCs showed significantly higher EPO levels by 180%, compared with DMOG-treated atrial CDCs (Figure 6.22), even though BIC-treated atrial CDCs had a lower HIF-1α protein level by 36%, compared with DMOG-treated atrial CDCs (as shown in Figure 6.20). Secondly, BIC did not induce the upregulation of VEGF mRNA in both atria and apical CDCs, but DMOG and EDBA treated CDCs did (Figure 6.23).

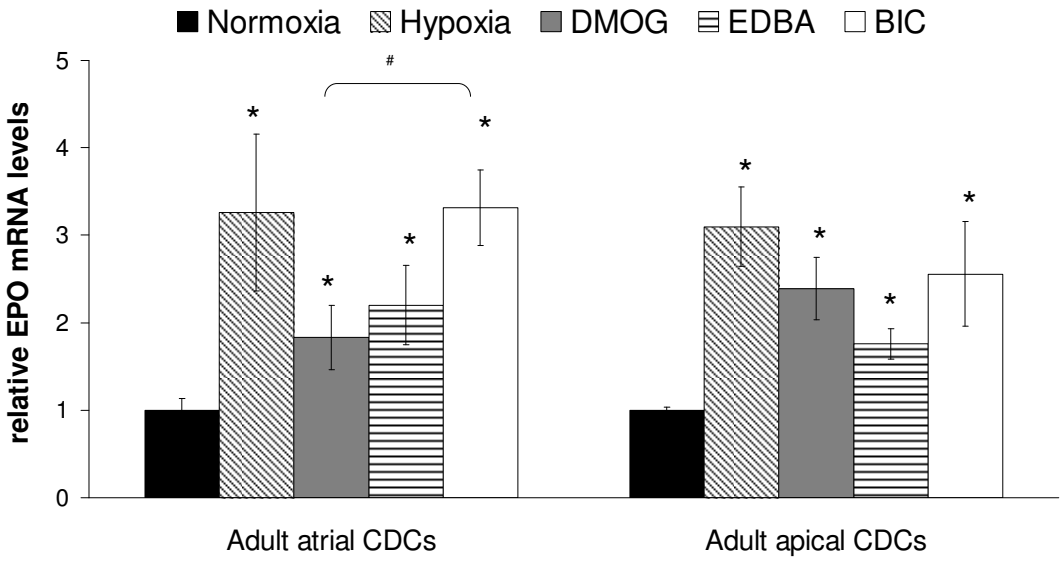

Figure 6.22 *The relative mRNA expression of EPO in adult atrial and apical CDCs (n = 4) using qRT-PCR. mRNA expression in hypoxic, DMOG-, EDBA- and BIC-treated CDCs was normalized to the geometric mean of GAPDH and Actb (housekeeping genes) and normoxic cells (calibrator). * $p < 0.05$ vs. normoxia; # $p < 0.05$ between the two groups linked with arrow.*

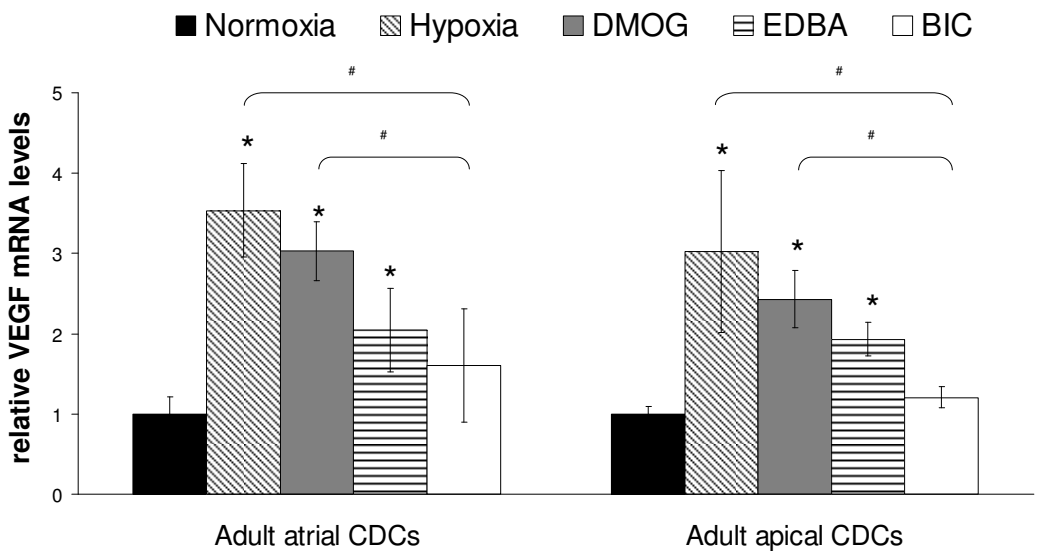

Figure 6.23 *The relative mRNA expression of VEGF in adult atrial and apical CDCs (n = 4) using qRT-PCR.. mRNA expression in hypoxic, DMOG-, EDBA- and BIC-treated CDCs was normalized to the geometric mean of GAPDH and Actb (housekeeping genes) and normoxic cells (calibrator). * $p < 0.05$ vs. normoxia; $^{\#}$ $p < 0.05$ between the two groups linked with arrow.*

6.4.9 Increased cardiac progenitor cells

Under hypoxia, CDC culture caused significant increases of c-Kit levels in both atrial (2.3 ± 0.1-fold) and apical (2.2 ± 0.1-fold) cells, compared with cells from these locations cultured under normoxia (Figure 6.24).

DMOG, EDBA and BIC treatment increased the c-Kit levels, by 1.59 ± 0.17-fold, 1.48 ± 0.16-fold and 1.60 ± 0.17-fold, respectively in atrial CDCs and by 1.54 ± 0.14-fold, 1.72 ± 0.15-fold and 1.61 ± 0.16-fold, respectively in apical CDCs, compared with non-treated normoxic CDCs. However, the induction of c-Kit expression by these PHDIs was significantly lower than the c-Kit levels induced by hypoxic culture (Figure 6.24).

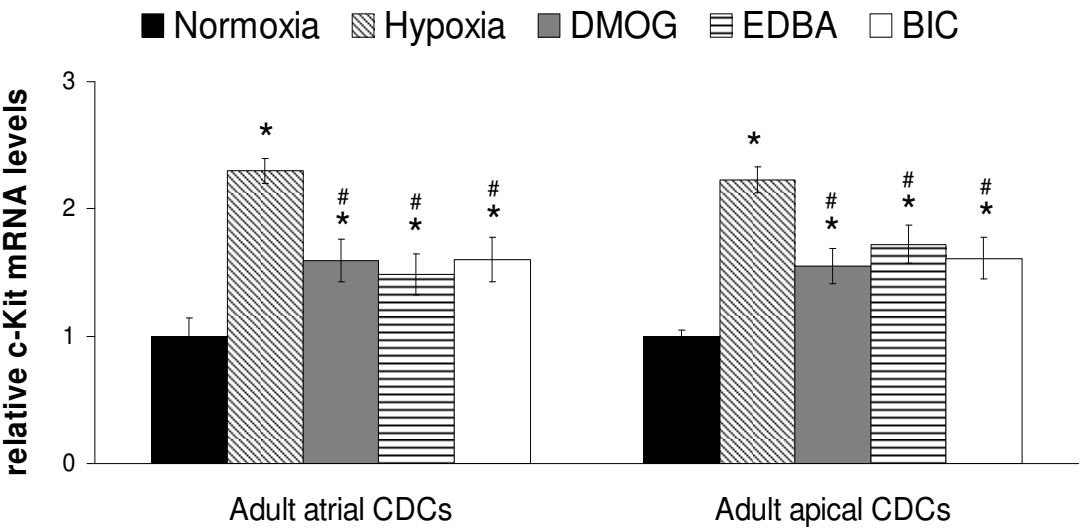

Figure 6.24 *The relative mRNA expression of c-Kit in adult atrial and apical CDCs (n = 4) using qRT-PCR. mRNA expression in hypoxic, DMOG-, EDBA- and BIC-treated CDCs was normalized to the geometric mean of GAPDH and Actb (housekeeping genes) and normoxic cells (calibrator). * $p < 0.05$ vs. normoxia; # $p < 0.05$ vs. hypoxia.*

All the hypoxic or PHDI-preconditioned atrial and apical CDCs had significantly reduced CD90 mRNA levels, compared with normoxic cells (Figure 6.25). On the other hand, only hypoxia and EDBA significantly reduced the expression of CD105 in atrial and apical CDCs (Figure 6.26).

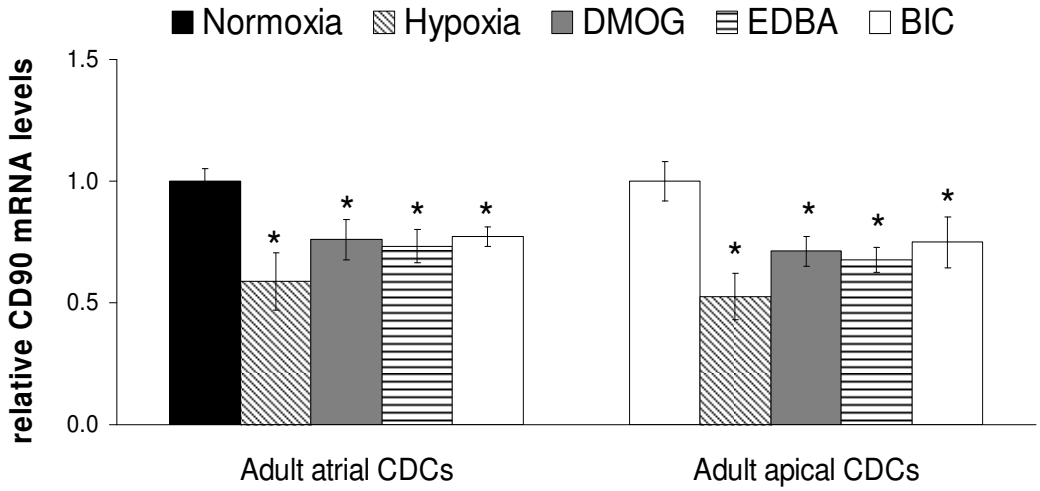

Figure 6.25 *The relative mRNA expression of CD90 in adult atrial and apical CDCs (n = 4) using qRT-PCR. mRNA expression in hypoxic, DMOG-, EDBA- and BIC-treated CDCs was normalized to the geometric mean of GAPDH and Actb (housekeeping genes) and normoxic cells (calibrator). * $p < 0.05$ vs. normoxia.*

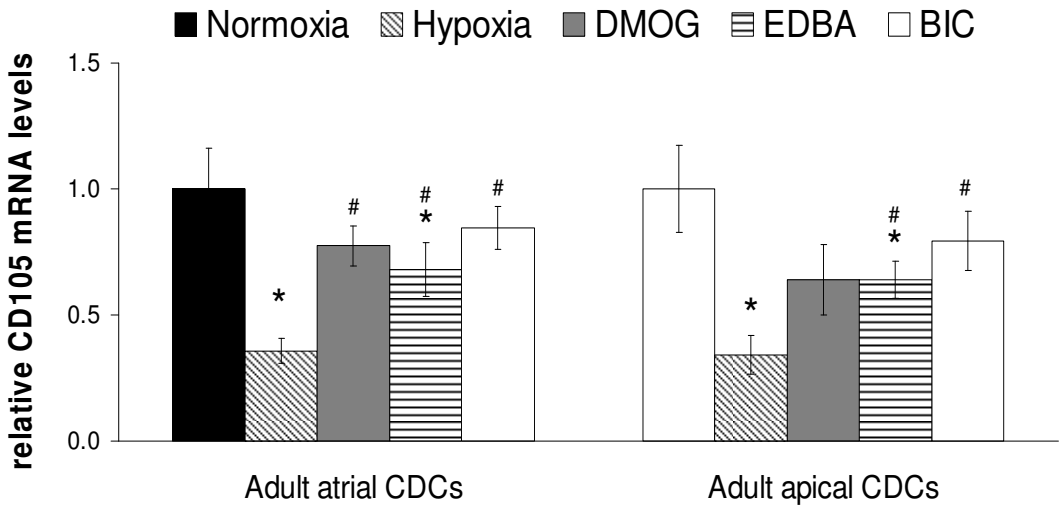

Figure 6.26 *The relative mRNA expression of CD105 in adult atrial and apical CDCs (n = 4) using qRT-PCR.. mRNA expression in hypoxic, DMOG-, EDBA- and BIC-treated CDCs was normalized to the geometric mean of GAPDH and Actb (housekeeping genes) and normoxic cells (calibrator). * $p < 0.05$ vs. normoxia; # $p < 0.05$ vs. hypoxia; # $p < 0.05$ vs. hypoxia.*

6.4.10 Increased glucose metabolism and reduced oxygen respiration

Following hypoxic and PHDI-preconditioning, CDCs had adapted to the hypoxic condition by reducing oxygen consumption rates (Figure 6.27) and switching to glycolytic metabolism, confirmed by the significant upregulation of glucose uptake and lactate production were also observed in CDCs (Figure 6.28).

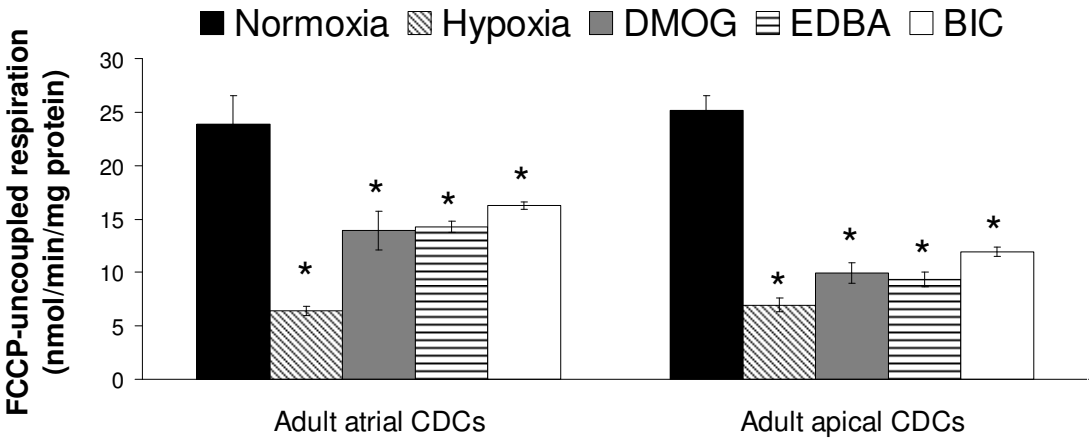

Figure 6.27 *FCCP-uncoupled respiration rates of non-treated normoxic CDCs (control) and hypoxic, DMOG-, EDBA- and BIC-treated CDCs. * $p < 0.05$ vs. control.*

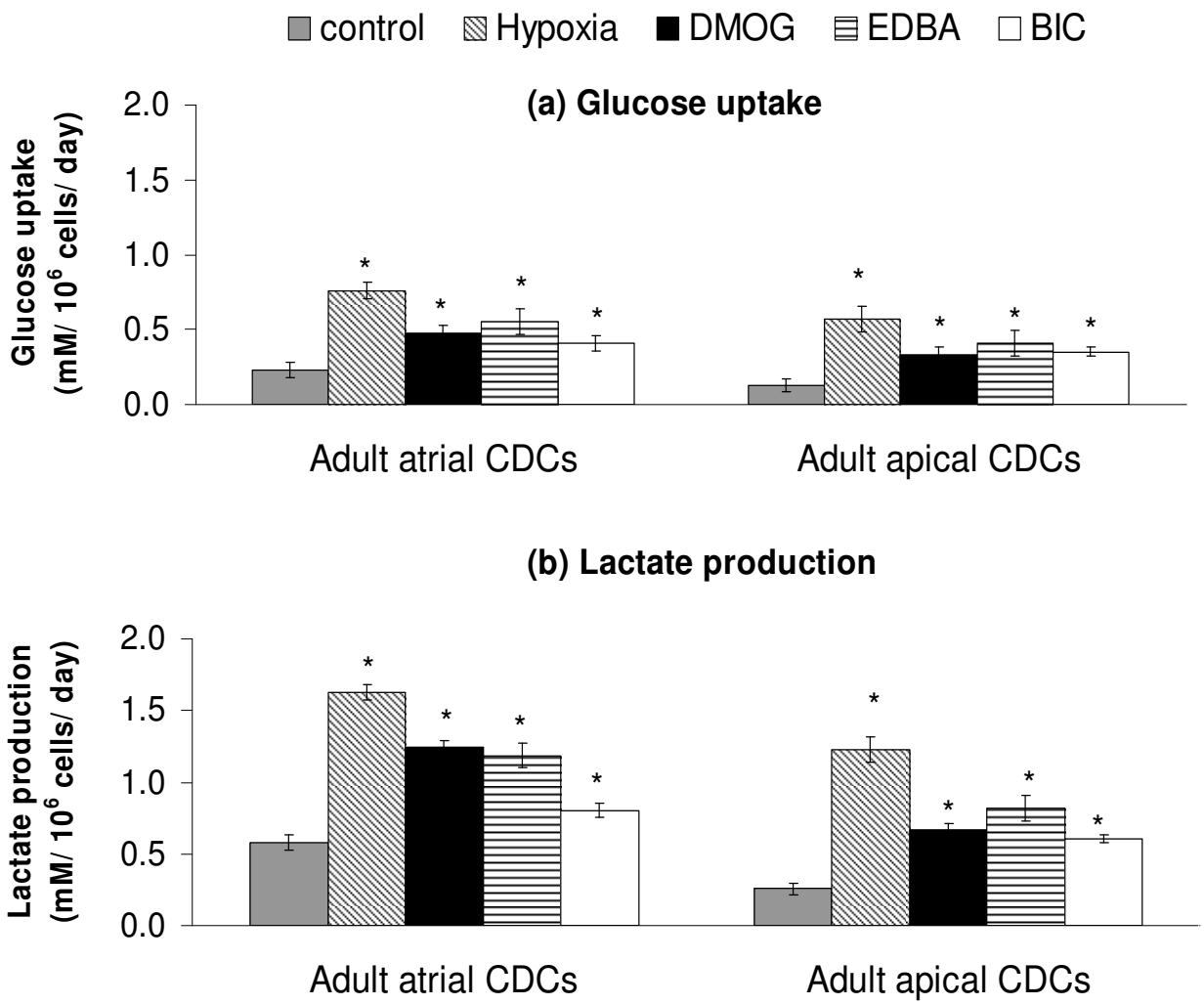

Figure 6.28 *Levels of (a) glucose uptake and (b) lactate production in non-treated normoxic CDCs (control) and hypoxic, DMOG-, EDBA- and BIC-treated CDCs. Glucose utilization and lactate production are expressed as mM of glucose/lactate per million cells per day. * $p < 0.05$ vs. control.*

6.4.11 Hypoxic preconditioning increased cell proliferation and TERT mRNA expression

Hypoxic precondiotioning significantly increased the proliferation rate of adult atrial and apical CDCs, to an average rate of 1.7 ± 0.1-fold higher than normoxic CDCs (Figure 6.29). TERT enzyme expression remained higher in hypoxic CDCs, on an average 4.1 ± 0.7-fold compared with normoxic CDCs (Figure 6.30).

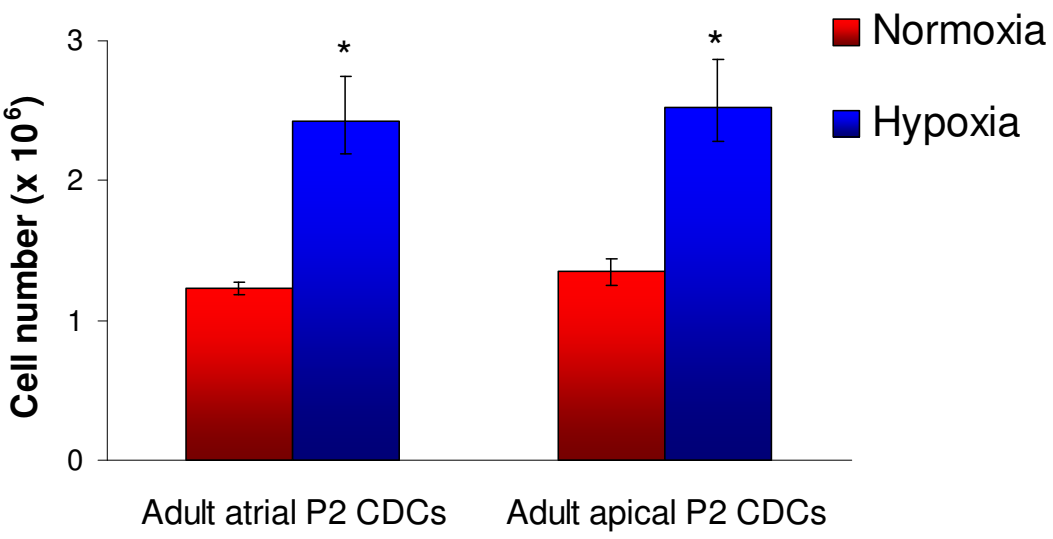

Figure 6.29 *Cell numbers of normoxic and hypoxic P2 atrial and apical CDC at 5 days post-plating. * $p < 0.01$ vs. normoxia.*

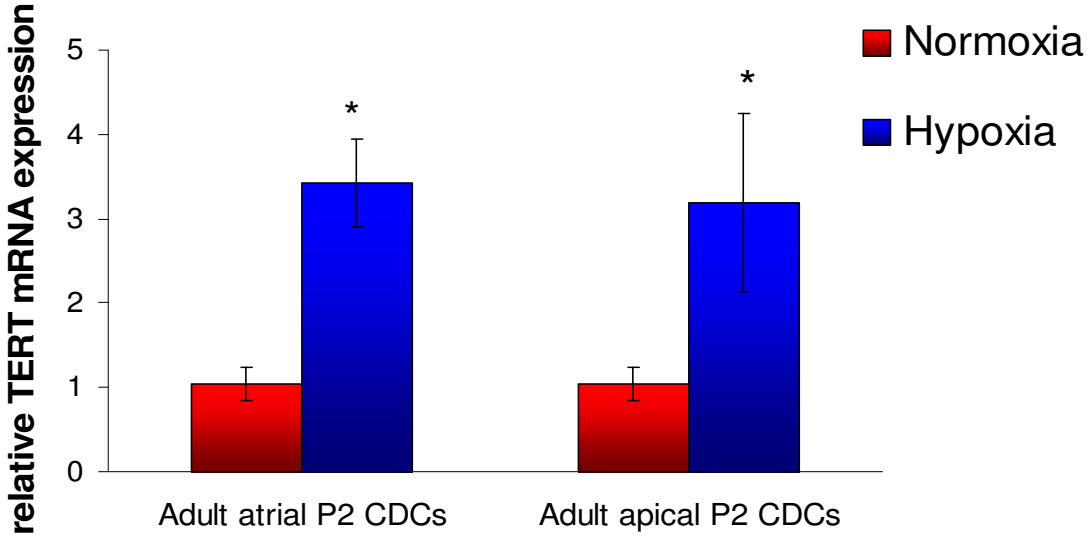

Figure 6.30 *The relative mRNA expression of TERT for normoxic and hypoxic P2 atrial and apical CDCs (n=3) using qRT-PCR. All values were normalized to GAPDH and Actb (housekeeping genes). mRNA expression of hypoxic CDCs were expressed relative to the normoxic CDCs. * $p < 0.05$ vs. normoxia.*

6.5 Discussion

The aims of the work described in the first part of this chapter were to determine the effects of ageing on the CSC numbers, proliferative ability, and differentiation potential, while the second part discussed the optimization of CDCs using hypoxia and PHDI-preconditioning.

Effects of ageing on primary cardiac stem cell proliferation

In this study, CSCs were isolated from neonatal rats (1-3 days old) and adult rats (4 months old). As hypothesized, the proliferation rates of CSCs were significantly decreased from the aged donors. Approximately 6 x 10^6 CDCs were obtained from neonatal rat heart within 26 ± 6 days, from adult atrial tissue within 36 ± 7 days and from adult apical tissue within 42 ± 7 days, comparable to Smith *et al.* who obtained 1.7 ± 0.4 x 10^6 CDCs from human biopies within 45 ± 7 days using the same technique [108]. *In vitro* expansion of neonatal rat explants successfully yielded adequate cell numbers for transplantation approximately 2 weeks faster than adult rat explants. This is in agreement with studies which demonstrated the impacts of ageing on low cell cycling or division in endothelial progenitor cells [284], bone marrow-derived mesenchymal stem cells [285], skeletal muscle [286] and precursor cells in the subventricular zone of rat brain [287].

A potential cause of reduced proliferative potential in aged CSCs is the shortening of telomeres [94]. Telomeres are DNA-protein complexes that cap chromosomal ends, promoting the genome from damage. At each cellular division, telomeric DNA terminal regions are not fully replicated, thus causing the shortening of telomere after every cell cycle, unless the telomere length is reversed by telomerase reverse transcriptase enzyme (TERT) which elongates the length of the telomere [92, 288].

When telomeric DNA reaches a critically short length, cells become susceptible to senescence or apoptosis [289, 290]. Here, a negative relationship was found between telomere length and age in CDC population. Also, a reduced expression of telomerase enzyme in CDCs was observed with increasing age. These data indicated that the ageing processes decreased telomere length, and thereby accelerated cell senescence or mortality, which in turn impaired cardiac stem cell proliferation/self renewal rate.

Effects of ageing on CSC gene expression profile and differentiation potential

CDCs generated from both adult atrial and apical tissue expressed cardiac stem cell and pluripotent cell markers, c-Kit, Oct-4, Klf4 and Sox 2. However, it was observed that the expression of these genes was significantly lower in adult CDCs compared with neonatal CDCs. Extensive reports have revealed that the changes in phenotypic and functional properties of adult stem/progenitor cells may occur during chronological aging [291-293]. In some cases, chronological aging triggered stem cell death and lead to a depletion of the stem cell pool [294-296]. For example, the number of neural stem cells [297], melanocyte stem cells [298], circulating endothelial progenitor cells [299] and c-kit$^+$ cells in rats testis and epididymis [300], were found to be reduced in elderly animals. Many factors may account for the reduced stem cell density in aged donors, including intense oxidative and metabolic stress, or genotype factors such as telomere shortening and defects in DNA repair mechanisms [301, 302].

The fate of CDCs was modulated by the environmental factors and mediated by signalling pathways based on the tissue in which they reside [182, 303]. In fully developed adult heart CDCs, an upregulation of the cardiac differentiation marker (Nkx 2.5), matured cardiomyocytes markers (Tnnt and MyHC), and a downregulation of mesenchymal stem cells marker (CD105) were observed, compared with the

postnatal heart CDCs. In line with this, it was found that the adult CDCs were more committed to differentiate into cardiomyocyte lineage rather than into adipocyte lineage. Taken together, these data suggest that adult CDCs exhibited age-related changes in stem cell density and stem cell fate. The replicative activity and density of cardiac stem cells from young rats was higher than that from aged rats, however, the activation of cardiomyocytes markers in aged CDCs lead the cells into more lineage specific cell fate.

Effects of stem cells niche organisation in primary cardiac stem cell isolation

Stem cells are stored in niches that are located deep in the tissue for protection from damaging stimuli [181, 303, 304]. These CSC niches are scattered throughout the myocardium [279]. Due to consideration of clinical accessibility, adult hearts were cut into small portions of atrial, midregion and apical tissue, representing the nature of biopsies commonly obtained from patients. Ideally, the neonatal rat hearts should be dissected into 3 parts for a more detailed comparison between neonatal rat CSCs and adult rat CSCs, however, it is not practical due to the small sizes of neonatal hearts.

Stem cell niches play a important role in signaling the stem cell division, function and differentiation [182, 183]. Although scattered throughout myocardium, Leri *et al.,* suggested that the frequency of lineage negative CSC clusters was inversely related to the hemodynamic load sustained by each section of the heart [279]. The very high degree of stress at the base-midregion of the ventricular wall may induce a higher turnover rate of the progeny cells residing in this area towards matured cardiomyocyte lineage in order to replace old/damaged cells with newly generated cells. On the other hand, in the atrial microenvironment, which is an area of low wall stress, the CSCs are preserved through symmetric division or self-renewal, while in ventricular apical

niches, CSCs are mostly involved in the formation of transient amplifying cells for cardiomyocyte commitment in ventricular tissue [279]. This is supported by Beltrami *et al.* who reported that lineage negative CSCs were found more densely in the atria and ventricular apex than other regions [86] and Urbaneck *et al.* who demonstrated that the atrial niches were 2-fold larger than ventricular apex niches, and thus contained more CSCs [305]. Here we found that the midregion of adult rat heart did not generate any EDCs, while atrial explants generated an average 0.6-fold more EDCs from day 6 to day 12 in culture, with 0.2-fold higher c-Kit level, than the apical explants. Further, apical EDCs took approximately 3 to 4 days longer to form cardiospheres, compared with atrial EDCs. CSC numbers were higher in atrial tissue than apical tissue, ideally it would be preferable for surgical biopsies for CSC isolation to be taken from the atrium. However, this may not be practical as often biopsies are taken via a catheter as an outpatient.

Effects of passage number on cardiac progenitor and mesenchymal cell population

An important factor in the success of stem cell-based therapy is to obtain sufficient quality cell numbers from a limited tissue biopsy. Passaging the CSCs could expand the cell line and generate more cells for transplantation, but the passaging process could induce *in vitro* cellular ageing due to the prolonged cell culture period. It has been shown that cells were aged by multiple *in vitro* passages, triggering variability of stem cell phenotypic and functional characteristics [306]. For example, a decline in progenitor cell numbers [307] and loss of multipotency [308] was reported during *in vitro* expansion of bone marrow mesenchymal stem cells. Here, we examined the effects of passaging on the gene expression of cardiac progenitor and mesenchymal cells in EDCs, cardiospheres and CDCs from P0 up to P10. It was found that c-Kit showed a gradual decrease in expression, while CD105 and CD90 showed a gradual

increasing expression upon *in vitro* propagation of CDCs. A possible explanation is that the CDC *in vitro* expansion process favored the expansion of $CD105^+CD90^+$ mesenchymal stem cells. It has been found that c-kit^+ CSCs were spontaneously differentiated into adipocytes over long-term culture [98]. Also, the increasing CD90 mRNA expression could be due to contamination of CDC cultures with $CD90^+$ fibroblasts [309, 310]. In this situation, identification and elimination of fibroblasts from the CDC culture could improve the c-Kit yield and CDC differentiation potential [311]. In future work, purification of the heterogenous CDC population based on reliable specific markers, such as CD146 (specific mesenchymal stem cells marker) [311] or DDR2 (specific cardiac fibroblast marker) [312], which discriminates between $CD90^+CD105^+$ mesenchymal stem cells and $CD90^+$ fibroblasts is suggested.

Optimization of adult CDCs

Stem cells reside in tissues where they maintain pluripotency and the potential for self-replication. However, during each round of DNA replication, processes that underlie replicative aging could ultimately lead to the senescence of stem cells [302, 313]. In this study, we found that the c-Kit expression and stem cells proliferation deteriorated with age and *in vitro* multiple passaging. In order to optimize the therapeutic potential of adult CDCs, these cells were preconditioned with physiologically-induced hypoxia using low oxygen culture and pharmacologically-induced hypoxia using prolyl hydroxylase inhibitors, including DMOG, EDBA and BIC.

Physiologically-induced hypoxia and pharmacologically-induced hypoxia resulted in different effects on CDCs. For example, hypoxic preconditioning increased the proliferation rate of adult CDSs, but this effect was not observed in PHDI-preconditioned cells. Nonetheless, these two culture techniques generated CDCs with increased c-Kit^+ and reduced $CD105^+CD90^+$ cell population. Also, the HIF system was

activated under both culture methods and subsequently upregulated the expression of several important cytokines, including CXCR-4 which aids to recruit the CDCs to the infarcted myocardium [314], EPO [110] and VEGF [124] which play a role in neovascularisation. An *in vivo* animal study with optimized adult CDCs is planned in future work to verify the potential of these cells for the treatment of myocardial infarction.

6.6 Conclusion

In conclusion, CDCs grown from adult atrial and apical tissue had adult stem cell characteristics comparable to those previously described [108]. Although apical tissues generated EDCs slower than atrial tissue, CDCs generated from both atrial and apical EDCs expressed cardiac stem cell and pluripotent cell markers, c-Kit, Oct-4, Klf4, Sox 2 and Nanog. This population was complemented by a $CD105^{+}CD90^{+}$ mesenchymal-like population, likely serving as a feeder layer to the more primitive cell populations during *ex vivo* proliferation. Further, some adult CDC population expressed cardiac differentiation markers, Nkx 2.5, GATA 4, Tnnt and MyHC and were readily differentiated along the cardiomyocyte lineage with or without cardiomyogenic induction stimuli. Nonetheless, the expression of c-Kit decreased in aged animals and also after extended culture *in vitro*. Thus, hypoxic culture and PHDIs were used to optimize the adult CDC culture. Optimized cells showed increased c-Kit and decreased CD90 and CD105, giving a increased cardiac stem cell population in CDC culture. In addition, hypoxic- and PHDI-preconditioning enhanced the therapeutic potential of these cells for myocardial infarction by increasing the expression of several important cytokines such as CXCR-4, EPO and VEGF. This work introduced the prospect for autologous CDC therapy for myocardial infarction which predominantly affects more elderly patients.

Chapter 7

General Discussion

GENERAL DISCUSSION

Cardiosphere-derived cells (CDCs) isolated from rat heart tissue explants via the formation of explant-derived cells (EDC) and cardiospheres (Csp) are a potential endogenous cardiac stem cell (CSC) candidate for myocardial infarction therapy. These cells showed adult stem cell properties and have been proven to increase cardiac function *in vivo* [107-109, 201, 315-317]. Clinical application of CDCs is under investigation by the CADUCEUS trial (Clinical Trials.gov. Identifier NCT00893360) [180].

However, it has been shown by us and others, that CDCs need to be expanded *in vitro* over weeks in order to obtain sufficient cells for transplantation [108]. During this period, the infarcted heart will undergo the initial stages of scar formation and remodeling. Hence, optimization of the current CDC culture protocol to increase the cell proliferation rate without compromising the stem cell properties was the main objective of the studies in this thesis.

Isolation and phenotypic characterization of cardiosphere-derived cells

In *Chapter 3*, CDCs were isolated and characterized *in vitro*. Approximately 6 x 10^6 CDCs were obtained from a neonatal rat heart within 28 days. This heterogeneous population contained cells expressing the cardiac stem cell marker, c-Kit, and pluripotent cell markers, Oct-4, Klf4 Sox 2 and Nanog. CDCs also expressed cardiac differentiation markers, Nkx 2.5 and GATA 4, indicating that some cells were at the early stage of cardiac myogenic differentiation and were committed to the cardiac lineage. However, a relatively high expression of CD105 and CD90 was found in CDC heterogeneous culture, compared with neonatal heart total cells, indicating that the majority of CDCs had a $CD105^+$ $CD90^+$ mesenchymal stem cell (MSC) phenotype.

These $CD105^+$ $CD90^+$ mesenchymal-like cells possibly served as a feeder layer to the more primitive cardiac stem cell populations during *ex vivo* proliferation [108]. MSCs are multipotent, capable of differentiation into osteoblasts, chondrocytes and adipocytes under specific culture conditions [66], and recently have also been found to differentiate into cardiomyocytes [69]. In this study, approximately 30% of neonatal CDCs turned into adipocytes after induction with adipogenesis medium. Also, CDCs were found to be readily differentiated into the cardiomyocyte lineage with or without cardiomyogenic induction stimuli, revealed by the upregulation of cardiac troponin T (Tnnt) and myosin heavy chain (MyHC) mRNA expression. Furthermore, *in vivo* CDCs cardiomyogenic differentiation was observed in the infarcted myocardium, confirming the cardiomyogenic potential of CDCs. In brief, CDCs grown from direct outgrowth of cardiac tissue explants were a heterogeneous population resembling cardiac stem/pluripotent cells and mesenchymal cells and were capable of multipotent differentiation into adipocytes and most importantly cardiomyocytes, both *in vitro* and *in vivo*.

Cardiosphere-derived cells improved cardiac function

Transplanted CDCs were retained in the infarcted myocardium after injection and 49% were found to express troponin I (cTnI) 16 weeks after injection. MRI measurements of cardiac function showed that CDC-treated hearts had a significantly greater ejection fraction than control hearts by 9%, 6 weeks after myocardial infarction and CDC administration. This difference in EF was maintained up to 16 weeks after infarction. The increase in cardiac function was probably a result of both regeneration of viable myocardium by differentiation of transplanted CDCs, and of paracrine effects. This hyphothesis was supported by quantitative histological analysis which showed a significant decrease in infarcted scar volume by 33% and immunohistochemistry

which showed that 49% of transplanted CDCs differentiated into cardiomyocytes within the infarcted myocardium area. Paracrine release of cytokine by transplanted CDCs induced neoangiogenesis, confimed by the quantitative histological analysis which showed an increased capillary density by 9%. Our data are in agreement with Chimenti *et al.* who also demonstrated that the regenerative mechanism of CDCs resulted from both paracrine effects and via cardiomyocyte differentiation, with differentiation accounting for 20 - 50% of the observed effects [315]. Despite the relatively lower c-Kit level expressed in CDCs isolated in this study, than that reported by others [108], it has been proven that these CDCs had a therapeutic value to improve cardiac function. This is in agreement with previous study which also reported that a mixed cell population of cardiac mesenchymal stem cells and c-Kit$^+$ cardiac stem cells provided greater functional improvement than c-Kit$^+$ cells alone [178].

Hypoxic preconditioning of cardiac stem cells enhances the therapeutic potential for myocardial infarction therapy

In this study, CDCs improved cardiac function by injecting donor CDCs at the time of infarction, thus CDCs would be beneficial clinically if they could be administered as soon as possible after infarction. However, it has been shown, by us and others, that CDCs need to be expanded *in vitro* over a period of weeks in order to obtain sufficient cells for autologous transplantation [107, 108]. Hence, in *Chapter 4,* CSC cultures were optimized by preconditioning the cells under hypoxia. Enhanced cell proliferation rates were found for hypoxic EDCs and CDCs while larger cardiosphere sizes were formed under hypoxia, compared with normoxic cells. Hypoxic preconditioning successfully increased the proportion of c-Kit$^+$ cardiac progenitor cells and reduced the CD90$^+$ CD105$^+$ cardiac mesenchymal cells, giving an increased cardiac stem cell population in the heterogeneous CDC population. In addition, proliferating hypoxic

cells maintained pluripotency, with fewer cells spontaneously transdifferentiating into cardiomyocytes, compared with cells cultured under normoxia. This was probably due to the activation of essential factors for maintaining stem cell pluripotency, Oct-4, Klf-4, Sox 2 and Nanog, under hypoxia, which was in agreement with previous findings [164, 188, 215, 216]. Moreover, hypoxic preconditioned CDCs showed increased CXCR-4 (~3.2-fold), EPO (~3-fold) and VEGF (~1.5-fold), indicating that hypoxic preconditioning may stimulate stem cell homing and neovascularization in the infarcted myocardium. Notably, hypoxic CDCs had approximately 80% lower oxygen consumption and were able to switch to anaerobic glycolytic metabolism under deprived oxygen condition, suggesting that the hypoxic-preconditioned CDCs may be better adapted to survive within the hypoxic infarct scar, compared with normoxic CDCs. Implantation of the hypoxic CDCs into infarcted mice hearts *in vivo* has been shown to result in greater cell engraftment and better functional recovery than with conventionally cultured (normoxic) CDCs [211].

Mimicked hypoxic condition using prolyl-hydroxylase inhibitors

This is the first study using PHDIs to stabilize HIF in CDCs, mimicking the effects of hypoxic cell culture. In *Chapter 5*, three different prolyl-4-hydroxylase inhibitors (PHDIs) were used for HIF stabilization in CDC culture, DMOG, EDBA and BIC (also known as FG2216). Simulation of the hypoxic response by using PHD inhibitors will not only enable more practical treatment prior to *in vivo* application of stem cells, but will also allow more specific activation of HIF compared with hypoxic cell culture which will introduce a range of uncontrollable variables. In addition, manipulation of a pharmaceutical is also easier than physiological manipulation. The optimal PHDI treatment for CDCs, with respect to their negative cytotoxicity effects and optimal potential to activate HIF-1α expression, was found to be 1 mM DMOG, 0.5 mM

EDBA or 30 μM BIC for 24 hours. Cell proliferation was not affected by PHDI treatment under this condition. PHDI preconditioning using DMOG, EDBA and BIC partly mimicked the effects of hypoxia preconditioning as seen in *Chapter 4*. For example, all three PHDIs significantly stabilized and activated HIF, which induced metabolic changes and several important cytokines such as CXCR-4 in the CDCs. In addition, all three PHDIs significantly reduced the cardiac mesenchymal cell markers, CD90 and CD105, induced the expression of GLUT-1 protein, glucose uptake and lactate production, but decreased cellular oxygen respiration, indicating that PHDI-preconditioned CDCs had adapted to the PHDI-induced 'hypoxic' condition by reducing oxygen consumption and switching into glycolytic metabolism.

Different effects of DMOG, EDBA and BIC treatment on CDCs

Although all three PHDIs used in this study successful stabilized and activated HIF, they produced different effects in CDC culture. For example, only EDBA-treated CDCs had significantly increased c-Kit mRNA expression, and also, we found a significant increase of both EPO and VEGF in EDBA-treated CDCs, whereas, in contrast, only VEGF was found to significantly increase in DMOG-treated CDCs while only EPO was increased in BIC-treated CDCs. The difference in PHDI effects on CDCs was probably due to the different affinity of the PHDIs in activating HIF system. As described in *Chapter 1*, HIF is regulated by dual pathways involving oxygen-dependent prolyl and asparaginyl hydroxylation of its HIF-α subunits (refer Figure 1.1). Tian *et al.* [126] reported differences in the sensitivity of HIF hydroxylation sites by different types of PHDIs. They found that BIC efficiently inhibited the PHD enzyme, but was not able to prevent the FIH enzyme from degrading HIF-α subunits, causing an incomplete activation of HIF. This was in agreement with our data which showed that BIC-treated CDCs had a significantly

lower HIF-1α level, compared to DMOG and EDBA-treated CDCs. Also, Lienard *et al.* [127] found that EDBA was more potent in inducing HIF-1α stabilisation in cells than DMOG, confirming the data found in this study which showed that only EDBA-treated CDCs had significantly increased c-Kit mRNA expression, but not in the DMOG- and BIC-treated CDCs. In conclusion, the ability of different PHDIs in stabilizing the HIF system and activating HIF-regulated genes based on their feasibility and sensitivity of selectively inhibiting the prolyl or asparaginyl hydroxylation within cells. Hydroxylation and degradation of HIF-1α in CDC culture was suppressed by PHDIs in the order EDBA>DMOG>BIC.

Stem cell proliferation and c-Kit expression decreased in aged donor and after in vitro extended culture

In *Chapter 6*, the effects of donor age and *in vitro* cellular ageing were investigated. It was found that the proliferation rates of CSCs were significantly decreased in older animals. *In vitro* expansion of neonatal rat explants yielded 6 x 10^6 CDCs for transplantation approximately 2 weeks faster than adult rat explants. CDCs generated from adult rat heart tissue expressed cardiac stem cell and pluripotent cell markers, c-Kit, Oct-4, Klf4 and Sox 2. However, the expression of these genes was significantly lower compared with neonatal CDCs. Also, it was found that *in vitro* cellular ageing due to long term cell passaging gradually decreased the expression of c-Kit. A few recent studies have reported a similar reduction of c-Kit expression, in purified c-Kit cells and in CDCs over time in culture. Koninckx *et al.* demonstrated that clonogenic-derived c-Kit$^+$ cells and CDCs lost c-Kit expression after several passages in culture [318] while Gambini *et al.* showed that c-Kit expression was significantly down-regulated at the RNA level after 4 passages [319]. Although none of these papers discussed the mechanism of c-Kit shut down over *in vitro* culture, this could be

possibly explained by the destructive effect of trypsin (a serine protease found in the digestive system of many vertebrates, where it hydrolyses proteins) on the binding site of the c-Kit receptor during each passaging process [320] or that CDC *in vitro* expansion process favored the expansion of other cell types [309, 310]. The latter hypothesis was supported by the observation of gradually increasing $CD105^{+}CD90^{+}$ mesenchymal stem cells in later passages.

CDCs isolated from aged donor were more cardiac lineage committed

The fate of CDCs was modulated by the environmental factors and mediated by signalling pathways based on the age of the tissue in which they resided [182, 303]. In CDC isolated from fully developed adult heart, an upregulation of the cardiac differentiation marker (Nkx 2.5), the matured cardiomyocytes markers (Tnnt and MyHC), and a downregulation of mesenchymal stem cells marker (CD105) was observed, compared with CDC isolated from the postnatal heart. In line with this, it was found that the adult CDCs were more committed to differentiate into the cardiomyocytes lineage rather than into the adipocytes lineage.

Optimization of adult rat CSCs using hypoxic and PHDI-preconditioning

Resident CSCs exist, albeit in relatively small number, in adult rat hearts. In order to obtain sufficient cell numbers for transplantation, adult CSC culture was optimized using hypoxic and PHDI-preconditioning. Hypoxic treatment significantly increased the cell proliferation, shortening the time required to obtain adequate cell numbers for therapy, while both hypoxic and PHDI-preconditioning enhanced the therapeutic potential of CDCs by increasing the expression several important cytokines such as CXCR-4, EPO and VEGF. Also, hypoxic and PHDI-preconditioned CDCs had lower oxygen consumption rate, suggesting that they could survive better after

transplantation into hypoxic infarcted myocardium. This work improved the prospect for autologous CDC therapy for myocardial infarction which predominantly affects older patients.

Study limitation and future directions

Although several studies have shown that CDCs improve cardiac function after myocardial infarction, the optimized protocol used here altered the original characteristic and properties of the CDCs currently under investigation by the CADUCEUS trial (Clinical Trials.gov. Identifier NCT00893360) [180]. A concern with the optimized CDC culture using hypoxic and PHDI-preconditioning is that activation of HIF could induce a wide range of pathophysiological processes involving at least 100 other genes, some of which are oncogenic [141]. Since the effects on optimized cells could be diverse, it is in our interest to carefully evaluate the specific effects of these cells *in vivo*. My future research will focus on isolating and optimizing CDCs *in vitro* using hypoxia and PHDIs, followed by experiments in which CDCs will be administered to the infarcted heart *in vivo*, and the function of treated heart and the destiny of donor CDCs, monitored using MRI. Currently in our laboratory, a new approach to imaging cells *in vivo* using fluorine (F^{19})-based particles has been established to provide high specificity of detection, more accurate localization and quantification of the F^{19}-labelled cells [321] , and it is anticipated that *in vivo* studies will be started later this year.

REFERENCES:

1. Hellermann, J.P., et al., *Heart failure after myocardial infarction: a review.* Am J Med, 2002. **113**(4): p. 324-30.
2. Levy, D., et al., *Long-term trends in the incidence of and survival with heart failure.* N Engl J Med, 2002. **347**(18): p. 1397-402.
3. Véronique L. Roger, M.B., et al., *Heart Association Heart Disease and Stroke Statistics - 2011 Update: A Report From the American.* American Heart Association Circulation, 2011.
4. Sophie Petersen, M.R.a.J.W., *Coronary heart disease statistics: heart failure supplement 2010 edition*. 2010.
5. Soonpaa, M.H. and L.J. Field, *Survey of studies examining mammalian cardiomyocyte DNA synthesis.* Circ Res, 1998. **83**(1): p. 15-26.
6. Valentin Fuster, R.W.A., Robert A O'Rourke, *Hurst's The Heart*. 11th ed. Vol. 1. 2004, USA: McGraw-Hill Medical Publishing Division.
7. French, B.A. and C.M. Kramer, *Mechanisms of Post-Infarct Left Ventricular Remodeling.* Drug Discov Today Dis Mech, 2007. **4**(3): p. 185-196.
8. Lange, R.A. and L.D. Hillis, *Reperfusion therapy in acute myocardial infarction.* N Engl J Med, 2002. **346**(13): p. 954-5.
9. Stone, G.W., et al., *Comparison of angioplasty with stenting, with or without abciximab, in acute myocardial infarction.* N Engl J Med, 2002. **346**(13): p. 957-66.
10. Sunagawa, G., et al., *Coronary artery bypass surgery is superior to percutaneous coronary intervention with drug-eluting stents for patients with chronic renal failure on hemodialysis.* Ann Thorac Surg. **89**(6): p. 1896-900; discussion 1900.
11. Orozovic, V., et al., *Current therapy of the right ventricle myocardial infarction.* Vojnosanit Pregl, 2002. **59**(6): p. 587-92.
12. McCarthy, P.M., *Surgical therapies for post-myocardial infarction patients.* Am J Cardiol, 2008. **102**(5A): p. 42G-46G.
13. Anversa, P., M.A. Sussman, and R. Bolli, *Molecular genetic advances in cardiovascular medicine: focus on the myocyte.* Circulation, 2004. **109**(23): p. 2832-8.
14. Rippon, H.J. and A.E. Bishop, *Embryonic stem cells.* Cell Prolif, 2004. **37**(1): p. 23-34.
15. Thomson, J.A., et al., *Embryonic stem cell lines derived from human blastocysts.* Science, 1998. **282**(5391): p. 1145-7.
16. Amit, M. and J. Itskovitz-Eldor, *Feeder-free culture of human embryonic stem cells.* Methods Enzymol, 2006. **420**: p. 37-49.
17. Amit, M., et al., *Clonally derived human embryonic stem cell lines maintain pluripotency and proliferative potential for prolonged periods of culture.* Dev Biol, 2000. **227**(2): p. 271-8.
18. Itskovitz-Eldor, J., et al., *Differentiation of human embryonic stem cells into embryoid bodies compromising the three embryonic germ layers.* Mol Med, 2000. **6**(2): p. 88-95.
19. Levenberg, S., et al., *Endothelial cells derived from human embryonic stem cells.* Proc Natl Acad Sci U S A, 2002. **99**(7): p. 4391-6.
20. Carpenter, M.K., et al., *Enrichment of neurons and neural precursors from human embryonic stem cells.* Exp Neurol, 2001. **172**(2): p. 383-97.
21. Assady, S., et al., *Insulin production by human embryonic stem cells.* Diabetes, 2001. **50**(8): p. 1691-7.

22. Segev, H., et al., *Differentiation of human embryonic stem cells into insulin-producing clusters.* Stem Cells, 2004. **22**(3): p. 265-74.
23. Kehat, I., et al., *Human embryonic stem cells can differentiate into myocytes with structural and functional properties of cardiomyocytes.* J Clin Invest, 2001. **108**(3): p. 407-14.
24. Hodgson, D.M., et al., *Stable benefit of embryonic stem cell therapy in myocardial infarction.* Am J Physiol Heart Circ Physiol, 2004. **287**(2): p. H471-9.
25. Nir, S.G., et al., *Human embryonic stem cells for cardiovascular repair.* Cardiovasc Res, 2003. **58**(2): p. 313-23.
26. Nussbaum, J., et al., *Transplantation of undifferentiated murine embryonic stem cells in the heart: teratoma formation and immune response.* Faseb J, 2007. **21**(7): p. 1345-57.
27. Draper, J.S., et al., *Surface antigens of human embryonic stem cells: changes upon differentiation in culture.* J Anat, 2002. **200**(Pt 3): p. 249-58.
28. Orive, G., et al., *Controversies over stem cell research.* Trends Biotechnol, 2003. **21**(3): p. 109-12.
29. Takahashi, K. and S. Yamanaka, *Induction of pluripotent stem cells from mouse embryonic and adult fibroblast cultures by defined factors.* Cell, 2006. **126**(4): p. 663-76.
30. Takahashi, K., et al., *Induction of pluripotent stem cells from adult human fibroblasts by defined factors.* Cell, 2007. **131**(5): p. 861-72.
31. Mauritz, C., et al., *Generation of functional murine cardiac myocytes from induced pluripotent stem cells.* Circulation, 2008. **118**(5): p. 507-17.
32. Zhang, J., et al., *Functional cardiomyocytes derived from human induced pluripotent stem cells.* Circ Res, 2009. **104**(4): p. e30-41.
33. Laurent, L.C., et al., *Dynamic changes in the copy number of pluripotency and cell proliferation genes in human ESCs and iPSCs during reprogramming and time in culture.* Cell Stem Cell. **8**(1): p. 106-18.
34. Okita, K., T. Ichisaka, and S. Yamanaka, *Generation of germline-competent induced pluripotent stem cells.* Nature, 2007. **448**(7151): p. 313-7.
35. Lister, R., et al., *Hotspots of aberrant epigenomic reprogramming in human induced pluripotent stem cells.* Nature. **471**(7336): p. 68-73.
36. Panopoulos, A.D., S. Ruiz, and J.C. Izpisua Belmonte, *iPSCs: induced back to controversy.* Cell Stem Cell. **8**(4): p. 347-8.
37. Poulsom, R., et al., *Adult stem cell plasticity.* J Pathol, 2002. **197**(4): p. 441-56.
38. Forbes, S.J., et al., *Adult stem cell plasticity: new pathways of tissue regeneration become visible.* Clin Sci (Lond), 2002. **103**(4): p. 355-69.
39. Friedenstein, A.J., S. Piatetzky, II, and K.V. Petrakova, *Osteogenesis in transplants of bone marrow cells.* J Embryol Exp Morphol, 1966. **16**(3): p. 381-90.
40. Friedenstein, A.J., R.K. Chailakhjan, and K.S. Lalykina, *The development of fibroblast colonies in monolayer cultures of guinea-pig bone marrow and spleen cells.* Cell Tissue Kinet, 1970. **3**(4): p. 393-403.
41. Owen, M., *Marrow stromal stem cells.* J Cell Sci Suppl, 1988. **10**: p. 63-76.
42. Orlic, D., et al., *Bone marrow cells regenerate infarcted myocardium.* Nature, 2001. **410**(6829): p. 701-5.
43. Jackson, K.A., et al., *Regeneration of ischemic cardiac muscle and vascular endothelium by adult stem cells.* J Clin Invest, 2001. **107**(11): p. 1395-402.

44. Carr, C.A., et al., *Bone marrow-derived stromal cells home to and remain in the infarcted rat heart but fail to improve function: an in vivo cine-MRI study.* Am J Physiol Heart Circ Physiol, 2008. **295**(2): p. H533-42.
45. Lunde, K., et al., *Intracoronary injection of mononuclear bone marrow cells in acute myocardial infarction.* N Engl J Med, 2006. **355**(12): p. 1199-209.
46. Schachinger, V., et al., *Intracoronary bone marrow-derived progenitor cells in acute myocardial infarction.* N Engl J Med, 2006. **355**(12): p. 1210-21.
47. Adler, E.D. and T.M. Maddox, *Cell therapy for cardiac disease: where do we go from here?* Nat Clin Pract Cardiovasc Med, 2007. **4**(1): p. 2-3.
48. Strauer, B.E., et al., *Repair of infarcted myocardium by autologous intracoronary mononuclear bone marrow cell transplantation in humans.* Circulation, 2002. **106**(15): p. 1913-8.
49. Wollert, K.C., et al., *Intracoronary autologous bone-marrow cell transfer after myocardial infarction: the BOOST randomised controlled clinical trial.* Lancet, 2004. **364**(9429): p. 141-8.
50. Bartunek, J., et al., *Intracoronary injection of CD133-positive enriched bone marrow progenitor cells promotes cardiac recovery after recent myocardial infarction: feasibility and safety.* Circulation, 2005. **112**(9 Suppl): p. I178-83.
51. Meyer, G.P., et al., *Intracoronary bone marrow cell transfer after myocardial infarction: eighteen months' follow-up data from the randomized, controlled BOOST (BOne marrOw transfer to enhance ST-elevation infarct regeneration) trial.* Circulation, 2006. **113**(10): p. 1287-94.
52. Schachinger, V., et al., *Improved clinical outcome after intracoronary administration of bone-marrow-derived progenitor cells in acute myocardial infarction: final 1-year results of the REPAIR-AMI trial.* Eur Heart J, 2006. **27**(23): p. 2775-83.
53. Hirsch, A., et al., *Intracoronary infusion of autologous mononuclear bone marrow cells in patients with acute myocardial infarction treated with primary PCI: Pilot study of the multicenter HEBE trial.* Catheter Cardiovasc Interv, 2008. **71**(3): p. 273-81.
54. Tendera, M., et al., *Intracoronary infusion of bone marrow-derived selected CD34+CXCR4+ cells and non-selected mononuclear cells in patients with acute STEMI and reduced left ventricular ejection fraction: results of randomized, multicentre Myocardial Regeneration by Intracoronary Infusion of Selected Population of Stem Cells in Acute Myocardial Infarction (REGENT) Trial.* Eur Heart J, 2009. **30**(11): p. 1313-21.
55. Wohrle, J., et al., *Results of intracoronary stem cell therapy after acute myocardial infarction.* Am J Cardiol. **105**(6): p. 804-12.
56. Hirsch, A., et al., *Intracoronary infusion of mononuclear cells from bone marrow or peripheral blood compared with standard therapy in patients after acute myocardial infarction treated by primary percutaneous coronary intervention: results of the randomized controlled HEBE trial.* Eur Heart J.
57. Roncalli, J., et al., *Intracoronary autologous mononucleated bone marrow cell infusion for acute myocardial infarction: results of the randomized multicenter BONAMI trial.* Eur Heart J.
58. Peichev, M., et al., *Expression of VEGFR-2 and AC133 by circulating human CD34(+) cells identifies a population of functional endothelial precursors.* Blood, 2000. **95**(3): p. 952-8.
59. Yeh, E.T., et al., *Transdifferentiation of human peripheral blood CD34+-enriched cell population into cardiomyocytes, endothelial cells, and smooth muscle cells in vivo.* Circulation, 2003. **108**(17): p. 2070-3.

60. Kocher, A.A., et al., *Neovascularization of ischemic myocardium by human bone-marrow-derived angioblasts prevents cardiomyocyte apoptosis, reduces remodeling and improves cardiac function.* Nat Med, 2001. **7**(4): p. 430-6.
61. Kawamoto, A., et al., *Therapeutic potential of ex vivo expanded endothelial progenitor cells for myocardial ischemia.* Circulation, 2001. **103**(5): p. 634-7.
62. Purhonen, S., et al., *Bone marrow-derived circulating endothelial precursors do not contribute to vascular endothelium and are not needed for tumor growth.* Proc Natl Acad Sci U S A, 2008. **105**(18): p. 6620-5.
63. Yoder, M.C. and D.A. Ingram, *The definition of EPCs and other bone marrow cells contributing to neoangiogenesis and tumor growth: is there common ground for understanding the roles of numerous marrow-derived cells in the neoangiogenic process?* Biochim Biophys Acta, 2009. **1796**(1): p. 50-4.
64. Wu, Y., et al., *Essential role of ICAM-1/CD18 in mediating EPC recruitment, angiogenesis, and repair to the infarcted myocardium.* Circ Res, 2006. **99**(3): p. 315-22.
65. da Silva Meirelles, L., P.C. Chagastelles, and N.B. Nardi, *Mesenchymal stem cells reside in virtually all post-natal organs and tissues.* J Cell Sci, 2006. **119**(Pt 11): p. 2204-13.
66. Horwitz, E.M., et al., *Clarification of the nomenclature for MSC: The International Society for Cellular Therapy position statement.* Cytotherapy, 2005. **7**(5): p. 393-5.
67. Caplan, A.I., *Mesenchymal stem cells and gene therapy.* Clin Orthop Relat Res, 2000(379 Suppl): p. S67-70.
68. Cho, K.J., et al., *Neurons derived from human mesenchymal stem cells show synaptic transmission and can be induced to produce the neurotransmitter substance P by interleukin-1 alpha.* Stem Cells, 2005. **23**(3): p. 383-91.
69. Pittenger, M.F. and B.J. Martin, *Mesenchymal stem cells and their potential as cardiac therapeutics.* Circ Res, 2004. **95**(1): p. 9-20.
70. Rojas, M., et al., *Bone marrow-derived mesenchymal stem cells in repair of the injured lung.* Am J Respir Cell Mol Biol, 2005. **33**(2): p. 145-52.
71. Nagaya, N., et al., *Intravenous administration of mesenchymal stem cells improves cardiac function in rats with acute myocardial infarction through angiogenesis and myogenesis.* Am J Physiol Heart Circ Physiol, 2004. **287**(6): p. H2670-6.
72. Shake, J.G., et al., *Mesenchymal stem cell implantation in a swine myocardial infarct model: engraftment and functional effects.* Ann Thorac Surg, 2002. **73**(6): p. 1919-25; discussion 1926.
73. Menasche, P., *Skeletal myoblasts as a therapeutic agent.* Prog Cardiovasc Dis, 2007. **50**(1): p. 7-17.
74. Menasche, P., et al., *Autologous skeletal myoblast transplantation for severe postinfarction left ventricular dysfunction.* J Am Coll Cardiol, 2003. **41**(7): p. 1078-83.
75. Hagege, A.A., et al., *Skeletal myoblast transplantation in ischemic heart failure: long-term follow-up of the first phase I cohort of patients.* Circulation, 2006. **114**(1 Suppl): p. I108-13.
76. Chanseaume, S., et al., *Can erythropoietin improve skeletal myoblast engraftment in infarcted myocardium?* Interact Cardiovasc Thorac Surg, 2007. **6**(3): p. 293-7.
77. Menasche, P., *Skeletal myoblasts and cardiac repair.* J Mol Cell Cardiol, 2008. **45**(4): p. 545-53.

78. Menasche, P., *Towards the second generation of skeletal myoblasts?* Cardiovasc Res, 2008. **79**(3): p. 355-6.
79. Instituto Cientifico y Tecnologico de Navarra, U.d.N. *Study of the Efficacy of Percutaneous Implantation of Autologous Myoblasts in Patients With Old Infarction (PERCUTANEO).* 2009 [cited; Available from: http://www.clinicaltrials.gov/ct2/show/NCT00908622?term=myoblast&rank=1 .
80. Kucia, M., et al., *A population of very small embryonic-like (VSEL) CXCR4(+)SSEA-1(+)Oct-4+ stem cells identified in adult bone marrow.* Leukemia, 2006. **20**(5): p. 857-69.
81. Zuba-Surma, E.K., et al., *Morphological characterization of very small embryonic-like stem cells (VSELs) by ImageStream system analysis.* J Cell Mol Med, 2008. **12**(1): p. 292-303.
82. Zuba-Surma, E.K., et al., *Very small embryonic-like stem cells are present in adult murine organs: ImageStream-based morphological analysis and distribution studies.* Cytometry A, 2008. **73A**(12): p. 1116-27.
83. Zuba-Surma, E.K., et al., *Transplantation of expanded bone marrow-derived very small embryonic-like stem cells (VSEL-SCs) improves left ventricular function and remodelling after myocardial infarction.* J Cell Mol Med. **15**(6): p. 1319-28.
84. Quaini, F., et al., *Chimerism of the transplanted heart.* N Engl J Med, 2002. **346**(1): p. 5-15.
85. Urbanek, K., et al., *Intense myocyte formation from cardiac stem cells in human cardiac hypertrophy.* Proc Natl Acad Sci U S A, 2003. **100**(18): p. 10440-5.
86. Beltrami, A.P., et al., *Adult cardiac stem cells are multipotent and support myocardial regeneration.* Cell, 2003. **114**(6): p. 763-76.
87. Oh, H., et al., *Cardiac progenitor cells from adult myocardium: homing, differentiation, and fusion after infarction.* Proc Natl Acad Sci U S A, 2003. **100**(21): p. 12313-8.
88. Hierlihy, A.M., et al., *The post-natal heart contains a myocardial stem cell population.* FEBS Lett, 2002. **530**(1-3): p. 239-43.
89. Martin, C.M., et al., *Persistent expression of the ATP-binding cassette transporter, Abcg2, identifies cardiac SP cells in the developing and adult heart.* Dev Biol, 2004. **265**(1): p. 262-75.
90. Oyama, T., et al., *Cardiac side population cells have a potential to migrate and differentiate into cardiomyocytes in vitro and in vivo.* J Cell Biol, 2007. **176**(3): p. 329-41.
91. Pfister, O., et al., *CD31- but Not CD31+ cardiac side population cells exhibit functional cardiomyogenic differentiation.* Circ Res, 2005. **97**(1): p. 52-61.
92. Blackburn, E.H., *Structure and function of telomeres.* Nature, 1991. **350**(6319): p. 569-73.
93. Wu, K.J., et al., *Direct activation of TERT transcription by c-MYC.* Nat Genet, 1999. **21**(2): p. 220-4.
94. Allsopp, R.C., S. Cheshier, and I.L. Weissman, *Telomere shortening accompanies increased cell cycle activity during serial transplantation of hematopoietic stem cells.* J Exp Med, 2001. **193**(8): p. 917-24.
95. Coussens, M., et al., *RNAi screen for telomerase reverse transcriptase transcriptional regulators identifies HIF1alpha as critical for telomerase function in murine embryonic stem cells.* Proc Natl Acad Sci U S A. **107**(31): p. 13842-7.

96. Wang, X., et al., *The role of the sca-1+/CD31- cardiac progenitor cell population in postinfarction left ventricular remodeling.* Stem Cells, 2006. **24**(7): p. 1779-88.
97. Barile, L., et al., *Endogenous cardiac stem cells.* Prog Cardiovasc Dis, 2007. **50**(1): p. 31-48.
98. Miyamoto, S., et al., *Characterization of long-term cultured c-kit+ cardiac stem cells derived from adult rat hearts.* Stem Cells Dev. **19**(1): p. 105-16.
99. Tang, X.L., et al., *Intracoronary administration of cardiac progenitor cells alleviates left ventricular dysfunction in rats with a 30-day-old infarction.* Circulation. **121**(2): p. 293-305.
100. *Cardiac Stem Cell Infusion in Patients With Ischemic CardiOmyopathy (SCIPIO).* 2007 [cited; Available from: http://clinicaltrials.gov/ct2/show/NCT00474461.
101. Laugwitz, K.L., et al., *Postnatal isl1+ cardioblasts enter fully differentiated cardiomyocyte lineages.* Nature, 2005. **433**(7026): p. 647-53.
102. Moretti, A., et al., *Multipotent embryonic isl1+ progenitor cells lead to cardiac, smooth muscle, and endothelial cell diversification.* Cell, 2006. **127**(6): p. 1151-65.
103. Moretti, A., et al., *Biology of Isl1+ cardiac progenitor cells in development and disease.* Cell Mol Life Sci, 2007. **64**(6): p. 674-82.
104. Limana, F., et al., *Identification of myocardial and vascular precursor cells in human and mouse epicardium.* Circ Res, 2007. **101**(12): p. 1255-65.
105. Riley, P.R. and N. Smart, *Thymosin beta4 induces epicardium-derived neovascularization in the adult heart.* Biochem Soc Trans, 2009. **37**(Pt 6): p. 1218-20.
106. Smart, N., et al., *De novo cardiomyocytes from within the activated adult heart after injury.* Nature. **474**(7353): p. 640-4.
107. Messina, E., et al., *Isolation and expansion of adult cardiac stem cells from human and murine heart.* Circ Res, 2004. **95**(9): p. 911-21.
108. Smith, R.R., et al., *Regenerative potential of cardiosphere-derived cells expanded from percutaneous endomyocardial biopsy specimens.* Circulation, 2007. **115**(7): p. 896-908.
109. Davis, D.R., et al., *Validation of the cardiosphere method to culture cardiac progenitor cells from myocardial tissue.* PLoS One, 2009. **4**(9): p. e7195.
110. Stockmann, C. and J. Fandrey, *Hypoxia-induced erythropoietin production: a paradigm for oxygen-regulated gene expression.* Clin Exp Pharmacol Physiol, 2006. **33**(10): p. 968-79.
111. Carmeliet, P. and R.K. Jain, *Angiogenesis in cancer and other diseases.* Nature, 2000. **407**(6801): p. 249-57.
112. Shweiki, D., et al., *Induction of vascular endothelial growth factor expression by hypoxia and by glucose deficiency in multicell spheroids: implications for tumor angiogenesis.* Proc Natl Acad Sci U S A, 1995. **92**(3): p. 768-72.
113. Shweiki, D., et al., *Vascular endothelial growth factor induced by hypoxia may mediate hypoxia-initiated angiogenesis.* Nature, 1992. **359**(6398): p. 843-5.
114. Lopez-Barneo, J., R. Pardal, and P. Ortega-Saenz, *Cellular mechanism of oxygen sensing.* Annu Rev Physiol, 2001. **63**: p. 259-87.
115. Chen, C., et al., *Regulation of glut1 mRNA by hypoxia-inducible factor-1. Interaction between H-ras and hypoxia.* J Biol Chem, 2001. **276**(12): p. 9519-25.
116. Taylor, D.K., et al., *Thrombospondin-2 influences the proportion of cartilage and bone during fracture healing.* J Bone Miner Res, 2009. **24**(6): p. 1043-54.

117. Abbott, J.D., et al., *Stromal cell-derived factor-1alpha plays a critical role in stem cell recruitment to the heart after myocardial infarction but is not sufficient to induce homing in the absence of injury.* Circulation, 2004. **110**(21): p. 3300-5.
118. Ceradini, D.J., et al., *Progenitor cell trafficking is regulated by hypoxic gradients through HIF-1 induction of SDF-1.* Nat Med, 2004. **10**(8): p. 858-64.
119. Semenza, G.L. and G.L. Wang, *A nuclear factor induced by hypoxia via de novo protein synthesis binds to the human erythropoietin gene enhancer at a site required for transcriptional activation.* Mol Cell Biol, 1992. **12**(12): p. 5447-54.
120. Tian, H., S.L. McKnight, and D.W. Russell, *Endothelial PAS domain protein 1 (EPAS1), a transcription factor selectively expressed in endothelial cells.* Genes Dev, 1997. **11**(1): p. 72-82.
121. Gu, Y.Z., et al., *Molecular characterization and chromosomal localization of a third alpha-class hypoxia inducible factor subunit, HIF3alpha.* Gene Expr, 1998. **7**(3): p. 205-13.
122. Chowdhury, R., A. Hardy, and C.J. Schofield, *The human oxygen sensing machinery and its manipulation.* Chem Soc Rev, 2008. **37**(7): p. 1308-19.
123. Lisy, K. and D.J. Peet, *Turn me on: regulating HIF transcriptional activity.* Cell Death Differ, 2008. **15**(4): p. 642-9.
124. Asikainen, T.M., et al., *Stimulation of HIF-1alpha, HIF-2alpha, and VEGF by prolyl 4-hydroxylase inhibition in human lung endothelial and epithelial cells.* Free Radic Biol Med, 2005. **38**(8): p. 1002-13.
125. Cummins, E.P., et al., *The hydroxylase inhibitor dimethyloxalylglycine is protective in a murine model of colitis.* Gastroenterology, 2008. **134**(1): p. 156-65.
126. Tian, Y.M., et al., *Differential sensitivity of HIF hydroxylation sites to hypoxia and hydroxylase inhibitors.* J Biol Chem.
127. Lienard, B.M., et al., *Evaluation of aspirin metabolites as inhibitors of hypoxia-inducible factor hydroxylases.* Chem Commun (Camb), 2008(47): p. 6393-5.
128. Hirsila, M., et al., *Characterization of the human prolyl 4-hydroxylases that modify the hypoxia-inducible factor.* J Biol Chem, 2003. **278**(33): p. 30772-80.
129. Zhong, H., et al., *Nuclear expression of hypoxia-inducible factor 1alpha protein is heterogeneous in human malignant cells under normoxic conditions.* Cancer Lett, 2002. **181**(2): p. 233-8.
130. Akakura, N., et al., *Constitutive expression of hypoxia-inducible factor-1alpha renders pancreatic cancer cells resistant to apoptosis induced by hypoxia and nutrient deprivation.* Cancer Res, 2001. **61**(17): p. 6548-54.
131. Zhong, H., et al., *Increased expression of hypoxia inducible factor-1alpha in rat and human prostate cancer.* Cancer Res, 1998. **58**(23): p. 5280-4.
132. Zhong, H., et al., *Modulation of hypoxia-inducible factor 1alpha expression by the epidermal growth factor/phosphatidylinositol 3-kinase/PTEN/AKT/FRAP pathway in human prostate cancer cells: implications for tumor angiogenesis and therapeutics.* Cancer Res, 2000. **60**(6): p. 1541-5.
133. Zhang, M., et al., *Stem cell factor/c-kit signaling enhances invasion of pancreatic cancer cells via HIF-1alpha under normoxic condition.* Cancer Lett. **303**(2): p. 108-17.
134. Epstein, A.C., et al., *C. elegans EGL-9 and mammalian homologs define a family of dioxygenases that regulate HIF by prolyl hydroxylation.* Cell, 2001. **107**(1): p. 43-54.

135. Selak, M.A., et al., *Succinate links TCA cycle dysfunction to oncogenesis by inhibiting HIF-alpha prolyl hydroxylase.* Cancer Cell, 2005. **7**(1): p. 77-85.
136. Koivunen, P., et al., *Inhibition of hypoxia-inducible factor (HIF) hydroxylases by citric acid cycle intermediates: possible links between cell metabolism and stabilization of HIF.* J Biol Chem, 2007. **282**(7): p. 4524-32.
137. Deng, A., et al., *Renal protection in chronic kidney disease: hypoxia-inducible factor activation vs. angiotensin II blockade.* Am J Physiol Renal Physiol. **299**(6): p. F1365-73.
138. Nagel, S., et al., *Neuroprotection by dimethyloxalylglycine following permanent and transient focal cerebral ischemia in rats.* J Cereb Blood Flow Metab. **31**(1): p. 132-43.
139. Chen, W., et al., *HIF-1alpha inhibition ameliorates neonatal brain injury in a rat pup hypoxic-ischemic model.* Neurobiol Dis, 2008. **31**(3): p. 433-41.
140. Ivan, M., et al., *Biochemical purification and pharmacological inhibition of a mammalian prolyl hydroxylase acting on hypoxia-inducible factor.* Proc Natl Acad Sci U S A, 2002. **99**(21): p. 13459-64.
141. Jaakkola, P., et al., *Targeting of HIF-alpha to the von Hippel-Lindau ubiquitylation complex by O2-regulated prolyl hydroxylation.* Science, 2001. **292**(5516): p. 468-72.
142. Ockaili, R., et al., *HIF-1 activation attenuates postischemic myocardial injury: role for heme oxygenase-1 in modulating microvascular chemokine generation.* Am J Physiol Heart Circ Physiol, 2005. **289**(2): p. H542-8.
143. Jones, N.M., et al., *Long-term functional and protective actions of preconditioning with hypoxia, cobalt chloride, and desferrioxamine against hypoxic-ischemic injury in neonatal rats.* Pediatr Res, 2008. **63**(6): p. 620-4.
144. Li, Y.X., et al., *Desferoxamine preconditioning protects against cerebral ischemia in rats by inducing expressions of hypoxia inducible factor 1 alpha and erythropoietin.* Neurosci Bull, 2008. **24**(2): p. 89-95.
145. Prass, K., et al., *Desferrioxamine induces delayed tolerance against cerebral ischemia in vivo and in vitro.* J Cereb Blood Flow Metab, 2002. **22**(5): p. 520-5.
146. Groenman, F.A., et al., *Effect of chemical stabilizers of hypoxia-inducible factors on early lung development.* Am J Physiol Lung Cell Mol Physiol, 2007. **293**(3): p. L557-67.
147. Huang, L.E., et al., *Regulation of hypoxia-inducible factor 1alpha is mediated by an O2-dependent degradation domain via the ubiquitin-proteasome pathway.* Proc Natl Acad Sci U S A, 1998. **95**(14): p. 7987-92.
148. Urquilla P, F.A., Oksanen S, Leigh S, Turtle E, Flippin L, Brenner M, Muthukrishnan E, Fourney P, Lin A, Yeowell D, Molineaux C: , *Upregulation of endogenous EPO in healthy subjects by inhibition of HIF-PH [Abstract].* Am Soc Nephrol, 2004. **15**.
149. Wiecek A, P.G., Ignacy W, Schmidt R, Neumayer HH, Scigalla P, Urquilla P, *Pharmacological stabilization of HIF increases hemoglobin concentration in anemic patients with chronic kidney disease [Abstract].* . Nephrol Dial Transplant, 2005. **195**.
150. Inc:, A.P. *Adverse Event of FG-2216 for the Treatment of Anemia [News release],* . 2007 [cited; Available from: http://http://www.astellas.com/global/about/news/2007/pdf/070507_eg.pdf.
151. Tang, Y.L., et al., *A novel two-step procedure to expand cardiac Sca-1+ cells clonally.* Biochem Biophys Res Commun, 2007. **359**(4): p. 877-83.

152. Cao, F., et al., *In vivo visualization of embryonic stem cell survival, proliferation, and migration after cardiac delivery.* Circulation, 2006. **113**(7): p. 1005-14.
153. Burton, R.A., et al., *Three-dimensional models of individual cardiac histoanatomy: tools and challenges.* Ann N Y Acad Sci, 2006. **1080**: p. 301-19.
154. Evers, A.S., et al., *Effects of endogenously produced leukotrienes, thromboxane, and prostaglandins on coronary vascular resistance in rabbit myocardial infarction.* J Clin Invest, 1985. **75**(3): p. 992-9.
155. Tateishi, K., et al., *Human cardiac stem cells exhibit mesenchymal features and are maintained through Akt/GSK-3beta signaling.* Biochem Biophys Res Commun, 2007. **352**(3): p. 635-41.
156. Orlic, D., et al., *Purification and characterization of heterogeneous pluripotent hematopoietic stem cell populations expressing high levels of c-kit receptor.* Blood, 1993. **82**(3): p. 762-70.
157. Wolf, S.S. and A. Cohen, *Expression of cytokines and their receptors by human thymocytes and thymic stromal cells.* Immunology, 1992. **77**(3): p. 362-8.
158. Visser, J.W., et al., *The expression of cytokine receptors by purified hemopoietic stem cells.* Stem Cells, 1993. **11 Suppl 2**: p. 49-55.
159. Massa, S., et al., *Critical role for c-kit (CD117) in T cell lineage commitment and early thymocyte development in vitro.* Eur J Immunol, 2006. **36**(3): p. 526-32.
160. Wong, S.H., et al., *Evaluation of Sca-1 and c-Kit as selective markers for muscle remodelling by nonhemopoietic bone marrow cells.* Stem Cells, 2007. **25**(6): p. 1364-74.
161. Andersen, D.C., et al., *Murine "cardiospheres" are not a source of stem cells with cardiomyogenic potential.* Stem Cells, 2009. **27**(7): p. 1571-81.
162. Scholer, H.R., et al., *New type of POU domain in germ line-specific protein Oct-4.* Nature, 1990. **344**(6265): p. 435-9.
163. Boyer, L.A., et al., *Core transcriptional regulatory circuitry in human embryonic stem cells.* Cell, 2005. **122**(6): p. 947-56.
164. Covello, K.L., et al., *HIF-2alpha regulates Oct-4: effects of hypoxia on stem cell function, embryonic development, and tumor growth.* Genes Dev, 2006. **20**(5): p. 557-70.
165. Jiang, Y., et al., *Pluripotency of mesenchymal stem cells derived from adult marrow.* Nature, 2002. **418**(6893): p. 41-9.
166. Tai, M.H., et al., *Oct4 expression in adult human stem cells: evidence in support of the stem cell theory of carcinogenesis.* Carcinogenesis, 2005. **26**(2): p. 495-502.
167. Bhatia, B., et al., *SOX2 is required for adult human muller stem cell survival and maintenance of progenicity in vitro.* Invest Ophthalmol Vis Sci. **52**(1): p. 136-45.
168. Biernaskie, J., et al., *SKPs derive from hair follicle precursors and exhibit properties of adult dermal stem cells.* Cell Stem Cell, 2009. **5**(6): p. 610-23.
169. Kellner, J.C. and P.A. Coulombe, *Preview. SKPing a hurdle: Sox2 and adult dermal stem cells.* Cell Stem Cell, 2009. **5**(6): p. 569-70.
170. Katz, J.P., et al., *Loss of Klf4 in mice causes altered proliferation and differentiation and precancerous changes in the adult stomach.* Gastroenterology, 2005. **128**(4): p. 935-45.
171. Guan, K., et al., *Pluripotency of spermatogonial stem cells from adult mouse testis.* Nature, 2006. **440**(7088): p. 1199-203.

172. Cyranoski, D., *Stem cells from testes: could it work?* Nature, 2006. **440**(7084): p. 586-7.
173. Komashko, V.M. and P.J. Farnham, *5-azacytidine treatment reorganizes genomic histone modification patterns.* Epigenetics. **5**(3).
174. Iwatani, M., et al., *Dimethyl sulfoxide has an impact on epigenetic profile in mouse embryoid body.* Stem Cells, 2006. **24**(11): p. 2549-56.
175. Martin-Rendon, E., et al., *5-Azacytidine-treated human mesenchymal stem/progenitor cells derived from umbilical cord, cord blood and bone marrow do not generate cardiomyocytes in vitro at high frequencies.* Vox Sang, 2008. **95**(2): p. 137-48.
176. Yoon, J., et al., *Transdifferentiation of mesenchymal stem cells into cardiomyocytes by direct cell-to-cell contact with neonatal cardiomyocyte but not adult cardiomyocytes.* Ann Hematol, 2005. **84**(11): p. 715-21.
177. Davis, D.R., et al., *Isolation and expansion of functionally-competent cardiac progenitor cells directly from heart biopsies.* J Mol Cell Cardiol. **49**(2): p. 312-21.
178. Smith RR, C.I., Marban E, *Abstract 3417: Unselected Human Cardiosphere-derived Cells are Functionally Superior to c-Kit- or CD90-Purified Cardiosphere-derived Cells.* Circulation. 2008;118(18_Meeting Abstract):S_420-a, 2008.
179. Taylor, D.A. and A.G. Zenovich, *Cardiovascular cell therapy and endogenous repair.* Diabetes Obes Metab, 2008. **10 Suppl 4**: p. 5-15.
180. Center, C.-S.M. *CArdiosphere-Derived aUtologous Stem CElls to Reverse ventricUlar dySfunction (CADUCEUS).* 2009 [cited; Available from: http://clinicaltrials.gov/ct2/show/NCT00893360.
181. Spradling, A., D. Drummond-Barbosa, and T. Kai, *Stem cells find their niche.* Nature, 2001. **414**(6859): p. 98-104.
182. Li, L. and T. Xie, *Stem cell niche: structure and function.* Annu Rev Cell Dev Biol, 2005. **21**: p. 605-31.
183. Scadden, D.T., *The stem-cell niche as an entity of action.* Nature, 2006. **441**(7097): p. 1075-9.
184. Csete, M., *Oxygen in the cultivation of stem cells.* Ann N Y Acad Sci, 2005. **1049**: p. 1-8.
185. Simon, M.C. and B. Keith, *The role of oxygen availability in embryonic development and stem cell function.* Nat Rev Mol Cell Biol, 2008. **9**(4): p. 285-96.
186. Rodesch, F., et al., *Oxygen measurements in endometrial and trophoblastic tissues during early pregnancy.* Obstet Gynecol, 1992. **80**(2): p. 283-5.
187. Bruder, S.P., N. Jaiswal, and S.E. Haynesworth, *Growth kinetics, self-renewal, and the osteogenic potential of purified human mesenchymal stem cells during extensive subcultivation and following cryopreservation.* J Cell Biochem, 1997. **64**(2): p. 278-94.
188. Grayson, W.L., et al., *Hypoxia enhances proliferation and tissue formation of human mesenchymal stem cells.* Biochem Biophys Res Commun, 2007. **358**(3): p. 948-53.
189. Lennon, D.P., J.M. Edmison, and A.I. Caplan, *Cultivation of rat marrow-derived mesenchymal stem cells in reduced oxygen tension: effects on in vitro and in vivo osteochondrogenesis.* J Cell Physiol, 2001. **187**(3): p. 345-55.
190. Studer, L., et al., *Enhanced proliferation, survival, and dopaminergic differentiation of CNS precursors in lowered oxygen.* J Neurosci, 2000. **20**(19): p. 7377-83.

191. Zhao, T., et al., *[Effect of low glucose and/or hypoxia on the proliferation and metabolism of neural stem cells].* Zhongguo Ying Yong Sheng Li Xue Za Zhi. **26**(4): p. 412-5.
192. Chen, X., et al., *Hypoxia stimulates proliferation of rat neural stem cells with influence on the expression of cyclin D1 and c-Jun N-terminal protein kinase signaling pathway in vitro.* Neuroscience. **165**(3): p. 705-14.
193. Ingraham, C.A., et al., *Matrix metalloproteinase (MMP)-9 induced by Wnt signaling increases the proliferation and migration of embryonic neural stem cells at low O2 levels.* J Biol Chem.
194. Lee, E.Y., et al., *Hypoxia-enhanced wound-healing function of adipose-derived stem cells: increase in stem cell proliferation and up-regulation of VEGF and bFGF.* Wound Repair Regen, 2009. **17**(4): p. 540-7.
195. Ju, S.Y., et al., *Effect of hypoxic treatment on bone marrow cells that are able to migrate to the injured liver.* Cell Biol Int, 2009. **33**(1): p. 31-5.
196. Theus, M.H., et al., *In vitro hypoxic preconditioning of embryonic stem cells as a strategy of promoting cell survival and functional benefits after transplantation into the ischemic rat brain.* Exp Neurol, 2008. **210**(2): p. 656-70.
197. Rehman, J., et al., *Secretion of angiogenic and antiapoptotic factors by human adipose stromal cells.* Circulation, 2004. **109**(10): p. 1292-8.
198. Hollenberg, M., N. Honbo, and A.J. Samorodin, *Effects of hypoxia on cardiac growth in neonatal rat.* Am J Physiol, 1976. **231**(5 Pt. 1): p. 1445-50.
199. Schafer, M., et al., *Signaling of hypoxia-induced autonomous proliferation of endothelial cells.* Faseb J, 2003. **17**(3): p. 449-51.
200. Ott, H.C., et al., *The adult human heart as a source for stem cells: repair strategies with embryonic-like progenitor cells.* Nat Clin Pract Cardiovasc Med, 2007. **4 Suppl 1**: p. S27-39.
201. Davis, D.R., R. Ruckdeschel Smith, and E. Marban, *Human cardiospheres are a source of stem cells with cardiomyogenic potential.* Stem Cells. **28**(5): p. 903-4.
202. Li, Z., et al., *Imaging survival and function of transplanted cardiac resident stem cells.* J Am Coll Cardiol, 2009. **53**(14): p. 1229-40.
203. Koninckx, R., et al., *Mesenchymal stem cells or cardiac progenitors for cardiac repair? A comparative study.* Cell Mol Life Sci.
204. Li, T.S., et al., *Cardiospheres recapitulate a niche-like microenvironment rich in stemness and cell-matrix interactions, rationalizing their enhanced functional potency for myocardial repair.* Stem Cells. **28**(11): p. 2088-98.
205. Pugh, C.W. and P.J. Ratcliffe, *Regulation of angiogenesis by hypoxia: role of the HIF system.* Nat Med, 2003. **9**(6): p. 677-84.
206. Bartosh, T.J., et al., *3D-model of adult cardiac stem cells promotes cardiac differentiation and resistance to oxidative stress.* J Cell Biochem, 2008. **105**(2): p. 612-23.
207. Lyon, A. and S. Harding, *The potential of cardiac stem cell therapy for heart failure.* Curr Opin Pharmacol, 2007. **7**(2): p. 164-70.
208. Smith, P., *Effect of hypoxia upon the growth and sprouting activity of cultured aortic endothelium from the rat.* J Cell Sci, 1989. **92 (Pt 3)**: p. 505-12.
209. Gordan, J.D., et al., *HIF-2alpha promotes hypoxic cell proliferation by enhancing c-myc transcriptional activity.* Cancer Cell, 2007. **11**(4): p. 335-47.
210. Denis, N., et al., *Stimulation of methotrexate resistance and dihydrofolate reductase gene amplification by c-myc.* Oncogene, 1991. **6**(8): p. 1453-7.

211. Li, T.S., et al., *Expansion of human cardiac stem cells in physiological oxygen improves cell production efficiency and potency for myocardial repair.* Cardiovasc Res. **89**(1): p. 157-65.
212. Wang, F., S. Thirumangalathu, and M.R. Loeken, *Establishment of new mouse embryonic stem cell lines is improved by physiological glucose and oxygen.* Cloning Stem Cells, 2006. **8**(2): p. 108-16.
213. Fehrer, C., et al., *Reduced oxygen tension attenuates differentiation capacity of human mesenchymal stem cells and prolongs their lifespan.* Aging Cell, 2007. **6**(6): p. 745-57.
214. *Human embryonic stem cell research.* Hum Reprod Genet Ethics, 2001. **7**(1): p. 14.
215. Forristal, C.E., et al., *Hypoxia inducible factors regulate pluripotency and proliferation in human embryonic stem cells cultured at reduced oxygen tensions.* Reproduction. **139**(1): p. 85-97.
216. Ji, L., et al., *Self-renewal and pluripotency is maintained in human embryonic stem cells by co-culture with human fetal liver stromal cells expressing hypoxia inducible factor 1alpha.* J Cell Physiol, 2009. **221**(1): p. 54-66.
217. Shafer, J., et al., *Oxygen tension directs chondrogenic differentiation of myelo-monocytic progenitors during endochondral bone formation.* Tissue Eng, 2007. **13**(8): p. 2011-9.
218. Khan, W.S., A.B. Adesida, and T.E. Hardingham, *Hypoxic conditions increase hypoxia-inducible transcription factor 2alpha and enhance chondrogenesis in stem cells from the infrapatellar fat pad of osteoarthritis patients.* Arthritis Res Ther, 2007. **9**(3): p. R55.
219. Abdollahi, H., et al., *The role of hypoxia in stem cell differentiation and therapeutics.* J Surg Res. **165**(1): p. 112-7.
220. Fink, T., et al., *Induction of adipocyte-like phenotype in human mesenchymal stem cells by hypoxia.* Stem Cells, 2004. **22**(7): p. 1346-55.
221. Csete, M., et al., *Oxygen-mediated regulation of skeletal muscle satellite cell proliferation and adipogenesis in culture.* J Cell Physiol, 2001. **189**(2): p. 189-96.
222. Yun, Z., et al., *Inhibition of PPAR gamma 2 gene expression by the HIF-1-regulated gene DEC1/Stra13: a mechanism for regulation of adipogenesis by hypoxia.* Dev Cell, 2002. **2**(3): p. 331-41.
223. Mizuno, S., et al., *Hypoxia regulates human lung fibroblast proliferation via p53-dependent and -independent pathways.* Respir Res, 2009. **10**: p. 17.
224. Siddiqui, A., et al., *Differential effects of oxygen on human dermal fibroblasts: acute versus chronic hypoxia.* Wound Repair Regen, 1996. **4**(2): p. 211-8.
225. Xiong, L., et al., *Heat shock protein 90 is involved in regulation of hypoxia-driven proliferation of embryonic neural stem/progenitor cells.* Cell Stress Chaperones, 2009. **14**(2): p. 183-92.
226. Ramirez-Bergeron, D.L. and M.C. Simon, *Hypoxia-inducible factor and the development of stem cells of the cardiovascular system.* Stem Cells, 2001. **19**(4): p. 279-86.
227. Beguin, Y., *Erythropoietin and platelet production.* Haematologica, 1999. **84**(6): p. 541-7.
228. Orn, S., et al., *Effect of left ventricular scar size, location, and transmurality on left ventricular remodeling with healed myocardial infarction.* Am J Cardiol, 2007. **99**(8): p. 1109-14.
229. Carmeliet, P., *Angiogenesis in health and disease.* Nat Med, 2003. **9**(6): p. 653-60.

230. Varma, S. and H.J. Cohen, *Co-transactivation of the 3' erythropoietin hypoxia inducible enhancer by the HIF-1 protein.* Blood Cells Mol Dis, 1997. **23**(2): p. 169-76.
231. Fong, G.H., *Regulation of angiogenesis by oxygen sensing mechanisms.* J Mol Med, 2009. **87**(6): p. 549-60.
232. Hu, X., et al., *Stromal cell derived factor-1 alpha confers protection against myocardial ischemia/reperfusion injury: role of the cardiac stromal cell derived factor-1 alpha CXCR4 axis.* Circulation, 2007. **116**(6): p. 654-63.
233. Dimmeler, S., A.M. Zeiher, and M.D. Schneider, *Unchain my heart: the scientific foundations of cardiac repair.* J Clin Invest, 2005. **115**(3): p. 572-83.
234. Stuckey, D.J., *Stem Cell Therapy for Myocardial Infarction*, in *Department of Physiology, Anatomy and Genetics*. 2007, University of Oxford: Oxford. p. 179.
235. Wood, I.S. and P. Trayhurn, *Glucose transporters (GLUT and SGLT): expanded families of sugar transport proteins.* Br J Nutr, 2003. **89**(1): p. 3-9.
236. Charron, M.J., et al., *A glucose transport protein expressed predominately in insulin-responsive tissues.* Proc Natl Acad Sci U S A, 1989. **86**(8): p. 2535-9.
237. Airley, R.E. and A. Mobasheri, *Hypoxic regulation of glucose transport, anaerobic metabolism and angiogenesis in cancer: novel pathways and targets for anticancer therapeutics.* Chemotherapy, 2007. **53**(4): p. 233-56.
238. Warburg, O., *On the origin of cancer cells.* Science, 1956. **123**(3191): p. 309-14.
239. Vander Heiden, M.G., L.C. Cantley, and C.B. Thompson, *Understanding the Warburg effect: the metabolic requirements of cell proliferation.* Science, 2009. **324**(5930): p. 1029-33.
240. Guppy, M., E. Greiner, and K. Brand, *The role of the Crabtree effect and an endogenous fuel in the energy metabolism of resting and proliferating thymocytes.* Eur J Biochem, 1993. **212**(1): p. 95-9.
241. Kondoh, H., et al., *A high glycolytic flux supports the proliferative potential of murine embryonic stem cells.* Antioxid Redox Signal, 2007. **9**(3): p. 293-9.
242. Brand, K., *Aerobic glycolysis by proliferating cells: protection against oxidative stress at the expense of energy yield.* J Bioenerg Biomembr, 1997. **29**(4): p. 355-64.
243. DeBerardinis, R.J., et al., *The biology of cancer: metabolic reprogramming fuels cell growth and proliferation.* Cell Metab, 2008. **7**(1): p. 11-20.
244. Song, S.W., et al., *Integrin-linked kinase is required in hypoxic mesenchymal stem cells for strengthening cell adhesion to ischemic myocardium.* Stem Cells, 2009. **27**(6): p. 1358-65.
245. Sridharan, V., et al., *The prolyl hydroxylase oxygen-sensing pathway is cytoprotective and allows maintenance of mitochondrial membrane potential during metabolic inhibition.* Am J Physiol Cell Physiol, 2007. **292**(2): p. C719-28.
246. Fong, G.H. and K. Takeda, *Role and regulation of prolyl hydroxylase domain proteins.* Cell Death Differ, 2008. **15**(4): p. 635-41.
247. Schofield, C.J. and P.J. Ratcliffe, *Signalling hypoxia by HIF hydroxylases.* Biochem Biophys Res Commun, 2005. **338**(1): p. 617-26.
248. Huang, L.E., et al., *Activation of hypoxia-inducible transcription factor depends primarily upon redox-sensitive stabilization of its alpha subunit.* J Biol Chem, 1996. **271**(50): p. 32253-9.

249. Wenger, R.H., *Cellular adaptation to hypoxia: O2-sensing protein hydroxylases, hypoxia-inducible transcription factors, and O2-regulated gene expression.* Faseb J, 2002. **16**(10): p. 1151-62.
250. Forest, L., N. Glade, and J. Demongeot, *Lienard systems and potential-Hamiltonian decomposition: applications in biology.* C R Biol, 2007. **330**(2): p. 97-106.
251. Myllyharju, J., *HIF prolyl 4-hydroxylases and their potential as drug targets.* Curr Pharm Des, 2009. **15**(33): p. 3878-85.
252. Wenger, R.H., et al., *HIF prolyl-4-hydroxylase interacting proteins: consequences for drug targeting.* Curr Pharm Des, 2009. **15**(33): p. 3886-94.
253. Hsieh, M.M., et al., *HIF prolyl hydroxylase inhibition results in endogenous erythropoietin induction, erythrocytosis, and modest fetal hemoglobin expression in rhesus macaques.* Blood, 2007. **110**(6): p. 2140-7.
254. Imperatore, A., et al., *Hypoxia and preeclampsia: increased expression of urocortin 2 and urocortin 3.* Reprod Sci. **17**(9): p. 833-43.
255. Li, X., et al., *Integrity of the prolyl hydroxylase domain protein 2:erythropoietin pathway in aging mice.* Blood Cells Mol Dis. **45**(1): p. 9-19.
256. Gong, Y. and F.H. Agani, *Oligomycin inhibits HIF-1alpha expression in hypoxic tumor cells.* Am J Physiol Cell Physiol, 2005. **288**(5): p. C1023-9.
257. Vogel, S., et al., *Prolyl hydroxylase domain (PHD) 2 affects cell migration and F-actin formation via RhoA/rho-associated kinase-dependent cofilin phosphorylation.* J Biol Chem. **285**(44): p. 33756-63.
258. Jokilehto, T. and P.M. Jaakkola, *The role of HIF prolyl hydroxylases in tumour growth.* J Cell Mol Med. **14**(4): p. 758-70.
259. Song, Y.R., et al., *Activation of hypoxia-inducible factor attenuates renal injury in rat remnant kidney.* Nephrol Dial Transplant. **25**(1): p. 77-85.
260. Mole, D.R., et al., *2-oxoglutarate analogue inhibitors of HIF prolyl hydroxylase.* Bioorg Med Chem Lett, 2003. **13**(16): p. 2677-80.
261. Oliver, R.J., et al., *Prognostic value of facilitative glucose transporter Glut-1 in oral squamous cell carcinomas treated by surgical resection; results of EORTC Translational Research Fund studies.* Eur J Cancer, 2004. **40**(4): p. 503-7.
262. Mohle, R., et al., *Regulation of transendothelial migration of hematopoietic progenitor cells.* Ann N Y Acad Sci, 1999. **872**: p. 176-85; discussion 185-6.
263. McQuibban, G.A., et al., *Matrix metalloproteinase activity inactivates the CXC chemokine stromal cell-derived factor-1.* J Biol Chem, 2001. **276**(47): p. 43503-8.
264. Al-Adnani, M.S., J.A. Kirrane, and J.O. McGee, *Inappropriate production of collagen and prolyl hydroxylase by human breast cancer cells in vivo.* Br J Cancer, 1975. **31**(6): p. 653-60.
265. Kobayashi, K., et al., *Secreted Frizzled-related protein 2 is a procollagen C proteinase enhancer with a role in fibrosis associated with myocardial infarction.* Nat Cell Biol, 2009. **11**(1): p. 46-55.
266. Conejo-Garcia, A., et al., *Structural basis for binding of cyclic 2-oxoglutarate analogues to factor-inhibiting hypoxia-inducible factor.* Bioorg Med Chem Lett. **20**(20): p. 6125-8.
267. FibroGen. *Clinical results demonstrate ability of HIF-PHI to treat patients with anemia*. [cited; Available from: http://www.fibrogen.com/Anemia_Clinical_Studies.
268. Roger, V.L., et al., *Heart disease and stroke statistics--2011 update: a report from the American Heart Association.* Circulation. **123**(4): p. e18-e209.

269. Lloyd-Jones, D., et al., *Heart disease and stroke statistics--2010 update: a report from the American Heart Association.* Circulation. **121**(7): p. e46-e215.
270. Lloyd-Jones, D., et al., *Heart disease and stroke statistics--2009 update: a report from the American Heart Association Statistics Committee and Stroke Statistics Subcommittee.* Circulation, 2009. **119**(3): p. 480-6.
271. Hobbs, F.D., L.R. Erhardt, and C. Rycroft, *The From The Heart study: a global survey of patient understanding of cholesterol management and cardiovascular risk, and physician-patient communication.* Curr Med Res Opin, 2008. **24**(5): p. 1267-78.
272. Liu, L., *Cardiovascular diseases in China.* Biochem Cell Biol, 2007. **85**(2): p. 157-63.
273. Ballard, V.L. and J.M. Edelberg, *Stem cells for cardiovascular repair - the challenges of the aging heart.* J Mol Cell Cardiol, 2008. **45**(4): p. 582-92.
274. Mayani, H., *Biological differences between neonatal and adult human hematopoietic stem/progenitor cells.* Stem Cells Dev. **19**(3): p. 285-98.
275. Nishino, J., et al., *Hmga2 promotes neural stem cell self-renewal in young but not old mice by reducing p16Ink4a and p19Arf Expression.* Cell, 2008. **135**(2): p. 227-39.
276. Fan, M., et al., *The effect of age on the efficacy of human mesenchymal stem cell transplantation after a myocardial infarction.* Rejuvenation Res. **13**(4): p. 429-38.
277. Sopko, N.A., et al., *Bone marrow support of the heart in pressure overload is lost with aging.* PLoS One. **5**(12): p. e15187.
278. Conboy, I.M., et al., *Rejuvenation of aged progenitor cells by exposure to a young systemic environment.* Nature, 2005. **433**(7027): p. 760-4.
279. Leri, A., J. Kajstura, and P. Anversa, *Cardiac stem cells and mechanisms of myocardial regeneration.* Physiol Rev, 2005. **85**(4): p. 1373-416.
280. Cheng, W., et al., *Stretch-induced programmed myocyte cell death.* J Clin Invest, 1995. **96**(5): p. 2247-59.
281. Estes, B.T., J.M. Gimble, and F. Guilak, *Mechanical signals as regulators of stem cell fate.* Curr Top Dev Biol, 2004. **60**: p. 91-126.
282. Guilak, F., et al., *Control of stem cell fate by physical interactions with the extracellular matrix.* Cell Stem Cell, 2009. **5**(1): p. 17-26.
283. Cawthon, R.M., *Telomere measurement by quantitative PCR.* Nucleic Acids Res, 2002. **30**(10): p. e47.
284. Zhu, G., et al., *Young environment reverses the declined activity of aged rat-derived endothelial progenitor cells: involvement of the phosphatidylinositol 3-kinase/Akt signaling pathway.* Ann Vasc Surg, 2009. **23**(4): p. 519-34.
285. Xin, Y., et al., *Aging adversely impacts biological properties of human bone marrow-derived mesenchymal stem cells: implications for tissue engineering heart valve construction.* Artif Organs. **34**(3): p. 215-22.
286. Jump, S.S., et al., *Fibroblast growth factor 2-stimulated proliferation is lower in muscle precursor cells from old rats.* Exp Physiol, 2009. **94**(6): p. 739-48.
287. Belluardo, N., et al., *Nicotine-induced fibroblast growth factor-2 restores the age-related decline of precursor cell proliferation in the subventricular zone of rat brain.* Brain Res, 2008. **1193**: p. 12-24.
288. Puterman, E., et al., *The power of exercise: buffering the effect of chronic stress on telomere length.* PLoS One. **5**(5): p. e10837.
289. Blackburn, E.H., *Telomere states and cell fates.* Nature, 2000. **408**(6808): p. 53-6.

290. Calado, R.T. and N.S. Young, *Telomere maintenance and human bone marrow failure.* Blood, 2008. **111**(9): p. 4446-55.
291. Jiang, S., et al., *Transcriptional profiling of young and old mesenchymal stem cells in response to oxygen deprivation and reparability of the infarcted myocardium.* J Mol Cell Cardiol, 2008. **44**(3): p. 582-96.
292. Rossi, D.J., et al., *Cell intrinsic alterations underlie hematopoietic stem cell aging.* Proc Natl Acad Sci U S A, 2005. **102**(26): p. 9194-9.
293. Stolzing, A., S. Sethe, and A.M. Scutt, *Stressed stem cells: Temperature response in aged mesenchymal stem cells.* Stem Cells Dev, 2006. **15**(4): p. 478-87.
294. Mimeault, M. and S.K. Batra, *Aging of tissue-resident adult stem/progenitor cells and their pathological consequences.* Panminerva Med, 2009. **51**(2): p. 57-79.
295. Mimeault, M. and S.K. Batra, *Recent insights into the molecular mechanisms involved in aging and the malignant transformation of adult stem/progenitor cells and their therapeutic implications.* Ageing Res Rev, 2009. **8**(2): p. 94-112.
296. Kirkwood, T.B., *Understanding the odd science of aging.* Cell, 2005. **120**(4): p. 437-47.
297. Maslov, A.Y., et al., *Neural stem cell detection, characterization, and age-related changes in the subventricular zone of mice.* J Neurosci, 2004. **24**(7): p. 1726-33.
298. Inomata, K., et al., *Genotoxic stress abrogates renewal of melanocyte stem cells by triggering their differentiation.* Cell, 2009. **137**(6): p. 1088-99.
299. Mieno, S., et al., *Aging is associated with an impaired coronary microvascular response to vascular endothelial growth factor in patients.* J Thorac Cardiovasc Surg, 2006. **132**(6): p. 1348-55.
300. Duan, Y.G., et al., *[Expression patterns of age-related molecule c-kit, HIWI and vimentin in the rat testis and epididymis].* Zhonghua Nan Ke Xue, 2007. **13**(11): p. 992-6.
301. Rajawat, Y.S., Z. Hilioti, and I. Bossis, *Aging: central role for autophagy and the lysosomal degradative system.* Ageing Res Rev, 2009. **8**(3): p. 199-213.
302. Liu, L. and T.A. Rando, *Manifestations and mechanisms of stem cell aging.* J Cell Biol. **193**(2): p. 257-66.
303. Fuchs, E., T. Tumbar, and G. Guasch, *Socializing with the neighbors: stem cells and their niche.* Cell, 2004. **116**(6): p. 769-78.
304. Tumbar, T., et al., *Defining the epithelial stem cell niche in skin.* Science, 2004. **303**(5656): p. 359-63.
305. Urbanek, K., et al., *Stem cell niches in the adult mouse heart.* Proc Natl Acad Sci U S A, 2006. **103**(24): p. 9226-31.
306. Peterson, W.J., K.H. Tachiki, and D.T. Yamaguchi, *Serial passage of MC3T3-E1 cells down-regulates proliferation during osteogenesis in vitro.* Cell Prolif, 2004. **37**(5): p. 325-36.
307. Katsara, O., et al., *Effects of Donor Age, Gender, and In Vitro Cellular Aging on the Phenotypic, Functional, and Molecular Characteristics of Mouse Bone Marrow-Derived Mesenchymal Stem Cells.* Stem Cells Dev.
308. Siddappa, R., et al., *Donor variation and loss of multipotency during in vitro expansion of human mesenchymal stem cells for bone tissue engineering.* J Orthop Res, 2007. **25**(8): p. 1029-41.

309. Ratajczak, M.Z., et al., *Heterogeneous populations of bone marrow stem cells--are we spotting on the same cells from the different angles?* Folia Histochem Cytobiol, 2004. **42**(3): p. 139-46.
310. Ho, A.D., W. Wagner, and W. Franke, *Heterogeneity of mesenchymal stromal cell preparations.* Cytotherapy, 2008. **10**(4): p. 320-30.
311. Halfon, S., et al., *Markers distinguishing mesenchymal stem cells from fibroblasts are downregulated with passaging.* Stem Cells Dev. **20**(1): p. 53-66.
312. Haudek, S.B., et al., *Monocytic fibroblast precursors mediate fibrosis in angiotensin-II-induced cardiac hypertrophy.* J Mol Cell Cardiol. **49**(3): p. 499-507.
313. Waterstrat, A. and G. Van Zant, *Effects of aging on hematopoietic stem and progenitor cells.* Curr Opin Immunol, 2009. **21**(4): p. 408-13.
314. Schioppa, T., et al., *Regulation of the chemokine receptor CXCR4 by hypoxia.* J Exp Med, 2003. **198**(9): p. 1391-402.
315. Chimenti, I., et al., *Relative roles of direct regeneration versus paracrine effects of human cardiosphere-derived cells transplanted into infarcted mice.* Circ Res. **106**(5): p. 971-80.
316. Aghila Rani, K.G. and C.C. Kartha, *Effects of epidermal growth factor on proliferation and migration of cardiosphere-derived cells expanded from adult human heart.* Growth Factors. **28**(3): p. 157-65.
317. Johnston, P.V., et al., *Engraftment, differentiation, and functional benefits of autologous cardiosphere-derived cells in porcine ischemic cardiomyopathy.* Circulation, 2009. **120**(12): p. 1075-83, 7 p following 1083.
318. Koninckx, R., et al., *Mesenchymal stem cells or cardiac progenitors for cardiac repair? A comparative study.* Cell Mol Life Sci. **68**(12): p. 2141-56.
319. Gambini, E., et al., *C-kit+ cardiac progenitors exhibit mesenchymal markers and preferential cardiovascular commitment.* Cardiovasc Res. **89**(2): p. 362-73.
320. Geller, L.I. and M.M. Pashko, *[The significance of trypsin, amylase and lipase activities in the blood serum for the differential,diagnosis of chronic pancreatitis and other diseases of the abdominal organs].* Vrach Delo, 1990(3): p. 86-8.
321. Chen, J., G.M. Lanza, and S.A. Wickline, *Quantitative magnetic resonance fluorine imaging: today and tomorrow.* Wiley Interdiscip Rev Nanomed Nanobiotechnol. **2**(4): p. 431-40.
322. O'Callaghan, N.J. and M. Fenech, *A quantitative PCR method for measuring absolute telomere length.* Biol Proced Online. **13**: p. 3.
323. Rasband, W.S., *ImageJ, U. S. National Institutes of Health, Bethesda, Maryland, USA,*. http://rsb.info.nih.gov/ij/, 1997-2009.

Appendix 1 Media composition

Medium	Composition
Complete Explant Medium (CEM)	400 ml Ischove's Modified Dulbeccon's Medium (IMDM) (invitrogen) 100 ml Fetal Bovine Serum (FBS) (Invitrogen) 5 ml Penicilin streptomycin glutamine (PSG) (100U/ml penicillin, 100U/ml streptomycin, 0.2mM L-glutamine)
Medium Supplement (MS)	500 ml Dulbecco's Modified Eagle's Medium and Ham's F-12 (DMEM/F12) (invitrogen) 5 ml PSG
Cardiosphere Growing Medium (CGM)	65% DMEM/F12 35% IMDM 7% FBS Growth factors (as described below)

Growth factor in CGM	Concentration	Manufacture
B27	2%	Invitrogen
Cardiotrophin	25 ng/ml	Peprotech
Human Recombinant Epidermal Growth Factor (EGF)	10 ng/ml	Promega
Human Recombinant Fibroblast Growth Factor (FGF)	20 ng/ml	Peprotech
Thrombin	5 units	Sigma

Appendix 2 Adipogenesis assay medium

Medium	Composition	Medium	Composition
Adipogenic Induction Medium (AIM)	400 ml (DMEM/F12) 100 ml FBS 5 ml PSG 10μg/ml insulin 1 μM dexamathasone 200 μM indomethacin 500 μM 1-methyl-3-isobutylxanthine	Maintenance Medium (MM)	400 ml DMEM/F12 100 ml FBS 5 ml PSG

Appendix 3 Cardiomyocyte differentiation medium

Medium	**Composition**
Cardiomyocytes Differentiation Medium (CDM)	245 ml IMDM 245 ml DMEM/F12 10 ml FBS ESQ (embroyonic stem cell-qualified) (Invitrogen) 5 ml insulin transferring selenium (Invitrogen)

Appendix 4 List of primer sequences

No.	Function	Primer	Gene name	Forward primer 5' to 3'	Reverse primer 3' to 5'	Gene accession number
1	Markers for pluripotent stem cells	OCT-4	POU class 5 homeobox 1 (Pou5f1)	GAGGGATGTGGTTCGAGTGT	CCAGAGCAGTGACAGGAACA	NM_001009178.2 #
2		Sox-2	SRY (sex determining region Y)-box 2	CACAACTCGGAGATCAGCAA	CTCCGGGAAGCGTGTACTTA	NM_001109181.1 #
3		Klf-4	Kruppel-like factor 4	CCACAGACCTGGAAAGTGGT	GGAAGACGAGGATGAAGCTG	NM_053713.1#
4		Nanog	Homeobox protein NANOG	TACCTCAGCCTCCAGCAGAT	AGGCCGTTGCTAGTCTTCAA	AB275459 #
5	Cardiac stem cell marker	c-Kit	Stem cell factor cytokine receptor	AATCCGACAACCAAAGCAAC	TGACATCAGAGTTGGACACCA	ENSRNOG00000002227 *
6	Involved in the signaling for stem cell homing to infarcted heart	CXCR-4	chemokine receptor type 4	GCTACCTTGCCATTGTCCAC	ACATCGGCGAAGATGATGTC	NM_022205.3
7	Early cardiac transcription markers	Nkx 2.5	Homeobox protein NKX2-5	CATTTTATCCGCGAGCCTAC	GTCTGTCTCGGCTTTGTCCA	ENSRNOG00000020747 *
8		GATA 4	GATA binding protein 4	CAGTCCTGCACAGCCTACCT	CCGCAGTTGACACACTCTCT	NM_144730

* Exon sequences browsed using Ensembl Genome Browser; others were browsed using GenBank Genome Browser.
# Primer sequences were kindly provided by Dr. Georgina M. Ellison.

Appendix 4 List of primer sequences (continue)

No.	Function	Primer	Gene name	Forward primer 5' to 3'	Reverse primer 3' to 5'	Gene accession number
9	Markers of matured cardiomyocyte	Tnnt 2	Troponin T type 2 (cardiac)	CGTATTCGCAATGAACGAGA	CTGTTCTCCTCCTCCTCACG	NM_012676
10		MyHC	Myosin heavy chain	TATGAGACGGACGCCATACA	CTCCAGAGAGGAGCACTTGG	NM_017239.2
11	Markers for mesenchymal cells or fibroblasts	CD90	Thy-1 cell surface antigen	CAGAATCCCACAAGCTCCAA	GCCAGGAAGTGTTTTGAACC	NM_012673
12		CD105	Endoglin	GGTACAGTGCATCGACATGG	GCTGGCCTAGCTCTATGGTG	NM_001010968
13	Hypoxia induced transcription factor	HIF-1α	Hypoxia induced factor-1 alpha	GGTGGATATGTCTGGGTTGAG	TTCAACTGGTTTGAGGACAGA	NM_024359
14	Induce production of red blood cell	EPO	Erythropoietin	CCAGCCACCAGAGAGTCTTC	TGTGAGTGTTCGGAGTGGAG	NM_017001.1
15	Stimulate vasculogenesis and angiogenesis	VEGF-α	Vascular endothelial growth factor A	AATGATGAAGCCCTGGAGTG	ATGCTGCAGGAAGCTCATCT	ENSRNOG00000019598 *
16	Catalytic subunit of the enzyme telomerase	TERT	telomerase reverse transcriptase	AGTGGTGAACTTCCCTGTGG	CAACCGCAAGACTGACAAGA	NM_053423 #

* Exon sequences browsed using Ensembl Genome Browser; others were browsed using GenBank Genome Browser.
# Primer sequences were kindly provided by Dr. Georgina M. Ellison.

Appendix 4 List of primer sequences (continue)

No.	Function	Primer	Gene name	Forward primer 5' to 3'	Reverse primer 3' to 5'	Gene accession number
17	Housekeeping genes	GAPDH	glyceraldehyde-3-phosphate dehydrogenase	GGGTGTGAACCACGAGAAAT	ACTGTGGTCATGAGCCCTTC	NM_017008
18		Actb	Beta-actin	CTAAGGCCAACCGTGAAAAG	AACACAGCCTGGATGGCTAC	NM_031144
19	Telomere length	Tel	Telomere	GGTTTTTGAGGGTGAGGGTGAGGGTGAGGGTGAGGGT	TCCCGACTATCCCTATCCCTATCCCTATCCCTATCCCTA	Sequence obtained from published paper [283].
20	Encodes acidic ribosomal phosphoprotein. Used as housekeeping gene in telomere length measurement assay.	36β4	acidic ribosomal phosphoprotein	ACTGGTCTAGGACCCGAGAAG	TCAATGGTGCCTCTGGAGATT	Sequence obtained from published paper [322].

* Exon sequences browsed using Ensembl Genome Browser; others were browsed using GenBank Genome Browser.
# Primer sequences were kindly provided by Dr. Georgina M. Ellison
.

Appendix 5 Buffer for western blot

Medium	Composition	Medium	Composition
Lysis buffer	75mM Tris-HCL pH 6.8	TBS-tween	0.9% NaCl (w/v)
	3.8% SDS (w/v)		10mM Tris-base
	4M urea		0.05% tween (v/v)
	20% glycerol (v/v)		
	0.1% triton (v/v)	SDS transfer	48mM Tris-HCl
	Protease inhibitors	buffer	30mM glycine
			0.0375% SDS
			20% methanol

Appendix 6 Respiratory medium for Clarke-type oxygen electrode

Medium	Composition
Respiratory medium	100 mM KCl
	50mM MOPS
	1 mM EGTA
	5mM KH_2PO_4
	1 mg.ml BSA
	pH 7..4

Appendix 7 Magnetic Resonance Imaging (MRI)

Rats underwent *in vivo* cine MRI to characterize cardiac function and morphology. Anaesthesia was induced in a chamber with isoflurane vaporized to 2.5% in O_2. Animals were positioned supine in a purpose-built rat holder and maintained at 2.5% isoflurane throughout the experiment. Temperature was maintained using air heated by a heating blanket. The electrocardiogram (ECG) and respiration rates were monitored and recorded. The imaging was performed using an 11.7 T (500 MHz) vertical bore MRI scanner (Magnex Scientific, Oxon, UK), a Bruker Avance console (Bruker Medical, Ettlingen, Germany) and a shielded gradient system (Magnex Scientific, Oxon, UK). A 60 mm diameter birdcage radiofrequency (RF) coil (Bruker Medical,

Ettlingen, Germany) was used to transmit and receive MRI signals. Scout images were acquired to determine the position of the heart. After scouting for long and short axis views of the heart, seven to nine contiguous slices of 1.5 mm thickness covering the entire left ventricle (LV) were acquired (Figure A1). Image data were segmented using Image J program [323]. End-diastole (ED) and end-systole (ES), corresponding to the frames of maximal and minimal ventricular volume, respectively, were identified (Figure 3.1 b and c). The epicardial and endocardial borders were outlined using the free hand drawing tool. End-diastole volume (EDV), end-systole volume (ESV), stroke volume (SV = EDV – ESV) and ejection fraction (EF = SV / EDV) were calculated (work done by Dr Carolyn Carr and Dr. Daniel Stuckey).

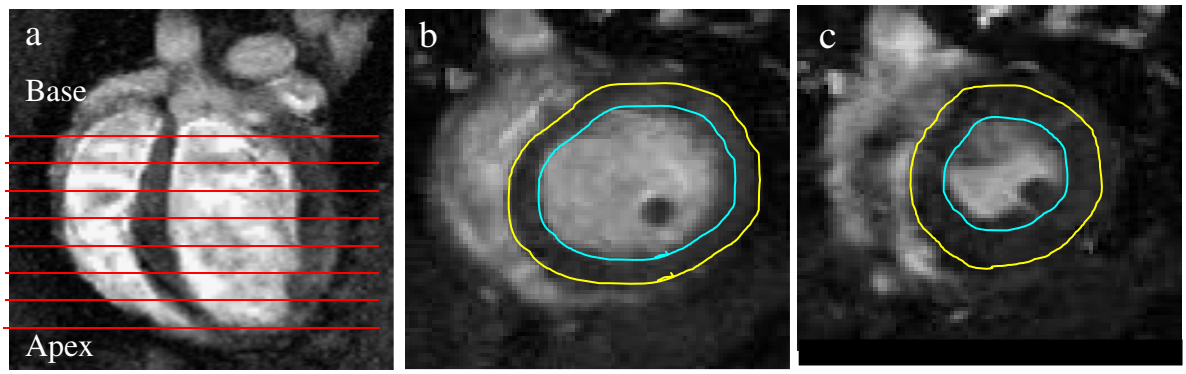

Figure A1 *(a) Long axis view of the rat heart showing eight continuous slices of 1.5 mm thickness covering the entire heart from base to apex. (b) End diastolic and (c) End systolic short axis images of heart showing the outlined epicardial (yellow line) and endocardial (blue line) border of the left ventricle.*

Appendix 8 Publication arising from this thesis (paper submitted)

Identification of valid housekeeping genes for quantitative RT-PCR analysis of cardiosphere-derived cells

Suat Cheng Tan[1], Carolyn A. Carr[1], Kar Kheng Yeoh[2], Christopher J. Schofield[2], Kay E. Davies[1], Kieran Clarke[1]

[1]Department of Physiology, Anatomy & Genetics, University of Oxford, Sherrington Building, Parks Road, Oxford, OX1 3PT, UK

[2]Department of Chemistry, University of Oxford, Chemistry Research Laboratory, Mansfield Road, Oxford, OX1 3TA, UK.

Corresponding author:

Dr. Carolyn A. Carr

Cardiac Metabolism Research Group,

Department of Physiology,

Anatomy & Genetics,

University of Oxford,

Sherrington Building,

Parks Road, Oxford, OX1 3PT, UK.

Tel: 01865 282247; Fax 01865 282272

Email addresses:

SCT: suat.tan@dpag.ox.ac.uk

CAC: carolyn.carr@dpag.ox.ac.uk

KKY: karkheng.yeoh@chem.ox.ac.uk

CJS: christopher.schofield@chem.ox.ac.uk

KD: kay.davies@dpag.ox.ac.uk

KC: kieran.clarke@dpag.ox.ac.uk

Abstract:

Resident stem cells (CSCs) in the heart may be isolated *in vitro,* via the formation of cardiospheres (Csp), to give cardiosphere-derived cells (CDCs). Although qRT-PCR analyses of CDCs have been performed, no justification for the selection of housekeeping genes has been reported. As a housekeeping gene is important for the interpretation of qRT-PCR results, here we evaluated the most suitable housekeeping gene for RNA expression analyses in CDCs cultured under normoxia, hypoxia or with prolyl-4-hydroxylase inhibitors (PHIs), from both neonatal and adult rats, to determine the effects of aging and different culture conditions on the stability of the housekeeping gene. Six candidate housekeeping genes, [glyceraldehyde-3-phosphate dehydrogenase (GAPDH), beta-actin (Actb), hypoxanthine phosphoribosyltransferase 1 (HPRT-1), beta-2-microtubulin (β2M), 60S acidic ribosomal protein large P1 (RPLP-1) and TATA box binding protein (Tbp)] were evaluated. Analyses using geNorm and NormFinder revealed that GAPDH was the most consistently expressed housekeeping gene among all genes tested under normoxia for both neonatal and adult CDCs. However, Actb was the most stable housekeeping gene under hypoxia. For the PHI-treated CDCs, overall, GADPH, Actb and β2M were more consistently expressed, whereas HPRT-1, RPLP-1 and Tbp showed unstable expression. The ranking for β2M, HPRT- and RPLP-1 stability was different for neonatal and adult cells, indicating that expression of these genes is age-dependent. Lastly, independent of age or culture conditions, Tbp was the least stable housekeeping gene. A combination of Actb and GADPH gives the most reliable normalization for comparative analyses of gene transcription in neonatal and adult rat CDCs preconditioned by hypoxia or PHIs.

Introduction:

The identification of stem cells within the heart [1] challenged the generally accepted paradigm that the heart is a postmitotic organ [2, 3]. In 2004, Messina *et al.* developed a method to isolate stem cells from human and murine heart, expanding them as cardiospheres (CSp) [4]. Such CSp were clonogenic, expressed stem and endothelial progenitor cell antigens/markers, and appeared to have the properties of adult cardiac stem cells. The CSp were expanded to obtain sufficient cardiosphere-derived cells (CDC) for transplantation [5]. CSp and CDCs derived from heart explant culture *in vitro* caused myocardial regeneration and functional improvement when injected into the infarcted mouse heart *in vivo* [4, 5].

Preconditioning of stem cells to enable survival in the hypoxic environment has been postulated to improve both stem cell production efficiency and potency for myocardial repair [6]. The implantation of hypoxic (5% O_2) CDCs into infarcted hearts of mice *in vivo* resulted in greater cell engraftment and better functional recovery than with conventionally cultured (normoxic) CDCs [6]. Hypoxia triggers multiple physiological and cellular adaptations to reduced oxygen, with many processes involved in oxygen homeostasis being mediated by the hypoxia-inducible factor (HIF) transcriptional complex, which is negatively regulated by the prolyl-4-hydroxylase (PHD) (also known as HIF prolyl hydroxylases, HPH and Egg-laying deficient nine, EGLN) [7]. The PHD enzyme is a conserved subfamily of dioxygenases that uses oxygen and 2-oxoglutarate as a co-substrate and iron as a co-factor to catalyse the post-translational hydroxylation of specific prolyl residues of HIF-α subunits [8-10]. Upon hydroxylation, the HIF-1α subunit is recognized by the von Hippel-Lindau protein which targets the subunit for efficient proteasomal degradation [10]. PHD hydroxylase activity in cells depends on the availability of 2-oxoglutarate, oxygen and ferrous ion. Thus, limited oxygen supply or inhibition of the 2-oxoglutarate or iron binding can inhibit PHD activity and thus activate the HIF response [11-14].

Here, we cultured CDCs under hypoxia (2% oxygen) or used three different prolyl-4-hydroxylase inhibitors (PHIs) to enable CDC HIF stabilization. The PHIs used in this study included dimethyloxaloylglycine (DMOG) – a cell permeable, competitive inhibitor of 2-oxoglutarate [12], ethyl 2-(2,3-dihyroxybenzamido) acetate (EDBA) - an aspirin metabolite that activates the HIF system via generic 2-oxoglutarate oxygenase inhibition [15], and 2-(1-chloro-4-hydroxyisoquinoline-3-carboxamido) acetic acid (BIC) - a specific PHD inhibitor reported in the patent literature [16], which has been used in clinical trials as a pro-angiogenic compound acting via the HIF-1α system [13].

Changes in the CDC genotype after hypoxic and PHI treatment are of interest. The most commonly used technique for gene expression analysis is quantitative (real-time) reverse transcriptase polymerase chain reaction (qRT-PCR), in which expression magnitude is normalized to a reference gene. This gene, referred to as a housekeeping gene, is typically a constitutive gene that is expressed at relatively constant levels in all cells independent of experimental conditions. Selection of an appropriate housekeeping gene is crucial because it directly influences the interpretation of the qRT-PCR data. However, no one housekeeping gene is universal under all experimental conditions.

Many papers have been published using qRT-PCR analysis of CDCs [17-19], hypoxic CDCs [6] or other cells treated with PHIs [20-23], but none have described the background for selecting a suitable housekeeping gene for quantification. Therefore, in this study, we evaluated the most suitable housekeeping gene for RNA expression analysis in normoxic, hypoxic and PHI-preconditioned CDCs isolated from both neonatal and adult rat hearts, using a panel of 6 housekeeping genes, glyceraldehyde-3-phosphate dehydrogenase (GAPDH), beta-actin (Actb), hypoxanthine phosphoribosyltransferase 1 (HPRT-1), beta-2-microtubulin (β2M), 60S acidic ribosomal protein large P1 (RPLP-1) and TATA box binding protein (Tbp) (Table 1). These genes were chosen as they are most commonly used as reference genes in rat qRT-PCR studies [18, 24-34] (Additional file 1).

Methods:

Animals

Sprague Dawley (SD) rats were used for all experiments. All experiments were performed with the approval from The University of Oxford Animal Ethics Review Committees and the Home Office (London, UK).

Primary cardiac stem cell culture

CDCs were isolated and expanded according to a protocol described previously [5]. In brief, neonatal (1-3 days) and adult (4 months) SD rat hearts were isolated, and minced into small explants in 0.05% trypsin-EDTA (Invitrogen). Explants were plated on fibronectin-coated petri dishes with 1.5 ml of complete explant medium (CEM, Additional file 3) to generate explant-derived cells (EDCs). EDC, once confluent, were isolated and seeded onto poly-*D*-lysine coated 24-well plates with cardiosphere growth medium (CGM, Additional file 1) to form spherical cell clusters, known as cardiospheres (Csp). Loosely attached Csp were harvested and plated onto fibronectin-coated T75 flasks with CEM, at a density of 1 x 10^4 cells/flask for expansion into cardiosphere derived cells (CDCs). All the cells were cultured in incubator under 21% O_2 and 5% CO_2, at 37°C, unless otherwise stated.

CDC preconditioned with hypoxia and PHIs

For hypoxic-preconditioned cells, CDCs were cultured under 2% O_2 (hypoxia) and 5% CO_2 at 37°C using an incubator (Wolf Laboratories, UK) adjustable to different oxygen concentrations by infusion of nitrogen (N_2). The O_2 concentration was monitored continuously using an O_2 sensor. For PHI-preconditioning, normoxic CDCs

(cultured under 21% O_2 and 5% CO_2, at 37°C) were treated with 1 mM of DMOG, 0.5 mM of EDBA or 30 μM of BIC for 24 hours at 80% cell confluency.

Western blot analysis for HIF-1α protein

Normoxic, hypoxic and PHI-preconditioned CDCs were lysed in cell lysis buffer containing protease inhibitor. The homogenate was boiled and centrifuged for 5 min, the supernatant frozen and stored at −80°C. The lysate (50 μg/ul) was subjected to SDS–polyacrylamide gel (10%) electrophoresis, and protein was subsequently transferred to a nitrocellulose membrane (Pall Life Science, Mexico). The membrane was incubated overnight with rat HIF-1α primary antibody diluted (1:2000) in 5% milk in TBS-Tween (Novus, NB100-479). The secondary antibody used was goat anti-rabbit conjugated to horseradish peroxidase (1:2000) (Santa Cruz Biotechnology, Santa Cruz, CA). The immunoreactive protein signal was visualized by an ECL plus detection kit (Perkin Elmer). Protein bands were quantified using Un-Scan-It, Version 6.1 (Silk Scientific, USA).

Primer design and optimization

Primers were designed using Primer3 software based on interpretation of GenBank or Ensembl Genome Browser search results (Table 2). Primer specificity was enhanced by designing a primer pair that flanked the exon-exon border of the gene of interest, to avoid the primers amplifying genomic DNA that may be contained in samples. Primer specificity was confirmed by BLASTing the primer sequence against genomic databases available at NCBI. No significant homology sequence should be found, to ensure gene specific amplification rather than amplification of several transcripts with one primer pair.

RNA extraction and DNase treatment

Total RNA was extracted from cultured CDCs using Trizol reagent (Sigma) according to the manufacturer's instructions. DNase treatment was performed using Turbo DNA-free (Ambion) to degrade any DNA present. The concentration and purity of RNA was determined by measuring the absorbance at 260 nm (A260) and 280 nm (A280) using a Nanodrop ND-1000 Spectrophotometer (Nanodrop Technologies Inc., USA). A ratio of A260/A280 ≈ 2.0 is generally accepted as pure RNA.

cDNA synthesis

cDNA was synthesized from the RNA template using AB high capacity transcriptase kit (Applied Biosystem). Every 1 ug RNA sample was reverse transcribed using 1 µl reverse transcriptase, 2 µl random primer, 0.8 µl dNTPs (10 mM each), 2 µl buffer and topped up by RNase free water to a total volume of 20 µl. The reaction mixture was subjected to incubation for 10 mins at 25 °C, 120 mins at 37 °C and 5 secs at 85 °C.

Quantitative RT-PCR (qRT-PCR)

qRT-PCR amplification was performed using Applied Biosystems StepOnePlus Real-Time PCR System (AB International, CA). The qRT-PCR mastermix was prepared by adding 10 µl AB Sybrgreen PCR mastermix (AB International, CA), 1 µl reverse primer, 1 µl forward primer, 1 µl cDNA and 7 µl distilled water. The total volume for each real-time PCR reaction was 20 µl. The PCR program was set up with an initial heat activation step at 95 °C for 10 mins. Then, 40 cycles of thermocycling were performed with a denaturation step at 95 °C for 15 secs, an annealing step at 60 °C for 30 secs and an extension step at 72 °C for 30 secs. Fluorescence was measured at the end of each extension step. After amplification, a melting curve was acquired by heating the product at 4 °C/sec to 95 °C, cooling it at 4 °C/sec to 70 °C, keeping it at 70 °C for 20 secs, and then slowly heating it at 4 °C/sec to 95 °C. Fluorescence was measured through the slow heating phase. Melting curves were used to determine the specificity of PCR products.

Analysis of housekeeping gene expression stability

Raw Ct values of housekeeping genes were converted to linear values compatible with the geNorm and NormFinder programs. For comparison of housekeeping gene stability between groups, the software geNorm, version 3.4 (Visual Basic application tool for Microsoft Excel) [35] was used, while for housekeeping genes stability comparison within group, NormFinder (a Microsoft Excel Add-in) [36] was used. Both programs were used according to developer's recommendations as published.

Analysis of target gene expression

Raw Ct values of the target gene (HIF-1α) were analyzed using two different methods to determine the importance of normalization to different housekeeping gene(s) in qRT-PCR data analysis.

Data analysis using $2^{-\Delta\Delta Ct}$ method

Simple relative quantification of target gene expression normalized to one housekeeping gene was performed using the $2^{-\Delta\Delta Ct}$ method. Derivation of the equation, including assumptions, experimental design and validation test, have been described in Applied Biosystem User Bulletin No. 2 (P/N 4303859). Analyses of gene expression data using this method have appeared in the literature [37-39].

Data analysis using geNorm method

Relative quantification of target gene expression normalized to more than one housekeeping gene was performed using the geNorm method. In this method, target gene expression was normalized to the geometric mean expression of the best combination of housekeeping genes subjected to expression stability analysis using geNorm software. Analyses of gene expression data using this method have appeared in the literature [25, 40-42].

Statistical analysis

The software program, SPSS version 18 was used for further statistical analysis of gene and protein expression among experimental groups. In all cases expression data were compared by one-way analysis of variance (ANOVA) (statistical significance <0.05). The significance level (α) was set at 0.05.

Results:

Hypoxic response

Western blot analyseis showed that CDCs cultured either under hypoxia or after treatment with PHIs had significantly increased HIF-1α protein levels, compared to normoxic CDCs (Figure 1). As anticipated [13], this observation showed that the hypoxic challenge to the cells and the PHI treatments successfully elevated HIF-1α.

RNA and cDNA quality

RNA was isolated from neonatal and adult CDCs subjected to five different culture conditions (Table 2). The RNA purity was measured using a NanoDrop® Spectrophotometer (NanoDrop Technologies). On average, the $A_{260/280}$ ratio of RNA samples was 2.01 ± 0.04, indicating protein-free pure RNA, and the ratio of $A_{260/230}$ was 1.98 ± 0.21, indicating that the RNA was phenol and ethanol free. cDNA was synthesized from the pure RNA template and cDNA purity was verified with the mean ratio of $A_{260/280}$ = 1.81 ± 0.01.

Primer efficiency

Primers for GAPDH, Actb, HPRT-1, β2M, RPLP-1, Tbp and HIF-1α were designed using the Primer3 software. A primer efficiency test using serial dilution curves gave efficiencies for all primers from 92% to 99% with a correlation coefficient (R^2) ranging from 0.92 to 0.99 (Table 3), indicating that all the designed primers worked successfully and gave consistent results throughout efficiency testing.

The expression profiles of candidate housekeeping genes

qRT-PCR was performed and the cycle threshold (Ct) values were plotted directly, assuming the same threshold for all genes. Ct is the number of cycles needed for fluorescence to reach a specific threshold level of detection and is inversely related to the amount of initial RNA template present in the sample. The six candidate housekeeping genes showed a wide Ct expression range (Figure 2), with RPLP-1 being the most abundantly expressed gene, presenting average Ct values below 16 cycles. Actb, β2M and GAPDH were moderately expressed in these samples, with average Ct values between 16 and 22 cycles, while Tbp and HPRT-1 were the least expressed housekeeping genes, with Ct values above 24 cycles. For qRT-PCR normalization, a moderately expressed housekeeping gene is preferred because extremely high or low expression of a housekeeping gene can introduce variability to the data analysis.

HKGs stability test using geNorm and Normfinder

To identify the candidate housekeeping gene with the most stable expression in the CDC samples, two software-based methods were used: geNorm and NormFinder.

geNorm analysis

geNorm is an established Microsoft Excel based program designed to validate stability of housekeeping gene expression. The underlying principles and calculations are described in Vandesompele *et al.* [35]. geNorm ranks gene stability by an average expression stability value (M), which is the average pairwise variation of a single candidate housekeeping gene with all other candidate housekeeping genes. More stable gene expression is indicated by lower M values.

To investigate the effects of aging on the ranking of candidate genes, housekeeping gene stability was determined in neonatal and adult CDCs (Figure 3a and 3b). In the neonatal cells, both Actb and GAPDH genes had the lowest M value, followed by

RPLP-1, β2M, HPRT-1 and Tbp. This indicates that in neonatal CDCs preconditioned with either hypoxia or PHI, Actb and GAPDH were the most stable genes and Tbp was the least stable gene (Figure 3a). In the adult cells, a combination of Actb and GAPDH genes was found to be the most stable housekeeping genes, compared to other candidate genes. However, the ranking for β2M, HPRT-1 and RPLP-1 was different from that found in the neonatal group (Figure 3b), indicating that expression of β2M, HPRT-1 and RPLP-1 is age-dependent. Independent of age, Tbp was the least stable housekeeping gene. When neonatal and adult CDCs were analyzed in combination, a similar ranking of candidate genes was observed (Figure 3c).

In addition, geNorm analysis revealed the optimal number of housekeeping genes required for reliable and accurate normalization of qRT-PCR expression data, based on the average pairwise variation V_n/V_{n+1} calculated between n and n+1 housekeeping genes (recommended cut-off threshold of $V_n/V_{n+1} = 0.15$) [35]. In both neonatal and adult groups, the pairwise variation $V_{2/3} < 0.15$ indicated there was no need to include a third gene to calculate the normalization factor. Therefore, the two best performing housekeeping genes, GAPDH and Actb, could accurately normalize qRT-PCR expression (Figure 4).

A limitation of this software is that the M value measured is the expression of a single gene as a ratio of the other genes tested. Thus, we could not resolve the best gene out of the two best performing genes, GADPH and Actb. In addition, geNorm analysis relies on the principle that the two best performing genes are identical in all samples, regardless of the experimental conditions or treatments, which is not necessarily true. To address this problem, NormFinder software was also used.

NormFinder analysis

NormFinder, introduced by Andersen *et al.* [36], assesses the expression stability of a gene by evaluating the variation of expression within groups or between groups. Genes with the lowest variation values (V) have the most stable expression and are therefore ideal reference genes. This program allows not only the estimation of overall expression variation of the candidate housekeeping genes across a group of samples, but also of the variation between subgroups of a sample, eg: normoxic CDCs vs. hypoxic CDCs or non-treated CDCs vs. PHI-treated CDCs. Using NormFinder, we found that GADPH was the most stable gene expressed in both neonatal and adult

normoxic cells, while Actb was the most stable gene expressed in both neonatal and adult hypoxic cell groups. For DMOG and EDBA-treated samples, GADPH was the best housekeeping gene for neonatal cells and Actb was best for adult cells. For BIC-treated samples, GADPH was the best housekeeping gene for neonatal cells and β2M was the best for adult cells (Tables 4a and 4b). Overall, NormFinder analysis predicted that GADPH, Actb and β2M were the most consistently expressed housekeeping genes, always being ranked in the first three places, while HPRT-1, RPLP-1 and Tbp were predicted to be unstable, ranked in the last three places (Table 4c). Intergroup stability showed that a combination of GAPDH and Actb were the best housekeeping genes (Figure 5) (Additional file 2).

HIF-1α mRNA expression normalized by different HKGs

We used normalization to different housekeeping genes to compare the gene expression of HIF-1α in CDCs preconditioned under normoxia or hypoxia or with PHIs, for CDCs from both neonatal and adult rat hearts. Normalization was performed using GAPDH, Actb, HPRT-1, RPLP-1, β2M, Tbp and a combination of GAPDH and Actb as reference genes. As shown in Figure 6, when expression levels were normalized to the non-stable housekeeping genes, HPRT-1, RPLP-1 or Tbp, HIF-1α expression was the same for the normoxic, hypoxic and PHI-treated samples for either neonatal or adult groups. Normalization to GADPH, Actb or β2M gave significantly different results in some, but not all, samples. All hypoxic and PHI-treated samples from both neonatal and adult groups showed significant increases in HIF-1α expression, compared with the normoxic control, only when the qRT-PCR data were normalized to the combination of GAPDH and Actb, the optimal HKG combination validated using geNorm and NormFinder, demonstrating that the simultaneous use of two optimal housekeeping genes (GAPDH and Actb) is required to generate valid normalized qRT-PCR data.

Discussion:

This study clearly illustrates the differences in stability of housekeeping genes in rat CDCs cultured under normoxia (21% O_2), hypoxia (2% O_2) or in the presence of the PHIs: DMOG, EDBA or BIC.

Preconditioning of cells under hypoxia or in the presence of an iron chelator (EDBA), an inhibitor of 2-oxoglutarate oxygenases (DMOG) or a specific prolyl hydroxylation inhibitor (BIC), inhibits prolyl-4-hydroxylase (PHD) enzyme activity and subsequently

activates the HIF transcriptional complex [11-14]. Analysis of protein levels in hypoxic and PHI-treated CDCs revealed a significant increase in HIF-α expression, compared to normoxic CDCs, in both the neonatal and adult group, indicating that the hypoxic challenge to the cells was successful. Analysis of mRNA levels in hypoxic and PHI-treated CDCs using qRT-PCR is, however, not as straightforward as the protein analysis. The analysis of qRT-PCR data required normalization using a consistently expressed housekeeping gene.

RPLP-1, which plays role in the elongation step of protein synthesis [43], was the most abundantly expressed gene in the rat CDCs, whereas HPRT-1 (an enzyme which recycles purine in cells) [44] and Tbp (a transcription factor which binds to the TATA-box DNA sequence) [45], were the least expressed genes. Genes with extensive or low expression are not suitable reference genes for qRT-PCR due to their extreme transcription expression. Our conclusions were validated by the geNorm and Normfinder analysis, which showed that these three genes were relatively unstable, compared to GAPDH, β2M and Actb, which showed moderate expression in rat CDC.
To evaluate the effect of aging on HKG stability, we grouped the samples into neonatal and adult groups and analyzed the data either separately or as a combined set using geNorm. In both approaches, we found that a combination of GAPDH and Actb provided the best housekeeping gene, while the Tbp was the least stable among all the candidate genes. The instability of β2M, HPRT-1 and RPLP-1 at different stages of heart development is a drawback in their use as housekeeping genes.

Normalization with multiple reference genes is becoming more prevalent, but studies that apply this normalization approach are limited. Based on geNorm analysis, we found that an optimum of two housekeeping genes was needed to perform a valid normalization. To confirm this, we evaluated the expression of HIF-1α mRNA in the study samples normalized to only one housekeeping gene or to a combination of the two best housekeeping genes as selected by geNorm analysis. Interestingly, only the data set normalized to the geometric mean of GADPH and Actb genes showed a significant increase in HIF-1α expression in every sample. Thus, use of two housekeeping genes appears preferential for accurate normalization in the cell types analyzed.

In our experiments, the sample sets included different stages of heart development (neonatal vs. adult rat hearts), different oxygen tensions (normoxic vs. hypoxic) and

three different PHI drug treatments (DMOG, EDBA or BIC). For NormFinder analysis, we grouped the samples within each experiment, taking into account the genes associated with cardiac progenitor cells in normoxic and hypoxic CDCs or between physiologically-induced hypoxia using hypoxic culture and pharmaceutically-induced hypoxia using PHIs. We found that GADPH was the most stable gene expressed in the normoxic cell group. However, the expression of this gene was unstable in hypoxic CDCs where Actb was the most stable gene expressed. For the PHI-treated samples, there were different best housekeeping genes selected for each inhibitor, yet overall, GADPH, Actb and β2M were the most stable reference genes. Although different housekeeping genes were selected for the different experimental conditions, when the stability of housekeeping genes were considered over all groups, the best housekeeping genes revealed by NormFinder analysis was GADPH and Actb combined.

Conclusions:

In conclusion, both geNorm and NormFinder analysis revealed that GAPDH and Actb are the best housekeeping genes for the cell types analyzed in this study. geNorm also indicated that two housekeeping genes were required for valid qRT-PCR data normalization. In most cases, using multiple housekeeping genes resulted in more accurate and reliable normalization compared with the use of only one reference gene. Thus, we suggest that Actb and GADPH genes should be both used as the housekeeping genes in qRT-PCR involving normoxic, hypoxic and PHI-treated neonatal and adult rat CDCs.

Authors' contributions:

Conceived, designed and performed the experiments: SCT
Synthesized the PHIs: KKY
Analyzed the data: SCT
Wrote the paper: SCT, CAC, KC, CS
Supervisors of the first author (PhD student): CAC, KED, KC

Acknowledgements:

This work was supported by the British Heart Foundation (BHF). SCT and KKY thank the Malaysian Ministry of Higher Education and Univeristy of Science Malaysia for studentships.

1. Beltrami, A.P., et al., *Adult cardiac stem cells are multipotent and support myocardial regeneration.* Cell, 2003. **114**(6): p. 763-76.
2. Soonpaa, M.H. and L.J. Field, *Survey of studies examining mammalian cardiomyocyte DNA synthesis.* Circ Res, 1998. **83**(1): p. 15-26.
3. Anversa, P., M.A. Sussman, and R. Bolli, *Molecular genetic advances in cardiovascular medicine: focus on the myocyte.* Circulation, 2004. **109**(23): p. 2832-8.
4. Messina, E., et al., *Isolation and expansion of adult cardiac stem cells from human and murine heart.* Circ Res, 2004. **95**(9): p. 911-21.
5. Smith, R.R., et al., *Regenerative potential of cardiosphere-derived cells expanded from percutaneous endomyocardial biopsy specimens.* Circulation, 2007. **115**(7): p. 896-908.
6. Li, T.S., et al., *Expansion of human cardiac stem cells in physiological oxygen improves cell production efficiency and potency for myocardial repair.* Cardiovasc Res. **89**(1): p. 157-65.
7. Jokilehto, T. and P.M. Jaakkola, *The role of HIF prolyl hydroxylases in tumour growth.* J Cell Mol Med. **14**(4): p. 758-70.
8. Epstein, A.C., et al., *C. elegans EGL-9 and mammalian homologs define a family of dioxygenases that regulate HIF by prolyl hydroxylation.* Cell, 2001. **107**(1): p. 43-54.
9. Bruick, R.K. and S.L. McKnight, *A conserved family of prolyl-4-hydroxylases that modify HIF.* Science, 2001. **294**(5545): p. 1337-40.
10. Schofield, C.J. and P.J. Ratcliffe, *Signalling hypoxia by HIF hydroxylases.* Biochem Biophys Res Commun, 2005. **338**(1): p. 617-26.
11. Asikainen, T.M., et al., *Stimulation of HIF-1alpha, HIF-2alpha, and VEGF by prolyl 4-hydroxylase inhibition in human lung endothelial and epithelial cells.* Free Radic Biol Med, 2005. **38**(8): p. 1002-13.
12. Cummins, E.P., et al., *The hydroxylase inhibitor dimethyloxalylglycine is protective in a murine model of colitis.* Gastroenterology, 2008. **134**(1): p. 156-65.
13. Tian, Y.M., et al., *Differential sensitivity of HIF hydroxylation sites to hypoxia and hydroxylase inhibitors.* J Biol Chem.
14. Lienard, B.M., et al., *Evaluation of aspirin metabolites as inhibitors of hypoxia-inducible factor hydroxylases.* Chem Commun (Camb), 2008(47): p. 6393-5.
15. Forest, L., N. Glade, and J. Demongeot, *Lienard systems and potential-Hamiltonian decomposition: applications in biology.* C R Biol, 2007. **330**(2): p. 97-106.
16. FibroGen. *Clinical results demonstrate ability of HIF-PHI to treat patients with anemia*. [cited; Available from: http://www.fibrogen.com/Anemia_Clinical_Studies.
17. Chimenti, I., et al., *Relative roles of direct regeneration versus paracrine effects of human cardiosphere-derived cells transplanted into infarcted mice.* Circ Res. **106**(5): p. 971-80.
18. Sun, J., et al., *Improvement in cardiac function after bone marrow cell thearpy is associated with an increase in myocardial inflammation.* Am J Physiol Heart Circ Physiol, 2009. **296**(1): p. H43-50.
19. Lisi, A., et al., *Ion cyclotron resonance as a tool in regenerative medicine.* Electromagn Biol Med, 2008. **27**(2): p. 127-33.
20. Deng, A., et al., *Renal protection in chronic kidney disease: hypoxia-inducible factor activation vs. angiotensin II blockade.* Am J Physiol Renal Physiol. **299**(6): p. F1365-73.

21. Imperatore, A., et al., *Hypoxia and preeclampsia: increased expression of urocortin 2 and urocortin 3.* Reprod Sci. **17**(9): p. 833-43.
22. Kroening, S., et al., *Hypoxia interferes with connective tissue growth factor (CTGF) gene expression in human proximal tubular cell lines.* Nephrol Dial Transplant, 2009. **24**(11): p. 3319-25.
23. Warnecke, C., et al., *Activation of the hypoxia-inducible factor-pathway and stimulation of angiogenesis by application of prolyl hydroxylase inhibitors.* Faseb J, 2003. **17**(9): p. 1186-8.
24. Yang, M.C., et al., *The cardiomyogenic differentiation of rat mesenchymal stem cells on silk fibroin-polysaccharide cardiac patches in vitro.* Biomaterials, 2009. **30**(22): p. 3757-65.
25. Wang, F., et al., *Normalizing genes for real-time polymerase chain reaction in epithelial and nonepithelial cells of mouse small intestine.* Anal Biochem. **399**(2): p. 211-7.
26. Miyamoto, S., et al., *Characterization of long-term cultured c-kit+ cardiac stem cells derived from adult rat hearts.* Stem Cells Dev. **19**(1): p. 105-16.
27. Li, H., et al., *Paracrine factors released by GATA-4 overexpressed mesenchymal stem cells increase angiogenesis and cell survival.* Am J Physiol Heart Circ Physiol. **299**(6): p. H1772-81.
28. Zakharova, L., et al., *Transplantation of cardiac progenitor cell sheet onto infarcted heart promotes cardiogenesis and improves function.* Cardiovasc Res. **87**(1): p. 40-9.
29. Zuba-Surma, E.K., et al., *Bone marrow-derived pluripotent very small embryonic-like stem cells (VSELs) are mobilized after acute myocardial infarction.* J Mol Cell Cardiol, 2008. **44**(5): p. 865-73.
30. Sluka, P., L. O'Donnell, and P.G. Stanton, *Stage-specific expression of genes associated with rat spermatogenesis: characterization by laser-capture microdissection and real-time polymerase chain reaction.* Biol Reprod, 2002. **67**(3): p. 820-8.
31. Nishimura, M., et al., *Effects of prototypical drug-metabolizing enzyme inducers on mRNA expression of housekeeping genes in primary cultures of human and rat hepatocytes.* Biochem Biophys Res Commun, 2006. **346**(3): p. 1033-9.
32. Takagi, H., et al., *Impact of maternal dietary exposure to endocrine-acting chemicals on progesterone receptor expression in microdissected hypothalamic medial preoptic areas of rat offspring.* Toxicol Appl Pharmacol, 2005. **208**(2): p. 127-36.
33. Wang, X., et al., *Quantification of platelet composition in experimental venous thrombosis by real-time polymerase chain reaction.* Thromb Res, 2007. **119**(5): p. 593-600.
34. Yuzbasioglu, A., et al., *Assessment of housekeeping genes for use in normalization of real time PCR in skeletal muscle with chronic degenerative changes.* Exp Mol Pathol. **88**(2): p. 326-9.
35. Vandesompele, J., et al., *Accurate normalization of real-time quantitative RT-PCR data by geometric averaging of multiple internal control genes.* Genome Biol, 2002. **3**(7): p. RESEARCH0034.
36. Andersen, C.L., J.L. Jensen, and T.F. Orntoft, *Normalization of real-time quantitative reverse transcription-PCR data: a model-based variance estimation approach to identify genes suited for normalization, applied to bladder and colon cancer data sets.* Cancer Res, 2004. **64**(15): p. 5245-50.

37. Winer, J., et al., *Development and validation of real-time quantitative reverse transcriptase-polymerase chain reaction for monitoring gene expression in cardiac myocytes in vitro.* Anal Biochem, 1999. **270**(1): p. 41-9.
38. Schmittgen, T.D. and B.A. Zakrajsek, *Effect of experimental treatment on housekeeping gene expression: validation by real-time, quantitative RT-PCR.* J Biochem Biophys Methods, 2000. **46**(1-2): p. 69-81.
39. Livak, K.J. and T.D. Schmittgen, *Analysis of relative gene expression data using real-time quantitative PCR and the 2(-Delta Delta C(T)) Method.* Methods, 2001. **25**(4): p. 402-8.
40. Kuijk, E.W., et al., *Validation of reference genes for quantitative RT-PCR studies in porcine oocytes and preimplantation embryos.* BMC Dev Biol, 2007. **7**: p. 58.
41. Kidd, M., et al., *GeneChip, geNorm, and gastrointestinal tumors: novel reference genes for real-time PCR.* Physiol Genomics, 2007. **30**(3): p. 363-70.
42. Van Zeveren, A.M., et al., *Evaluation of reference genes for quantitative real-time PCR in Ostertagia ostertagi by the coefficient of variation and geNorm approach.* Mol Biochem Parasitol, 2007. **153**(2): p. 224-7.
43. Rich, B.E. and J.A. Steitz, *Human acidic ribosomal phosphoproteins P0, P1, and P2: analysis of cDNA clones, in vitro synthesis, and assembly.* Mol Cell Biol, 1987. **7**(11): p. 4065-74.
44. Duan, J., L. Nilsson, and B. Lambert, *Structural and functional analysis of mutations at the human hypoxanthine phosphoribosyl transferase (HPRT1) locus.* Hum Mutat, 2004. **23**(6): p. 599-611.
45. Kornberg, R.D., *The molecular basis of eucaryotic transcription.* Cell Death Differ, 2007. **14**(12): p. 1989-97.

Figures:

Figure 1 Western blot analysis of HIF-1α protein levels in neonatal and adult P2 CDCs cultured under hypoxia or with DMOG, EDBA and BIC. In each group, all values were normalized to levels in normoxic CDCs (control). Culture under hypoxia or with PHIs increased expression of HIF-1α. * $p < 0.05$ vs. control, n = 4.

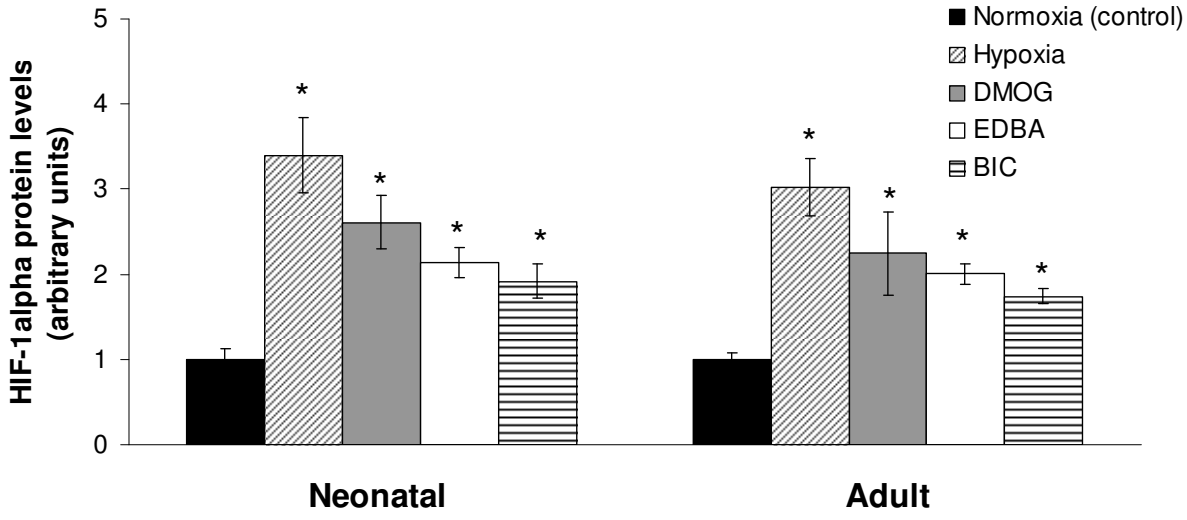

Figure 2 Expression levels of candidate housekeeping genes in normoxic, hypoxic and PHI-treated CDCs cultured from neonatal and adult rat hearts. Boxes represent lower and upper quartiles of cycle threshold ranges with the median indicated, whiskers represent the 10th and 90th percentiles. Grey boxes correspond to neonatal CDCs and hatched boxes correspond to adult CDCs. In both groups, RPLP-1 was the most highly expressed gene (lowest Ct value), followed by Actb, β2M, GAPDH and lastly the HPRT-1 and Tbp as the least expressed genes (highest Ct values).

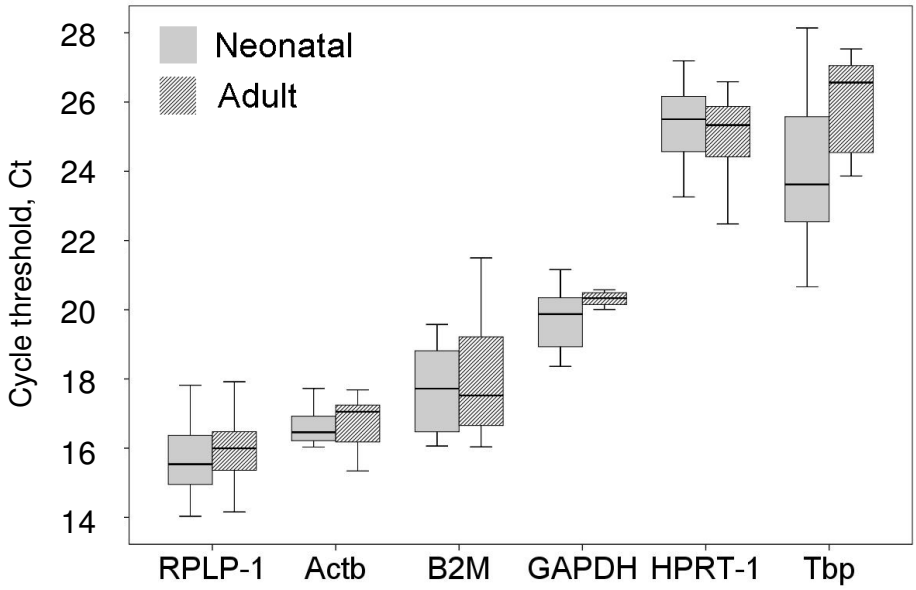

Figure 3 geNorm analysis of the candidate housekeeping genes average expression stability, M. Genes with highest M value represent the least stable gene. Samples were analyzed separately according to the age group: (a) neonatal, (b) adult, or (c) were analyzed in a combined set (results obtained from three sets of biological replicates).

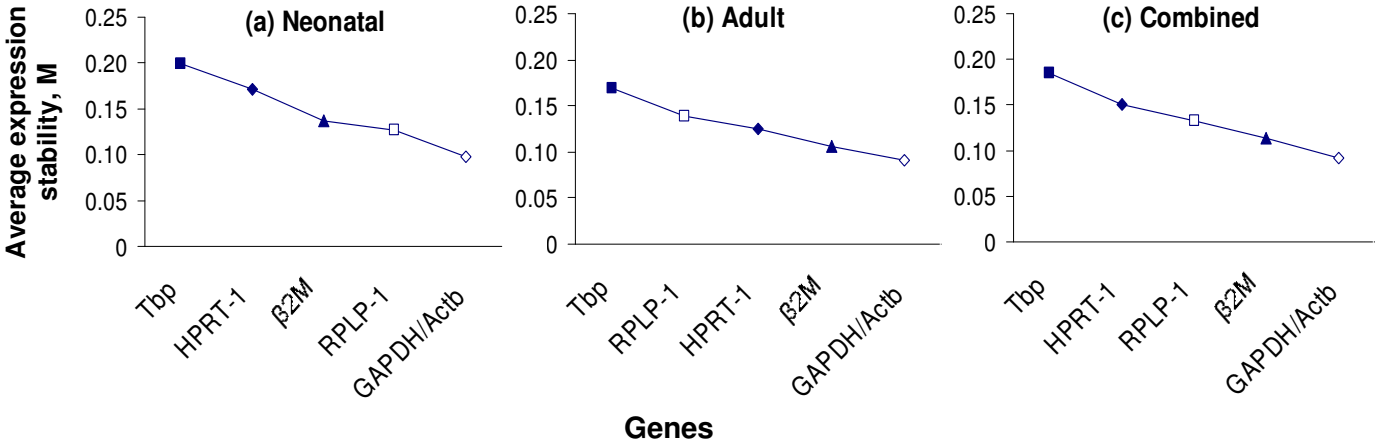

Figure 4 geNorm analysis of the optimal number of housekeeping genes required for data normalization. A variation coefficient, V, value below 0.15 was accepted as indicating the optimal number of genes required for the data normalization. V2/3 < 0.15 indicated that 2 genes were required for the data normalization (results obtained from three sets of biological replicates).

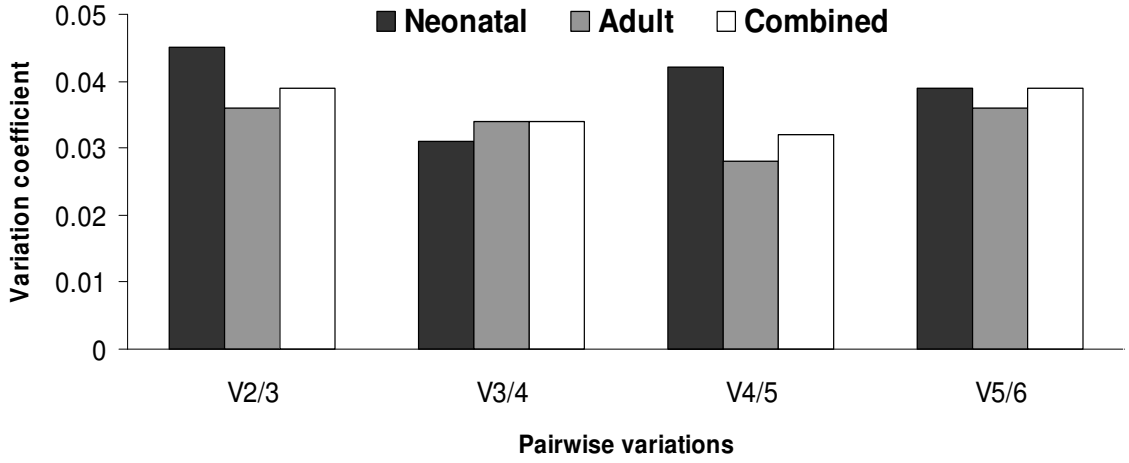

Figure 5 NormFinder analysis of the candidate housekeeping genes average expression stability values (V). Genes with highest V value represent the least stable gene. Ranking of candidate housekeeping genes were determined considering intra- and inter-group variation for (a) neonatal, (b) adult and (c) combined set of neonatal and adult CDCs (results obtained from three sets of biological replicates).

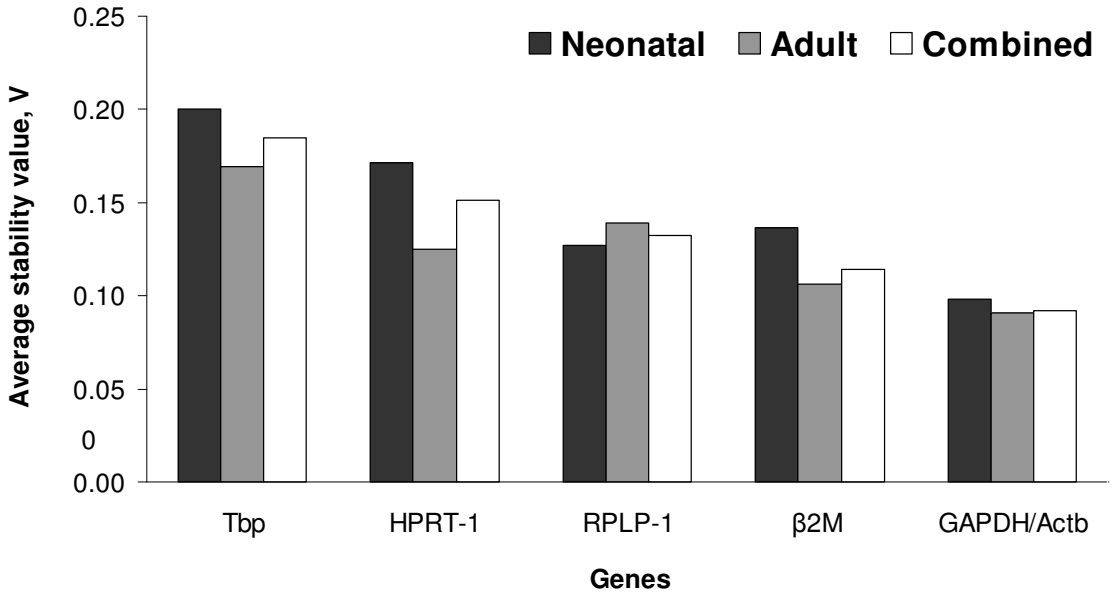

Figure 6 Expression level of HIF-1α mRNA in (a) neonatal and (b) adult CDCs upon normalization to different housekeeping gene. All data are relative to the normoxic sample (control). Normalization to the best combination of GAPDH/Actb validated by geNorm and NormFinder showed significantly increased expression of HIF-1α mRNA in both neonatal and adult group under all experimental conditions. * $p < 0.05$, # $p < 0.01$.

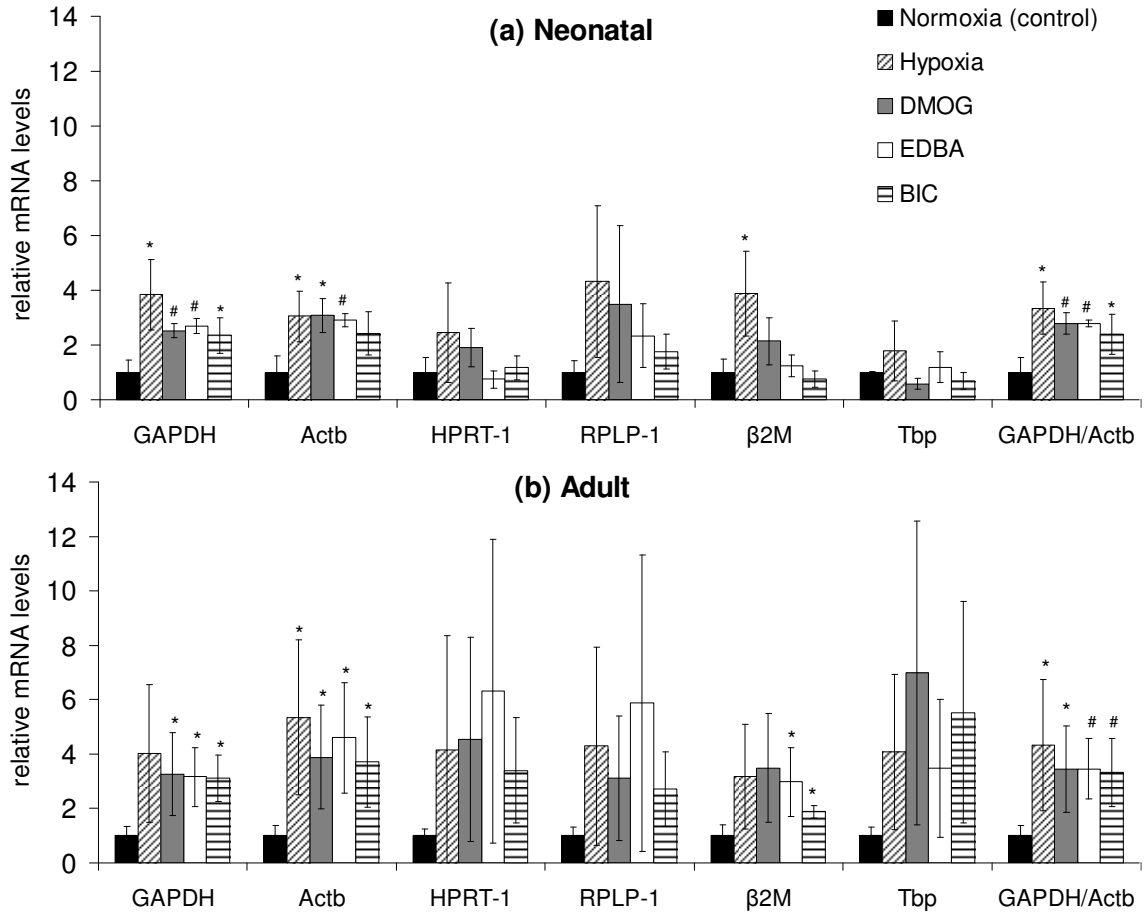

Tables

Table 1 List of reference genes and target gene used in the present study. Gene symbol, name, primer sequences, gene accession and function are shown.

No.	Code	Primer	Gene name	Forward primer 5' to 3'	Reverse primer 5' to 3'	Gene accession number	Function of the protein coded by this gene
1	HKG 1	GAPDH	glyceraldehyde-3-phosphate dehydrogenase	GGGTGTGAACC ACGAGAAAT	ACTGTGGTCATG AGCCCTTC	NM_017008	Oxidoreductase in glycolysis and gluconeogenesis
2	HKG 2	Actb	Beta-actin	CTAAGGCCAAC CGTGAAAAG	AACACAGCCTG GATGGCTAC	NM_031144	Cytoskeletal structure protein
3	HKG 3	HPRT-1	hypoxanthine phosphoribosyl-transferase 1	CTCATGGACTG ATTATGGACAG GAC	GCAGGTCAGCA AAGAACTTATA GCC	NM_012583	Recycle purines in cells
4	HKG 4	β2M	Beta-2-microtubulin	CCGTGATCTTTC TGGTGCTT	ATTTGAGGTGGG TGGAACTG	NM_012512	Highly conserved proteins that are involved in cell motility, structure and integrity
5	HKG 5	RPLP-1	60S acidic ribosomal protein large P1	AAAGCAGCTGG TGTCAATGTT	GCAGATGAGGC TTCCAATGT	ESNSRNOG00000 013874*	Protein synthesis
6	HKG 6	Tbp	TATA box binding protein	TTCTGGGAAAA TGGTGTGC	CCCACCATGTTC TGGATCTT	NM_001004198	Transcription factor that binds to TATA box located at upstream of the transcription start site in eukaryotic gene promoters
7	TG 1	HIF-1α	Hypoxia induced factor-1 alpha	GGTGGATATGT CTGGGTTGAG	TTCAACTGGTTT GAGGACAGA	NM_024359	Transcription factors that respond to reduced oxygen changes in the cellular environment

* Exon sequences browsed using Ensembl Genome Browser; others were browsed using GenBank Genome Browser. HKG = housekeeping gene, TG = target gene.

Table 2 CDC sample groups. CDCs were cultured from (a) neonatal and (b) adult rat hearts. CDCs from each group were subjected to five different culture conditions (i) – (v).

Age of animals	Culture conditions
(a) Neonatal (1-3 days)	(i) Normoxia (21% O_2) (control)
(b) Adult (4 months)	(ii) Hypoxia (2% O_2)
	(iii) Normoxia + 1 mM DMOG for 24 h
	(iv) Normoxia + 0.5 mM EDBA for 24 h
	(v) Normoxia + 30 μM BIC for 24 h

DMOG = dimethyloxalyl glycine; EDBA = Ethyl 2-(2,3-dihyroxybenzamido) acetate; BIC = 1-Chloro-4-hydroxyisoquinoline-3-carboxamido ethanoic acid.

Table 3 List of reference genes and target gene used in the present study. Gene name, primer efficiency and the correlation coefficient are shown.

Gene name	Primer efficiency	Correlation coefficient (R^2)
GAPDH	99.3	0.99
β2M	91.6	0.97
HPRT-1	92.3	0.99
Actb	92.7	0.99
RPLP-1	94.9	0.92
Tbp	93.8	0.93
HIF-1α	98.2	0.92

Table 4 Ranking of candidate HKGs and their expression stability,V in the different sample groups of the study evaluated using NormFinder. Samples were analyzed separately according to age group, (a) neonatal and (b) adult or were analyzed in a (c) combined set of neonatal and adult. Gene with the lowest stability value has the most stable expression. Stability values are listed from most stable to least stable.

(a) Neonatal CDCs

Normoxia		Hypoxia		DMOG 1mM		EDBA 0.5 mM		BIC 30µM	
Ranking	Stability value	Ranking	Stability value	Ranking	Stability value	Ranking	Stability value	Ranking	Stability value
1) GAPDH	0.053	***1) Actb***	0.139	***1) GAPDH***	0.087	***1) GAPDH***	0.051	***1) GAPDH***	0.092
2) Actb	0.113	***2) GAPDH***	0.160	***2) Actb***	0.362	***2) Actb***	0.121	***2) Actb***	0.192
3) β2M	0.158	***3) β2M***	0.189	***3) β2M***	2.224	***3) β2M***	0.152	***3) β2M***	0.591
4) RPLP-1	4.606	*4) Tbp*	1.910	*4) HPRT-1*	3.215	*4) HPRT-1*	2.951	*4) RPLP-1*	1.757
5) Tbp	14.744	*5) RPLP-1*	3.068	*5) RPLP-1*	4.935	*5) RPLP-1*	5.014	*5) HPRT-1*	3.055
6) HPRT-1	15.586	*6) HPRT-1*	17.241	*6) Tbp*	20.389	*6) Tbp*	11.328	*6) Tbp*	14.794

(b) Adult CDCs

Normoxia		Hypoxia		DMOG 1mM		EDBA 0.5 mM		BIC 30µM	
Ranking	Stability value	Ranking	Stability value	Ranking	Stability value	Ranking	Stability value	Ranking	Stability value
1) GAPDH	0.233	***1)Actb***	0.200	***1) Actb***	0.216	***1) Actb***	0.333	***1) β2M***	0.040
2) Actb	0.747	***2) β2M***	0.388	***2) GAPDH***	0.414	***2) GAPDH***	0.447	***2) Actb***	0.156
3) β2M	1.077	***3) GAPDH***	0.419	***3) β2M***	1.498	***3) β2M***	0.542	***3) GAPDH***	0.275
4) RPLP-1	2.502	*4) RPLP-1*	4.592	*4) HPRT-1*	4.380	*4) Tbp*	1.482	*4) RPLP-1*	1.495
5) HPRT-1	10.524	*5) HPRT-1*	8.784	*5) RPLP-1*	4.682	*5) RPLP-1*	2.106	*5) Tbp*	1.608
6) Tbp	13.181	*6) Tbp*	15.939	*6) Tbp*	6.490	*6) HPRT-1*	10.410	*6) HPRT-1*	3.381

(c) Combined (neonatal and adult CDCs)

Normoxia		Hypoxia		DMOG 1mM		EDBA 0.5 mM		BIC 30µM	
Ranking	Stability value	Ranking	Stability value	Ranking	Stability value	Ranking	Stability value	Ranking	Stability value
1) GAPDH	0.002	***1) GAPDH***	0.315	***1) Actb***	0.359	***1) Actb***	0.263	***1) β2M***	0.072
2) Actb	0.161	***2) Actb***	1.059	***2) GAPDH***	1.215	***2) β2M***	0.718	***2) Actb***	0.248
3) β2M	0.298	***3) β2M***	1.793	***3) β2M***	2.201	***3) GAPDH***	1.491	***3) GAPDH***	1.105
4) RPLP-1	3.981	*4) RPLP-1*	2.188	*4) HPRT-1*	3.160	*4) RPLP-1*	2.519	*4) RPLP-1*	1.263
5) HPRT-1	12.482	*5) Tbp*	4.208	*5) RPLP-1*	3.844	*5) Tbp*	4.834	*5) HPRT-1*	2.520
6) Tbp	25.530	*6) HPRT-1*	6.658	*6) Tbp*	16.492	*6) HPRT-1*	6.447	*6) Tbp*	9.298

Bold type indicates the reference genes that were consistently ranked the top places, and thus can be categorized as stable HKGs in this study as compared to other three candidate genes.

Additional files

Additional file 1 – List of recent papers published on rat qRT-PCR analysis. Cell types, experimental factors and housekeeping genes selected are shown.

Reference	Cell types and experimental factors	HKG selected
[26]	Characterization of long-term cultured c-Kit$^+$ cardiac cells	GAPDH
[24]	Rat MSC transdifferentiated into cardiomyocytes	GAPDH
[27]	GATA-4 overexpressed MSC	GADPH
[18]	CDCs encapsuled in hydrogels	Actb
[28]	Characterization of rat and human CFC seeded on double-coated plates (poly-l-lysine and collagen type IV from human placenta)	Actb
[29]	HSC cultured from myocardial infarcted rodents.	β2M
[30]	Adult rat testes	HPRT
[31]	Primary cultures of human and rat hepatocytes	HPRT and Actb
[32]	Rat brain tissue	HPRT and GAPDH
[33]	Characterization of cell marker cell components in rat vascular thrombosis	RPLP and GAPDH
[34]	Rat skeletal muscle with chronic degenerative changes	Tbp and Actb

MSC = mesenchymal stem cell; CDC = cardiosphere-derived cell; CFC = cardiosphere-forming cell; HSC = hematopoietic stem cell.

Additional file 2 - Ranking of candidate HKGs and their expression stability as evaluated by NormFinder considering intra- and inter-group variation for neonatal (a), adult (b) and combined set of neonatal and adult (c) CDCs. Stability values are listed from most stable to least stable.

(a) Neonatal		**(b) Adult**		**(c) Combined (neonatal and adult)**	
Ranking	Stability value	Ranking	Stability value	Ranking	Stability value
1) Actb	0.371	*1) Actb*	0.224	*1) Actb*	0.203
2) GAPDH	0.404	*2) GAPDH*	0.333	*2) GAPDH*	0.265
3) β2M	0.646	*3) β2M*	0.412	*3) β2M*	0.346
4) RPLP-1	1.118	*4) RPLP-1*	0.699	*4) RPLP-1*	0.543
5) HPRT-1	1.159	*5) Tbp*	0.945	*5) HPRT-1*	0.801
6) Tbp	1.972	*6) HPRT-1*	0.956	*6) Tbp*	1.047
Actb/GAPDH [a]	0.291	*Actb/GAPDH* [a]	0.207	*Actb/GAPDH* [a]	0.177

[a] the best combination of two most stable reference genes

Additional file 3 - Preparation of culture medium

Complete explant medium (CEM)

Iscove's modified Dulbecco's medium (IMDM; Invitrogen) supplemented with 20% (v/v) fetal bovine serum (FBS; Biosera), 100 U/ml penicillin, 100 µg/ml streptomycin, and 0.2 mM L-glutamine (PSG; Gibco).

Cardiosphere-growth medium (CGM)

65% (v/v) Dulbecco's modified Eagle's medium (DMEM/F12; Invitrogen) and 35% (v/v) CEM supplemented with: 7% (v/v) FBS, 100 U/ml penicillin, 100 µg/ml streptomycin, 0.2 mM L-glutamine (PSG; Gibco), 2% (v/v) B27 supplement (Invitrogen), 25 ng/ml cardiotrophin (Peprotech), 20 ng/ml bFGF (Promega), 10 ng/ml EGF (Peprotech), 5 U thrombin (Sigma).

Additional file 4 - **Figure A1** Structure of prolyl-4-hydroxylase inhibitors (PHDIs)

Dimethyloxaloylglycine (DMOG)

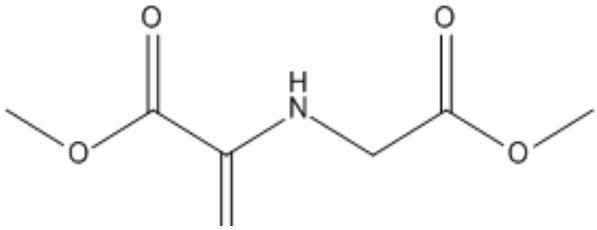

Ethyl 2-(2,3-dihyroxybenzamido) acetate (EDBA)

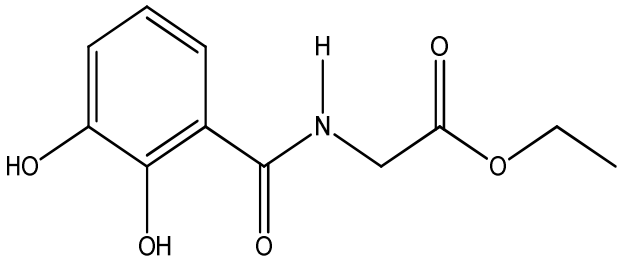

1-Chloro-4-hydroxyisoquinoline-3-carboxamido ethanoic acid (BIC)

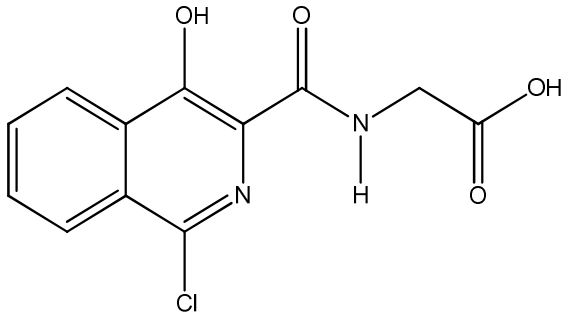

Supplemental data 1 *Comparison of cells being tested for myocardial regeneration. Cell markers expressed, cell sources, advantages and disadvantages of each cell types are listed.*

Cell Type	Markers	Source	Advantages	Disadvantages
Embryonic stem cells	• Oct-4 • Sox 2	• Existing stem cell lines • Aborted or miscarried embryos • Unused *in vitro* fertilized embryos • Cloned embryos	• Divide for indefinite periods • Pluripotent	• Major ethical opposition • Possibility of teratoma formation
Induced pluripotent cell	• Oct4 • Sox2	• Allogenic – donor tissue • Autologous – own tissue	• Readily obtained from skin and thus less invasive • Closely resemble embryonic stem cells • Pluripotent	• Potential for malignant transformation mutagenesis
Bone marrow stem cells / mononuclear cells	• c-Kit$^+$ • Lin$^-$	• Autologous	• Feasible and safe in humans • Readily prepared in hospitals	• Pluripotency uncertain • Limited success in clinical trials
Endothelial progenitor cells	• CD144 • CD34 • VEGFR • CD133	• Autologous	• Paracrine • Angiogenesis	• Isolation after BM aspiration • Cell processing

Supplemental data 1 (continued) *Comparison of cells being tested for myocardial regeneration. Cell markers expressed, cell sources, advantages and disadvantages of each cell types* are listed

Mesenchymal stem cells	• $CD105^+$ • $CD45^-$ • $CD90^+$ • $CD34^-$ • $CD74^+$	• Autologous – bone marrow • Allogenic - umbilical cord	• Multipotent • Paracrine Plastic-Adhesive cells	• Microembolization after intracoronary injection
Skeletal myoblasts	• Myo D • Myf5	• Autologous	• Readily obtained • Low risk of tumor formation • Survive and differentiate in human hearts • Myotube formation	• Ventricular arrhythmias in clinical trials
Very small-embryonic like cells	• $CXCR\text{-}4^+$ • $Oct\text{-}4^+$ • $Sca\text{-}1^+$ • $Nanog^+$ • $CD45^-$ • $Rex\text{-}^+$ • $SSEA\text{-}1^+$	• Autologous - bone marrow	• Pluripotent	• Potential for mutagenesis
Cardiac stem cells	• c-kit, • Sca-1 • Abg • Isl-1	• Autologous	• Cardiac origin • Cardiogenic Potential • Clinical trials underway	• More invasive because biopsy should be obtained for cell isolation • Long-term outcome not yet known • Cardiac stem cells isolated from an aging heart may not sufficiently improve function • requires cardiac biopsy and Ex-vivo expansion